UNIVERSITY OF LEEDS

Identifying differences in the tumour microenvironment between ER-positive and ER-negative invasive ductal breast cancer

Ahmed Jasim Mohammed

M.Sc. (Hons)

Submitted in accordance with the requirements for the Degree of Doctor philosophy

The University of Leeds

School of Medicine and Health

Leeds Institute of Cancer and Pathology

Declaration

The candidate confirms that the work submitted is his own, except where work which has formed part of jointly-authored publications has been included.
The contribution of the candidate and the other authors to this work has been explicitly indicated within the thesis.

The candidate confirms that appropriate credit has been given within the thesis where reference has been made to the work of others.

Acknowledgment

First and foremost, praises and thanks to Allah who generously conferred me with the strength and ability to get successfully through my PhD research studies. All praise is due to Allah, the Lord of the entire worlds, and Allah's peace and blessings be upon his final prophet Muhammad, his pure family, his noble companions, and all those who follow them with righteousness until the Day of Judgment. Indeed, it is Allah who bestows success. I also would like to share my emotional sorry for people who are bravely fighting against cancer, people who live with the disease patiently and optimistically. Then, I gratefully would like to express my deep and sincere gratitude and appreciation to my principal supervisor Dr. Peter Laslo for his support all along the highway of my scientific journey. I am extremely grateful for what he has offered me, for providing me invaluable guidance throughout my studies. His motivation, vision and dynamism have inspired me. He taught me the methodologies in order to carry out this research. I also owe my sincere thanks to my co-supervisor Prof. Christopher Twelves. Without the full support and encouragement of my supervisors, I could not have completed my thesis. I would also like to express my appreciation to University of Leeds, faculty of medicine and health, department of pathology. Special thanks also go to the Ministry of higher education and scientific research for their generous financial support, encouragement and granting me a full scholarship. I would like to extend my warmest thanks to my family specially my parents, brothers, sister. I mentioned them last to emphasise the peculiar nature of their encouragement, tremendous effort, patience and emotional support throughout my candidature.

Dedication

I would like to dedicate this thesis to my beloved Dad prof Jasim and mom who always picked me up on time and encouraged me to go on every adventure in my life especially this one. My beloved brothers Dr. Mohammed, Dr. Ali and Dr. Ibrahem, as well as my beautiful little sister Dr. Noor who always support me in every aspect in my life. Without their continuous and sincere advice, and full support, I could not have completed this thesis. I also dedicate this thesis to my honourable ministry of higher education and scientific research in Iraq for their financial support, encouragement and granting me a full scholarship. I would like to offer my special thanks and gratitude for all the people of Iraq. With my deepest gratitude and warmest affection that I dedicate this PhD thesis to my both supervisors Dr. Peter Laslo and Prof. Christopher Twelves who have been a constant source of knowledge and inspiration. Finally, I would like to dedicate my entire work in this thesis to my special friend Dr. Haidar Arkawazi for his support during my PhD journey.

Abstract

The tumour microenvironment plays an essential role in tumour growth and progression. The tumour microenvironment is composed of different cell types, including macrophages, fibroblasts, various inflammatory cells, fat cells and endothelial cells, collectively known as stroma. Most recent studies believe that the tumour microenvironment in many solid tumours including breast cancer defines outcome in oestrogen receptor positive (ER+) and triple negative breast cancer (TNBC). This PhD project was established in order to test the hypothesis that cells within the tumour microenvironment influence breast cancer outcome and this differs in ER+ versus TNBC disease. As part of the project, 7 biomarkers were used to identify stromal cells including fibroblasts and various immune cells. Furthermore, our results from positive pixel count (PPC) revealed CD3+ (n=4.01), CD4+ (n=1.28) and CD8+ (n=4.71) numbers were positively correlated with higher histologic grade in TNBC cases, while in ER+ samples, the cell number of CD3+ (n=2.1), CD4+ (n=0.5) and CD8+ (n=2.3) was negatively correlated with high grade tumour. High levels of CD68 were found to be associated with high tumour grade in both ER+ (n=5.5) and TNBC (n=6.41) breast cancer samples. Pirfenidone PFD drug displayed a sign of acute toxic at 100µm, while it showed inhibitory effect on cell proliferation of MCF-7, MDA-MB-231 and CAFs derived from ER+ positive breast cancer. Our data from qRT-PCR and immunofluorescence revealed that MCF-7 expressed ER-α gene but it was absent in MDA-MB-231 breast cancer cells. Human monocytic Thp-1 cells have been considered as an alternative model for human peripheral-blood macrophages. 25ng/ml PMA concentration was chosen as an optimal concentration among others to differentiate monocytic Thp-1 into macrophages. The co-culture of macrophages with

MCF-7 or MDA-MB-231 has shown lower proliferative rate in both breast cancer subtypes, whereas breast cancer cells were more proliferative when co-cultured with fibroblasts and macrophages using triple culture model. Moreover, breast cancer cells co-cultured with macrophages for different time points were termed as following; control or untreated were labelled as (C), short-term co-culture (3-5 days) were labelled as (S) ,long-term co-culture (30 days) were labelled as (L) and those cells that grew individually after 1 month incubation with macrophages were labelled as programmed (P). However, long-term co-culture of macrophages with breast cancer subtypes has chronically promoted cell migration of programmed MDA-MB-231 but not MCF-7 clones compared to those co-cultured under short-term and control samples. Differential gene expression analysis revealed that programmed MDA-MB-231 clones share the highest number of up-regulated (5591) and down-regulated (6093) genes among other samples including short-term and long-term in contrast with control, indicating that the incubation of macrophages with MDA-MB-231 for 30 days has chronically regulated gene expression in programmed MDA-MB231 which has reflected in their migration and proliferation behaviour.

Table of Contents

Declaration I
Acknowledgment II
Dedication III
Abstract IV
Contents VI
List of tables XI
List of figures XII
Table of common abbreviations XVI

Chapter 1. Introduction

1.1 Overview of breast cancer 2
1.2 Breast cancer initiation and progression 4
1.3 Oestrogen receptor positive breast cancer 6
1.4 Triple negative breast cancer 9
1.5 The role of tumour microenvironment in breast cancer 11
1.6 Immune system and breast cancer 14
1.7 The role of cytotoxic T lymphocytes in breast cancer 16
1.8 The role of T helper cell in breast cancer 19
1.9 The role of regulatory T cell in breast cancer 21
1.10 B Cells and the breast tumour microenvironment 23
1.11 Tumour associated macrophages 26
1.12 Cancer associated fibroblasts in breast cancer 28
1.13 The relationship between tumour stroma ratio and survival outcome 32
1.14 Cellular reprogramming during cancer progression 34
1.15 Cytokines mediated tumour progression 35
Hypothesis 37
Aims and objective 37

Chapter 2. Materials and Methods

2.1 Immunohistochemistry 39
2.1.1 Tumor samples and antibody optimisation for immunohistochemistry staining 39
2.1.2 Antibody optimisation 41

2.1.3 Positive pixel count algorithm 43
2.1.4 Positive pixel count analysis 44
2.1.5 Quantification of positive pixel analysis 46
2.1.6 Positive pixel count optimisation 47
2.1.7 Picro Sirius Red Staining 47
2.2 Cell culture 48
2.2.1 Cell maintenance 48
2.2.2 Generation of Conditioned Medium (CM) 49
2.2.3 Generation of NF and CAFa from human breast tumours 49
2.2.4 The effect of CM on cell proliferation 50
2.2.5 The effect of PFD on breast cancer cell lines and fibroblasts 51
2.3 Assessing ER status in human breast cancer cell lines and fibroblasts 52
2.3.1 RNA extraction 52
2.3.2 Quantification of RNA purity using NanoDrop 52
2.3.3 First-strand cDNA synthesis 53
2.3.4 Real-Time Polymer Chain Reaction RTPCR 54
2.3.5 Immunofluorescence 54
2.4 Raman Imaging 55
2.4.1 Slide silanisation 55
2.4.2 Sample preparation 55
2.4.3 Raman measurements 56
2.5 Thp-1 differentiation into marophages 59
2.5.1 Optimisation of PMA concentration 59
2.5.2 RNA isolation 59
2.5.3 cDNA synthesis 60
2.5.4 PCR primer design 60
2.5.5 Polymer Chain Reaction (PCR) 61
2.5.6 Evaluating gene expression on gel electrophoresis 62
2.6 Determining resting phase in stimulated Thp-1 post PMA removal 62
2.7 Evaluating gene expression analysis in detahed cells 63
2.8 Evaluating macrophages differentiation co-cltured with BC cells 63
2.9 Assessment of gene expression analysis in BC post co-culture with macrophages 64
2.10 Determining co-culture cell ratio 65
2.11 Assessment of macrophages cell morphology in presence of BC 66

2.12 CM effect on BC 66
2.13 Characterization of BC in double and triple culture model 67
2.13.1 Determining fibroblasts and BC cell ratio 67
2.13.2 Cell migration assay 68
2.13.3 Cell invasion assay 69
2.13.3.1 Determining optimal matrigel concentration 69
2.13.3.2 Matrigel chambers preparation 69
2.13.3.3 Cell lines preparation 70
2.13.3.1 Matrigel invasion assay performance 70
2.13.4 Cell proliferation assay 72
2.14 Evaluating macrophages role in BC single cell clone 72
2.14.1 Generating single cell clone 72
2.14.2 Long term co-culture of macrophages with BC 73
2.14.3 Evaluating gene expression in BC single cell clones 74
2.14.4 Cell migration assay 74
2.14.5 Cell proliferation assay 75
2.15 Next generation RNA sequencing 75
2.15.1 Differential gene expression analysis 76
2.15.2 Analysis of genes related cell migration and proliferation 77
2.16 Statistical analysis 78

Chapter 3. The findings of immunohistochemistry analysis

3.1. Antibody optimisation 80
3.1.1 CD3 81
3.1.2 CD4 82
3.1.3 CD8 83
3.1.4 CD20 84
3.1.5 CD68 85
3.1.6 αSMA 86
3.1.7 FOXP3 87
3.2 Localization of T cell subsets, CD20+, CD68+ and αSMA in BC subtypes 88
3.3 Positive pixel count optimisation 92
3.4 Quantification of immunohistochemistry 94
3.5 Collagen quantification by Picro Sirius red histochemistry 98

3.6 Determination of ERα expression in fibroblasts 99
3.6.1 qRT-PCR 99
3.6.2 Immunofluorescence 100
3.7 Raman Imaging 101
3.8 The effect of conditioned medium on cell proliferation 102
3.9 The effect of Pirfenidone on cell proliferation 104
Discussion 107

Chapter 4 Assessment of macrophages differentiation and their role in BC

4 Macrophages cell line selection and differentiation 111
4.1 The optimal PMA concentration 112
4.2 Resting priod of macrophages post PMA removal 116
4.3 Gene expression in detached cells 119
4.4 BC cells promoted macrophages differentiation 121
4.5 Gene expression in BC cells upon co-culture with macrophages 125
4.6 Determining co-culture cell ratio 127
4.7 Macrophages cell morphology co-cultured with BC cells 129
4.8 Evaluating macrophages CM effect on BC cells 131
4.9 Characterization of BC using triple culture model 134
4.10 Determining fibroblast-BC cell ratio 136
4.11 BC cell migration in triple culture model 138
4.12 The optimal concentration of matrix matrigel 143
4.13 Macrophages and fibroblasts promoted BC cell proliferation 146
Discussion 148

Chapter 5 Evaluation of cellular reprogramming of breast cancer after long-term co-culture with macrophages

5.1 Characterisation of BC after long-term co-culture with macrophages 152
5.1.1 Generating single cell clone 153
5.1.2 Gene expression in programmed BC 153
5.1.3 Long term incubation with macrophages promoted BC cell migration 155
5.1.4 Macrophages inhibited breast cancer cell proliferation 159

5.2 Next Generation RNA sequensing 162
5.2.1 Assessment of RNA isolation and integrity 162
5.2.2 Analysis of KEGG pathways and Gene Ontology enrichment 164
5.2.3 Differential gene expression between samples..... 166
5.2.4 Clustering and grouping of MDA-MB-231 samples..... 167
5.3 Identification of genes-related cell migration 169
5.4 Identification of genes-related cell proliferation 171
5.5 Analysis of gene expression related cell migration and proliferation 175
5.6 Validation of gene expression related cell migration 175
5.7 Validation of gene expression related cell proliferation 177
Discussion..... 179

Chapter 6 Discussion and summary findings

Discussion..... 182
Summary findings..... 194
Future direction. 198
APPENDIXES 200
References..... 211

List of tables

Table 1. Clinicopathological features of triple-negative breast cancer patients 40
Table 2. Clinicopathological features of oestrogen receptor positive breast cancer patients..... 41
Table 3. Primary antibodies used for immunohistochemistry 42
Table 4. Primers used for RT-PCR analysis to evaluate Thp-1 differentiation into macrophages 61
Table 5. List of primers were used for PCR to detect gene expression in MDA-MB-231 breast cancer cells after co-culture with macrophages derived Thp-1 65
Table 6. List of primers were used for PCR to detect gene expression in MCF-7 breast cancer cells after co-culture with macrophages derived Thp-1 65
Table 7. List or primers used for RT-PCR amplification in order to evaluate genes-related cell migration expression in MDA-MB-231 and MCF-7 breast cancer cells...77
Table 8. List or primers used for RT-PCR amplification in order to evaluate genes-related cell proliferation expression in breast cancer cells.. 77
Table 9. Immunohistochemical quantification of biomarkers analysed in 20 oestrogen receptor positive samples..... 97
Table 10. Immunohistochemical quantification of biomarkers analysed in 50 oestrogen receptor negative samples 97
Table 11. Collagen density in ER+ and TN breast cancers..... 98
Table 12. Top 10 up-regulated genes-related MDA-MB-231 cell migration identified by NGS..... 170
Table 13. Top 10 down-regulated genes-related MDA-MB-231 cell migration identified by NGS 171
Table 14. Top 10 up-regulated genes-related MDA-MB-231 cell proliferation identified by NGS 174
Table 15. Top 10 down-regulated genes-related MDA-MB-231 proliferation identified by NGS..... 174

List of figures

Figure 1. An overview of breast cancer initiation and development from DCIS to IDC. 6
Figure 2. Kaplan-Meier curves shows the association between breast cancer subtypes. 8
Figure 3. Representative images of invasive ductal carcinoma of TNBC subtype 11
Figure 4. The tumour microenvironment of invasive ductal breast cancer. 13
Figure 5. The cross-talk between T cell and tumour cells through PD-1 and PDL-1 pathway. 16
Figure 6. Representative images showing the difference in density of cytotoxic T lymphocytes in patients before and after received primary systematic therapy 19
Figure 7. Kaplan–Meier curves of RFS and OR in TNBC patients. 21
Figure 8. Kaplan–Meier analysis show the prognostic value of infiltrated regulatory Treg cells in breast cancer. 23
Figure 9. The immunological function of B lymphocytes in breast cancer. 25
Figure 10. Survival analysis of CD68 and CD163 expression in ER+ and TNBC breast cancer cohorts. 28
Figure 11. Kaplar-meier analysis of OS and DSS in relation with α-SMA and FAP expression in TNBC cancer patients. 31
Figure 12. . Kaplan-Meier analysis for recurrence-free survival of TNBC and ER+ breast cancer subtypes stratified by tumour-stroma ratio. 33
Figure 13. The thresholds of total intensity: weak, positive and strong. 43
Figure 14. Examples of hand drawn annotation type. 44
Figure 15. The spot generation screen shows the number of boxes to be generated on the slide. 45
Figure 16. Positive pixel count analysis after generating boxes on the slide. 45
Figure 17. Examples of CD3 abundance characterized as high (a), moderate (b) and low (c) abundance. 47
Figure 18. Representative example shows Picro serius red histochemistry staining. 48
Figure 19. Fibroblasts generated from human breast tumours 50
Figure 21. Concentration of RNA extracted from cells in ng/µl. 53

Figure 21. False colour images of the mapped region. 58
Figure 22. CD3 antibody optimisation. 81
Figure 23. CD4 antibody optimisation. 82
Figure 24. CD8 antibody optimisation. 83
Figure 25. CD20 antibody optimisation. 84
Figure 26. CD68 antibody optimisation. 85
Figure 27. α-SMA antibody optimisation. 86
Figure 28. Foxp3 antibody optimisation..... 87
Figure 29. Representative example shows the localization of CD3+, CD4+, CD8+, CD20+, CD68+, Foxp3+ and αSMA in one case triple negative breast cancer..... 90
Figure 30. Representative example shows the localization of CD3+, CD4+, CD8+, CD20+, CD68+, Foxp3+ and αSMA in one case of ER+ breast cancer. 91
Figure 31. Example of box generation on a single sample..... 92
Figure 32. Greater significance detection by positive pixel analysis with 30 boxes compared with 20 or 10..... 93
Figure 33. ER alpha expression by qrt-PCR analysis in MCF-7, MDA-MB 231, LS12-041 and TBCI samples..... 99
Figure 34. Immunofluorescent analysis of MCF-7 (+ve and –ve control), MDA-MB231 and CAFs using ERα antibody. 100
Figure 35. Raman map showing the intensity of the Raman shift at different points for triple positive and triple negative breast cancer tissue on stainless slides. 101
Figure 36. The effect of conditioned medium on MCF-7 cell growth. 102
Figure 37. The effect of conditioned medium on MDA-MB-231 cell growth..... 103
Figure 38. The effect of conditioned medium on cell growth of CAFs derived from ER+ BC patients..... 104
Figure 39. The effect of pirfenidone on MCF-7 cell growth..... 105
Figure 40. The effect of pirfenidone on MDA-MB-231 cell growth..... 106
Figure 41. The effect of pirfenidone on CAFs cell growth..... 106
Figure 42. MCF-7 cell proliferation after 5 days incubation. 106
Figure 43. Phase contrast microscopy of monocytic Thp-1 and macrophages-like cell morphology after exposure to different concentrations of PMA treatment..... 114
Figure 44. Gene expression of CD11b, CD14, CD68 and TLR-4 in macrophages-like 115

Figure 45. Representative image of gene expression including CD11b, CD14, CD68 and TLR-4 in Thp-1 cells (control), NoR, 2DR and 4DR 117
Figure 46. Cell survival rate in non-rested and resting cells macrophages post PMA removal relative to untreated Thp-1 119
Figure 47. RT-PCR analysis of gene expression in suspension cells and differentiated macrophages post PMA removal 120
Figure 48. Macrophages cell survival in single culture and co-cultured with breast cancer cells post PMA removal 122
Figure 49. Gene expression of macrophages-specific markers including CD11b, CD14, CD68 and TLR-4 124
Figure 50A. Up-regulated gene in MDA-MB-231 breast cancer cells co-cultured with macrophages represented by PCR analysis 126
Figure 50B. Up-regulated gene in MCF-7 breast cancer cells co-cultured with macrophages represented by PCR analysis 126
Figure 51A. Gene expression level in MDA-MB-231 breast cancer cells co-cultured with macrophages at different ratios..... 128
Figure 51B. Gene expression level in MCF-7 breast cancer cells co-cultured with macrophages at different ratios 129
Figure 52. Representative images of macrophages cell morphology in single culture or co-cultured with breast cancer cells 130
Figure 53. Representative image of RT-PCR analysis shows the expression levels of BIRC3, LAMC2, DKK1, PER1 and NR1D1 genes in MDA-MB-231 cells 132
Figure 54. Representative image of RT-PCR analysis shows the expression levels of BIRC3, LAMC2, DKK1, PER1 and NR1D1 genes in MCF-7 cells 133
Figure 55. Determining fibroblasts cell ratio. MCF-7 and MDA-MB-231 were incubated with fibroblasts at different ratios 137
Figure 56. Representative images of MDA-MB-231 wound healing during 12 hours 141
Figure 57. Representative images of MCF-7 wound healing during 12 hours..... 142
Figure 58. Optimization of matrix matrigel concentration 145
Figure 59. Proliferation assay of MDA-MB-231 and MCF-7 breast cancer cells in single culture as control or co-cultured with fibroblasts or macrophages or in triple culture with both fibroblasts and macrophages 147

Figure 60. RT-PCR analysis of gene expression level in Programmed (P), short term incubation (S) and control MDA-MB-231 and MCF-7 cells 155
Figure 61. Representative images of MDA-MB-231 clones wound healing during 12 hours 157
Figure 62. Representative images of MCF-7 clones wound healing during 12 hours 158
Figure 63. Cell proliferation assay of MCF-7 and MDA-MB-231 single cell clones ..... .161
Figure 64. Analysis of gene expression and RNA quality 163
Figure 65. Top 20 functional enrichment analysis of Gene Ontology (GO) and Kyoto Encyclopedia of Genes and Genomes (KEGG) pathways 165
Figure 66. Differentially gene expression and Venn diagram in MDA-MB-23 samples under different cultures..... 167
Figure 67. Gene expression pattern of the MDA-MB-231 samples represented by the heat map 168
Figure 68. Validation of genes-related cell migration in programmed (P) MDA-MB-231 and MCF-7 relative to control breast cancer cells 176
Figure 69. Validation of genes-related cell proliferation in programmed (P) MDA-MB-231 and MCF-7 relative to control breast cancer cells 178

Abbreviations List

Abbreviation	Definition
APCs	Antigen-presenting cells
BC	Breast cancer
C	Control or parental breast cancer clones
CaF2	Calcium fluoride
CAFs	Cancer associated fibroblasts
CD11b	Cluster of differentiation molecule 11B
CD14	Cluster of differentiation 14
CD20	Cluster of differentiation 20
CD3	Cluster of differentiation 3
CD4	Cluster of differentiation 4
CD68	Cluster of differentiation 68
CD8	Cluster of differentiation 8
CKs	Cytokeratins
CM	Conditioned medium
CSF-1	Colony stimulating factor 1
CTLs	Cytotoxic T lymphocytes
DAB	Diaminobenzidine
DCIS	Ductal carcinoma in situ
DIC	Ductal invasive carcinoma
DMEM	Dulbecco's modified eagle medium
DNA	Deoxyribonucleic acid
DPBS	Dulbecco’s phosphate buffered saline
ECM	Extracellular matrix
ER	Estrogen receptor
FFPE	Formalin fixed paraffin embedded
Foxp3	Forkhead Box P3
GAPDH	Glyceraldehyde 3-phosphate dehydrogenase
GO	Gene Ontology
H and E	Haematoxylin and Eosin
HER-2	Human epidermal growth factor receptor 2
IF	Immunofluorescence
IHC	Immunohistochemistry
IL	Interleukin

KEGG	Kyoto encyclopedia of genes and genomes
L	Long term incubated breast cancer clones
M1	Macrophages 1
M2	Macrophages 2
MCF-7	Michigan cancer foundation-7
MDA-MB-231	Breast cancer cell line derived at M.D. Anderson
MHC	Major histocompatibility complex
NF	Normal fibroblasts
NGS	Next generation sequencing
OCR	Oxygen consumption rate
P	Programmed breast cancer clones
PBS	Phosphate-buffered saline
PFD	Pirfenidone
PMA	Phorbol 12-myristate 13-acetate
PPC	Positive pixel count
PR	Progesterone receptor
RNA	Ribonucleic acid
RT-PCR	Reverse transcription-polymerase chain reaction
S	Short term incubated breast cancer clones
TBS	Tris buffered saline
TGF- β	Transforming growth factor beta
Th1	T helper 1 cells
Th2	T helper 2 cells
Thp-1	Human Monocytic cell line
TILs	Tumour infiltrating lymphocytes
TLRs	Toll-like receptors
TNBC	Triple Negative Breast Cancer
T-reg	T regulatory cells
X	Times

Chapter 1

Introduction

Introduction

1.1 Overview of breast cancer

Breast cancer is a heterogeneous disease that comprises several biological characteristics and most commonly diagnosed malignant disease in women worldwide [1, 2]. Immunohistochemistry studies and gene expression profile have revealed the different biological features of breast cancer such as hormone receptor status, histological grade, tumour size and lymph node involvement of breast cancer that exhibit distinct behaviours including cell proliferation, response to therapy and distant metastasis. This has led to a variety of treatment options and therapeutic strategies [3]. Breast cancer has been divided into two types; breast carcinoma *in situ* and infiltrated. Both *in situ* and infiltrated tumours arise from epithelial cells. The *in situ* carcinomas are pre-invasive tumours which has not spread beyond basement membrane, but when these carcinomas extend beyond basement membrane to the nearby breast tissues then they are referred to as infiltrated breast cancers [4]. According to the gene expression investigations, breast cancers have been characterised into various subtypes that lead to different treatment modalities and clinical outcome: luminal A/B group or oestrogen receptor positive (ER+) are characterised by the relatively over expression of oestrogen receptor in tumour cells and luminal cytokeratins and other luminal epithelial associated markers [5]. Human epidermal growth factor 2 (HER-2) is characterised by over expression of HER-2 gene and other genes associated HER-2 pathway that regulate cell proliferation[6]. Tumours that do not express ER+, PR+ and HER-2+ are characterised as triple negative breast cancer (TNBC). These tumours are also known as basal-like due to high expression of basal myoepithelial markers, such as CK5, CK 14, CK 17 and laminin [7, 8]. The

treatment of breast cancer is various depending on the hormone receptor expression. Patients with ER+ breast cancer are treated with hormonal therapies such as Tamoxifen which blocks oestrogen receptor leading to reduced proliferation rate [9]. HER-2 is treated with monoclonal antibodies such as Herceptin, this antibody is designed to attack and target HER2 cells to stop their growth [10]. TNBC is treated with standard chemotherapies, which are not targeted therapies, such as, Doxorubicin [11]. Current breast cancer treatments focus on targeting breast tumour cells only but there is now good evidence to suggest that targeting cells in the stroma, which support the tumour, may be appropriate. Recent studies, have shown that breast cancer initiates with epithelial cells supported by alterations in the tumour microenvironment that drives tumour development and progression [12, 13]. The tumour microenvironment of breast cancer is composed of tumour epithelial cells and stromal cells including, various inflammatory cells, endothelial cells that line blood vessels, fat cells, soluble factors, fibroblasts and extracellular matrix (ECM). These microenvironments effectively play a central role in tumour progression and growth as well as a potential therapeutic targets [14]. It has been widely believed that during tumour formation, the surrounding microenvironment gradually changes to foster tumour progression through secreting factors to support tumour growth, angiogenesis, invasiveness and facilitating cancer cell migration [15]. This PhD project will provide information on the role of the stroma in the most common type of breast cancer, invasive ductal breast cancer, potentially identifying therapeutic targets within breast stroma to develop in future studies.

1.2 Breast cancer initiation and progression

Breast cancer usually initiates from terminal duct-lobular units which are the functional units of women breast. Breast cancer can be classified into two types depending on the origin of malignancy; (i) carcinoma is breast cancer that initiates from epithelial cells that line both lobules and ducts terminals. (ii) sarcoma breast cancer which is considered as a rarer type of breast cancer that represents 1% or less of all breast cancer arising from stromal cells such as fibroblasts, myoepithelial cells and endothelial cells that form blood vessels [16-20]. Carcinoma breast cancer usually initiates from abnormal growth of epithelial cells that line lobules and ducts milk, this type of breast cancer is called ductal carcinoma *in situ* (DCIS) or pre-invasive breast cancer where malignant cells grow and proliferate that are confine within basement membrane [21, 22]. The development of breast cancer from DCIS lesion to invasive ductal carcinoma (IDC) is not well established yet, four evolutionary models have been assumed that describe the biological progression of malignant cells from DCIS to IDC. Independent lineage is the first model of breast cancer development which demonstrate that both DCIS and IDC arise and develop in a parallel independently from different cell lineages [23-25]. To better understand this, Narod *et al*. in support of this theory have stated that clusters of tumour cells are various in their behavior depending on their location and clones heterogeneity, some clusters progress aggressively that have the ability to spread concomitantly through different routes to other organs, while other clusters behave differently which do not display the ability to spread outside the membrane but proliferate and grow within breast ducts (Figure. 1) [26]. The second model of developing breast cancer from DCIS to IDC is convergent phenotype model, this model proposes that malignant cells arise with various genotype of DCIS that result in the same phenotype of IDC [27, 28]. Hernandez et al.

in support of this theory have demonstrated that DCIS and IDC may differ in their genomic profile but the similarity in their phenotype still exist (Figure. 1) [29]. Evolutionary bottleneck is the third model that assumes individual subpopulations of malignant cells within the same duct that have different genetic aberrations are capable to invade into adjacent tissues [24, 25, 28]. In support of this theory, comprehensive studies reported the similarities and differences between some DCIS and IDC in their genetic concordance indicating some DCIS share the same genetic profile with IDC (Figure. 1) [30]. The fourth model of breast cancer progression from DCIS to IDC is multiclonal invasion, this model suggests that some clones with a specific genetic aberrations have the ability to escape into adjacent tissues [30]. Single cell sequencing studies was performed by Casasent *et al*. which demonstrate that some clones displayed genetic aberration and mutations that evolve invasive properties in comparison with the others clones in the same duct, indicating not all clones have the ability to invade to adjacent tissues (Figure. 1) [24]. Based on these theories, the mechanism of breast cancer development from DCIS to IDC seems to be complex and not fully understood and more studies are required in order to better understand the mechanism underlying invasive process.

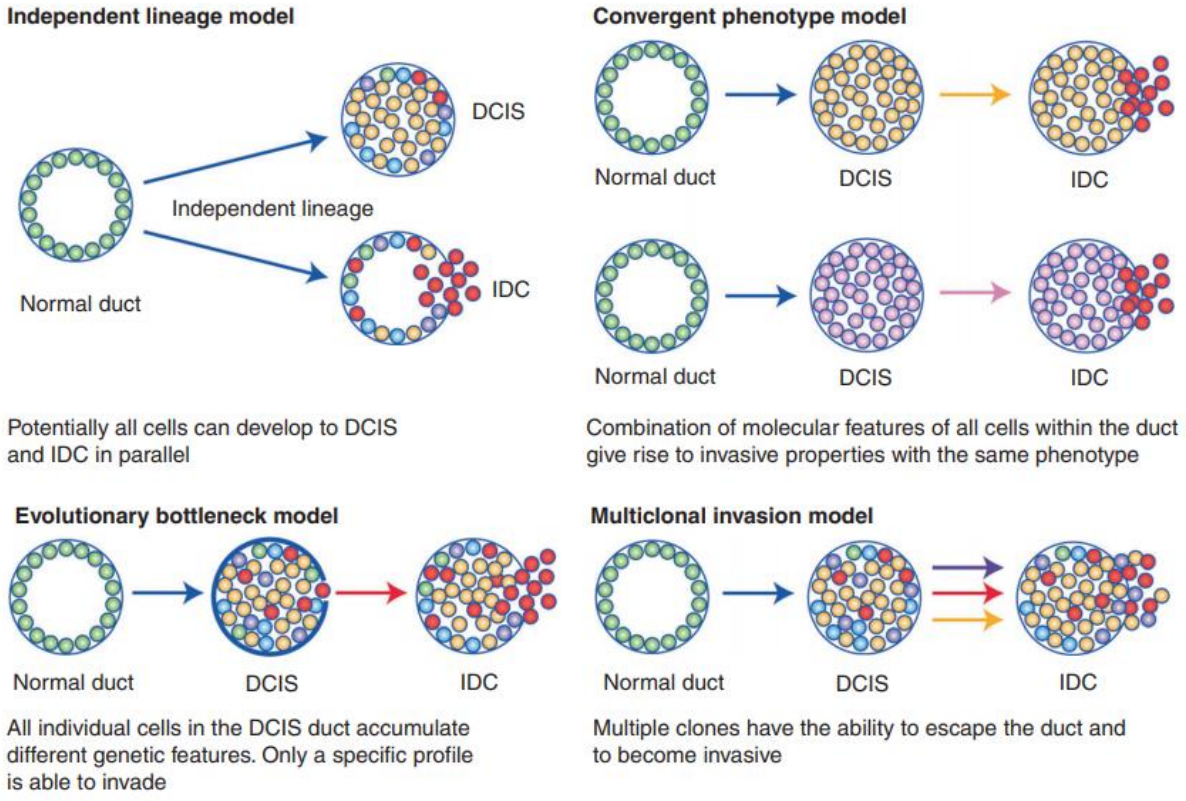

Figure 1 An overview of breast cancer initiation and development from DCIS to IDC. The four theories explain the potential progression of tumour cells evading from ducts into adjacent tissues. The figure was permitted and re-presented from van Seijen, M., Lips, E.H., Thompson, A.M. *et al.* [21].

1.3 Oestrogen receptor positive breast cancer

Oestrogen receptor positive (ER+) breast cancer, is the most frequent subtype that represents approximately 70-80% of all breast cancer molecular subtypes [31].The ER status was termed according to the postoperative therapeutic strategies, also the ER expression is the main identification marker can be used to distinguish between ER+ and ER- subtypes [32, 33]. The ER+ breast cancer is subdivided into two major subtypes: luminal A and luminal B. Luminal A breast cancer is the most common

subtype that represents 50-60% of all breast cancer. Histologically, luminal A has been characterised as a low grade tumour, with a low expression level of Ki-67 that regulates cell proliferation [34]. Clinical studies have reported that luminal A tumours have a favourable outcome in comparison to other subtypes of breast cancer [35].The remaining 15-20% of all breast cancer subtypes is represented by luminal B breast cancer. Studies have indicated that the luminal B subtype shares the same signatures with TNBC such as, the high expression of survivin gene that inhibits the cell apoptosis as well as high expression of the proliferation marker Ki-67, which distinguishes luminal A from luminal B [35]. In addition, the clinicopathological studies have reported that luminal B is more aggressive than luminal A subtype, this is due to high Ki-67 expression, high tumour grade and high expression of HER-2, leading to worse prognosis compared with luminal A breast cancer subtype [36]. In term of identifying differences in gene expression between luminal A and B, most subsequent studies have reported that luminal A shows high levels of luminal epithelial cytokeratins (CKs) genes, zinc transporter (LIV-1), forkhead box protein A1 (FOXA1), X-box binding protein 1 (XBP1) and more genes associated with ER receptor-1 (ESR1) in contrast with luminal B which shows low levels of genes mentioned above in addition to high levels of genes associated with cell proliferation such as lysosomal-associated transmembrane protein 4B (LAPTMB4), Gamma-glutamyl hydrolase (GGH) and Nuclease sensitive element binding protein 1 (NSEP1) [37-40]. Furthermore, studies were carried by Perou *et al.* to identify difference in gene expression profile of 36 invasive ductal carcinomas, these studies revealed that 1737 genes showed significant variation in their expression among different samples. These findings indicate that patients with breast cancer of the same molecular subtype are treated with different therapeutic strategies due to breast cancer heterogeneity [33].

Luminal like tumours are not homogenous groups therefore not all luminal like tumours are responsive to endocrine therapy. Luminal A tumours which are categorised with low grade tumours are more sensitive to endocrine therapy, but generally patients who are diagnosed with luminal breast cancer are treated with endocrine therapy, such as Tamoxifen to block oestrogen receptors, and aromatase inhibitors to reduce oestrogen production [41-43]. Clinical studies have reported that patients with luminal-like A have a favourable prognosis than those with luminal-like B and other breast cancer subtypes (Figure 2) [44].

Although these therapeutic strategies have been effective for ER+ patients, these strategies may interrupt the oestrogen signalling pathway, and cause effects during chemotherapies. Future therapeutic strategies are required, including an understanding of the tumour cells behaviour and the effect of the tumour microenvironment on the tumour progression. In this study we are trying to determine if any stromal cells within the tumour microenvironment contribute to the outcome.

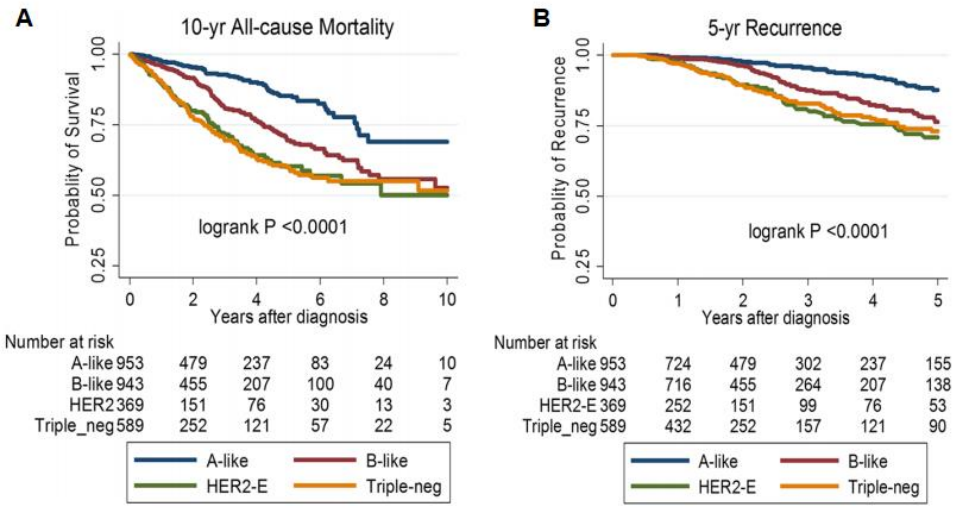

Figure 2 Kaplan-Meier curves shows the association between breast cancer subtypes including luminal A, luminal B, HER-2 and triple negative breast cancer and (A) 10 years cause mortality and (B) 5 years recurrence-free survival among 3012 women. The figure was permitted and re-presented from Abubakar M, Sung H, Bcr D, *et al* [44].

1.4 Triple negative breast cancer

Triple negative breast cancer (TNBC) is one of the breast cancer subtypes that does not express oestrogen and progesterone receptors, as well as no overexpression and amplification of HER-2 [45]. TNBC which represents about 15% of all breast cancer, has been clinically reported to be aggressive subtype due to relatively less response to treatment, rapid growth, high grade (Figure 3a), highly invasive nature, distant metastasis and most patients show poor prognosis in comparison with other subtypes of breast cancer [46]. TNBC is also known as basal-like breast cancer due to variable expression of basal cytokeratins such as CK5 (Figure 3b), CK6, CK14 and CK17 in addition to high expression of vimentin, P-cadherin and others [47-52]. Immunohistochemistry studies of 1944 cases were performed in order to determine differences in cytokeratins expression in basal-like and luminal-like tumours as well as their association with prognostic relevance. The findings revealed that luminal breast cancers express high levels of CK7, CK8, CK18 and CK19 unlike basal-like tumours which showed high levels of CK5, CK6, CK14. These cytokeratins can be used as identification markers for both breast cancer subtypes, sites of distant relapse and tumour progression [53, 54]. The progression of TNBC is not fully illustrated but many studies have found that various factors were found to be implicated in TNBC initiation and progression, BRCA1 and BRCA2 are high-penetrance breast cancer susceptibility genes known as tumour suppressor genes. Dysfunction of BRCA1 and BRCA2 genes in women leads to up to 85% chance to develop breast cancer as a result of disruption of double-strand DNA repair [55, 56]. Apoptosis resistance is one of TNBC hallmarks due to defects in TP53 expression which plays an important role in pathogenesis of cancer. Dysregulation in TP53 expression synergistically with BRCA1 abnormalities were found to drive tumour initiation and progression [57-59]. TNBC is characterised

as high proliferative tumours due to dysregulation in several genes involved in cell cycle and DNA damage, one of these genes is epidermal growth factor receptor (EGFR) which plays an essential role in promoting cell proliferation via activating MAPK kinase pathway [50, 60]. Furthermore, TNBC cells tend to have invasion and migration properties via gaining epithelial-mesenchymal transition (EMT) features which is the key step in the metastatic cascade. Several studies reported that high expression of E-cadherin, vimentin and N-cadherin was found to be frequently associated with cell adhesion and polarity [61-63].

TNBC is treated with different types of susceptible chemotherapy such as doxorubicin. Due to resistance development of tumour cell against doxorubicin drug and side effects such as cardiotoxicity [64]. Retrospective analysis suggested Cyclophosphamide Methotrexate Fluorouracil (CMF) to be effective for TNBC patients. Whereas, meta-analysis studies collected from different clinical trials have shown that doxorubicin was more effective than CMF in breast cancer patients [46]. Gene expression analysis have been performed on several targetable molecular pathways including mitogen activated protein kinase (MAPK), BRCA1, BRCA2, poly ADP-ribose polymerase 1 (PARP1) and other genes, these genes were highly mutated, these mutations are associated with the pathogenesis of TNBC [65]. Other studies have reported that p53 mutations were highly expressed in TNBC [46]. Overall, several studies are aiming to improve the treatment strategies with regards to chemotherapy. Another therapeutic targets is also being considered such as the tumour microenvironment that have been reported to be implicated in tumour prevention and formation.

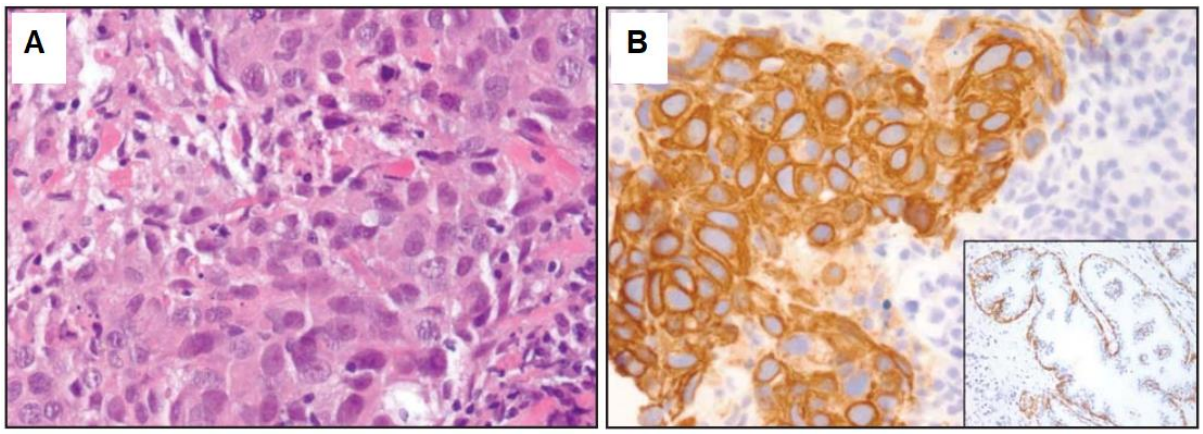

Figure 3 Representative images of invasive ductal carcinoma of TNBC subtype. **(A)** An example of hematoxylin and eosin staining (x400) which shows the grade 3 of tumour cells stained with purple colour. **(B)** Immunohistochemistry staining shows the positivity of cytokeratin 5 (CK5) expression (x400). The figure was permitted and re-presented from Ismail-Khan*, et.al [66].*

1.5 The role of tumour microenvironment cells in breast cancer

In the past few years, studies of the tumour microenvironment in breast cancer, have focused on the interaction between tumour cells and surrounding stromal cells in order to understand the signalling pathway and DNA changes [67]. The evidence has suggested, the tumour progression depends on the interaction within tumour microenvironment which may promote tumour growth, aggressiveness, invasion and metastasis [68] .More evidence shows that the interaction between tumour cells with surrounding stromal cell may actively contribute to genetic and epigenetic changes in host microenvironmental cells, this potentially leads to facilitate tumour progression. Therefore, the cross-talk between neoplastic cells and host stromal cells has attracted a lot of interest in order to understand the role of surrounding stromal cells in the microenvironment of breast cancer [69]. The tumour microenvironment of breast

cancer is composed of multiple cell types including neoplastic epithelial cells, fibroblasts, myoepithelial cells, adipocytes, endothelial cells and various immune cells as well as the extracellular matrix (ECM) and soluble factors (Figure 4) [70, 71]. The role of ECM is widely believed to be essentially involved during tumour progression. The ECM supports tumour progression by providing various chemicals such as Tenascin C and Fibronectin that are required for tumour progression and metastasis [72, 73]. In addition, matrix metalloproteinases (MMPs), which are predominantly produced by fibroblast. MMPs play a key role in tissue remodelling, chemokines activation and wound healing which participate in tumour cell proliferation and angiogenesis promotion [74]. Vascular endothelial growth factor (VEGF), growth factor produced mainly by tumour cells and inflammatory cells such as macrophages, and is a major factor that is involved during tumour progression and metastasis [75]. VEGF plays a critical role in forming new blood vessels in normal and pathological conditions. Clinicopathological assessments indicated that high expression of VEGF was positively associated with high histological grade, tumour size and lymph node positive [76]. Immune cells play a crucial role in preventing and promoting the tumour progression. For instance, the clinicopathological assessment have revealed that high expression of cytotoxic and helper T cell was associated with good prognosis [77], whereas, high expression of regulatory T cell was strongly associated with poor prognosis [78]. Cancer associated fibroblasts (CAFs) are the most abundant cells in the tumour microenvironment, that play a central role in the tumour progression and immune system suppression. CAFs are responsible for collagen synthesis which is implicated in cancer development. It has been stipulated that breast cancer density is attributed to collagen deposition [79]. CAFs also favour the microenvironment for tumour progression by secreting growth factors, such as transforming growth factor

beta (TGF-β) and IL-6 that play a key role in immune system suppression [80]. Macrophages are the important component in the tumour microenvironment, as they release factors that play an important role when defending against foreign substances including cancer. Macrophages that are infiltrated within tumour cells are called tumour associated macrophages (TAMs). TAMs function is not fully elucidated during cancer progression, but they were found to be implicated in releasing some factors that contribute to tumour progression and development. Clinical studies have reported that TAMs number correlated with poor prognosis in breast, prostate, bladder and ovarian cancers [81]. Although the role of tumour microenvironment in tumour development and progression has been reported in several studies, there is still a need for further investigations to identifying the role of each cell type in stroma component in breast cancer microenvironment and their effect on patients' outcomes.

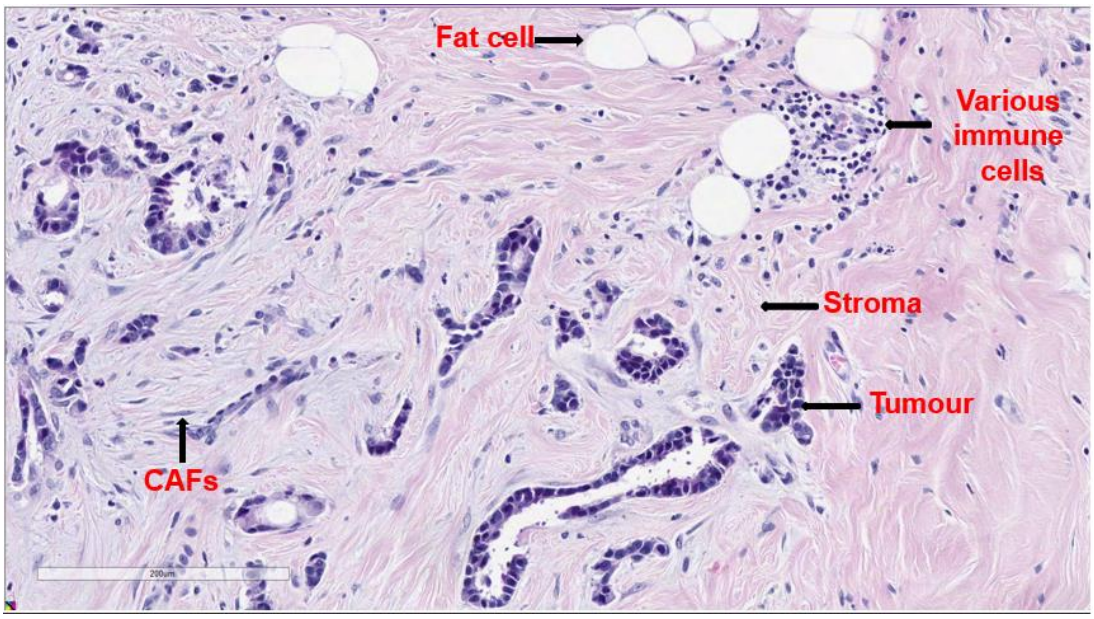

Figure 4 The tumour microenvironment of invasive ductal breast cancer. The tumour microenvironment is composed of several cell types including malignant cells surrounded by stroma tissue which comprises from various immune cells, cancer associated fibroblasts (CAFs) and fat cells as well as extracellular matrix and other soluble factors.

1.6 Immune system and breast cancer

The relationship between immune system and breast cancer is believed to play a pivotal role during cancer progression through a variety of mechanisms, in which they eliminate malignant cells or promote tumour growth and invasion into metastatic sites [82]. The immune infiltration in breast cancer microenvironment is composed of different cells including, T lymphocytes (CD8+ and CD4+), B lymphocytes, macrophages, natural killer cells, dendritic cells and others [83, 84]. The interaction between immune cells and tumour cells is dynamic and complex due to tumors cells heterogeneity and the distribution of immune cells in the breast cancer microenvironment.

In the first stage of cancer initiation, immune cells successfully eliminate malignant cells depending on antigen recognition that triggers immune response. In case the tumour has not been completely eliminated and due to breast cancer heterogeneity, transformed cells start to proliferate and escape immune-surveillance leading to tumour progression and metastasis [85].

The mechanism in which transformed cells capable to manipulate immune cells activity is not fully understood, however, extensive studies have reported that high levels of tumour-secreted factors such as VEGF, IL-6, M-CSF, IL-10 TGF-β were positively associated with increased numbers of regulatory T-cells and negatively with antigen-presenting cell functions [86]. In addition, alterations in HLA-I expression in tumour cells could negatively impede cytotoxic T lymphocyte activation and antigen recognition [87].

Furthermore, alterations in T lymphocytes signaling such as low expression of CD3 which work as co-stimulatory receptor were associated with highly proliferative

tumours and T cell exhaustion [88]. These findings have contributed in developing immunotherapy models which target not only primary tumours but also metastatic and recurrent tumors [89-91]. Programmed cell death-1 (PD-1) and programmed cell death ligand-1 pathway play an essential role in immune system inhibition and high expression of PDL-1 on tumour cells was associated with unfavorable prognosis in breast cancer [92-94].

In addition, the blockade of PD-1 and PDL-1 pathway by monoclonal antibodies such as nivolumab and pembrolizumab disrupted the negative cellular signals that regulate T cell proliferation and immune cells activation [95] as shown in figure (5). It was reported that TNBC patients have higher levels of tumour infiltrating lymphocytes and PDL-1 proteins compared with ER+ patients due to low PDL-1 expression was detected in ER+ samples [96, 97]. However, recent studies have reported that TNBC patients who received pembrolizumab in combination with neoadjuvant chemotherapy has shown a better prognosis, indicating that immunotherapy has shown a promising therapy for TNBC breast cancer [98]. More studies are still required in order to develop immunotherapeutic strategies in breast cancer and their association with patient survival outcome.

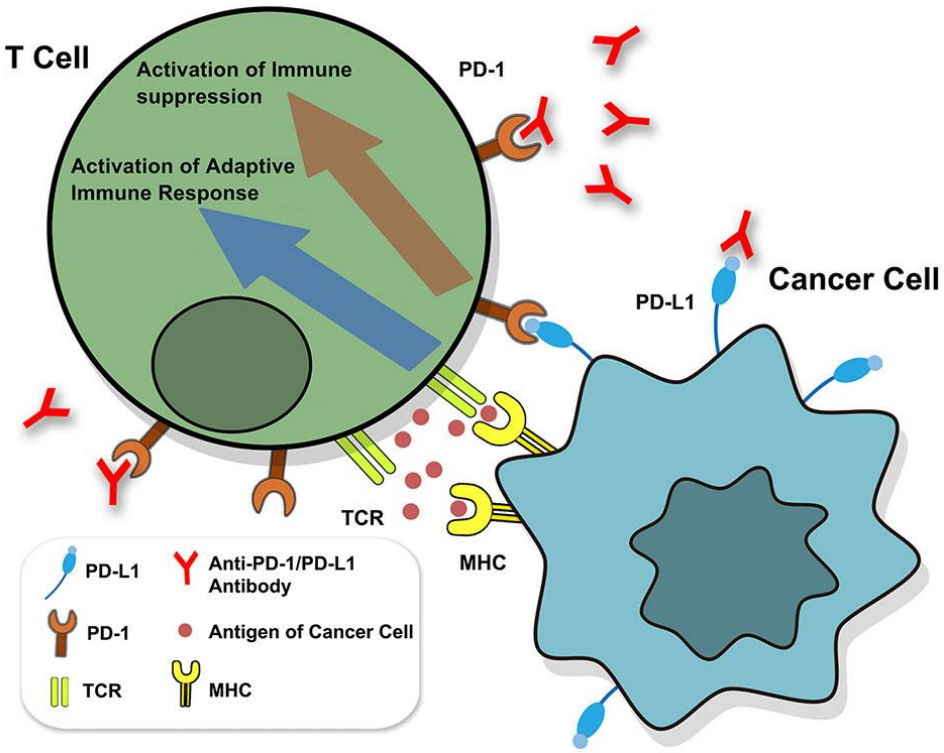

Figure 5 The cross-talk between T cell and tumour cells through PD-1 and PDL-1 pathway which inhibits immune response via preventing the signaling transduction of T lymphocyte. The use of monoclonal antibody has abrogated this pathway which therefore promoted immune cell response against tumour cells. The figure was permitted and presented from *Zhang, Jian-ye et.al* [99]

1.7 The role of cytotoxic T lymphocytes in breast cancer

T cells is the major component of adaptive immunity that represent the second essential cell type in immune system after macrophages [100]. Cytotoxic T lymphocytes cells (CTLs), are a T cell subset that expresses CD8 co-receptor as well as the T cell receptors that recognise foreign antigens presented by major histocompatibility class I molecule (MHC I). During the early stage of cancer, naiive T cells enter the tumour microenvironment to gain their differentiation and activation in response to immunogenic intigenes produced by affected cells. Histopathological

studies have reported that cytotoxic T cells accumulate the tumour edge as well infiltrate within tumour cells in order to participate in eliminating immunogenic tumour cells [101, 102]. Activated CD8+ T cells are directed for killing infected, tumour and damaged cells through three mechanisms, by secreting IFN-γ and TNF-α, releasing cytotoxic granules such as perforin and granzymes and via FAS/FASL pathway**.** Therefore, they are characterised as killer T cells [103].

The presence of CD8+ T cells at the tumour margin and among tumour cells leads to eliminating the tumour as CD8+ cell display their antitumoural function when they are in direct contact with tumour cells [104]. Several studies have examined the role of CTLs in the tumour microenvironment, in order to evaluate the relationship between clinical patient outcome and the presence of CTLs in variety of tumours including pancreatic, lung and breast cancers. In general, the findings of these studies have indicated that CTLs have shown to be good prognosis indicator [105-107].

The mechanism underlying the distribution of various levels of CD8+ T cell at the tumour edge or inside the tumour core is not fully understood yet. However, the prognostic value of CTLs in TNBC breast cancer has shown various results. However, limited numbers of studies were carried out to evaluate the importance of CTLs especially in TNBC. Some studies have evidenced that CTLs density at tumour margin and intratumoural stroma was not significant relative to clinical outcome [108] Whereas, the number of infiltrated CTLs in both intratumoral and stromal regions was positively associated with a high response to chemotherapy relative to patients with low number of CTLs who have lower response rate to chemotherapy [109]. The univariate survival analysis have demonstrated that the density of CTLs positively correlated with histological grade and pathological complete response (pCR) and negatively with patient age [110, 111]

In ER+ breast cancer, several investigations were carried out to evaluate the association between CD8+ cell numbers, and survival outcome. The findings illustrated that the number of infiltrated CD8+ was negatively correlated with disease-specific survival in ER+ breast cancer patients, and positively with those who were diagnosed with TNBC breast cancers. More investigations have reported that the density of intratumoural CD8+ was positively associated with higher histological grade in TNBC breast cancer phenotype, and inversely associated with ER+ phenotype [112]. Histopathological studies conducted on different cases of ER+ and TNBC included 155 patients to evaluate the density of CD8+ cells in patients after receiving conserving surgery with anthracycline alone and/or in combination with taxane based on primary systematic therapy (PST), compared with pre-PST biopsies.

The number of intratumoural CD8+ cells has largely increased in post-PST patients relative to those who did didn't undergo PST, the mechanism underlying increased CD8+ cell number post receiving PST is not fully clear, but it could potentially relate to the chemotherapeutic agents effect which result in increased immune responses (Figure 6) [113]. Although a high level of studies have been conducted on the role of CTLs in breast cancers, further studies are required to identify the utility of CTLs in the tumour microenvironment and their effect on patient survival regarding ER-positive and TNBC breast cancers.

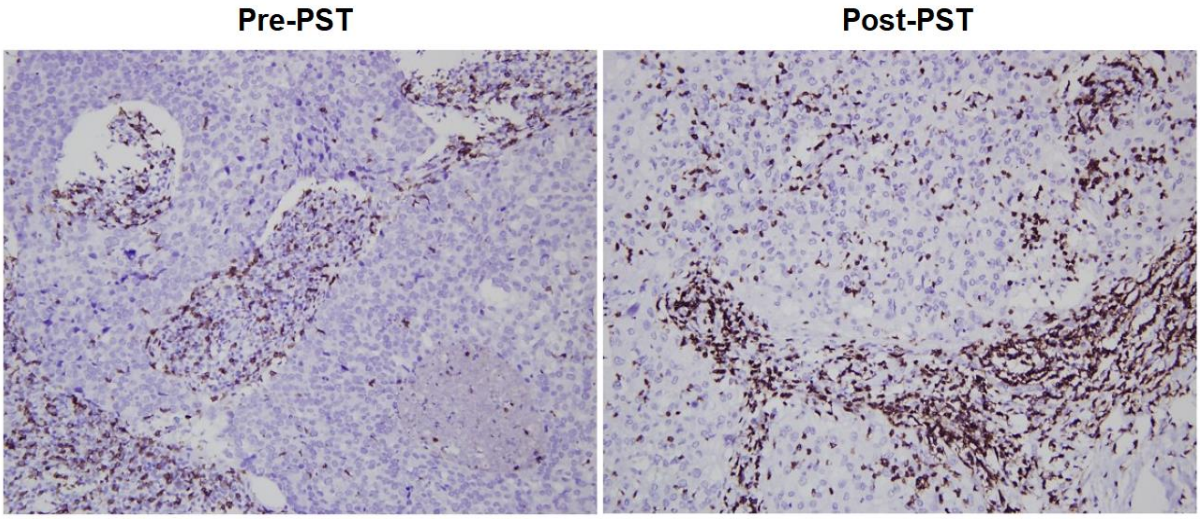

Figure 6 Representative images showing the difference in density of cytotoxic T lymphocytes in patients before and after received primary systematic therapy. The figure was permitted and re-presented from Ahn S, *et. al* [113].

1.8 The role of T helper cell in breast cancer

T helper cells are an important contributor in tumour progression that play a central role in suppressing and stimulating adaptive immune response, through activating other inflammatory cells including, macrophages and cytotoxic T cells to target foreign antigens such as tumour cells [114]. T helper cells express CD4 receptor, which is found on the surface of the cell. CD4 receptor helps the cells to recognise MHC class II molecule, found on antigen presenting cells. Once the CD4 T helper cell binds to MHC II, the cell starts secreting cytokines to stimulate the adaptive immune response. T helper cells functionally polarise into T helper 1 (Th1) and T helper 2 (Th2).

The Th1 cell is responsible for promoting antitumour immunity by producing different cytokines such as interferon-gamma (IFN-γ) interleukin 2 (IL-2) and tumour necrosis factor beta (TNF-β) which have been shown to play a pivotal role in activating adaptive and innate immunity. In contrast, the Th2 cell is involved in immunosuppression

mechanism by secreting IL-3, 4, 5, 6, 8, 9, 10 and IL-13 that play a key role in the activation and inhibition of the immune system [114, 115]. Although the role of the T helper cells in breast cancer is still not fully understood, evidence from clinical outcomes has shown different functions of Th1 and Th2 phenotypes. It has been found that the Th1 cell is associated with favourable prognosis. While, Th2 has been found to be implicated in promoting an anti-inflammatory response, as well as it could dysfunction CTLs through IL-10 production [116, 117].

Immunohistochemistry studies were conducted, to evaluate the association between CD4+ T cell and clinical outcomes. These studies showed high levels of intratumoral and stromal CD4+ T cells was significantly associated with better overall survival in TNBC breast cancer patients [118]. Other studies have shown the opposite role of infiltrating CD4+ T cell. The findings indicated that the number of intratumoral CD4+ T cell was positively correlated with tumour size, high histologic stages and inversely with relapse-free survival (RFS) of breast cancer patients [119]. Another studies of immunohistochemistry showed the correlation between CD4 T cell density and patient's survival outcome, these studies indicated that high CD4 T cell density was negatively associated with overall survival (OS) and lymph node status [120]. Clinicohistological analysis were conducted to evaluate the prognostic impact of intratumoural and stromal CD4+ on TNBC patients, high levels of intratumoural CD4+ were significantly associated with longer RFS and OS, whereas lower stromal CD4+ density were prognostically significant than those with higher stromal CD4+ levels (Figure 7)[121]. These contradictions in the role of CD4+ T cell in the tumour microenvironment of breast cancer, indicate that CD4+ T cell role may alter, this promoting tumour progression rather than tumour surveillance. Therefore, more

investigations need to be done in order to evaluate the role of T helper subset in the tumour microenvironment of breast cancer subtypes.

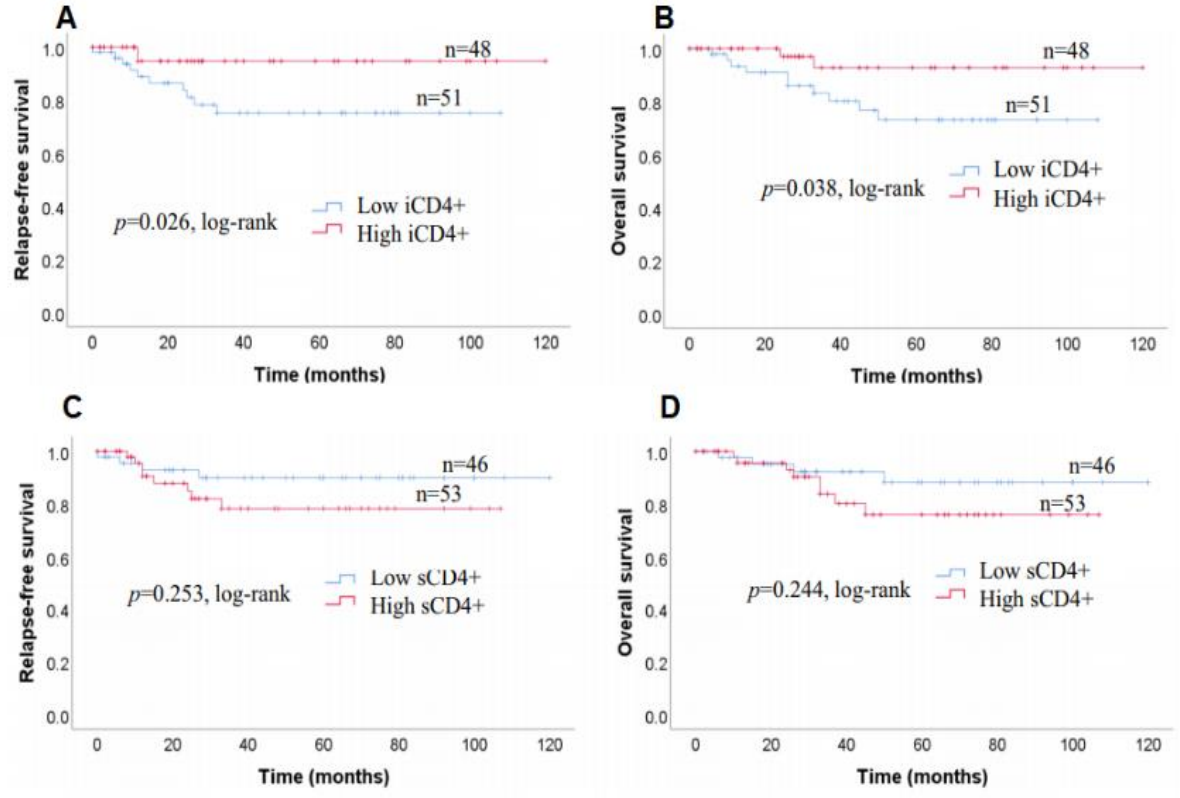

Figure 7 Kaplan–Meier curves of RFS and OR in TNBC patients, **(A,B)** curves show the prognostic value of high intratumoural CD4+ levels whereas patients with higher stromal CD4+ levels **(C,D)** where associated with poorer prognosis. The figure was permitted and re-presented from Jamiyan, T., Kuroda, H., Yamaguchi, R. *et al [122].*

1.9 The role of regulatory T cell in breast cancer

Regulatory T cells are known (Treg), play a crucial role in regulating or suppressing the immune response. Although the mechanism suppression role of Treg cells is not fully understood, many studies have reported that Treg cells are implicated in suppressing adaptive immune cells such as CD4+, and CD8+ T cell, and monocytes including macrophages and dendritic cells (DCs) [120].

In the early stages of the tumour progression, the presence of Treg cells in the tumour microenvironment, has an effective role in the immunological response through maintaining of immune homeostasis and self-tolerance. After interaction and chronic stimulation with tumour cells, Treg cells might contribute to tumour development, rather than inhibiting and suppressing the tumour progression. Treg cell expresses Foxp3 molecule which is a specific marker for Treg cell, and its immunosuppressive function [123]. The immunosuppressive mechanisms of Treg cell have been described in numerous studies, high expression of cytotoxic T-lymphocyte-associated protein 4 (CTLA-4) on Treg cell, which binds to CD80-CD86 molecules on APCs, resulting in reducing APCs activity [124]. Another mechanism of suppressive Treg cell, Treg cell produces numerous cytokines such as IL-10 and TGF-β. These cytokines play a central role in suppressing immune cells response and reducing granzyme/perforin expression on CTLs which weaken their killing activity against tumour cells [125]. On the other hand, the production of IL-10 and TGF-β play a crucial role in naïve T cell differentiation during an immune response, as well as they inhibit T and B cell proliferation and macrophages activity [126].

Although the clinicopathological and prognostic value of Treg cells in breast cancer has not yet been well elucidated and is controversial, limited meta-analysis studies have summarised the role of Treg cells in breast cancer subsets to show the importance of Treg cells in the breast tumour microenvironment. Several studies have indicated that high densities of Treg cells were significantly associated with improved overall-survival (OS) and recurrence free survival (RFS) in TNBC breast cancers [127-129]. Contrarily, another investigations have indicated that high expression of a tumour infiltrating Foxp3 cells was correlated with high histological grade and poor prognosis in oestrogen receptor-positive breast cancer [123, 130].

However, the univariate analysis have reported that high expression of Foxp3 was negatively correlated with OS and progression free survival (PFS) in both ER+ and ER- breast cancer subtypes (Figure 8) [123, 131, 132]. Although few studies have shown the effective role of Treg cells in the breast tumour microenvironment, more investigations need to be done to determine if Treg cells expression has a significant impact on the survival outcome in ER+ and TNBC breast cancer.

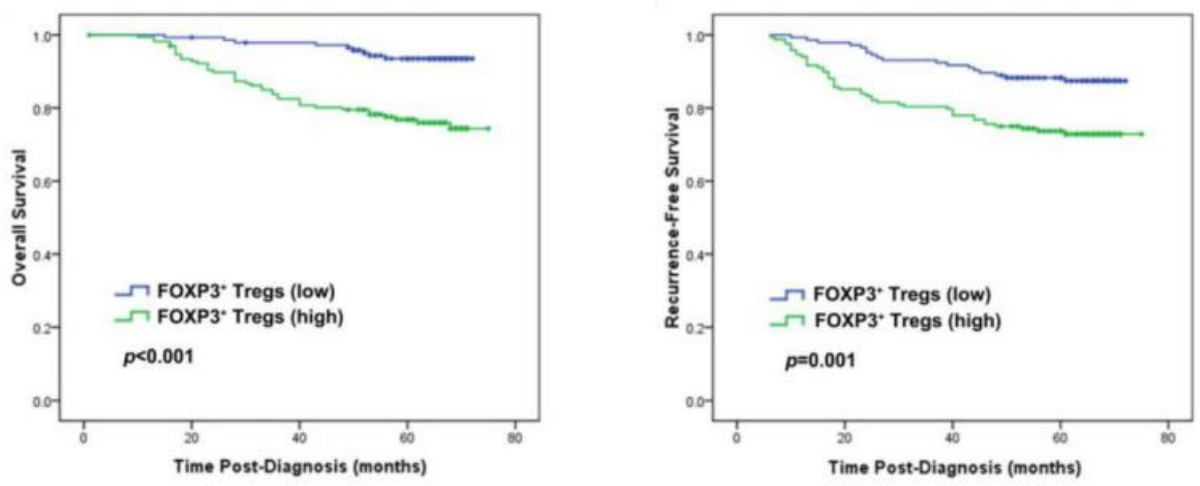

Figure 8 Kaplan–Meier analysis show the prognostic value of infiltrated regulatory Treg cells in breast cancer. High levels of FOXP3 was associated with unfavoural prognosis in both luminal and basal-like breast cancer subtypes. The figure was permitted and re-presented from Zhenhua Li, Pengzhi Dong, Meijing Ren *el al [133].*

1.10 B Cells and the breast tumour microenvironment

The tumour microenvironment contains various populations of B cell that functionally contribute to both pro-inflammatory as well as anti-immune response. The presence of B-cells infiltrated in the tumour microenvironment has been thought to play role in the tumour progression. B cells represent the predominant lymphocytic population, which represents approximately 20% of invasive breast carcinomas and 60% of

tumour associated lymphocyte in the breast tumour microenvironment [134, 135]. It has been suggested that the B cells role in the tumour microenvironment extends beyond eliciting humoral immune responses. By secreting antibodies and various cytokines, B cells recognise antigens and modulate T cell activation, as well as regulating antigen processing and presentation. The negative role of B lymphocytes in the tumour microenvironment has also been taken in consideration, B lymphocytes can promote tumour progression through lymphotoxin secretion that induces angiogenesis (Figure 9) [136]. It has been reported that B lymphocyte is implicated in T cells suppression by secreting interleukin 10 (IL-10) and TGF-β that polarise CD4 cell into regularity T cell (Foxp3) that plays a big role immune system suppression (Figure 9) [137]. Contrarily, B lymphocytes play an important role in the tumour microenvironment, B cells produce antibodies against tumour antigens. B cells secrete Immunoglobulin G (IgG) that binds to β-actin and ganglioside GD3 tumour antigens leading to immune system recognition (Figure 9). In addition, another studies have indicated that B cell is involved in tumour elimination by cell to cell contact through FAS/FASL mechanism or through CXCL-12 pathway (Figure 9) [138].

The clinicopathological studies have suggested the association between B lymphocytes and patient's survival, the presence of B lymphocytes in the tumour microenvironment was positively associated with breast cancer survival and longer free disease and a predictive for pathologic complete response (pCR) [138]. Whereas other studies of 134 breast cancer cases have reported that high numbers of B lymphocytes were positively correlated with high tumour grade, lymph node positive and ER/PR negativity indicating to a bad prognosis of B cells in the breast tumour microenvironment [138].

Although elevated populations of activated B-cells are seen in tumour progression, the pathological impact of these cells in the tumour microenvironment has not been well understood. It remains to be described if the role of tumour infiltrated B lymphocytes impacts the prognosis of breast cancer patients with specific subtypes.

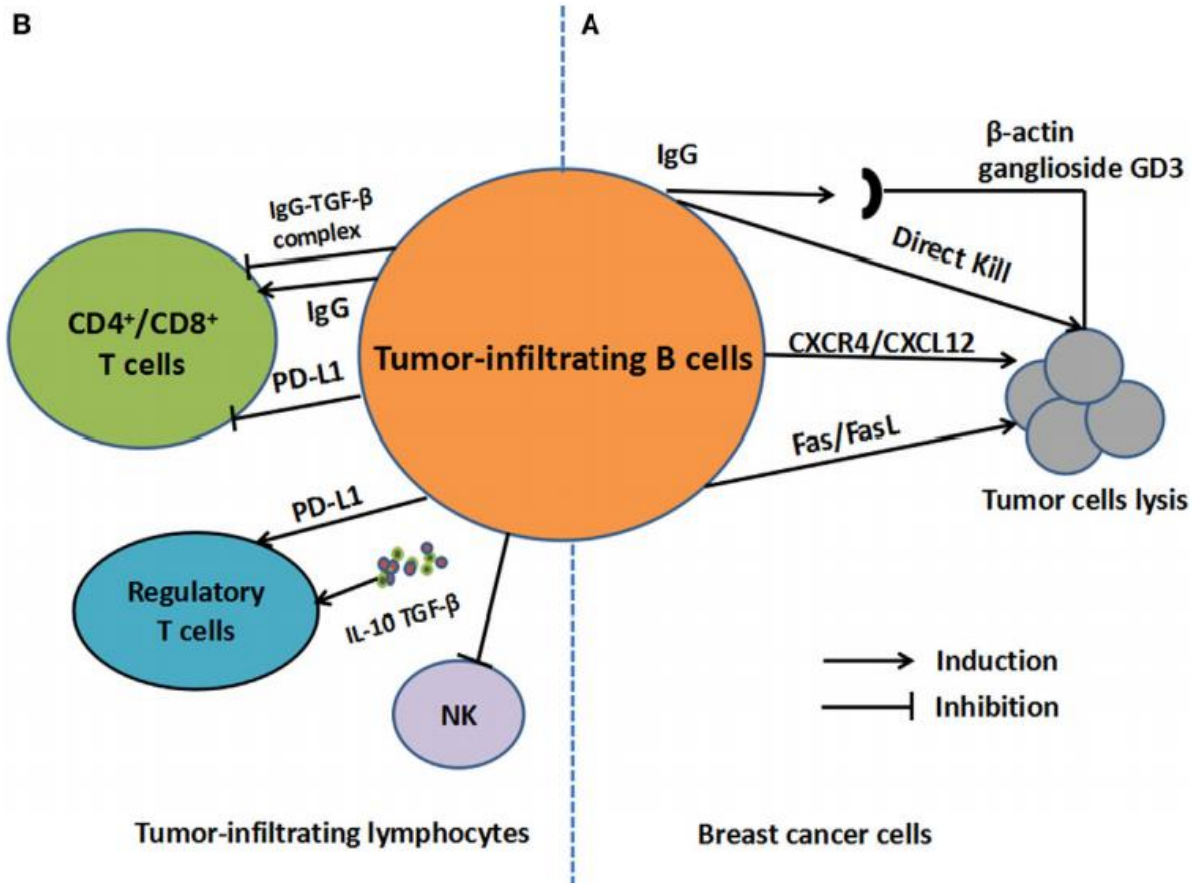

Figure 9 The immunological function of B lymphocytes in breast cancer. (A) B lymphocytes eliminate tumour cells via cell-cell contact through several pathways including CXCR4/CXCL12 and FAS/FASL and through antigens presented via tumour cells. (B) B lymphocytes involvement in regulating other lymphocytes cells including CD4+, CD8+ and FOXP3. The figure was permitted and re-presented from Meng Shen, Jian Wang, Xiubao Ren *et al [139].*

1.11 Tumour associated macrophages

Macrophages are one of the major group of immune cells that play a significant role in defence against abnormal substances in the tumour microenvironment of many solid tumours including breast cancer [140] Macrophages originate as progenitor cells from the bone morrow then develop into monocytes, which migrate under the influence of monocyte chemotactic protein CCL2 toward damaged or inflamed tissue where they differentiate into tissue macrophages [141]. Macrophages recruitment and their infiltration within tumour cells depends on cytokines and chemokines secreted by malignant cells, fibroblasts and various immune cells [142]. It was reported that CCL2 expression was found to be positively associated with macrophages abundance within tumour nest and angiogenesis [143].

Macrophages can further differentiate into 2 distinct functional phenotypes as a reaction to specific microenvironmental stimuli and signals, this process is known as macrophages polarisation [144]. Macrophages exposure to LPS, IFN-γ and GM-CSF, macrophages polarise into classical macrophages 1 (M1). While macrophages exposure to monocyte chemoattractant protein 1 (MCP1) secreted by tumour epithelial cells, which recruits macrophages into activated M2 in order to facilitate tumour progression [145]. In addition, Th2 produce anti-inflammatory cytokines IL-10, IL-4 and TGF-β as well as macrophage colony-stimulating factor (M-CFS) which is highly secreted by tumour epithelial cells are involved in differentiating macrophages toward M2 phenotype [146]. Macrophages that infiltrate within tumour cells are called tumour associated macrophages (TAMs).

M1 macrophages possess anti-tumour and pro-inflammatory characteristic through releasing chemical molecules such as IFN-γ and IL-12 whereas, TAMs macrophages

display immune suppression characteristic, tissue damage, support tumour growth and metastasis by producing TGF-β and IL-10 and others [147]. TAMs have been reported to promote tumour progression by providing a favourable microenvironment for tumour angiogenesis, tumour survival, tumour growth and metastasis. [148]. CD68 is a glycoprotein expressed on classical M1 and activated M2 macrophages and useful tool to evaluate their role in the tumour progression. In contrast, CD163 is expressed by activated M2 macrophages which has been reported to promote tumour progression via secreting several chemokines that play a crucial role in promoting tumour growth and progression [149-151]. In the breast tumour microenvironment, studies conducted by Adrian Harris group, which have found that a high level of CD68 cells was associated with increased nodal metastasis and vascularity as well as decreased overall survival and recurrence free [152, 153]. More studies have reported that TAMs density was negatively correlated with unfavourable outcome in TNBC patients [146, 154]. Another study has been carried out by Jin *et al*, they indicated that IL-1β which is secreted by CD68+ cells is associated with aggressive breast cancer [153]. High levels of infiltration TAMs in tumour microenvironment was an indicator of poor DFS, OS, high histological grade and overexpression of the proliferation index Ki-67 in hormone receptor positive and TNBC patients [155, 156]. Furthermore, studies from Yale university indicated that high expressions of CD68 were not significantly prognostic in both ER+ and TNBC samples, while high levels of CD163 were significantly associated with favourable OS in TNBC but not in ER+ (Figure 10) [157]. Although several studies have reported that TAMs favour the microenvironment and serve the need of the tumour proliferation and invasion instead of exhibiting anti-tumour function, further studies need to be conducted to understand

the cross-talk between TAMs and neoplastic cells to translate the emerging role of TAMs as a new therapeutic target for breast cancers.

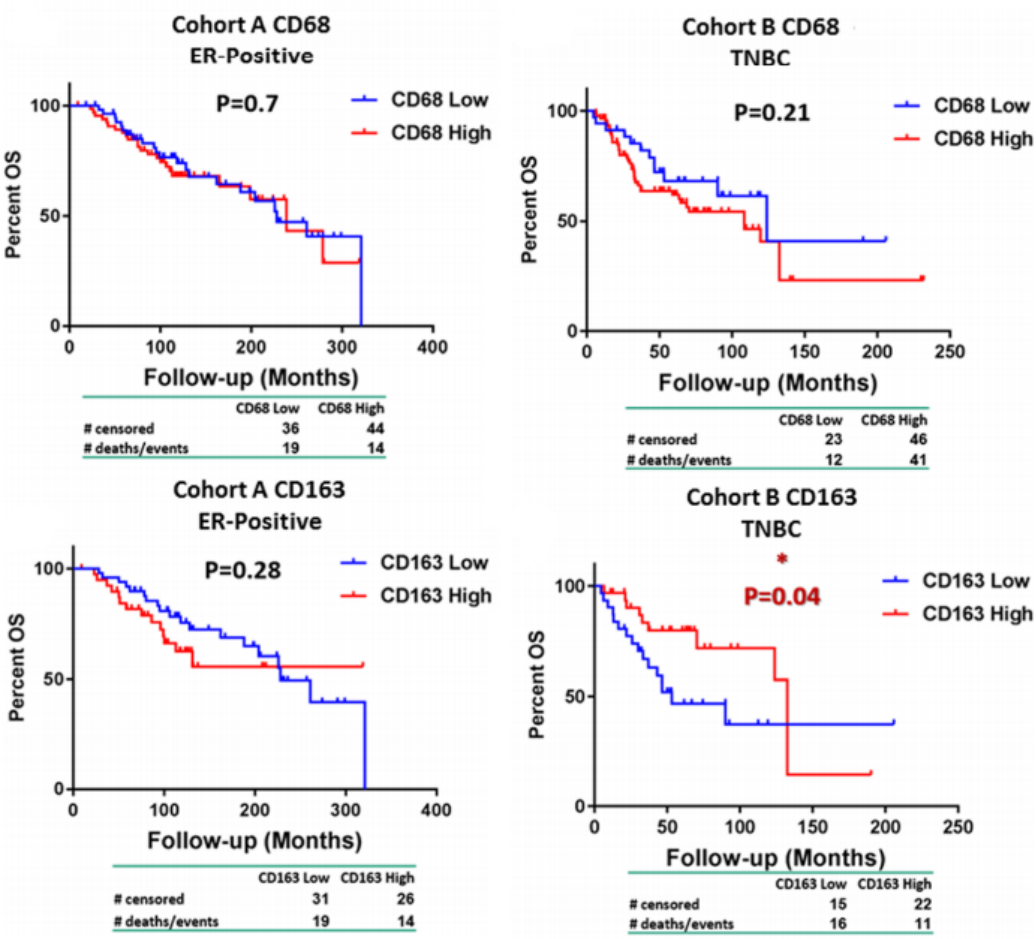

Figure 10 Survival analysis of CD68 and CD163 expression in ER+ and TNBC breast cancer cohorts. The expression of CD68 did not show significant changes in both ER+ and TNBC samples. CD163 was significantly prognostic in TNBC but not in ER+. The figure was permitted and re-presented from Pelekanou, V., Villarroel-Espindola, F., Schalper. *et al [157].*

1.12 The role of cancer associated fibroblasts in breast cancer

The tumour microenvironment of breast cancer is a multicellular system composed from different types of cells that interact directly or indirectly with tumour cells contributing to either tumour elimination or tumour promotion [158]. Recently, the tumour microenvironment has been given an intense interest to study the biological

function of stromal cells and their contribution to tumour progression [159]. Breast cancer microenvironment is composed of variety of cell types including fibroblasts, macrophages, immune cells, endothelial cells, extracellular matrix and others, fibroblasts are one of the major contributor in tumour development and the abundant cell type in stroma composition [160, 161]. Although the heterogeneity of fibroblasts and lack of specific markers as well as their origin, several studies have recently referred to the importance of fibroblasts in tumour progression in their role in regulating and shaping anti-tumour immune response [161, 162]. Quiescent fibroblasts become activated during wound healing response, and as activated fibroblasts are involved in tumour wound that never heal therefor they are called cancer associated fibroblasts (CAFs). Fibroblasts activation depends on several factors that contribute to their activation such as oxidative stress, local hypoxia and growth factors including PDGF, TGF-β, EGF and others secreted by surrounding tumour cells and other immune cells [163, 164]. The biological and morphological properties of CAFs differ from normal fibroblasts. Generally, normal fibroblasts are embedded in extra cellular matrix to facilitate wound healing during injury. In process of cancer, quiescent fibroblasts become activated known as CAFs to be involved in tumour development and fibrosis [161, 162]. In comparison with normal fibroblasts, CAFs display larger nuclei with a branched cytoplasm, CAFs proliferate and migrate faster than normal fibroblasts as well as CAFs are metabolically more active than normal fibroblasts. In breast cancer, Alpha-Smooth muscle actin (α-SMA) and the fibroblasts activating protein (FAP) are specific markers to identify CAFs in tissue specimens [165]. In breast cancer, CAFs contribute to tumour initiation, migration and potential invasion via secreting soluble mediators (i.e. growth factors and cytokines). In addition, Suda and collaborators demonstrated that 17-β estradiol (E2) production from aromatase in postmenopausal

women could be attributed to stromal CAFs activity [166]. Furthermore, the rapid proliferation and migration of tumour cells require an ideal platform in order to cope a local hypoxia and metabolic demands, CAFs play an essential role to facilitate angiogenesis process via secreting variety of growth factors, cytokines and Vascular Endothelial Growth Factor (VEGF) that mediate new blood vessels forming [167]. In addition, CAFs play a big role in modulating immune response and circumventing anti-tumour defense via secreting variety of chemokines and inflammatory cytokines that mediate immune response, these mediators include SDF-1, IL-10, IL-8, IL-6, CXCL1, TGF-β1, VEGFs, CCL2 and indoleamine-2,3-dioxygenase (IDO) [168]. Moreover, breast CAFs contribute to macrophages polorisation toward M2 phenotype which mediate immune-suppressive response through enhanced TGF-β secretion, also big amount of collagen deposition by CAFs may contribute to form a rigid and thick ECM generating a physical barrier which may restrain immune cells establishment and infiltration [169]. Further studies have found that CAFs contribute to therapeutic resistance in ER+ breast cancer subtype. These studies have identified two types of CAFs based on positive and negative CD146 expression, CD146-positive was associated with tamoxifen sensitivity, whereas the negative expression of CD146 contribute to consequently resistance to tamoxifen. In addition, a continuous growth factors secretion from CAFs leads to proliferative/survival pathways activation reducing in anti-oestrogen sensitivity [170, 171]. Meta-analysis studies were conducted to evaluate the prognostic value of CAFs in breast cancer, these studies revealed that high densities of activated fibroblasts in breast tumour microenvironment were positively correlated with OS and DFS. In luminal breast cancer, CAFs enhance apoptosis and resistance to therapy via favoring MCL-1 expression which shapes BCL-2 dependency in tumour cells [172]. In TNBC breast cancer samples,

immunohistochemistry studies revealed that high densities of CAFs were positively correlated with elevated CD136 TAM expression. In stratified analysis, high expressions of both CAFs markers including α-SMA and fibroblasts activated protein (FAP) were found to be negatively associated with OS and DSS and positively with high histological grade and lymph node involvement (Figure 11)[173] . Further studies of CAFs biological role are still required as CAFs could be a potential therapeutic and prognostic target in breast cancer.

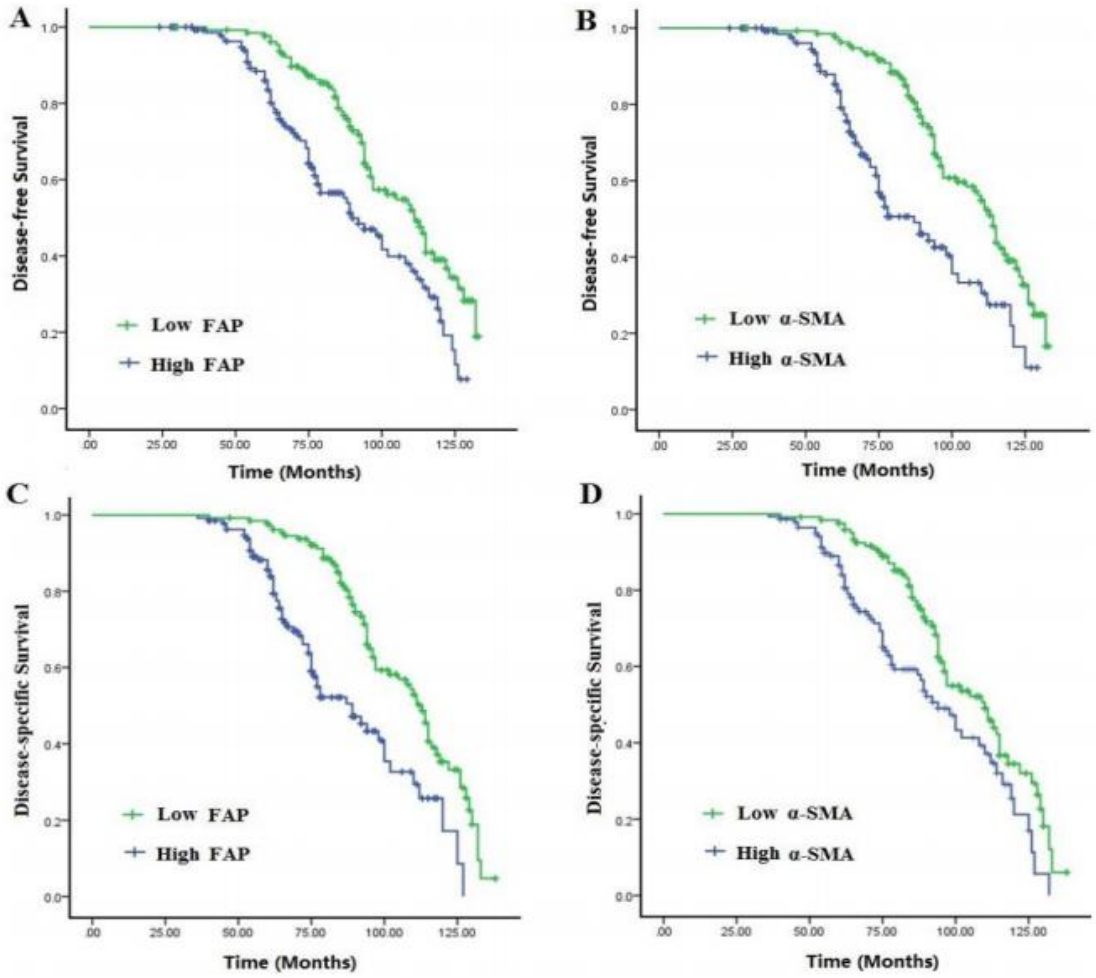

Figure 11 Kaplar-meier analysis of OS and DSS in relation with α-SMA and FAP expression in TNBC cancer patients. The figure was permitted and re-presented from Zhou J, Wang XH, Zhao YX, *et al [174].*

1.13 The relationship between tumour stroma ratio and survival outcome

The tumour microenvironment of breast is a complex tissue which is constituting not only from malignant cells but also from stromal cells. Tumour cells represent approximately 20% of total breast tumour microenvironment in most breast cancer, the remaining cell types include fibroblasts, endothelial cells, various immune cells, adipocytes and myofibroblasts, stromal cells are collectively known as tumour-associated stroma [175, 176]. In the recent decades, the role of stroma in breast cancer development and progression has become an area of interest due to its ability to promote tumour progression. More recent studies have demonstrated that breast cancer progression depends on the amount of support from stromal cells which have been repeatedly reported to play a central role in breast cancer initiation and development [177, 178].

Despite the new discoveries of an effective therapies, the tumour microenvironment has not extensively been involved in clinical decision making. The ratio of tumour stroma is the only parameter which can be used to translate the biological function of tumour associated stroma in tumour progression. The potential prognostic value of tumour stroma ratio (TSR) has been given an intention to be considered in different cancer types including breast cancer [179-182]. In breast tumour microenvironment high stroma content has been pointed toward worse prognosis in primary TNBC [183, 184], while high stroma percentage was reported to be a prognostic in ER+ breast cancer [185].

Furthermore, Kiki M H Vangangelt , Andrew R Green *et al*. demonstrated that high stroma content was negatively correlated with recurrence-free survival in both TNBC and ER+ breast cancer subtype (Figure 12) [186]. This has increased attention that

the tumour microenvironment role is dependent in ER+ and TNBC breast cancer subtypes, which displays different behaviours leading to promoting tumour initiation and progression [185].

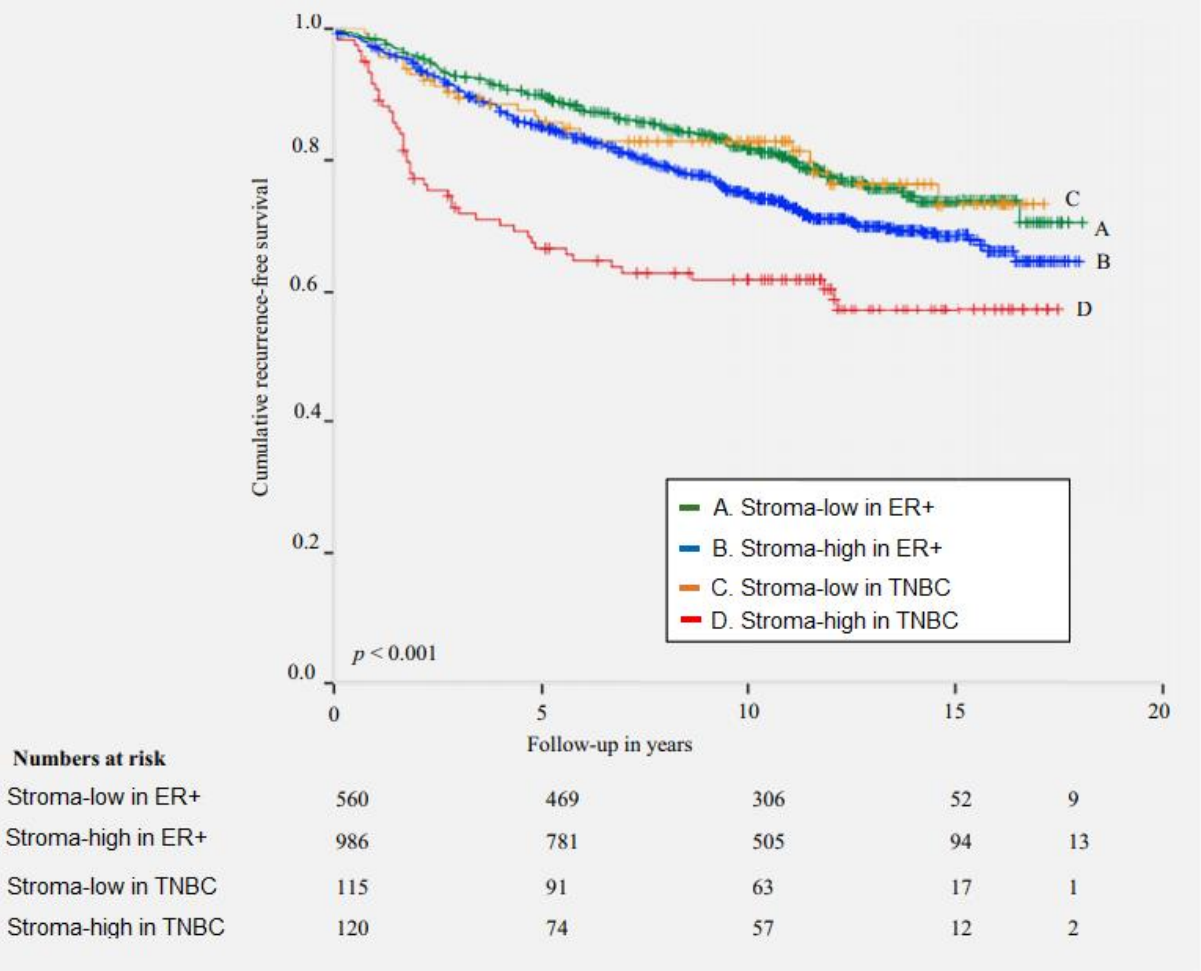

Figure 12 Kaplan-Meier analysis for recurrence-free survival of TNBC and ER+ breast cancer subtypes stratified by tumour-stroma ratio. The figure was permitted and re-presented from Vangangelt, Kiki M H *et al [187].*

1.14 Cellular reprogramming during cancer progression

In several occasions it has been reported that breast tumour microenvironment is constituted not only from malignant cells but also from non-transformed cells such as fibroblasts, macrophages, adipocytes and various immune cells. The tumour elimination or promotion is driven by a dynamic and a complex interaction between malignant cells and non-transforming cells via secreting variety of cytokines, chemokines, growth factors and matrix remodelling enzymes [188-190]. During cancer development, tumour cells acquire different molecular and morphological changes known as “cell reprogramming” as a result of the complex interaction between malignant and stromal cells. If the tumour has not been well eliminated by immune system, tumour cells will continuously gain a cellular changes which therefore result in more aggressive and resistant tumours to therapy. The biology of tumour progression can be understood not only by malignant cells itself, but also by studying other tumour microenvironment composition such as macrophages and fibroblasts using various methodologies including co-culture models. Although the findings of these studies contributed to prognostic outcomes, it is still difficult to determine the true efficiency of the biological effect of stromal cells on tumour cells due to the duration of co-culture and it’s mechanism of action [191]. Several conducted studies have used a short-term co-culture in order to evaluate the biological interaction between stromal and transformed cells. These evaluations may indicate inaccurate assessments due to the short-term (3-5 days) co-culture duration as tumour cells develop from long-term “weeks-months” communication with stromal cells [191]. In addition, studies were conducted by Dominguez-Andres J *et.al,* which demonstrate that long term exposure of innate immune cells such as macrophages, dendritic cells and natural killer cells to stimuli has genetically reprogrammed their biological function

and developing changed responses to subsequent challenges [192]. Other studies have reported that the tumour microenvironment plays a crucial role in reprogramming the immune system in order to functionally counteract the antitumour effect which therefore promote tumour progression [193]. Given these observations, we hypothesis that long-term co-culture system reprograms the cellular function not only the immune system but also tumour cells.

1.15 Cytokines mediated tumour progression

During cancer progression, malignant cells acquire several genomic abnormalities to facilitate their cellular activity including cell proliferation, cell survival, escaping immune surveillance, cell migration and metastasis to another parts of the body. Stromal cells play an important role in driving tumour progression through secreting variety of cytokines and chemokines such as TNF-*α*, IL-6, TGF-*β*, and IL-10. These cytokines and chemokines mediate several cellular activities such as immune system activation to either eliminate and reject cancer cells or to facilitate tumour progression through cell-cell communication [194]. TGB-β is a highly pleiotropic and multifunctional protein that plays an important role in immunoregulation, cancer progression, angiogenesis and other chronic diseases such as Asthma and Rheumatoid Arthritis [195-197]. In cancer progression, TGF-β is involved during the process of tumour initiation, proliferation, survival and metastasis. In the first step of tumour initiation, TGF-β works as a cyclin kinase regulator which therefore inhibits tumour growth, but most cancers including breast tumours become refractory to growth suppression due to having mutated TGB-β signaling pathway [198]. Teicher and his colleagues have reported that tumours that have high expression of TGF-β are more resistant to chemotherapeutic drugs via promoting cell arrest activity which therefore facilitate the

mechanism of DNA repair [199]. In addition, TGF-β plays a key role in accumulating and activating fibroblasts that drive fibrosis and secreting high protein levels of extra cellular protein through SMAD-SMAD independent signaling pathway, this activity was found to play an important role in tumour progression [200]. Furthermore, it was found that TGF-β involved in epithelial-mesenchymal transition through TGF-β-SMAD pathway which eventually contributes to upregulation of Snail and Slug expression that are involved in tumour invasion [201]. TNF-α is another multifunctional cytokine that plays a pivotal role in pro-inflammatory response and another cellular activity including proliferation, survival and cell death by necrosis and apoptosis [202]. TNF-α is a double-dealer cytokine during tumour progression, it promotes cancer cell proliferation, growth, invasion and angiogenesis. Conversely, it inhibits tumour cells survival through NF-κB pathway which therefore induces the mechanism of cell death known as apoptosis [203, 204]. During tumour progression, cancer cells undergo a variety of cellular changes known as “cellular reprogramming” as a result of genomic changes in order to facilitate their progression which could take weeks to months or even years from their initiation to metastasis to another parts of the body. These changes in cellular activity are driven not only by tumour cells itself, but also from micro-environment cells such as macrophages, fibroblasts, immune cells and others which have been reported to be implicated in either tumour rejection or promotion [205, 206]. Among tumour microenvironment cells, macropahges and fibroblasts play an essential role in the biology of tumour progression through secreting different chemokines and cytokines such as TGF-β and TNF-α which have been found to be involved in each step of tumour progression.

Hypothesis

This PhD project will test the hypothesis that cells involving CAFs and various immune cells within the tumour microenvironment influence breast cancer outcome and this differs in ER+ versus ER- breast cancer. In addition, this project will test the biological behaviour of cancer epithelial cells from both ER+ and TNBC subtypes will change under co-cultured with macrophages or fibroblasts using double culture model, compared with those co-cultured with macrophages and fibroblasts using our triple culture model.

Aims and objective

Aim 1: Determine if CAFs and/or inflammatory cells in breast stroma contribute to outcome in both triple negative and oestrogen receptor positive breast cancer.

Aim 2: Evaluate the interactive effects and functional role of CAFs or macrophages in double culture and/or in triple culture with MCF-7 and MDA-MB-231 breast cancer subtypes.

Aim 3: Conduct RNA-seq analysis to Identify gene expression profile in TNBC breast cancer cells after short-term and long-term co-culture with macrophages in order to evaluate whether long-term (30 days) co-culture will chronically up-down-regulate gene expression in tumour cells compared with those co-cultured with macrophages for short-term (3 days) incubation.

Aim 4: Identify genes underlying cell migration and proliferation in MDA-MB-231 and test their expression in MCF-7 cells to evaluate whether both breast cancer cells subtypes display the same/different patterns of selected genes.

Chapter 2

Materials and Methods

2.1 Immunohistochemistry

2.1.1 Tumor samples and antibody optimisation for immunohistochemistry staining

Formalin-fixed Paraffin-embedded (FFPE) tissue samples were obtained from The Leeds Breast Cancer Tissue Bank. The ethical approval committee reference (REC) of this study was 15/YH/0025. 70 cases (20 ER+ and 50 TNBC) were obtained from consented patients who underwent surgery and were diagnosed at the Leeds Teaching Hospitals NHS Trust with follow up between 2010 and 2016. The clinicopathological characteristics of patient samples of this study are shown in Table 1 & 2. FFPE cohorts were 10 x 5µm thick serial sectioned and mounted on super frost plus slides (Life Technologies, Paisley). Slides were dried for 1 hour at room temperature and incubated overnight at 37°C for staining. An additional paraffin coating was applied for longer term storage to preserve antigenicity. Prior to antigen retrieval, slides were heated to 70°C for 30 minutes to ensure the tissue was stuck to the super frost plus slide. Antigen retrieval solution 10x (Menarini Diagnostics MP-607-X500) was used to unmask protein epitopes using a pressure cooker (Access Retrieval Unit) at 125°C 40 minutes. For visualizing primary antibody, NovolinkTM Polymer Detection System kit (Leica RE7260-K) was used according to the standard protocol. Block endogenous peroxidase activity by incubating in peroxidase block 15 minutes at room temperature. Slides were rinse 1x in Tris-Buffered Saline (TBS Menarini diagnostics MP-945-X500x). Non-specific bindings were blocked using primary block reagent 15 minutes at 37ºC followed by washing slides in 1 x TBS. Antibodies were diluted in antibody diluent reagent solution (Thermo Fisher Scientific Ref: 003218), before incubating with primary antibody. After washing in PBS, samples were incubated with Horseradish Peroxidase (HRP) 30 minutes, and stained with

diaminobenzidine (DAB) for 5 minutes for immunodetection, followed by counterstaining with hematoxylin. Slide were rinsed in Scott's tap water followed by dehydration through graded ethanol and mounting using Distyrene Plasticizer Xylene (DPX) before drying overnight. Slides were scanned at x20 magnification using Leica Bioscience Aperio AT2- scanner.

Table 1 Clinicopathological features of triple-negative breast cancer patients.

Characteristic		Frequency
Gender	Female	50
Mean age (range)		65 (38-98)
Tumour type	Infiltrating ductal carcinoma (IDC) No specific type	38
	Lobular	2
	Others	10
Grade	I	3
	II	7
	III	40
Tumour size	≤20 mm	12
	21-30 mm	23
	≥30 mm	15
Lymph node status	Negative	4
	Positive	46

Table 2 Clinicopathological features of oestrogen receptor positive breast cancer patients.

Characteristic		Frequency
Gender	Female	20
Mean age (range)		70 (48-85)
	N/A	8
Tumour type	Infiltrating ductal carcinoma (IDC) No specific type	10
	Lobular	4
	Others	6
Grade	I	3
	II	9
	III	8
Tumour size	≤20 mm	0
	21-30 mm	4
	≥30 mm	16
Lymph node status	Negative	2
	Positive	18

2.1.2 Antibody optimisation

Antibody optimisation is the most important step for reliable immunohistochemistry technique. Several factors including incubation time and temperature, antibody dilution and concentration all impact the staining quality such as no background, strength of staining and non-specific binding. However, samples were stained with recommended positive and negative controls selected from the Human Atlas Protein (www.proteinatlas.org). 5µm tumour breast tissue was sectioned as described above. Slides were stained using immunohistochemistry as described above using serial dilutions (1-50, 1-100, 1-200) for each antibody (CD3, CD4, CD8, CD20, CD68, FOXP3 and α-SMA). Antibody information is shown in Table 3. Slides were counterstained with Haematoxylin, and rinsed in running water for 5 minutes. Using graded alcohol, slides were dehydrated and cleared using xylene. The final step was to mount the sections with DPX. Slides were dried overnight, and digitally scanned

with VENTANA iScan HT and then viewed to determine the specific concentration required.

Table 3 Primary antibodies used for immunohistochemistry.

Antibody	Code	Supplier	Dilution	Biological Features	Incubation time
CD3	M 7254	Dako	1-100	Binds to CD3 chain located on T-cytotoxic. It works as co-receptor that helps to activate T-cell	30 minutes at room temperature
CD4	M7310	Dako	1-50	Binds to CD4 that found on T helper cells. It plays an important role in T helper cells activation	20 minutes at room temperature
CD8	M7103	Dako	1-100	Binds to T lymphocyte cell. CD8 works as co-receptor for T cells.	30 minutes at room temperature
CD20	M0755	Dako	1-100	The antibody binds to CD20 receptor expressed on the surface of all B-cells	30 minutes at room temperature
CD68	M 0876	Dako	1-100	Binds to CD68 cells. It is found on the surface of macrophages cell.	30 minutes at room temperature
αSMA	M0851	Dako	1-100	The antibody binds to smooth muscle cells, myofibroblasts, fibroblasts, endothelial and myoepithelial cells.	30 minutes at room temperature
Foxp3	ab20034	Abcam	1-100	The antibody binds to Foxp3 protein found on the surface of regulatory T cells.	30 minutes at room temperature

2.1.3 Positive pixel count algorithm

Image analysis was applied to the scanned slides using the Leica-Aperio Positive Pixel Count algorithm (PPC). Regions of interest were manually selected by drawing annotation on all tissue, and pixel values were thresholded based on hue, saturation and intensity values. Background pixels were discarded based on their Saturation and Intensity values, to create a count of foreground pixels. Pixels were classified as positive or negative based on their Hue value (Positive = .1 +/-.25), and the intensity of the positive pixels was binned into three groups; Weak Positive, Positive and Strong Positive. The thresholds for each group were 175-220, 101-175 and < 100 respectively as depicted in figure (13). A single measure of positivity was calculated using the ratio of the sum of all positive pixel groups, to all foreground pixels. In the context of this analysis, pixels were used as a surrogate for tissue area.

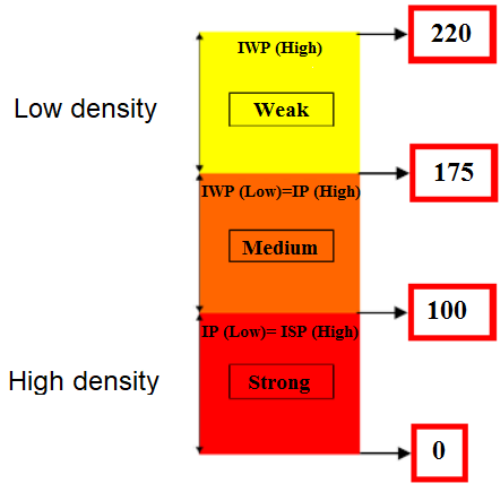

Figure 13 The thresholds of total intensity: weak, positive and strong

2.1.4 Positive pixel count analysis (PPC)

To reduce computational overhead on the image analysis scatter, digital slide images were randomly sampled using the RandomSpot Algorithm [207]. Firstly, regions of interest were manually annotated on each slide by drawing around desired areas as shown in figure (14). Annotated areas were exported and stored in XML format.

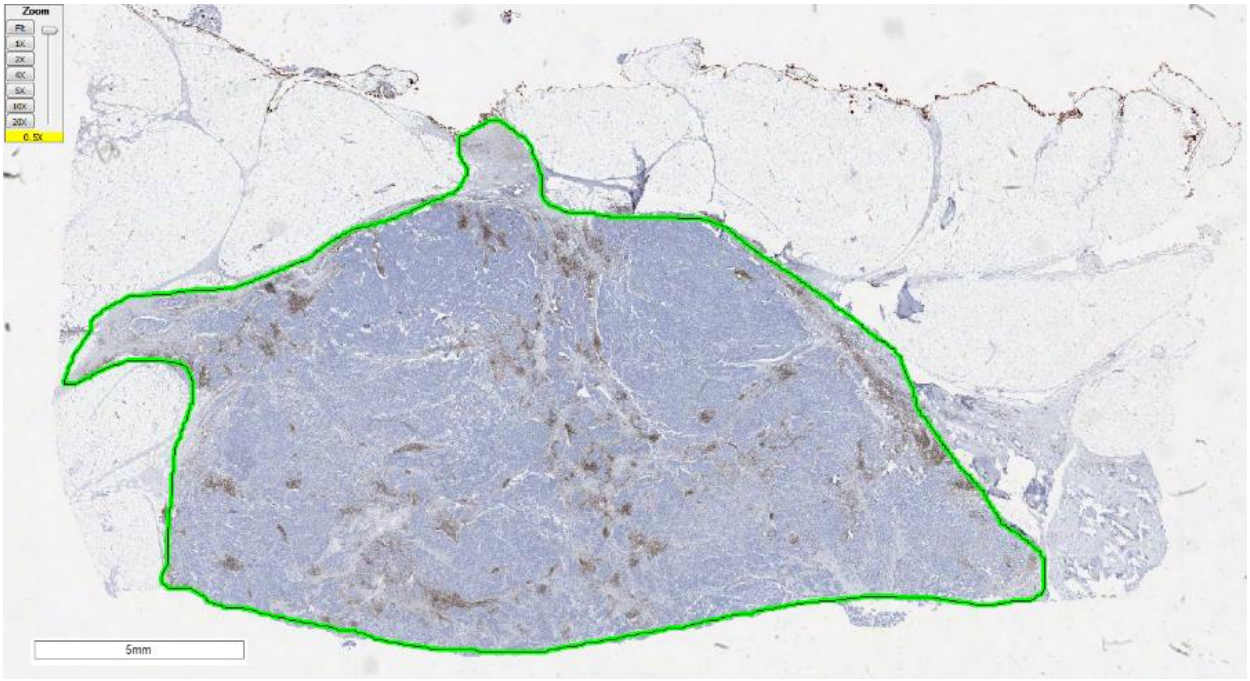

Figure 14 Examples of hand drawn annotation type, used as a region of interest to generate random boxes within annotated area.

The XML file was uploaded to Random Spot website http://129.11.65.182/RandomSpot/ . These regions of interest were used to generate sampling points in the RandomSpot software, generating 30 boxes with a tolerance of 1%. Each box was 1000 pixel in size as shown in figure (15).

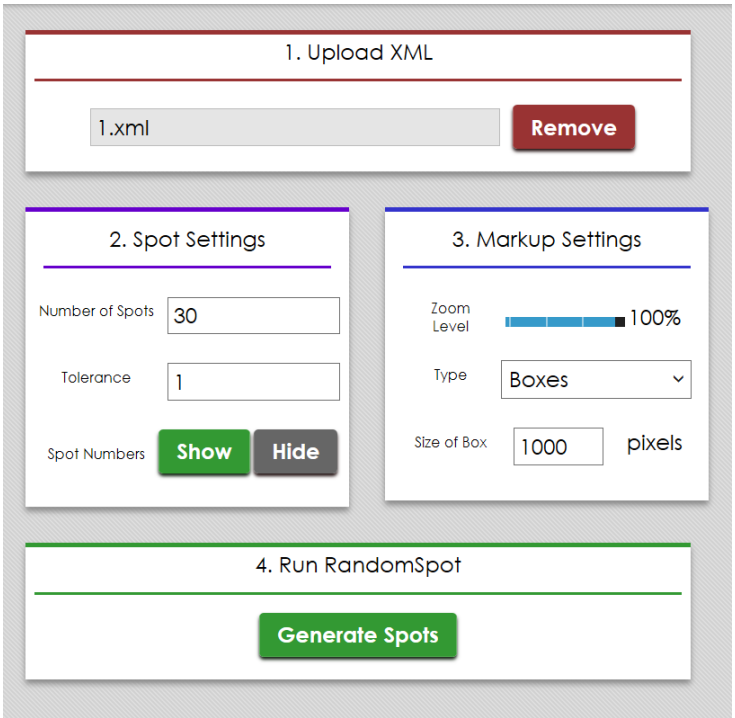

Figure 15 The spot generation screen shows the number of boxes to be generated on the slide.

Once the boxes have been generated, the XML was imported into positive pixel count for analysis as shown in figure (16) and each box annotation (box) was analysed to assess the presence of DAB stain.

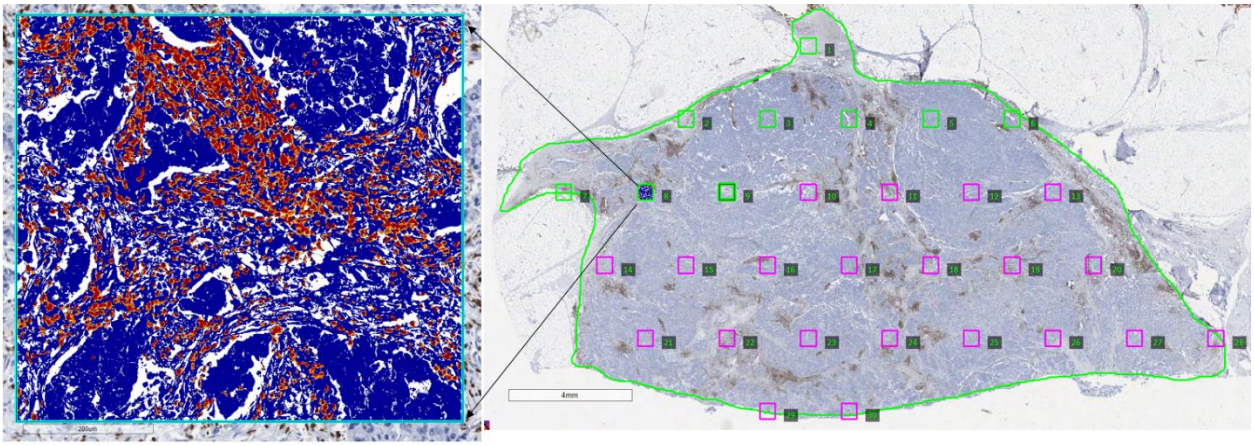

Figure 16 Positive pixel count analysis after generating boxes on the slide.

2.1.5 Quantification of positive pixel analysis

The algorithm generates data for all region of analysis as shown below:

Number of weak positive (Yellow in mark-up image).

Number of positive pixels (Orange in mark-up image).

Number of strong positive pixels (Red in mark-up image).

Total intensity of weak positive.

Total intensity of positive.

Total Intensity of strong positive.

Number of negative.

Total intensity of negative.

Total number (Positive+Negative).

Total area (millimetre-squared).

Positivity: NPositive/NTotal. The total number of positivity is recommended to quantifying specific staining. And to get this number we use the equation below.

$$\textit{Positivity total of brown stain in the tissue} = \frac{Weak\ Positive + Strong\ Positive + positivepixels}{total\ number\ (positive\ and\ negative)} * 100$$

2.1.6 Positive pixel count optimisation

For PPC optimization, 15 patient samples were immunohistochemically stained using CD3 antibody. Slides were scanned and the positive staining was counted using PPC software. According to CD3+ abundance, slides were characterised to 3 groups of high, moderate and low staining abundance as presented in figure (17), 5 patients per group. Regions of interest were manually annotated and exported to Random spot website to generate boxes as described above. 10, 20 and 30 boxes were generated on each slide and analysed (Leica-Aperio Positive Pixel Count algorithm). The outcome of PPC for each group was statistically calculated using Graph Pad prism to determine the actual box number to be used for PPC analysis.

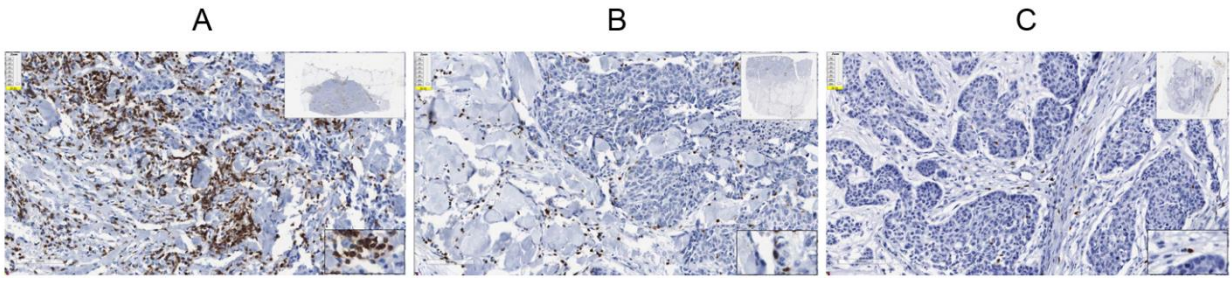

Figure 17 Examples of CD3 abundance characterized as high (a), moderate (b) and low (c) abundance.

2.1.7 Picro Sirius Red Staining

Picro serius red histochemistry is the best technique used to assess the localisation, distribution and density of collagen in tissue samples. For Sirius red staining, 20 ER+ and 20 TNBC cases were sectioned as described previously. Slides were hot plated at 70°C for 30 minutes and then dewaxed through xylene and then ethanol 100% 4 times 3 minutes respectively. Slides were incubated with Weigert's haematoxylin 20

minutes followed by washing in tap water. Slides were then differentiated in acid alcohol and stained in saturated picric acid with 0.1% Sirius Red (F3BA). Slides were rapidly dehydrated through alcohols and cleaned in xylene, and mounted with DPX. Collagen fibres stained red, the nuclei and cytoplasm stained black and yellow, respectively as shown in figure (18). Slides were scanned at x20 magnification as described previously and analysed using PPC analysis.

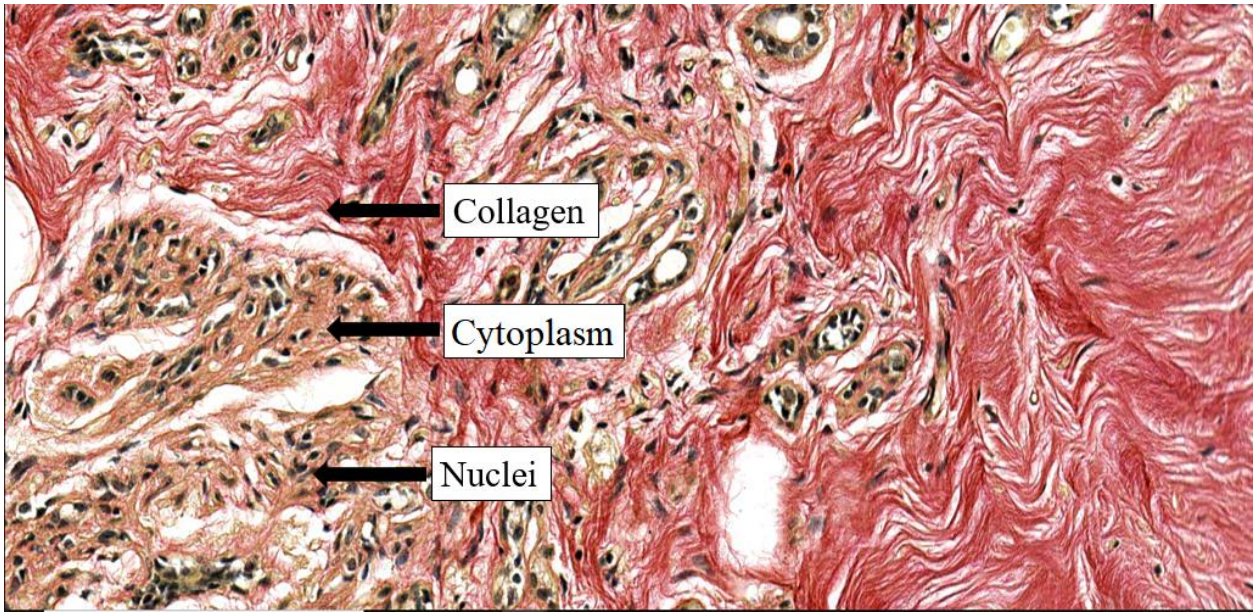

Figure 18 Representative example shows Picro serius red histochemistry staining. Collagen stains red, cytoplasm stains yellow and the nuclei stains black.

2.2 Cell culture

2.2.1 Cell maintenance

MCF-7 and MDA-MB-231 cell lines were obtained from the European collection of authenticated cell cultures (ECACC). Fibroblasts were derived in-house from tissue from ER+ breast cancer patients who consented at St. James's University Hospital Leeds East (Ethics reference: 15/YH/0025). Cell lines and fibroblasts were cultured in suitable media RPMI 1640 and DMEM respectively (both media were purchased from

Gibco™ life technologies. Both media were supplemented with 10% fetal bovine serum (FBS) (Labtech FCS-SA 30502). Cells were then gently rinsed using Dulbecco's Phosphate Buffered Saline (DPBS) supplied from Gibco™ life technologies. Adherent cells were detached by trypsinisation using 1x Trypsin (Thermofisher, Paisley). Cells were transferred into a 25ml universal tube using a pasteur pipet and centrifuged at 1200rpm for 5 minutes. 10ml of fresh media was added to re-suspend the cell pellet. 2ml were taken from re-suspended solution and seeded with 14ml medium in T75 flask and incubated at 37°C.

2.2.2 Generation of Conditioned Medium (CM)

The human breast cancer cell lines MCF-7 and MDA-MB-231 were maintained as described in previous section and incubated at 37°C. Cells were cultured in T75 flasks, and incubated until 60–70% confluent. The media was discarded and the cell monolayer rinsed in DPBS (Gibco). Serum-free media was added 5ml into T75 flask, and cells cultured for a further 24h at 37°C. Medium was transferred into 25ml universal tube and centrifuged at 1000rpm for 5 minutes and passed through a 0.22-µm filter. Medium was stored at -20 until use.

2.2.3 Generation of primary cultures of normal and cancer-associated fibroblasts from human breast tumours

Breast tumour and normal tissues were isolated from consented patient samples obtained at St. James's University Hospital. Briefly rinsing the sample in 70% ethanol. Tissues were then washed with DPBS and placed in a 10cm petri dish. 5ml DMEM supplemented with 10% FCS, Gibco™ Penicillin-Streptomycin 1% and fungizone Gibco™ Amphotericin B 0.25 % were added to the tissues . The samples was then

diced with scalpels into small fragments. 1% collagenase type 1A and hyaluronidase was added to the macro dissociated sample in the 10cm petri dish and left to digest for between 4-12 hours at $37^{O}C$, 5% CO_2. The sample was visually inspected to monitor the dissociation. Tissue fragments were then transferred to a universal tube and centrifuged at 1200rpm for 5 minutes and the supernatant discarded. The pellet of disassociated organoids were then transferred into several T25 culture flasks depending on the size of the sample. Tissues were incubated for 1-3 days at 37°C. Organoid attachment was visually inspected at 3 days and by differential trypsinisation fibroblasts were carefully transferred into T75 flasks as shown in figure (19). Media was replaced on the attached organoids for further fibroblast generation.

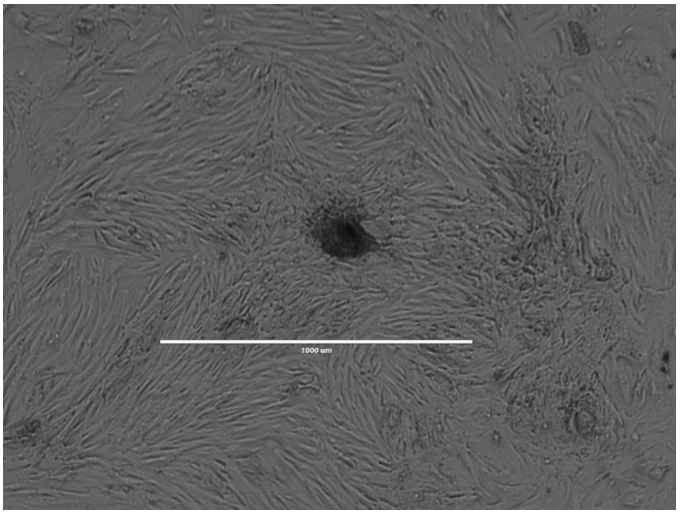

Figure 19 Fibroblasts generated from human breast tumours.

2.2.4 The effect of conditioned media on cell proliferation

MCF-7, MDA-MB-231 and fibroblasts derived from ER+ breast cancer patient were seeded in T75 flasks. Cells were dispersed from nearly confluent culture by 1x Trypsin

(Thermofisher, Paisley) and centrifuged at 1200rpm for 5 minutes. Cell pellets were suspended by adding 10 ml medium. Cell counting was performed using a hemocytometer. 5000 cells from each cell line and fibroblasts were pipetted into each well of a 96 well plate and incubated over night at 37°C. Next day medium was discarded and replaced with the CM being tested, cells were incubated for 5 days imaged using Microscope - Live Cell Imager - Essen IncuCyte Zoom to investigate the effect of CM on the cell proliferation.

2.2.5 The effect of Pirfenidone treatment on breast cancer cell lines and fibroblasts

Pirfenidone (PFD) (5-methyl-N-phenyl-2-(1H)-pyridone) is an anti-fibrosis drug that is widely used to decrease collagen deposition and fibroblasts proliferation, as well as it regulates various cytokines such as TGF-β1, PDGF and TNF-α in order to reduce or eliminate inflammation and fibrosis such as in TNBC [208]. PFD was purchased (Sigma-Aldrich). A 10mM stock concentration of PFD was prepared in 100% DMSO, stock solution was aliquoted into 100µl and stored at -20°C. To assess its effects, MCF-7 and MDA-MB-231 cells and fibroblasts derived from ER+ breast cancer patient were cultured in 96-well plate at 5000 cells per well at 200µl in the presence of 10 fold serial dilutions of PFD (100µm-1µm). Serial dilutions were conducted in the 96 well plate. A 100 fold dilution of the 10mM stock was conducted by adding 2µl to the 200µl in the well. This resulted in a treatment concentration of 100µM with a DMSO concentration of no more than 1% per well. 10 fold dilutions were then conducted in subsequent wells by transfer of 20µl from the treated wells in to 180µl of media in the untreated wells. Mixing by multi-channel pipette was done to achieve concentration

dilution. A 1% DMSO control well was included, in the absence of PFD. Cell proliferation assay was performed by using Essen IncuCyte Zoom.

2.3 Assessing ER status in human breast cell lines and fibroblasts

2.3.1 RNA extraction

Cells were harvested from regularly maintained T75 flasks, as described previously. Cells were centrifuged as described before. Cells were lysed by adding 350µl of lysis buffer (RLT buffer) and lysed using a syringe followed by adding 1 volume 70% alcohol to the homogenized cells and carefully mixed by pipette. 700µl from the homogenized cells were transferred including any precipitate into an RNeasy Mini spin column for. 700µl of washing membrane-bound RNA buffer **(**RW1) were pipetted to the homogenized cells and centrifuged 1 minute 10.000 rpm. After removing the supernatant, 500µl of a mild washing buffer (RPE) was pipetted to the pellet to remove traces of salts and centrifuged for 2 minutes. RNeasy filter was placed into fresh 2ml collection tube followed by adding add 30–50µl RNase-free water and to elute the RNA. RNA purification was measured by Agilent Bioanalyzer and NanoDrop.

2.3.2 Quantification of RNA purity using NanoDrop

After RNA extracting, the RNA was quantified using the NanoDrop 2000/2000c spectrophotometer Software. Both pedestals surfaces were cleaned using distilled water and a clean tissue. To perform a blank measurement, 1µl of distilled water was dispensed onto the lower pedestal surface. Once completed, both optical surfaces were cleaned as above. 1µL of the sample was pipetted onto the lower optical pedestal

before closing the level arm followed by RNA measurement. The RNA concentration was determined and viewed on screen as shown in figure (20).

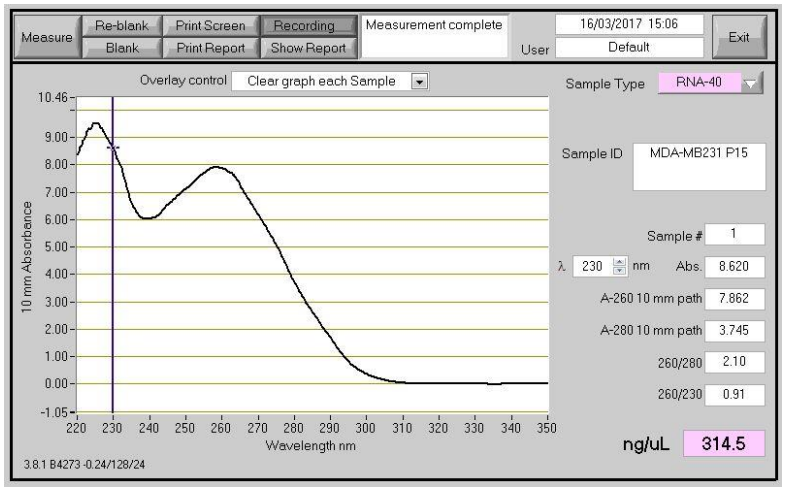

Figure 20 Concentration of RNA extracted from cells in ng/µl

2.3.3 First-strand cDNA synthesis

The SuperScript™II Reverse Transcriptase multiple temperature cDNA synthesis kit (SuperScript™ II Reverse Transcriptase, Catalog number 18064014) was used to reverse transcribe RNA to cDNA. 10µl of RNA (3145ng) was incubated on ice and 1µl of both random hexamers and deoxyribonucleotide triphosphate (dNTP) were then pipetted to the sample and incubated for 5 minutes at 65°C. 4µl 5x First Strand Buffer were added to control the pH followed by adding 2µl 0.1M DL-Dithiothreitol (DTT) to reduce disulphide bonds in proteins and enzymes RNases followed by adding 1µl RNase out. The reaction tubes were incubated at 42°C for 2 minutes followed by adding 1µl of Superscript II enzyme to polymerize DNA. Samples were incubated at 42°C for 50 minutes and finally, reactions terminated at 70°C for 15 minutes. Samples were stored at -20°C until use.

2.3.4 Real-Time Polymer Chain Reaction

The assessment of ER was carried out using a real-time PCR system (LightCycler® 480). The primers for ERα were used for gene expression detection, 180 µl of RNA free water was added to 20µl cDNA sample chilled on ice, followed by adding 90µl TaqMan Genotyping (4369016) Master Mix to the sample. The mixture was vortexed for 30 seconds and then divided into 2 tubes by adding 76µl to each tube. To the first tube, 4µl ER-α primer was added and centrifuged for 30 seconds 10,000 rpm. 4µl ribomsomal protein (RPLP) housekeeping gene was added to the second tube and centrifuged for 30 seconds 10,000 rpm. In separate tube, the negative control was prepared by adding 4µl ERα to 36 µl RNAse free water without chemical additives and 40µl Master Mix. Samples were pipetted into 3 different 96 well plates at 20µl and analysed.

2.3.5 Immunofluorescence

MCF-7, MDA-MB-231 and fibroblasts derived from ER+ breast cancer cells were seeded on sterilized glass coverslips in 12-well plates and grown to achieve 60-65% confluency. Cells were first washed with DPBS. For cells fixation, 4% formaldehyde was added to the cells and incubated at room temperature for 15-30 minutes in a rocker. 0.5% Triton in DPBD was prepared and pipetted to the cells for 15 minutes to permeabilise the cells. Non-specific bindings were blocked by adding 2-3 drops of avidin and biotin kit Vector Laboratories (SP-2001) and covered by parafilm for 30 minutes at room temperature. Cells were then washed with DPBS on a rocker. Cells were incubated with 5% skimmed milk for 1 hour on the rocker. Cells were stained with ER-α (DAKO 1D5 M74047 dilution 1-25) followed by incubating in dark with

secondary antibody (Alexa Fluor® 488 #A21202 dilution: 1-2000) at room temperature for 30 minutes for each antibody. Coverslips were mounted onto slides placed with one drop of fluoroshield mounting medium containing DAPI (Abcam ab104139). Fluorescent images were captured on Zeiss LSM880 FL Imaging System.

2.4 Raman Imaging

2.4.1 Slide silanisation

For Raman imaging stainless steel grade 304 supermirror of 0.9-mm thickness were obtained from Renishaw PLC (Gloucester, UK). Standard glass histological slides (75 × 25 × 1 mm) were prepared alongside. Both slides were dipped in trichloroethylene, acetone and isopropanol 30 minutes each in a sonication. Slides were silanised in 5% Dimethyldichlorosilane solution for 10 minutes and incubated with 100% ethanol for 10 minutes and finally through tap water 3 times 30 seconds each. Slides were dried at room temperature for 30 minutes before heating to 180ºC for 90 minutes.

2.4.2 Sample preparation

For this pilot study of Raman imaging, 8µm sections of one ER+ and one TNBC were sectioned and fixed onto stainless steel and standard glass slides and incubated overnight. Samples were hot plated at 70°C 40 minutes. Each section was dewaxed in 3 consecutive 100% xylene solutions for 15 minutes each time and rehydrated through graded ethanol (100%, 75%, 50% and 25%). Slides were washed using tap water for 60 seconds. On the next day, Samples were mapped using Raman imaging technique.

2.4.3 Raman measurements

The Raman measurements were conducted using a Raman confocal microscope (Renishaw inVia) integrated with a fluorescent confocal microscope (Leika SP8 microscope). The chosen laser was a 785 nm laser using a power of 45 mW on the sample. The camera used was an infrared enhanced Renishaw camera. The system was calibrated and detection of the Raman peak was at 520.5 cm^{-1} on a silicon sample. Visualisation was using a 40x dry objective (1.4 NA).

The background of the salinized stainless-steel slides was measured on the sample in a region free of tissue providing an overall background value (a broad peak between 1000 and 2000 cm^{-1}) and the sample returns a sharper peak at approximately 1250 cm^{-1}.

Some spectra regions of tissue on the sample were conducted to visualise the intensity of the tissue signal and also the contribution of any remaining wax to the spectra; these were completed using 10 second exposure time with an extended scan spectra. It has been previously reported that some of the peaks created by paraffin wax are located at: 1063, 1133, 1172, 1296, 1418, 1441 and 1463 cm^{-1} [209]. These peaks were not observed in the preliminary scans, indicating that the samples were successfully dewaxed. This was confirmed with Raman measurements at different stages of the dewaxing protocol.

To successfully map the specimen, a region of the sample with both tissue and empty regions, was selected (so-called fingerprint region). The streamline high resolution (HR) functionality of the Renishaw microscope was used for fast mapping of the fingerprint region (using a window centred at 1200 cm^{-1}). In this mapping, the laser is deformed into a line which allows obtaining multiple pixels simultaneously thus

reducing mapping time. The exposure time chosen was 0.7 s and the confocal option was removed to increase signal intensity.

A cosmic-ray removal algorithm, baseline subtraction and smoothing were performed on the datasets using the WiRE software. A noise filter based on Principal Components Analysis (PCA) was also performed to reduce the noise contribution on the sample. The PCA was applied and the components with higher variability were scored. A false colour image of the mapped region was obtained using the scores (PC1-5) of the components as shown in figure (21). Using this technique, a whole map took between 25 and 35 minutes, meaning that the exposure time could be increased to obtain a better signal-to-noise ratio and allow greater areas to be mapped overnight.

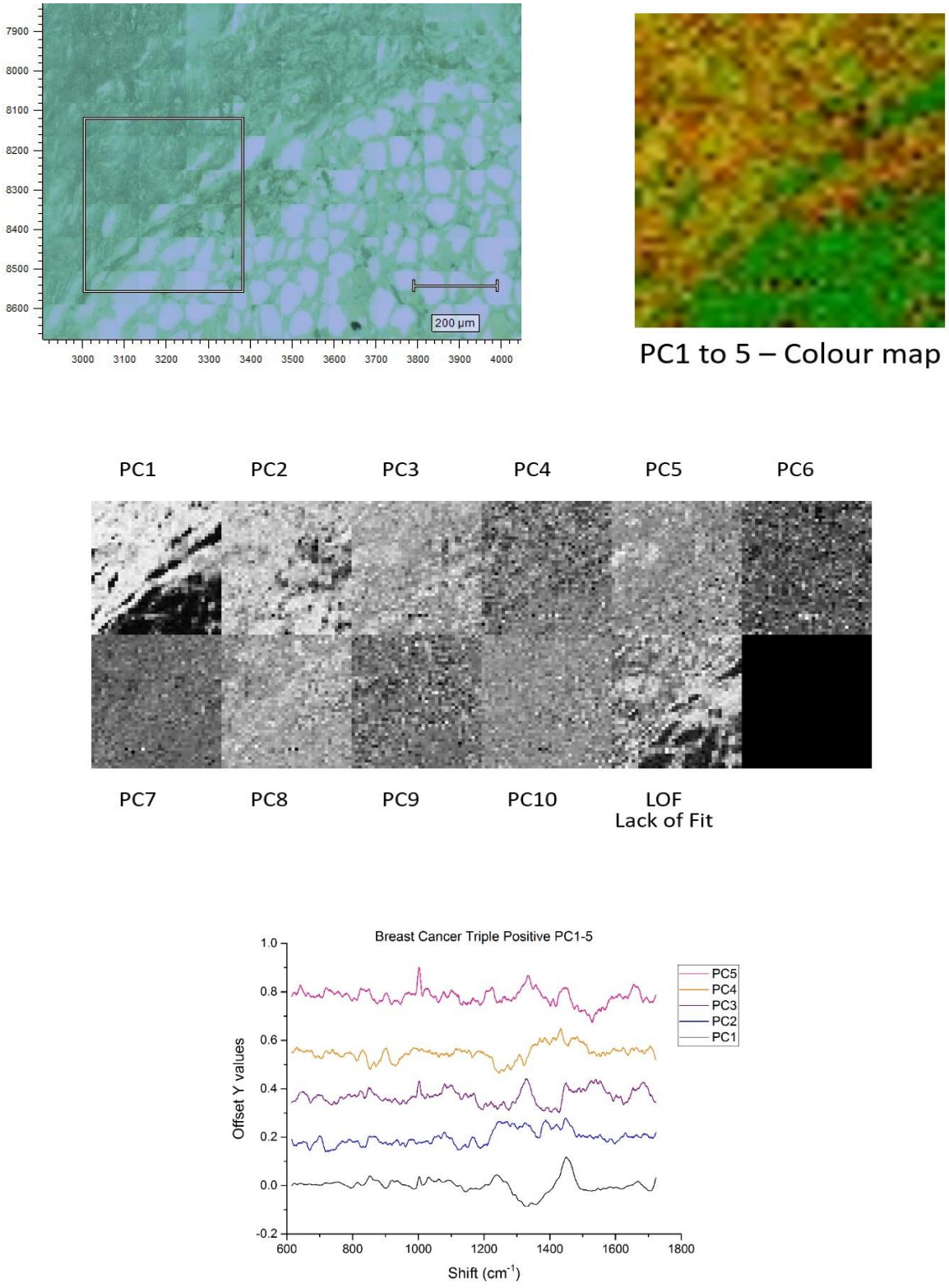

Figure 21 False colour images of the mapped region was obtained using the scores (1-5) of the components.

2.5. Human monocytic Thp-1 differentiation into macrophages

2.5.1 Optimisation of Thp-1 monocytes differentiation into macrophages using phorbol-12-myristate-13-acetate

This experiment is aiming to determine the lowest optimal PMA concentration which precisely reflects physiological conditions of macrophages. However, $1x10^6$ Thp-1 cells were pipetted into 6 well plates and treated with different concentrations of PMA treatment ranged from 10ng/ml-100ng/ml for 48hrs incubation, the length of exposure to PMA is commonly used in the literature [210-213]. Cells were washed with PBS and lysed with TRIzol reagent (Cat. No. 79306) for RNA extraction. The experiment was conducted 3x for the biological repeat.

2.5.2 RNA isolation

Lysed cells were thawed on ice for 20mins while preparing other reagents. 80µl phenol-chloroform were added to homogenate samples and the mixture was shaked vigorously for 15 second. The mixture was chilled on ice for 5 mins and centrifuged at 4ºC max speed 13.2g for 15 mins to get the phase separation. 200µl from aqueous phase where transferred to a fresh tube and 200µl isopropanol where then added to precipitate RNA. The mixture was incubated on ice for 15 mins followed by centrifuging for 15 mins at 4ºC max speed 13.2g. The supernatant was removed and washed by flicking with 70% ethanol at a volume 600µl. The mixture was centrifuged at 4ºC for 5 mins max speed 13.2g. The supernatant was carefully removed and air dry was applied for 10 mins to purify RNA from ethanol. The RNA pellet was dissolved in 20µl of RNase-free water and heated in the thermolyne heater at 55ºC for 5 mins. RNA quantity and purity was assessed using NanoDrop™ 2000 / 2000c

Spectrophotometers at 260 and 280 wavelengths. Ratios of 260/280 and 260/230 were above 2.0.

2.5.3 cDNA synthesis

Reverse transcriptase was performed to generate complementary DNA (cDNA) from RNA using Omniscript® RT Kit (QIAGEN 205111). Briefly, 14µl mixture of Diethyl pyrocarbonate (DEPC) water and 2µg RNA was prepared in 0.5ml microcentrifuge tube and chilled on ice. A master mix was prepared according to the standard protocol, for each sample 2µl 10x Buffer RT, 2µl dNTP Mix (5 mM each dNTP), 1µl Reverse Transcriptase and 1µl Random Nonamers Sigma product (R7647) were separately prepared. The master mix was added to the RNA and manually mixed. Samples were incubated in water path for 1.5 hrs at 37ºC. After incubation, 180µl RNase free water were then added to the sample to get 200µl cDNA as a final volume. Samples were stored in -20 until use.

2.5.4 PCR Primer Design

The choice of primer design is one of essential steps for amplification of small genetic materials. Primer 3 is an online program (http://primer3.ut.ee/) was used in order to generate primers for cloning and semi quantitative reverse transcription PCR (RTPCR) analysis using the codon region of each gene. The standard settings were modified as following, the primer length was between 300-500bp, this length was enough to easily bind to template. Annealing temperature and max self-complimentary were set at 58-60ºC and 5 respectively. Once generated, primers were purchased from Sigma-Aldrich. Primers were diluted in nuclear free water at 100µM concentration and stored in -20ºC until use.

2.5.5 Polymer Chain Reaction (PCR)

cDNA samples and PCR reagents were thawed on ice during master mix preparation. PCR Primers were purchased from (Sigma-Aldrich) and are listed in table 4 bellow. The Tag reagent was purchased from GENEFLOW (P8-0034). The master mix was prepared according to the standard protocol. Briefly, 10 µl RNase free water were pipetted into 0.5 microcentrifuge tube. 0.50µl of 2µM forward and reverse primers were added followed by adding 12.5 µl Tag DNA polymerase (please see the list of primers in table (4). Samples were vortexed and loaded into a sufficient PCR tube. Real-time PCR analyses were performed on a Biometra T3000 Thermocycler machine. The preheating was set on 95ºC for 15 minutes to allow polymerase activation, the system was cooled down for denaturation phase at 94ºC for 5 seconds. Followed by annealing phase at 56-58 independently and finally the extension step at 72º C. The PCR reaction result was visualised on Agarose Gel Electrophoresis.

Table 4 Primers used for RT-PCR analysis to evaluate Thp-1 differentiation into macrophages

Primer	Forward	Reverse
CD11b	TTTCTGCCCTTCTTTGCTTTGG	TAGTCGCACTGGTAGAGGCT
CD14	CAGAACCCTAGATGCCCTGC	CATCGTCCAGCTCACAAGGT
CD68	ACAGGGAATGACTGTCCTC	ACGTGTAGTCTCCAAGGTC
TLR-4	AGAATGCTAAGGTTGCCGCT	CGGAGTCTGAAAGCTCTGGG
GAPDH	TCCCATCACCATCTTCCA	CATCACGCCACAGTTTCC

2.5.6 Evaluating gene expression on gel electrophoresis

The agarose gel matrix was prepared by weighting 1.3g of agarose gel and added to the titration flask which contains 100ml of Tris-borate-EDTA x10 (TBE) (Cat. No. AM9863). The mixture was swirled thoroughly in order to get a homogenous mixture. The mixture was microwaved for 1-2 minutes with an interval swirl every 30 seconds until the agarose is completely dissolved. The solution was cooled down to 50ºC before adding 10µl of Ethidium Bromide (EtBr) (SIGMA-ALDRICH E1510-10ML) to visualise the DNA. The solution was swirled and slowly poured into gel casting apparatus which contains well comps in place. An air dry was applied for 15-20 minutes to solidify the gel. The gel box was attached to the power supply (EP-2000 RUNONE™ ELECTROPHORESIS SYSTEM) and 10x TBE running buffer was poured to the level which covers the gel surface. 12-15µl of DNA sample was pipetted into gel pores. The power supply was set up to the desired voltage 100V for 10-13 minutes. Once the electrophoresis has completed, the gel was exposed to uv light using ChemiDoc™ Imaging System (Cat. No. 17001402).

2.6 Determining resting phase period in stimulated Thp-1 post PMA removal

Human monocytic Thp-1 cells at density $1x10^6$ were incubated with 25ng/ml PMA treatment in 6 well plates for differentiation into macrophages-like. After 2 days incubation with PMA, cells were washed 3x with PBS which are termed non-resting phase (NOR), or cells were allowed to rest for 2 days (2DR) or 4 days (4DR) rest continuously in fresh media. RNA was extracted from each resting phase for PCR analysis. In order to evaluate cell adherence, cells were trypsinised after each resting

period and counted using hemocytometer technique. This experiment was conducted at least 3 independent times.

2.7 Evaluating gene expression of macrophages specific markers in detached cells

Human monocytic Thp-1 were seeded in 6 well plates at density $1x10^6$ and differentiated into macrophages-like with 25ng/ml PMA treatment for 48hrs. Cells were then washed 3x with PBS and incubated for further 4 days with fresh media. After 4 days incubation, suspension and adherent cells (as a positive control) were collected and RNA was extracted for RT-PCR analysis.

2.8 Evaluating macrophages differentiation co-cultured with breast cancer cells post PMA removal

Human monocytic Thp-1 were seeded in 6 well plates at density of $1x10^6$ and treated with 25ng/ml PMA to differentiate them into macrophages for 48hrs. Cells were washed 3x with PBS and incubated for 48hrs with fresh media to allow cells recovery post PMA removal. After 48hrs resting, $1x10^6$ MDA-MB-231 or MCF-7 breast cancer cells were cultured in Polyethylene Terephthalate (PET) Transwell membrane inserts (pore size 0.4 mm) (Ref. 3450) of 6 well plates 4hrs prior to co-culture experiment in order to allow cell attachment. Macrophages were incubated alone and/or with both breast cancer cell lines for different timescale. 2 days treatment with PMA is termed in the figure (2D PMA) then followed by resting phase for 2 days (2DR), 4 days rest (4DR) (the starting time of co-culture) and 6 days rest (6DR). After each incubation period, macrophages were washed with PBS in order to remove detachment cells and

counted using haemocytometer technique. To investigate the expression of macrophages-specific markers, macrophages were harvested and lysed with TRIzol after each resting period from cultures above for RT-PCR analysis. This experiment were repeated 3 individually times.

2.9 Assessment of gene expression in breast cancer cells upon co-culture with differentiated Thp-1 cells.

Thp-1 cells were seeded in transwell inserts (pore size 0.4 mm) of 6 well plates at density 1 x 10^6 Thp-1, cells were treated with 25ng/ml PMA treatment for 48hrs to stimulate Thp-1 differentiation to macrophages-like. Cells were washed 3X with PBS and rested for 48hrs in fresh media in order to allow cell recovery post PMA removal. 1 x 10^6 MDA-MB-231 or MCF-7 breast cancer cells were seeded in triplicate in the bottom compartment of 6 well plates and allowed to settle for 4 hours prior to co-culture incubation. Macrophages and/or untreated Thp-1 inserts were placed on top of breast cancer cells and incubated for 72hrs without changing media. Control breast cancer cells were incubated in single culture alongside with co-culture cells under the same conditions. After the incubation period, breast cancer cells were washed 3x with PBS and RNA was isolated for RT-PCR analysis. Primers for RT-PCR amplification are listed below in tables (5,6), and were designed using Primer3 software as described previously.

Table 5 List of primers were used for PCR to detect gene expression in MDA-MB-231 breast cancer cells after co-culture with macrophages derived Thp-1.

Primer	Forward	Reverse
DKK1	GTTCTCAATTCCAACGCTAT	TTTGAAGACAAGGTGGTTCT
hAEBP1	AGTCACACCGTATTGAGGAC	CATTCTGTGCGTAGTAGCTG
hBIRC3	CTGTGCAATGAATAACGAAA	CAAGCTGCTCAGGATTAACT
hLAMC2	ACTAACATTCCTGCCTCAGA	TACCAGGCTTGAGAGTGAAT
hNR1D1	CATCCTCCTCCTCCTTCTAT	CCCACAGAGAGACACTTCTT
hPPBP	AGCCTCAGACTTGATACCAC	TTCATCACCTGCCAATTT
hPRLR	TTTCTGCTGTCATCTGTTTG	GATTCTCTGGCTTCTCAATG
hSOCS1	GATTACCGGCGCATCACG	GAGCTCAGGTAGTCGCGG
hPCOTH	ACCAGGCTTTCCAATAGGGC	TCAGGGGCAGAAGGGGAATA
hPER1	GGACCAGGTGATTAAGTACG	CATCCAGCTCTGAGAAGAGT

Table 6 List of primers were used for PCR to detect gene expression in MCF-7 breast cancer cells after co-culture with macrophages derived Thp-1.

Primer	Forward	Reverse
FAS	ACATGGCTTAGAAGTGGAAA	TTCTGTTCTGCTGTGTCTTG
HLA-DPB1	AGGATGTGCAGACACAACTA	CTCCCGTCAATGTCTTACTC
HLA-DRA	TTTGACTTTGATGGTGATGA	GTCTCTGACACTCCTGTGGT
ICAM-1	GTGACCATCTACAGCTTTCC	AAAGTGCCATCCTTTAGACA
SOCS3	AGACCTTCAGCTCCAAGAG	CCGGAGTAGATGTAATAGGC

2.10 Determining co-culture cell ratio

MDA-MB-231 and MCF-7 breast cancer cells were placed in the lower compartment of 6 well plates at density of $1x10^6$ and incubated for 4hrs to allow cell attachment. Macrophages were differentiated and rested as mentioned previously and seeded at different ratios 0.5:1, 1:1, 2:1 and 3:1 in transwell inserts pore size 0.4 µm (Corning). Cells were incubated for 3 days alongside with control cells without macrophages on the top compartment. After 72hrs breast cancer cells were harvested and lysed with TRIzol for gene expression analysis. Gene expression level of BIRC3, LAMC2, DKK1,

PER1 and NR1D1 or FAS, ICAM1 and SOCS3 were tested in MDA-MB-231 and MCF-7 respectively and the experiment was repeated at least 3 times.

2.11 Assessment of Macrophages cell morphology in the presence of breast cancer cells

Human monocytic Thp-1 cells were plated in tissue culture 6 well plates at density $1x10^6$ and induced with 25ng/ml PMA for 48hrs. After 48hrs PMA treatment, cells were washed 3x with PBS and fresh media was added to cells to allow resting phase for another 48hrs without PMA treatment to attain macrophage cell morphological and functional status. After 48hrs resting, macrophages were incubated for another 4 days in single culture and/or co-cultured with breast cancer cell lines MDA-MB-231, MCF-7. Pictures were captured using a florescence microscope (EVOS FL).

2.12 Evaluation of conditioned media effect on breast cancer

Human monocytic Thp-1 cells at density $1x10^6$ were pipetted into 6 well plates inserts pore size 0.4 µm (Corning) and treated with 25ng/ml PMA in order to differentiate Thp-1 cells to macrophages. After the incubation period, macrophages were re-fed with fresh media for 48hrs to allow cells recovery. Same amount of MDA-MB-231 or MCF-7 breast cancer cell lines were cultured in 6 well plates 4hrs prior to co-culture incubation. For conditioned media generation, inserts of differentiated macrophages were incubated alone and/or with breast cancer cells for 3 days in order to obtain gene expression in breast cancer cells. The media was collected and stored in -20 for later use. Activated breast cancer cells were then washed 3x with PBS and replenished with new media and incubated for another 3 days. Media of activated breast cancer

cells was also harvested and stored in -20. In separate 6 well plates, breast cancer cells were also incubated with undifferentiated Thp-1 cells for 3 days using the same amount of cells. Media from all cultures above was centrifuged at 1200g for 5 minutes (4ºC) to pellet the detached cells and undesired debris. The supernatant was passed through a sterile 0.22 micron filter into 15ml tissue culture tube. Media was labeled and stored in -20 until use next day. Fresh MDA-MB-231 and MCF-7 cells were trypsinised and aliquotted into several tissue culture tubes at density $5x10^5$ and spun down at 1200g for 5 minutes. The supernatant was aspirated and cell pellet was re-suspended with 3mls of each CM that we generated on the day before. Cells were then plated into 6 well plates and incubated for 3 days. After the incubation period, cells were washed with PBS and lysed with TRIzol for RNA extraction.

2.13 Characterization of breast cancer cells in double and triple culture

2.13.1 Determining fibroblasts and breast cancer cells ratio

MDA-MB-231 and MCF-7 cells at density $1x10^5$ were seeded into 6 well plates and incubated for 4hrs to allow cell adherence. Fibroblasts at different ratios including 0.5, 1, 2 and $3x10^6$ were pipetted into transwell inserts and placed on top of breast cancer cells. Control breast cancer cells were incubated alongside with co-culture plates. Cells were incubated for different time points and cell count of breast cancer cells was daily performed using hemocytometer technique.

2.13.2 Cell migration assay (wound healing)

MDA-MB-231 and MCF-7 breast cancer cell lines and Thp-1 cells were maintained in RPMI tissue culture medium while fibroblasts were grown in high DMEM tissue culture medium. Both media were supplemented with 10% fetal bovine serum (FBS) (Gibco 10270-106), 5% antibiotics penicillin G/Streptomycin (Ref: 15140-122), 5% Glutamine (Ref. 25030-024) and 0.1% β- Mercaptoethanol (Cat.No. 60-24-2). Our 2D migration assay was assessed using transwell inserts (4µm pore size). $1x10^6$ Thp-1 cells were pipetted into upper wells and treated with 25ng/ml PMA for 48hrs in order to differentiate Thp-1 cells into macrophages. Cells were allowed to rest for 48hrs in fresh media as described previously. Same amount of normal fibroblasts were seeded into either individual inserts and/or into the same inserts that contain differentiated macrophages. MDA-MB-231 and MCF-7 breast cancer cell lines were previously seeded in the bottom compartments of 6 well plates until they reached 95-100% confluence. Breast cancer cell lines were washed 3x with PBS and media was replaced with serum free media 24hrs prior to experiment conduction. This was done to prevent cell growth in order to distinguish cell proliferation from cell migration. Next day, wounds were generated in breast cancer wells using 200µL sterile pipette tip by scratching across the centre of the well. Inserts of fibroblasts or macrophages or co-culture of fibroblasts and macrophages cells were placed on the top of breast cancer cells and incubated for different timescales 3, 6, 12 hrs. Control wells of breast cancer cells were incubated individually in fresh media contains 10% FBS for the same indicated time. Pictures of travelled breast cancer cells from intact zones into scratched region were taken using a florescence microscope (EVOS FL). Distance of recovered wounds was quantified using imageJ 1.52u software. The experiment conduction was repeated 3 times.

2.13.3 Cell invasion assay

2.13.3.1 Determining the optimal concentration of matrix matrigel

Corning@ Matrigel@ matrix growth factor reduced (GFR) (356230) was purchased from corning life sciences. Matrix matrigel was thawed on ice in the fridge overnight as recommended by the company. All tubes, pipetes and free serum media were precooled in cold room 24hrs before use. The matrigel bottle was shaked thoroughly several times in order to mix the solution. In order to determine the optimal concentration, matrigel was diluted in cold free serum media in variety of concentrations including 1.2mg/ml, 0.6mg/ml and 0.3mg/ml as recommended [214]. The mixture was stored in -20 not to be used immediately as recommended by the company.

2.13.3.2 Matrigel chambers preparation

The diluted matrigel was defrosted in the fridge overnight, all inserts, plates, pipets, tips and tubes were precooled alongside with matrigel in the fridge overnight. The defrosted matigel was mixed by pipetting up and down to assure all matrigel components are homogeneous. Permeable insert (Falcon® 353182) 8.0µm pore size were coated with 100µl of diluted matrigel. The insert was rotated in order to ensure the entire insert surface is coated. The insert was left in tissue culture hood for 1h then overlaid very carefully with 100µl double distilled water then incubated in tissue culture incubator overnight to solidify. After the incubation period, the matrigel was rehydrated by adding 100µl free serum media for 2hrs before performing the experiment. Cells were prepared while waiting for matrigel rehydration.

2.13.3.3 Cell lines preparation

MDA-MB-231 and MCF-7 breast cancer cells were cultured in RPMI 1640 media supplemented with 10% FCS in T75 cell culture flask until they reached 80% confluency. Cells were washed with PBS 3 times and incubated with serum free media overnight in order to inhibit cell proliferation. Next day, cells monolayer was washed 3 times with PBS then 2mls of 0.02% Ethylenediaminetetraacetic acid (EDTA) solution (Sigma: RNBH6583) were added to the flask, a gentle swirl was applied to assure all cells were covered with the solution then incubated in tissue culture incubator for 5 minutes to remove cell-cell adhesion. EDTA solution was aspirated and cells monolayer was washed once with PBS then incubated with 2mls Trypsin for 1 minute, the flask was gently nocked to detach cells attachment from the bottom. The trypsin action was inhibited after pipetting 8mls of cell culture medium supplemented with 10% FCS and the mixture was transferred into 15mls centrifuge tube. Cells were spun down at 1200rpm for 5 minutes. The supernatant was aspirated and the cell pellet was then suspended with 10mls serum free medium. Cell count was conducted using haemocytometer.

2.13.3.4 Matrigel invasion assay performance

Tissue culture cell media supplemented with 10 foetal calf serum were pre-warmed in water path 2-3 hours before conducting the experiment. 1-1.5ml media were pipetted to the bottom chamber of the 12 well plates Falcon® Corning® (Ref: 353503). $1x10^5$ cells/ml from cell suspension were pipetted to the matrigel insert then the insert was placed on the bottom plate which contains 1-1.5 serum free media. The control inserts were coated with all prepared concentrations alongside but without using fetal calf

serum in the bottom chamber. The invasion plates were incubated in tissue culture incubator for a different timescales 24hrs, 48hrs and 72hrs. After the incubation period, the free serum media was pipetted off and cells were washed with PBS 3 times. Cells were fixed by incubating them with 100% methanol for 30 minutes in the fridge. Non invading cells were removed by scrubbing of the upper chamber using a sterile cotton swab. This step was repeated for at least 3 times using a clean cotton swab to ensure all or majority of non-invaded cells were removed from the surface. The insert was washed with serum free media and then immersed in Mayer's hematoxylin for 3 minutes. Cells were blued by transferring them to tap water container for 1 minute with a gentle agitation. The tap water was aspirated and the insert was immerse in 1% w/v aqueous eosin solution for 30 seconds then rinsed in tap water by dipping in and out for a few seconds. The insert was dehydrated in 70% for one change then followed by 2 changes in 100% ethanol for 30 seconds each change. The insert was transferred to xylene for clearance by dipping the insert in and out for 1 minute. The membrane was cut out of the insert using a scalpel by rotating the insert against the blade. The membrane was placed on the slide which already contains a small drop of Depex, another small drop of Depex was also dropped on the top of the membrane before putting the coverslip on it. A gentle pressure was applied on coverslip to evict air bubbles out of the slide. The slide was left on bench overnight to apply air dry at room temperature. The experiment was conducted in triplicate and pictures were taken from the centre and the edge of the slide under the fluorescence microscope at approximately x100 magnification. Direct cell count was performed under the microscope and the percentage of invasive cells was evaluated using the equation below.

$$\%\ invasion = \frac{mean\ number\ of\ cells\ invading\ through\ matrix\ matrigl}{mean\ number\ of\ cells\ invading\ through\ control\ inserts}\ x\ 100$$

2.13.4 Cell proliferation assay

The rate of breast cancer cell proliferation was evaluated using transwell 6 well plates. $1x10^5$ MDA-MB-231 and MCF-7 breast cancer cells were plated in the bottom compartment of the well and allowed to adhere for 4hrs prior to experiment. $1x10^5$ macrophages or fibroblasts or macrophages cultured with fibroblasts were cultured in transwell inserts of 6 well plates. Cells were incubated at 37 °C, 5% CO2 for 1, 2,3,4,5 and 6 days and media was replaced with fresh media after 3 days of incubation. Inserts that contain macrophages were replenished with new differentiated macrophages after 3 days of culture. Cell count was daily performed using hemocytometer and the experiment was repeated 3 independent times.

2.14 Evaluating macrophages role in breast cancer single cell clones

2.14.1 Generating single cell clone

Breast cancer cells including MDA-MB-231 and MCF-7 were grown in RPMI media until they reached 80-90% confluence. Cells were trypsinised and counted at density approximately 15000 cells/ml as a final volume. In order to get a single cell, 200µl from cell suspension were pipetted into first column of 96 well plates (A1-G1) using a multichannel pipette. 100µl from first column were taken and added into second column (A2-G2) which already contains 200µl of fresh media. Cells were mixed up and down at least 3 times in order to get a second cell dilution. Another 100µl were taken from the second column and added into the third one (A3-G3). This was repeated for third, fourth and so until reaching (A11-G11) column. Another dilution was

applied in another 96 well plates by taking 100µl from (A11-G11) column and pipetted into the first column (A1-G1) of the other 96 wells which already contains 200µl of fresh media. This dilution was also applies sequentially to the last well of the second 96 well plates. Wells were incubated in tissue culture incubator with a regular monitoring once a week to ensure wells that contain 1 cell per well are healthy growing. Once cells started to proliferate and cloning, at least 3 different clones from each MDA-MB-231 and MCF-7 cells were washed 3 times with PBS and trypsinised with trypsin (10µl per well) and transferred into 12 well plates. Once the cells are confluent, cells were transferred into 6 well plates for cell expansion until they eventually were transferred into 25ml flask. Cells were frozen in -08 until use.

2.14.2 Co-culture of macrophages with breast cancer cells using long term model

Single cell clones from MDA-MB-231 and MCF-7 were grown in RPMI media until they reach 90% confluence. While breast cancer cells were grown, $1x10^6$ Thp-1 cells were pipetted into transwell inserts of 6 well plates and differentiated into macrophages-like by 25ng/ml PMA treatment for 48hrs. Macrophages were washed 3 times with PBS then allowed to rest in fresh media for another 48hrs. Same amount of MDA-MB-231 and MCF-7 breast cancer cells were seeded in triplicate into bottom compartment of 6 well plates 4hrs prior to experiment to allow cell attachment. Macrophages inserts were placed on top of breast cancer cells and incubated for 30 days in tissue culture incubator. Macrophages were replenished every 4 days and both breast cancer cells were split every 3 days deepening on cells confluence. After 30 days of co-culture, breast cancer cells were lysed with Trizol for RNA extraction and labelled as “long term incubation”, or cells were maintained in fresh media for another 1 moths post

macrophages removal, these cells were labelled as programmed breast cancer cells. Cells were expanded and frozen for future experiments.

2.14.3 Evaluating gene expression in breast cancer single cell clones

Single cell clones from MDA-MB-231 and MCF-7 were generated and incubated them with macrophages for short-term and long-term incubation as described previously. Here we have addressed a question whether programmed (P) breast cancer cell express genes including BIRC3, DKK, LAMC2, NRIDI and PER1 in MDA-MB-231 and FAS, ICAM1 and SOCS3 in MCF-7 cells compared to short-term (S) cells. However, breast cancer cells from different cultures including control C, S and P were harvested and lysed for RNA extraction. cDNA synthesis and RT-PCR analysis were conducted as described previously.

2.14.4 Cell migration assay

To overcome breast cancer heterogeneity and to evaluate macrophages effect on breast cancer cell migration after short-term and long term incubation with MDA-MB-231 and MCF-7 breast cancer cells, single cell clones were generated from heterogeneous MDA-MB-231 and MCF-7 cells. Breast cancer cells were incubated with macrophages either for 1 moth as described previously, or for 3 days. Breast cancer cells from long-term or short-term incubation with macrophages were labelled as programmed (P) or short-term (S) respectively. Activated breast cancer cells from both cultures above were allowed to rest for 1 moth in fresh media without incubation with macrophages. Cells were pipetted in triplicate into 6 well plates and allowed to grow until they reached a monolayer confluence. Cells were washed 3 times with PBS

then incubated overnight with serum-free media in order to prevent cell proliferation. To create a physical gap, cells monolayers were scraped with a 200µl pipet tip in a straight line in the middle of the well. Cells were incubated with different timescales and pictures of migrated cells were taken at different time points using a florescence microscope (EVOS FL). Wounds closure was quantified using imageJ 1.52u software.

2.14.5 Evaluating cell proliferation of programmed MDA-MB-231 and MCF-7 single cell clones

To better understand whether long-term incubation of macrophages with breast cancer cell clones differed from short-term incubation, and single cell clones of breast cancer cells will respond differently from heterogeneous breast cancer cells. We therefore set our experiment by generating single cell clones from both MDA-MB-231 and MCF-7 cell populations as described previously. Parental breast cancer cell clones at 1:1 ratio were co-cultured with macrophages for short-term incubation (5 days) or for long-term incubation (1 month). Cells from both cultures were allowed to rest in single culture for 1 month. $1x10^5$ MDA-MB-231 or MCF-7 in triplicate were plated into 6 well plates and incubated for 5 days without changing media. Cell count was performed ever 24hrs using hemocytometer technique.

2.15 Next Generation RNA Sequencing

MDA-MB-231 single cell clones at ratio 1:1 were cultured in triplicate with macrophages for 3 days and/or 30 days. After the indicated period of both cultures, breast cancer cells from long-term culture were allowed to grow individually in fresh media for further 30 days. Cells from all cultures were termed as following: Control

were labelled as (C), short-term co-culture were labelled as (S) ,long-term co-culture were labelled as (L) and those cells that grew individually after 1 month incubation with macrophages were labelled as programmed (P).

RNA was isolated from all cell populations as a first step of transcriptome sequencing. This step was performed accurately in order to ensure RNA concentration, purity and integrity values for this experiment. RNA purity was assessed by spectrophotometer and integrity was assessed by loading 1µg RNA on a standard 1.0% agarose gel, the RNA was mixed with Ethidium Bromide to enable bands visualisation on UV illuminator ChemiDoc imager.

2.15.1 Differential gene expression analysis

The analysis of differential gene expression is a process that calculates the total number of up and down-regulated in one sample under different cultures and conditions or between 2 or more samples. Three biological replicates were analysed using DESeq2 R and Volcano packages software. DESeq2 performs an internal normalisation for determining differential expression in digital gene expression data using a model based on the negative binomial distribution. The statistical *P* values for each step were arranged from smallest to largest using Benjamini and Hochberg's approach in order to decrease the False Discovery Rate (FDR). Clean data were obtained via removing adapter and poly-N, this step was performed via processing raw data of FASTQ through in-house scripts. All analysis of this step were performed with high quality and clean data. The threshold for significant expression was adjusted with 0.05 *p* values and $\log_2$ fold change. For gene overlapping, we used

an online “Venn” diagram web-tool (http://bioinformatics.psb.ugent.be/webtools/Venn/) in order to calculate the intersection between 2 or more lists of expressed genes.

2.15.2 Analysis of gene expression related cell migration and proliferation

Total RNA from programmed MDA-MB-231 and MCF-7 was isolated and reverse transcriptase was conducted as described previously. Primers for PCR amplification listed below in tables (7, 8) were designed using an online software system Primer3 (http://bioinfo.ut.ee/primer3-0.4.0/). RT-PCR reactions were conducted as shown before and GAPDH expression level was used to normalise our data. All reactions were separated on an agarose gel and visualised using ChemiDoc Imaging System.

Table 7 List or primers used for RT-PCR amplification in order to evaluate genes-related cell migration expression in MDA-MB-231 and MCF-7 breast cancer cells.

Gene name	Forward	Reverse
ARHGAP5	TCCCCCATCCTATACCATCA	CAGGCATTTGCTTCTGTTCA
PIK3R1	TTTGCCGAGCCCTATAACT	TGCATATACTGGGTAGGCTAGT
PIK3CA	TACCCAAATTGCTTCTGTCT	GCTTCAAATACATCCCACAT
ROCK2	TTCACGTCCGACCTGTTACC	GTGGCACCTACGGCACTCTA
ROCK1	TTCATGTCCGACCTGTAACC	TTGACAGCGTTCGAGGAGAG
PIK3CG	AGAGTTCCATATGATCCTGG	AATCTCTCCACTGCTGCCTG
MYL12A	CATTGCTCCCGTTGCCATTG	AACTGGAAGCAGTCGGAC
ITGB1	GATCAGTTCAGTTTGCTGTGT	TCCTTCCTGTAAAAATGTTGA

Table 8 List or primers used for RT-PCR amplification in order to evaluate genes-related cell proliferation expression in MDA-MB-231 and MCF-7 breast cancer cells.

Gene name	Forward	Reverse
ATR	CTCGCTGAACTGTACGTGGA	GCATAGCTCGACCATGGATT
MAD2L2	ACACGACAAGACCTCAACTT	CTGCTCCACATGAGACAAC
MCM2	CTCAGCATGGTCAAGTACAA	ACATCTTCATCGGTCAGTTC
MCM5	TTGACGAGTTTGACAAGATG	TAGCGGTTCTTCAGTTTCTC
GADD45G	AACTAGCTGCTGGTTGATCG	CGTTCAAGACTTTGGCTGAC
RB1	GTTTCATCTGTGGATGGAGT	AGCACCAATGCAGAATTTAT
CDC27	ACAGACAGCCTGAGACAGTT	GGCTATTTCCACTCTGTGAG

2.16 Statistical analysis

Statistical analysis of all graphs and calculations in chapters 3 and 4 were performed using GraphPad Prism software version 8.0. The statistical values of all analysed samples were reported as mean ± Standard Deviation (SD). T test or nonparametric tests of all data was performed by paired and two-tailed Student's t test (two independent groups), or one-way ANOVA test (multiple independent groups). P values of <0.05 were considered statistically significant of all tested samples. Differential expression analysis between two conditions/groups (three biological replicates per condition) was performed using DESeq2 R package. The use of DESeq2 software provided statistical routines for determining differential expression in digital gene expression data using a model based on the negative binomial distribution. P values were adjusted using the Benjamini and Hochberg's approach for controlling the False Discovery Rate (FDR). Genes with an adjusted P value < 0.05 found by DESeq2 were considered as differentially expressed. For RT-QPC analysis, bands intensity was calculated using using ImageJ (V. 1.38), and plotted in Prism V8.0 (GraphPad software). A p-value of ≤ 0.05 was considered as statistical significance between the samples of each group presented in figures.

Chapter 3

The findings of immunohistochemistry analysis

3. Immunohistochemistry

3.1 Antibody optimisation

Immunohistochemistry (IHC) is a critical technique used for detecting the location and abundance of specific protein in FFPE tissue section. Staining quality can be influenced by several factors such as antibody concentration, incubation time, temperature, regents used for IHC and the technique. Therefore, each antibody was serially diluted including the recommended dilution in order to achieve the specific staining with minimal background.

The following antibodies CD3, CD4, CD8, CD20, CD68, αSMA and Foxp3 were diluted using serial concentrations (1-50, 1-100, 1-200) including a negative control without using the primary antibody for each biomarker. Slides were viewed under a multi-header microscope (Olympus BX41opto-digital) using different resolutions (x10, x20, and x40) to determine the best antibody concentration, considering the staining intensity and specificity. Groups of slides were taken from each biomarker and scanned using Leica Bioscience Aperio AT2- scanner and viewed using the virtual pathology power wall to observe where the staining was located. For all optimisation images, scales within each image were set at 200µm, total slide image (slide thumbnail) on Aperio was shown on the top right of the screen, and the higher magnification window was shown on the bottom right screen.

3.1.1 CD3

CD3 is a co-receptor expressed on T lymphocyte cell surface which plays an important role in antigen recognition and T cell activation. CD3 was immunohistochemically stained by anti-CD3 antibody using serial concentrations (1-50, 1-100, 1-200) in order to get the desired concentration. 1-100 concentration was chosen as it showed the best quality of staining as shown in figure (22).

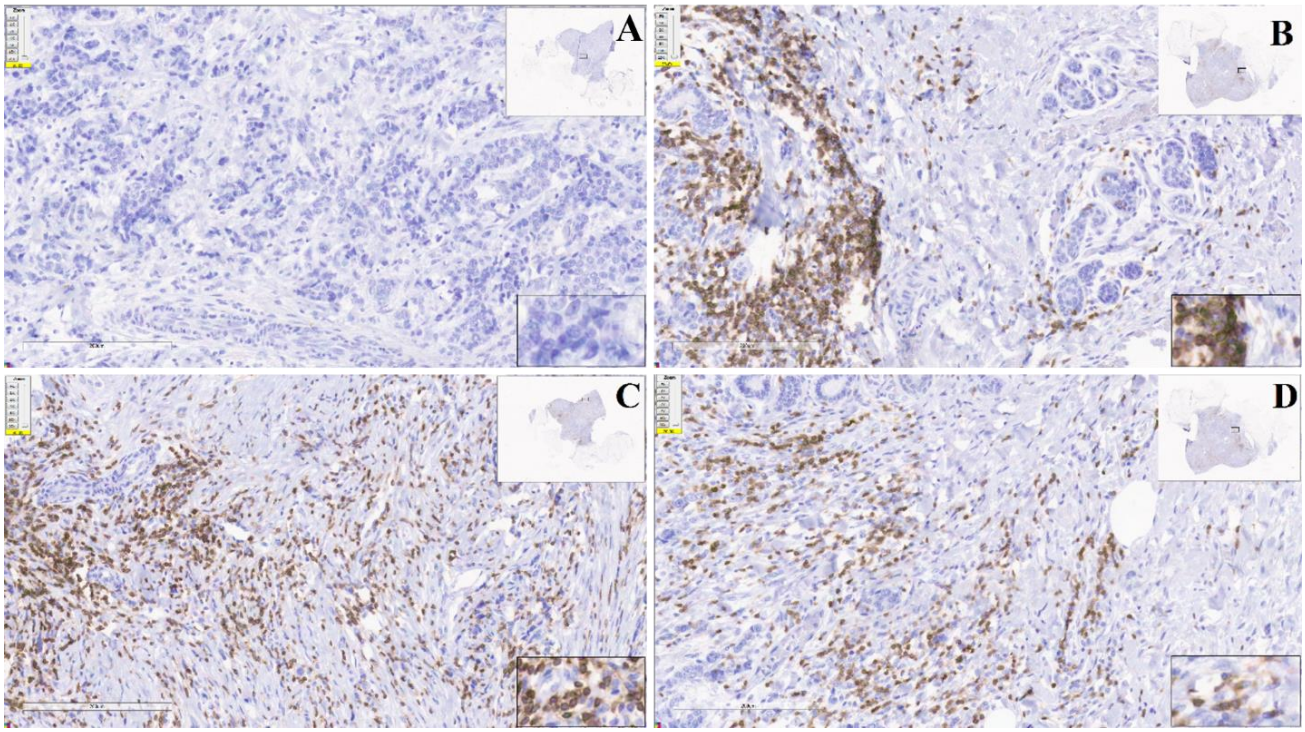

Figure 22 CD3 antibody optimisation **(A)** Negative control **(B)** 1-50 concentration **(C)** 1-100 concentration **(D)** 1-200 concentration. CD3 staining at 1-100 concentration yields low background and high specificity compared with other concentrations.

3.1.2 CD4

CD4 is a protein found on the surface of T helper cells that plays an essential role in augmenting cytotoxic T cell activation, also it participates in stimulating other type of inflammatory cells such as B cells and macrophages. CD4 receptor was stained by Anti-CD4 antibody using different concentrations (1-50, 1-100, 1-200). The 1-50 concentration was chosen due to it showed the best quality of staining because cells were uniformly stained by the antibody with no background staining (Figure. 23).

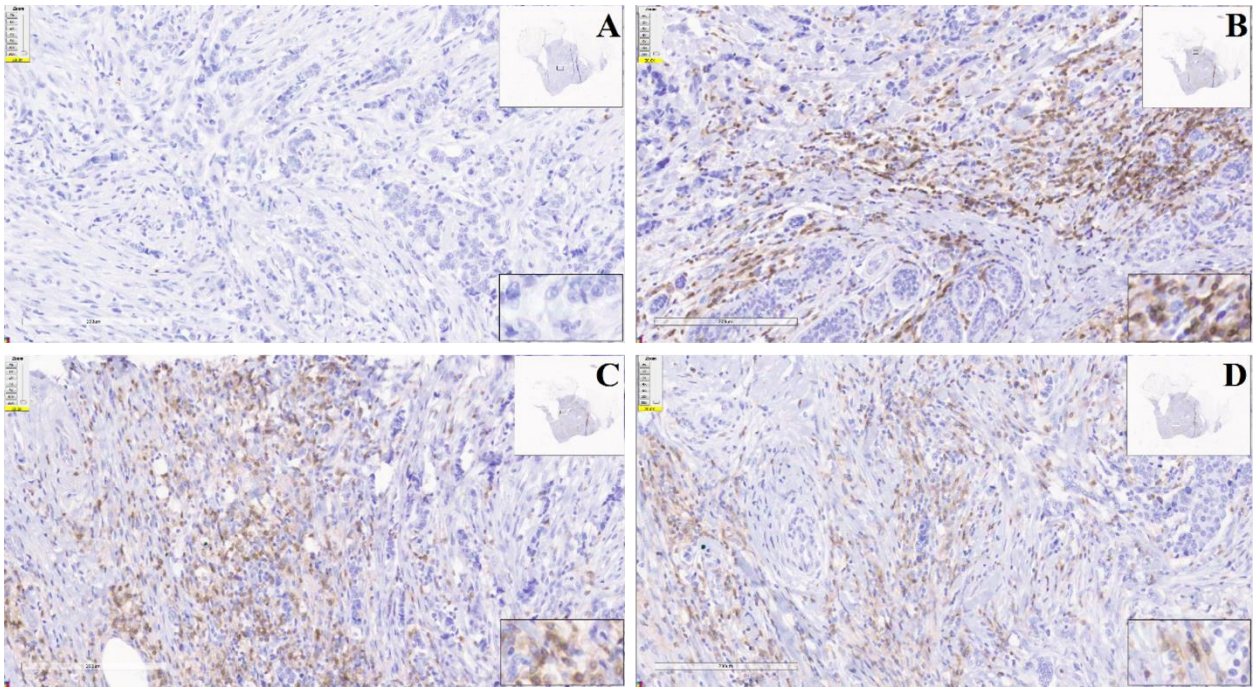

Figure 23 CD4 antibody optimisation **(A)** Negative control **(B)** 1-50 concentration **(C)** 1-100 concentration **(D)** 1-200 concentration. CD4 staining at 1-50 concentration yields low background and high specificity compared with other concentrations.

3.1.3 CD8

CD8 is a cell surface protein expressed mainly on cytotoxic T cell. CD8 plays a central role in antigens recognition presented on infected cells such as tumour cells. CD8 co-receptor can be detected by anti-CD8 antibody. The antibody was optimized using serial dilutions (1-50, 1-100, 1-200). The 1-100 concentration was chosen as it showed the best quality of staining with no background staining and the cells were uniformly stained (Figure 24).

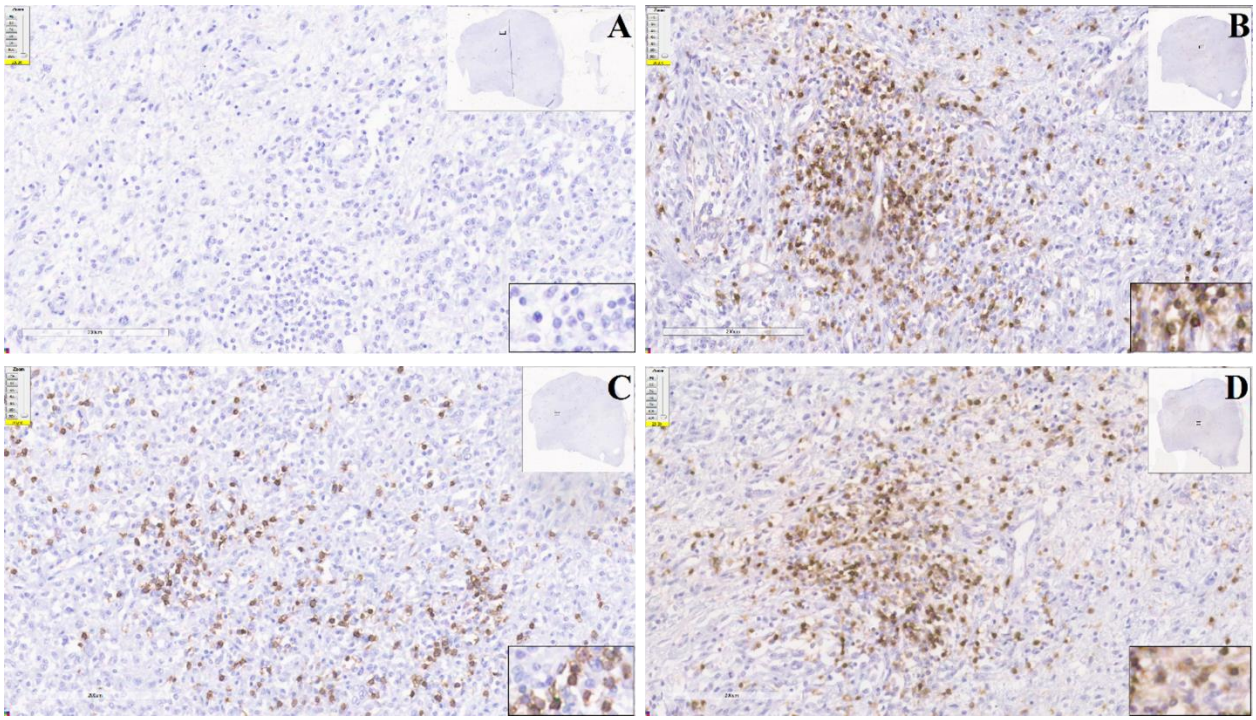

Figure 24 CD8 antibody optimisation **(A)** Negative control **(B)** 1-50 concentration **(C)** 1-100 concentration **(D)** 1-200 concentration. CD8 staining at 1-100 concentration yields low background and high specificity compared with other concentrations.

3.1.4 CD20

CD20 is a protein expressed on B cell surface. CD20 mediates B cell proliferation, development and B cell response against foreign antigens. CD20 protein was immunohistochemically stained by anti-CD20 antibody using serial dilutions (1-50, 1-100, and 1-200). The 1-100 concentration was chosen because it showed the best quality of staining and the cells appeared to be uniformly stained with no background staining (Figure. 25).

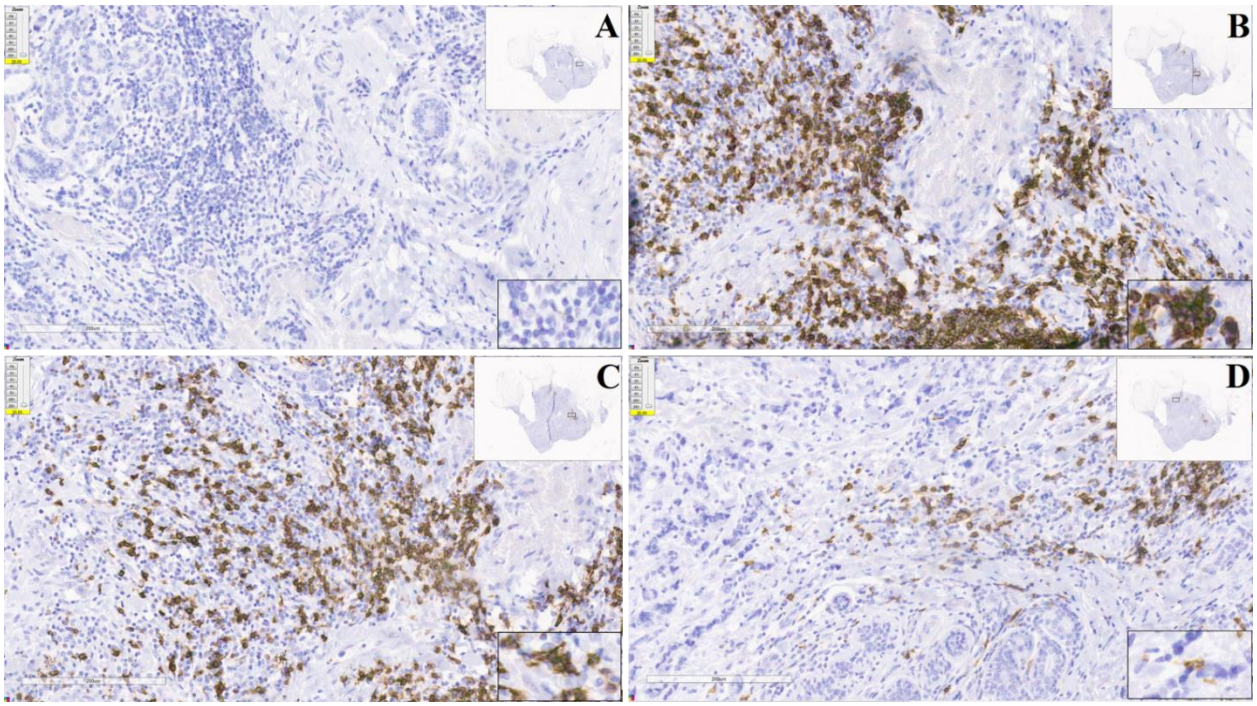

Figure 25 CD20 antibody optimisation **(A)** Negative control **(B)** 1-50 concentration **(C)** 1-100 concentration **(D)** 1-200 concentration. CD20 staining at 1-100 concentration yields low background and high specificity compared with other concentrations.

3.1.5 CD68

CD68 is a protein that is highly expressed by human monocytes and tissue macrophages. CD68 protein is involved in macrophages activation and recruitment, and promoting phagocytosis [215]. CD68 protein was immunohistochemically stained using serial dilutions (1-50, 1-100, 1-200). The 1-100 concentration showed the best quality of staining because it was specific to stain macrophages with no background (Figure 26).

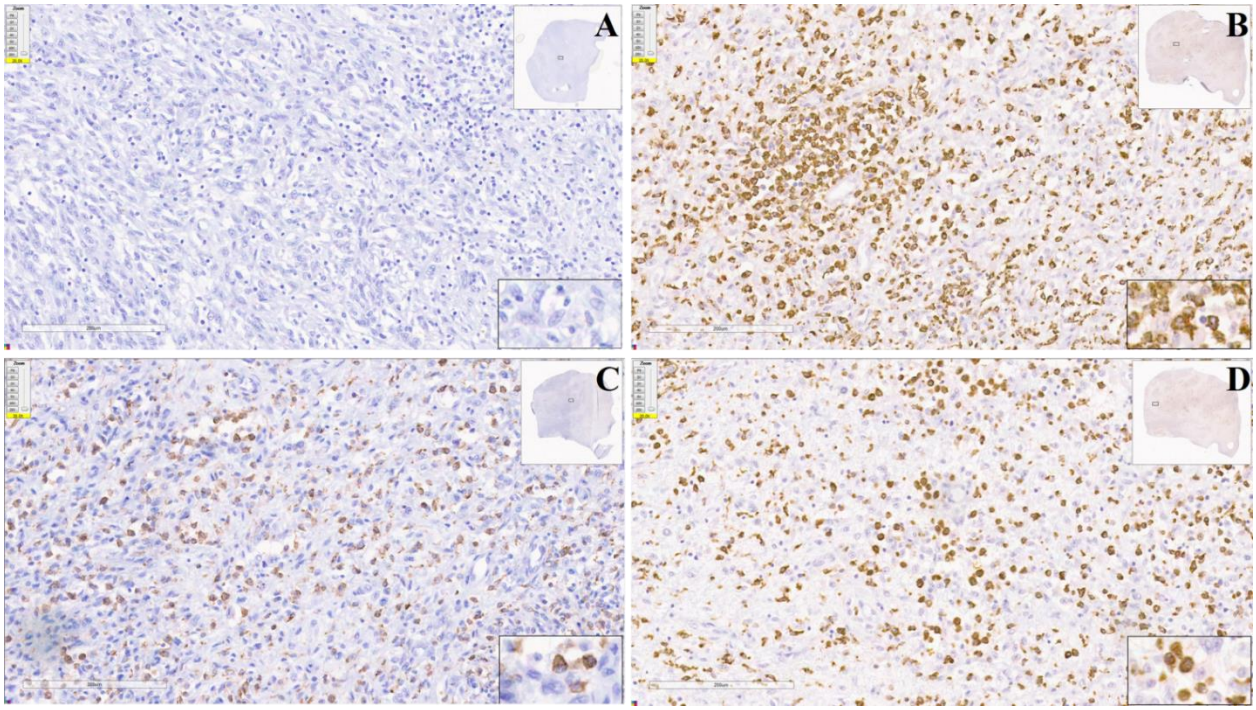

Figure 26 CD68 antibody optimisation **(A)** Negative control **(B)** 1-50 concentration **(C)** 1-100 concentration **(D)** 1-200 concentration. CD68 staining at 1-100 concentration yields low background and high specificity compared with other concentrations.

3.1.6 αSMA

Alpha-smooth muscle actin (αSMA) is a protein expresses predominantly in smooth muscle cells including fibroblasts, endothelial cells that lines blood vessels, myoepithelial cells and myofibroblasts. Anti-smooth muscle antibody is formed against smooth muscle cells. The antibody was optimized using serial dilutions (1-50, 1-100 and 1-200) in order to specifying the best quality of staining. The 1-100 concentration was chosen because cells were uniformly stained by the antibody with no background staining (Figure 27).

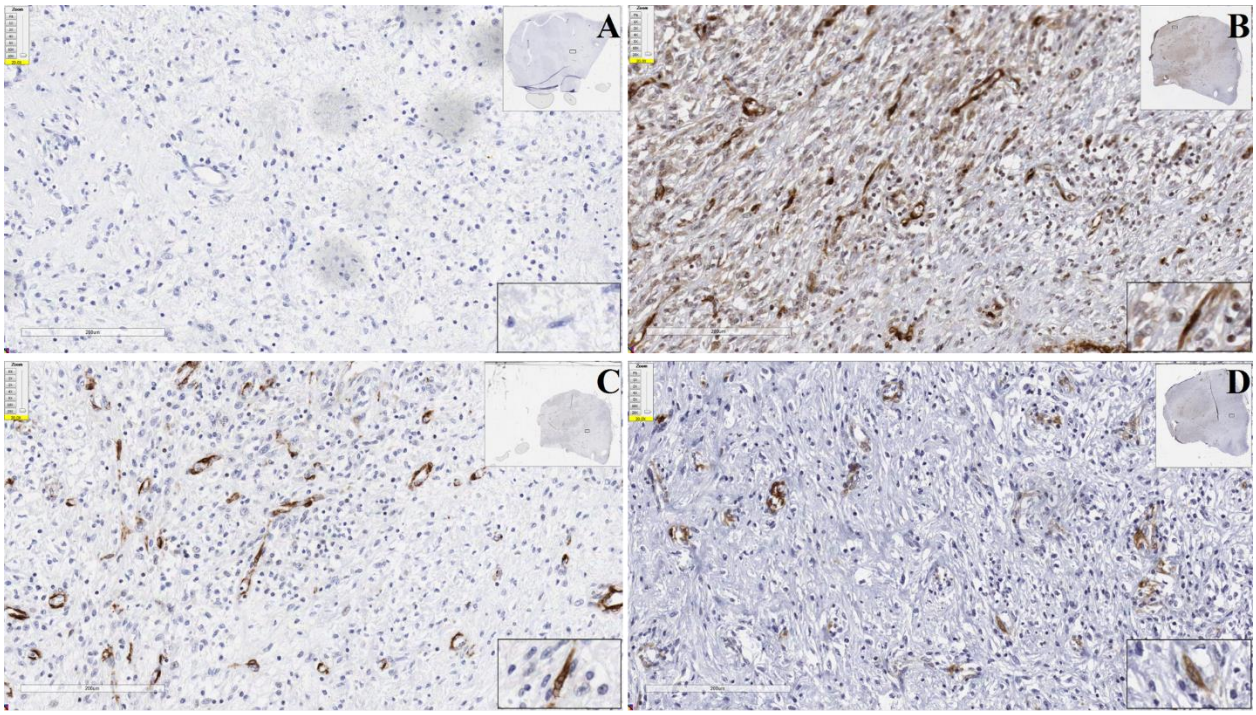

Figure 27 α-SMA antibody optimisation **(A)** Negative control **(B)** 1-50 concentration **(C)** 1-100 concentration **(D)** 1-200 concentration. A-SMA staining at 1-100 concentration yields low background and high specificity compared with other concentrations.

3.1.7 FOXP3

Forkhead box protein 3 (Foxp3) is an intracellular protein expressed in Treg cell, it plays an important role in Treg cell development and suppressing other immune cells. Treg cell was immunohistochemically stained by anti-Foxp3 antibody using serial dilutions (1-50, 1-100 and 1-200) to determine the specific concentration of the antibody. 1-100 concentration was used as the antibody uniformly stained Treg cells with low background as shown in figure (28).

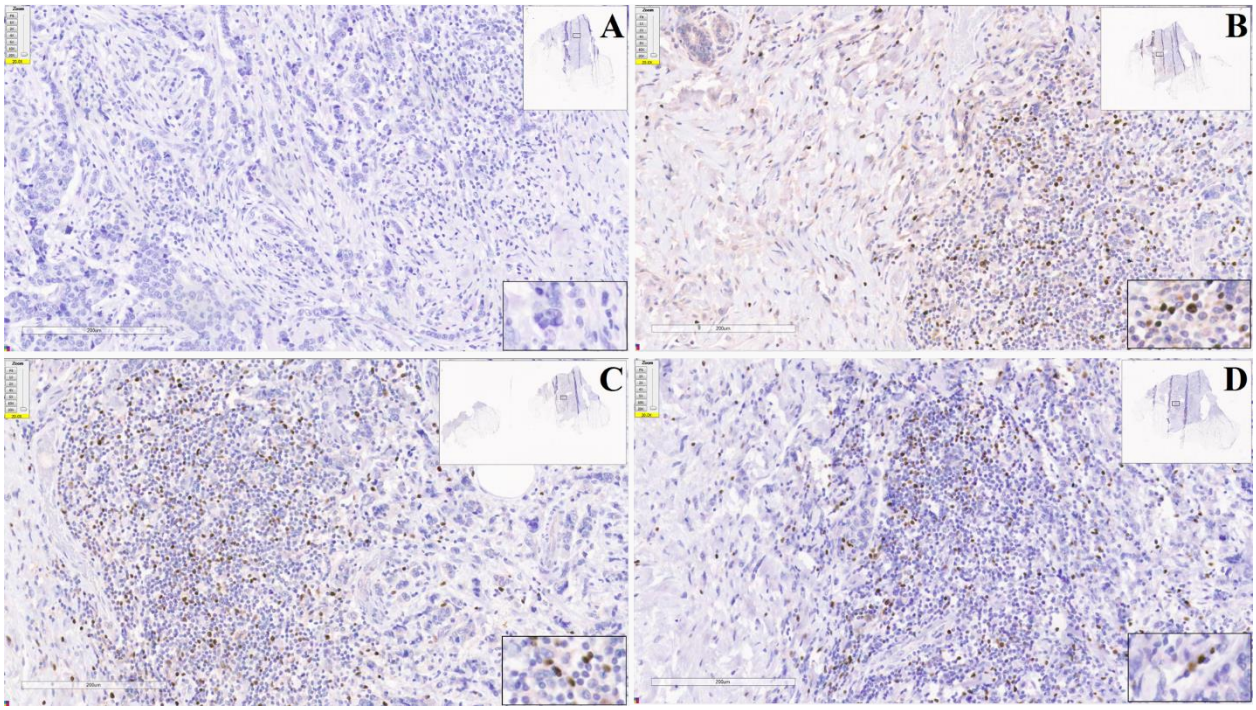

Figure 28 Foxp3 antibody optimisation **(A)** Negative control **(B)** 1-50 concentration **(C)** 1-100 concentration **(D)** 1-200 concentration. Foxp3 staining at 1-100 concentration yields low background and high specificity compared with other concentrations.

In summary, the antibody optimisation was conducted in tumour breast tissue using a range of biomarkers (CD3, CD4, CD8, CD20, CD68, α-SMA and Foxp3). Each primary antibody was serially diluted including negative controls. Considering strong and weak staining, the best concentration for each antibody was CD3, CD8, CD20, CD68, α-SMA and Foxp3 all in 1-100, CD4, 1-50.

3.2 Localization of T cell subsets, CD20+, CD68+ and αSMA in TNBC and ER+ breast cancer

A pilot assessment of full-face tissue sections from 50 TNBC and 20 ER+ breast cancer patient samples showed various distributions of lymphatic cells, macrophages and smooth muscle cells in the tumour and stroma tissue. The co-localisation of immune cells was determined using a power wall multi-screen viewer, which allowed us to view one tissue sample stained with different biomarkers.

In TNBC cases, high numbers of CD8+ and CD3+ T cells co-localized mainly in the stroma and the density of CD3+ and CD8+ was associated with other immune cells that accumulate at the tumour edge. Few CD3+ and CD8+ were seen in the tumour areas.

In the case of CD4+, occasional CD4+ cells infiltrated the stromal tissue. CD4+ cells were co-localised with CD3+ cells in stroma but were absent in the tumour. CD20+ cells were largely distributed in stromal tissue and CD20+ cell density was associated with other immune cells that accumulate in stroma tissue near to tumour cells. Occasional single CD20+ cells infiltrated within the tumour area. CD68+ cells were predominantly in the tumour with a large number of CD68+ cells also infiltrating the stromal tissue.

Foxp3+ cells were absent in the tumour, with occasional single Foxp3+ cells infiltrating in the stroma close to the tumour cells. αSMA+ cells were seen along the tumour edge, breast ducts and blood vessels. Few αSMA+ cells were seen in the tumour. Examples of these staining patterns are shown in figure (29).

In ER+ breast cancers, CD3+ and CD8+ cells were largely positive in the stroma as well as the tumour. The density of CD3+ and CD8+ cells was associated with other

immune cells that accumulated at tumour edge. A modest number of CD4+ cells infiltrated within tumour area. CD4+ cells were mainly distributed in the stroma. Few CD4+ cells were co-localised with CD3+ cells in stromal tissue. CD20+ cells were abundant in the stroma and the tumour is largely surrounded by CD20+. The density of CD20+ cells was associated with other immune cells that accumulate near to tumour cells. CD68+ were abundant in stroma tissue and the tumour was infiltrated with CD68+ cells. Large number of CD68+ and other immune cells infiltrated in stromal tissue surrounding the tumour cells. Foxp3+ cells were modest in the stroma and the majority of Foxp3+ cells were found with other immune cells near to tumour areas. Occasional Foxp3+ cells were seen within tumour area. αSMA+ cells were seen predominantly infiltrated within the stroma.αSMA cells were abundantly infiltrated at tumour edge as well as the tumour was largely infiltrated within CAFs with abundant αSMA+ cells among tumour cells with visible clusters shown in figure (30). Interestingly, the presence of CD3+, CD8+ and αSMA+ cells in the tumour microenvironment was different in both breast cancer subtypes, which showed high levels of infiltrated CD3+, CD8+ along with αSMA+ cells in the tumour and stroma tissue in ER+ specimens, whereas modest expression of CD3+ CD8+ and αSMA+ cells was assessed in TNBC samples. No differences were seen in CD68, Foxp3 and CD4 cells expression in both ER+ and TNBC breast cancer samples.

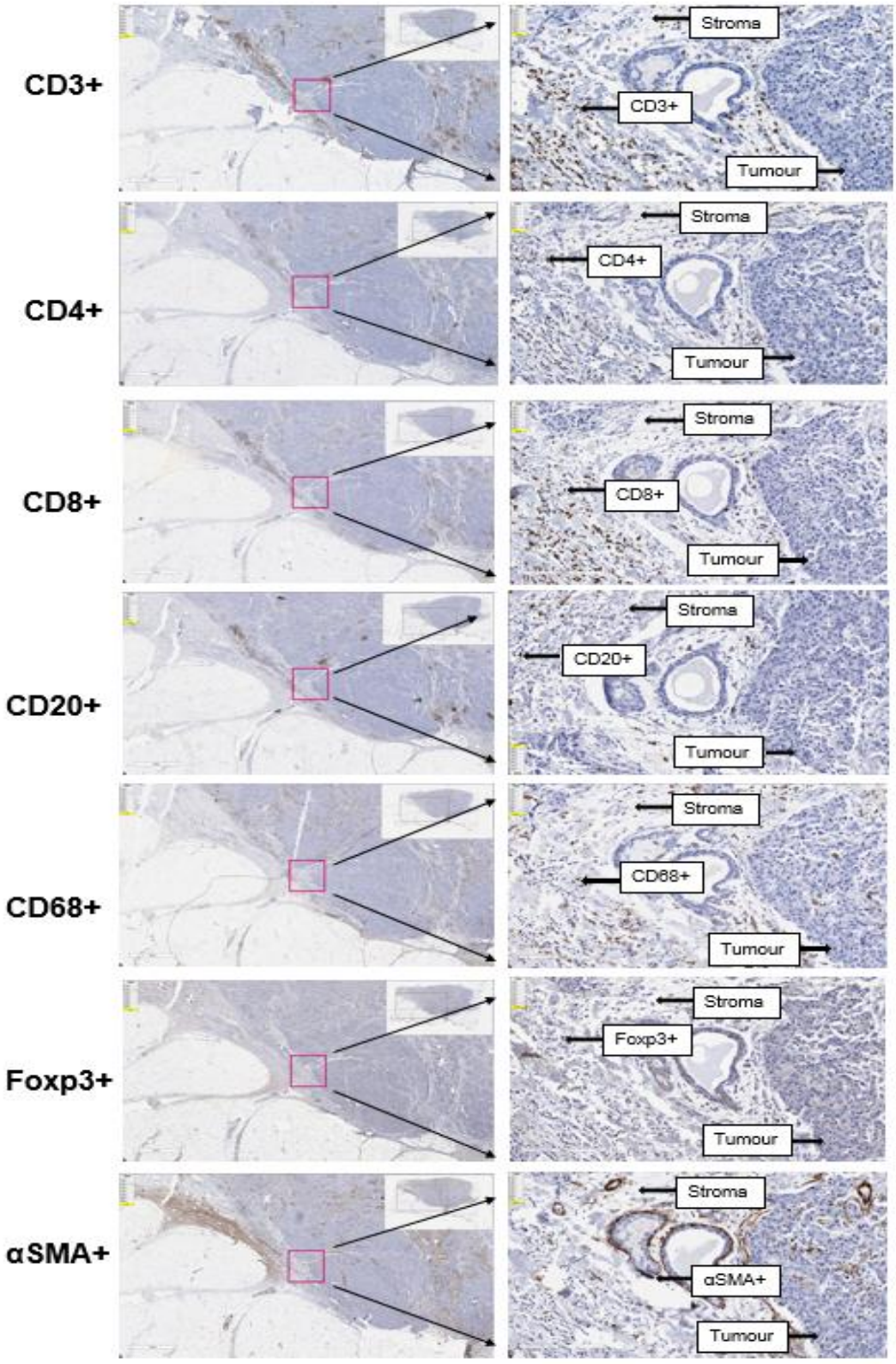

Figure 29 Representative example shows the localization of CD3+, CD4+, CD8+, CD20+, CD68+, Foxp3+ and αSMA in serial section from one case triple negative breast cancer. The distribution of stained cells was assessed using IHC staining and viewed using multi-screen viewer.

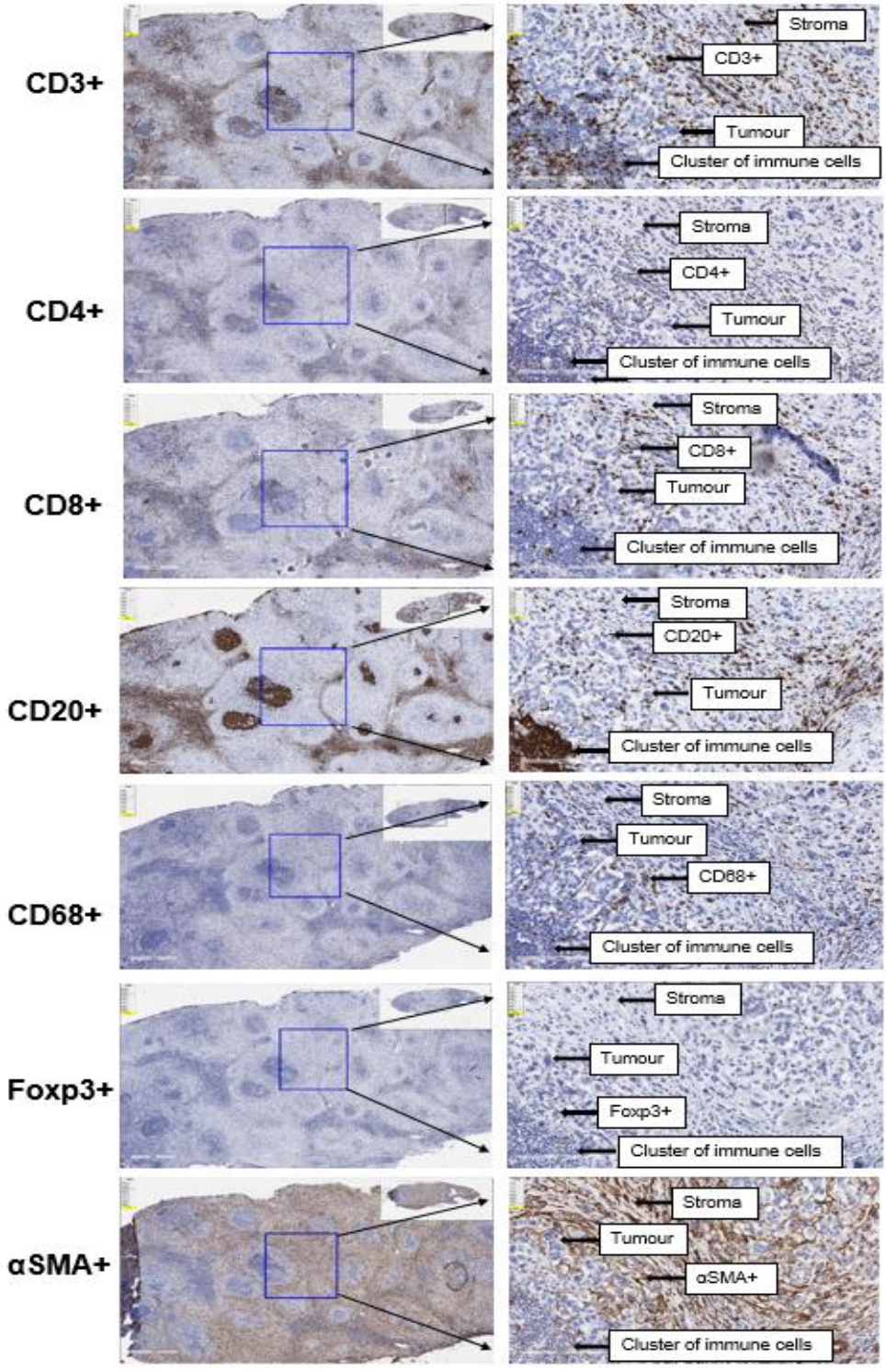

Figure 30 Representative example shows the localization of CD3+, CD4+, CD8+, CD20+, CD68+, Foxp3+ and αSMA in serial sections from one case of ER+ breast cancer. The distribution of stained cells was assessed using IHC staining and viewed using multi-screen viewer.

3.3 Positive pixel count optimisation (PPC)

The random generation of boxes was used to ensure the area selected were not biased. The number of boxes was examined to evaluate if a set number would detect an amount of positive pixels within the sample. To do this, 15 cases from ER+ and TNBC subtypes were immunohistochemically stained with CD3 antibody and visually characterized for 3 groups according to staining density high, moderate and low as described in methods (section 6). Slides were analysed using positive pixel count software after generating 10, 20 and 30 boxes on each slide as shown in figure (31).

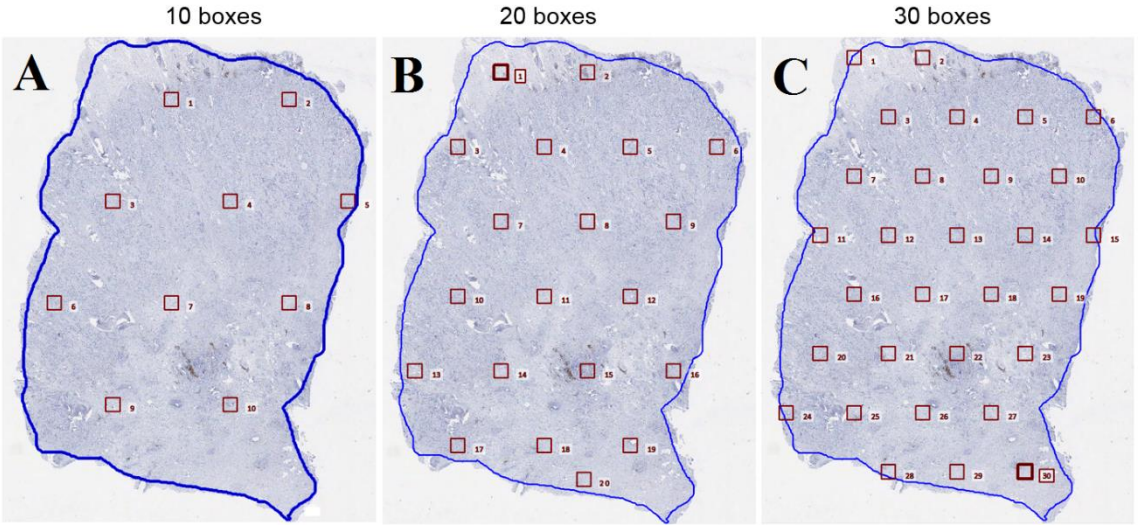

Figure 31 Example of box generation on a single sample. **(A)** 10 **(B)** 20 and **(C)** 30 boxes.

The mean value of CD3 abundance was calculated for each group. 10, 20 and 30 boxes across high, moderate and low abundance staining was evaluated. Results were presented in graph form using the Graph Pad (Figure 32).

The mean value of CD3 high abundance of 10 boxes was statistically analysed and compared with CD3 moderate abundance, this result was not significant. No significance was found when comparing CD3 moderate abundance 10 boxes with CD3

low abundance 10 boxes. Additionally, CD3 high abundance 10 boxes was also compared with CD3 low abundance 10 boxes and this was statistically significant. The same calculations were conducted on 20 and 30 boxes and CD3 high abundance was always significant when comparing with CD3 low abundance with 10, 20 and 30 boxes. The P value summary was more significant when comparing between CD3 high abundance and CD3 low abundance when using 30 boxes (P value = 0.0013) than when using 20 boxes (P value = 0.0040) and 10 boxes (P value = 00.75). Therefor 30 boxes were chosen to be generated on slides.

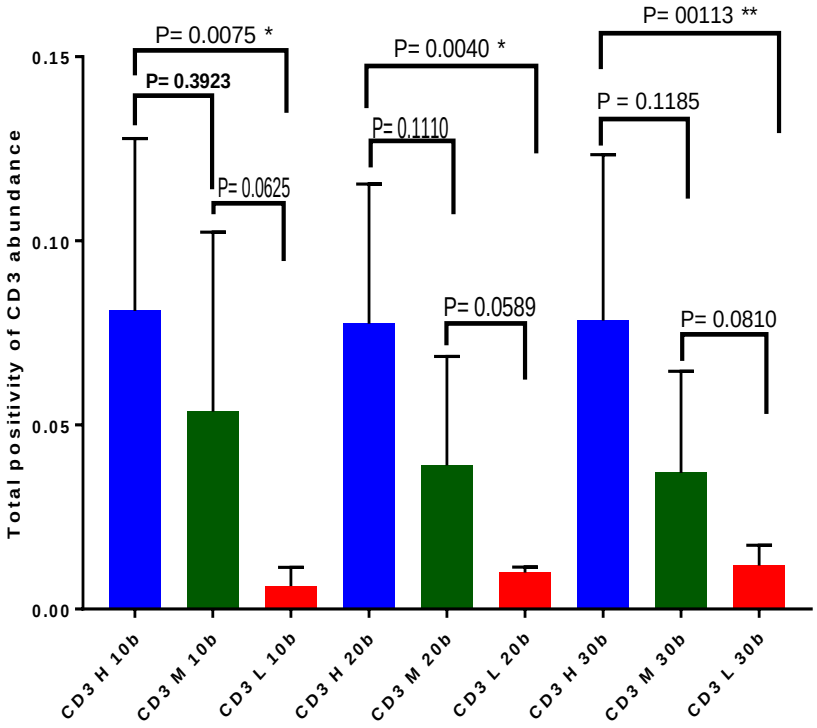

Figure 32 Greater significance detection by positive pixel analysis with 30 boxes compared with 20 or 10. Data shown was generated from 5 patient samples from low, moderate and high abundance of CD3 biomarker, in each group of boxes analysed. Data are presented as mean ± standard error and the analysis were performed and plotted in Prism V8.0 (GraphPad software). A p-value of ≤ 0.05 was considered as statistical significance between the samples presented in the figure.

3.4 Quantification of immunohistochemistry

Samples of 50 TNBC and 20 ER+ breast cancer were sectioned and immunohistochemically stained as described in methods section 1. The quantitative analysis of the lymphoid infiltrate, macrophages and smooth muscle cells was performed using PPC analysis. Clinical and pathological characteristics are shown in Table 1 (see methods section 1).

The mean value of PPC in ER+ breast cancer samples was CD3+ (4.2), CD4+ (1.2), CD8+ (4.1), CD20+ (3.9), CD68+ (3.7), FOXP3+ (0.3) and αSMA+ (25.4) while in TNBC the mean value of CD3+ was (3.6), CD4+ (1.17), CD8+ (4.3), CD20+ (2.4), CD68+ (5.8), FOXP3+ (2) and αSMA+ (19.6),

The staining profiles were evaluated in the total population under study and stratified as low/high grade, lymph node +/- and tumour size ≤20, 21-30 and ≥30 as shown in Tables 9, 10. Briefly, the mean value of cell number with high grade was CD3+ (4.01), CD8+ (4.71) and CD68+ (6.41) in TNBC samples. ER+ samples showed low positive cell numbers of CD3+ (2.1), CD8+ (2.3) and CD68+ (5.5). But no obvious difference was seen when comparing positive cells from low grade cases, CD3+ (0.48), CD8+ (0.91) and CD68+(2.40)) in triple negative cases compared to ER+ cases (CD3+ (10.9), CD8+ (11.3) and CD68+ (2.08)). The number of CD4+ (1.26) and CD20+ (2.56) positive cells in TNBC samples was higher than the positive cell number of CD4+ (0.5) and CD20+ (0.7) in ER+ with high grade tumour. In low grade tumour samples, the positive cell numbers of CD4+ (2.1) and CD20+ (9.2) were inversely correlated with low grade tumours in ER+ patient samples, while in TNBC patients CD4+ and CD20+ cell number was much lower (0.29 and 0.64 respectively). The number of Foxp3+ cells (1.80) in TNBC samples was far higher than Foxp3+ (0.2) cell number in ER+ in high

grade tumours. Also in low grade tumours, Foxp3+ (5.16) cell number in TNBC samples was higher than Foxp3+ (0.1) cell number in ER+ samples. In TNBC samples αSMA+ (20.4) cell number was lower than in ER+ samples (32.9) for high grade tumours. While this was not the case for αSMA+ in TNBC (15.7), compared to in ER+ samples (13.7) in low grade tumour.

ER+ and TNBC samples were stratified into lymph positive and negative cases. For lymph node negative samples the mean value of CD3+ (3.27), CD4+ (0.89), CD8+ (4.04), CD20+ (2.61), CD68+ (5.64) and Foxp3+ (1.46) in TNBC samples was higher than that seen in ER+ CD3+ (0.34), CD4+ (0.42), CD8+ (0.74), CD20+ (0.05), CD68+ (3.65) and Foxp3+ (0.26) cases. For αSMA, TNBC samples were lower (20.5) than that of ER+ samples (34.15).

In lymph node positive cases, which the exception of CD20, that same relationship was seen where the cell number of CD3+ (4.18), CD4+ (1.56), CD8+ (4.86), CD68+ (6.05) and Foxp3+ (2.79) in TNBC samples was higher than seen in ER+ samples (CD3+ (4.7), CD4+ (1.3), CD8+ (4.5), CD68+ (3.7) and Foxp3+ (0.3)). In TNBC the CD20+ (2.42) and αSMA+ (18.5) cells were lower than cells in ER+ samples (CD20+ (4.3) and αSMA (24.5)).

Furthermore, TNBC and ER+ samples were categorized into tumour size as shown in Table 1. The number of CD3+ (4.50), CD8+ (4.33), CD20+ (4.48) and αSMA+ (22.7) in ER+ was positively associated with larger tumour size (≥30 mm) in comparison with TNBC samples CD3+ (3.18) CD8+ (3.60), CD20+ (1.60) and αSMA+ (19.94) that was negatively correlated with large tumour size (≥30 mm). However, the opposite was true for CD4+ (1.46), CD68+ (5.48) and Foxp3 (2.20) in TNBC samples compared to ER+ cell number (CD4+ (1.28), CD68+ (3.81) and Foxp3+ (0.27) in tumours ≥30mm

in size. Within tumours sized 21-30mm, cell number of CD3+ (3.31), CD4+ (0.88), CD8+ (3.71), CD20+ (2.29), CD68+ (6.88) and Foxp3+ (2.21) was higher in TNBC than that seen in ER+ samples (CD3+ (2.94), CD4+ (0.83), CD8+ (2.97), CD20+ (0.93), CD68+ (3.40) and Foxp3+ (0.50)). For αSMA+ in this category (21-30mm), TNBC samples were lower (19.32) than αSMA+ in ER+ samples (40.7).

Interestingly, the number of CD3+ and CD8+ cells was significantly higher in high tumour grade than in low tumour grade in TNBC cases. In contrast, the number of CD3+ and CD8+ cells was positively correlated with low tumour grade and negatively with high tumour grade in ER+ samples. These findings have clearly showed the differences in the tumour microenvironment composition in both ER+ and TNBC breast cancer subtypes. No differences in the number of CD68+ and αSMA+ cells were observed in both subtypes, and the number of CD68+ and αSMA+ cells was significantly associated with high tumour grade in both ER+ and TNBC breast cancer samples.

Table 9 Immunohistochemical quantification of biomarkers analysed in 20 oestrogen receptor positive samples. Cell number count was conducted using PPC analysis and compared with clinicopathological features of breast cancer patients.

Biomarker	Total positivity % (mean)	Grade (N)			Lymph node (N)		Tumour size (N)		
		1(3) (15 %)	2 (10) (50%)	3(7) (35%)	+(18) (90%)	-(2) (10%)	≤20 (0)	21-30 (4) (20%)	≥30 (16) (80%)
CD3	4.2 (0.1-32.4)	10.9	3.78	2.1	4.7	0.34	N/A	2.94	4.50
CD4	1.2 (0.1-8.1)	2.1	1.42	0.5	1.3	0.42	N/A	0.83	1.28
CD8	4.1 (0.3-32)	11.3	3.23	2.3	4.5	0.74	N/A	2.97	4.33
CD20	3.9 (0.02-37.6)	9.2	4.56	0.7	4.3	0.05	N/A	0.93	4.48
CD68	3.7 (0.3-7.03)	2.08	2.97	5.5	3.7	3.65	N/A	3.40	3.81
FOXP3	0.3 (0.07-0.9)	0.1	0.38	0.2	0.3	0.26	N/A	0.50	0.27
αSMA	25.4 (1.7-48.1)	13.7	23.7	32.9	24.5	34.15	N/A	40.7	22.7

Table 10 Immunohistochemical quantification of biomarkers analysed in 50 oestrogen receptor negative samples. Cell number count was conducted using PPC analysis and compared with clinicopathological features of breast cancer patients.

Biomarker	Total positivity % (mean)	Grade (N) (%)			Lymph node (N) (%)		Tumour size (N) (%)		
		1 (3) (4%)	2 (7) (16%)	3 (40) (80%)	+ (46) (92%)	- (4) (8%)	≤ 20 (12) (24%)	21-30 (23) (46%)	≥ 30 (15) (30%)
CD3	3.6 (0.1-15.1)	0.48	2.82	4.01	4.18	3.27	4.84	3.31	3.18
CD4	1.17 (0.06-9.04)	0.29	1.01	1.26	1.56	0.89	1.32	0.88	1.46
CD8	4.3 (0.08-21.9)	0.91	3.76	4.71	4.86	4.04	6.50	3.71	3.60
CD20	2.4 (0.23-15.9)	0.64	2.84	2.56	2.42	2.61	4.02	2.29	1.60
CD68	5.8 (0.48-15.2)	2.40	3.79	6.41	6.05	5.64	4.26	6.88	5.48
FOXP3	2 (0.08-9.6)	5.16	2.14	1.80	2.79	1.46	1.57	2.21	2.20
αSMA	19.6 (2.8-37.2)	15.7	16.2	20.4	18.5	20.5	19.71	19.32	19.94

3.5 Collagen quantification by Picro Sirius red histochemistry

As collagen is the principal non-cellular component of the microenvironment, the potential difference in collagen density between ER+ and TNBC breast cancer patients (n = 20 per group) were histochemically evaluated using Picro Sirius Red staining and analysed using positive pixel count software as described in the methods section. The average total positivity in TNBC (88.6) was higher than in ER+ (83.5) samples. Cases were then stratified for grade, LN and tumour size and the results are shown in table 11. Collagen density in low-grade (88.5) was higher than high-grade (72) in ER+ cases, while there was no noticeable differences between low-grade (86.8) and high-grade (87.7) in TNBC cases. Collagen density was higher in node positive TNBC (88.9) than in ER+ (82.8). Furthermore, collagen density was higher in tumours ≥30mm in size in TNBC (88.1) than in ER+ (82.1) samples. In summary, overall, although collagen density was higher in TNBC than in ER+ cases, there was no statistical significance value between both breast cancer subtypes.

Table 11 Collagen density in ER+ and TN breast cancers. Cell number count was conducted using PPC analysis and compared with clinicopathological features of breast cancer patients.

Breast cancer subtype	**Total positivity % (mean)**	**Grade (N)**			**Lymph node (N)**		**Tumour size (N)**		
		1(3)	2(10)	3(7)	+(18)	-(2)	≤20 mm	21-30 mm (3)	≥30 mm (17)
ER+ (n = 20)	83.5 (33-99)	88.5	90	72	82.8	90.3	N/A	91.8	82.1
TNBC (n = 20)	88.6 (73-99)	86.8	93.7	87.7	88.9	88.2	93	88.1	88.1

3.6 Determination of ERα expression in fibroblasts

3.6.1 qRT-PCR

This study was conducted to determine if fibroblasts derived from ER+ breast cancer patients express ER-α gene, qRT-PCR was performed in three biological repeats as detailed in the methods section. Positive (MCF-7) and negative (MDA-MB-231) control samples, along with fibroblasts cells derived from ER+ (LS12-041) and TNBC (TCBI) breast cancer patients were analysed. ER-α was differentially expressed in these four samples. However, data from 3 independent experiments show that MCF-7 (positive control) cells showed significant expression of ER-α compared with MDA-MB-231(negative control). No expression was detected in MDA-MB-231 and fibroblasts cells derived from an ER+ (LS12-041) patient with low expression in the CAFs derived from a TNBC patient (TCBI) (Figure 33).

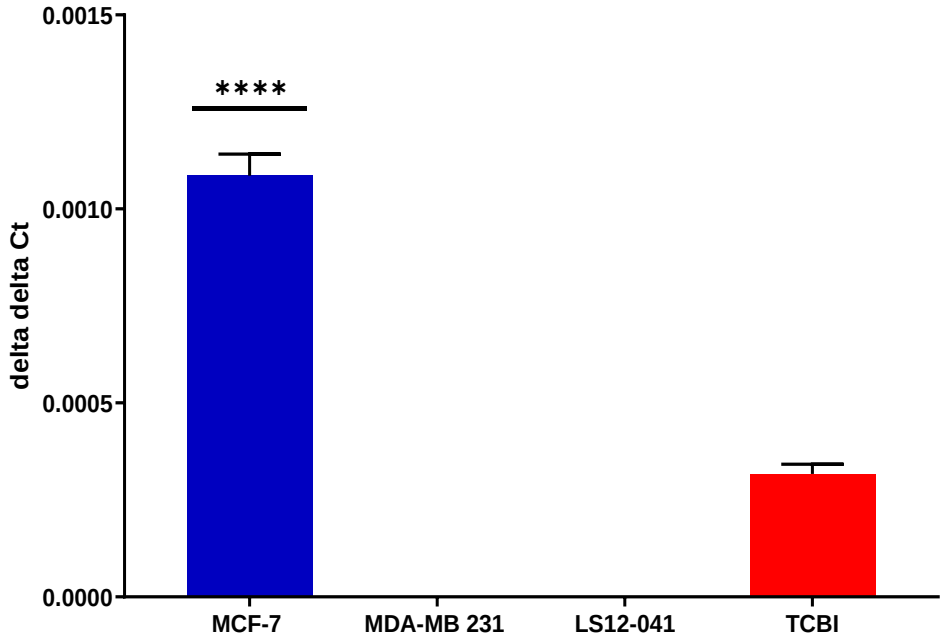

Figure 33 ER alpha expression by qrt-PCR analysis in MCF-7, MDA-MB 231 and fibroblasts cell line including LS12-041 and TBCI samples derived from ER+ and TNBC respectively. Data are displayed as mean values ± standard error of 3 independent experiments. A p-value of ≤ 0.05 was considered as statistical significance between the samples.

3.6.2 Immunofluorescence

MCF-7, MDA-MB-231 and fibroblasts (CAFs) derived from ER+ breast cancer cells were grown in a 12 well plate for 1 day in monolayer. MCF-7 cell lines were used as controls (+ve and –ve) alongside with MDA-MB-231 and CAFs were fixed using 4% PFA and incubated with specific primary antibody using ER-α and fluorochrome-conjugated secondary as described in the methods section. The fluorescent signal was captured with 20 seconds exposure time for the anti ER-α antibody. Results showed that MCF-7 displayed diffuse staining for ER-α which was localized to the cell nuclei. While ER-α expression was absent in MDA-MB-231 and CAFs derived from ER+ breast cancer patient as shown in figure (34).

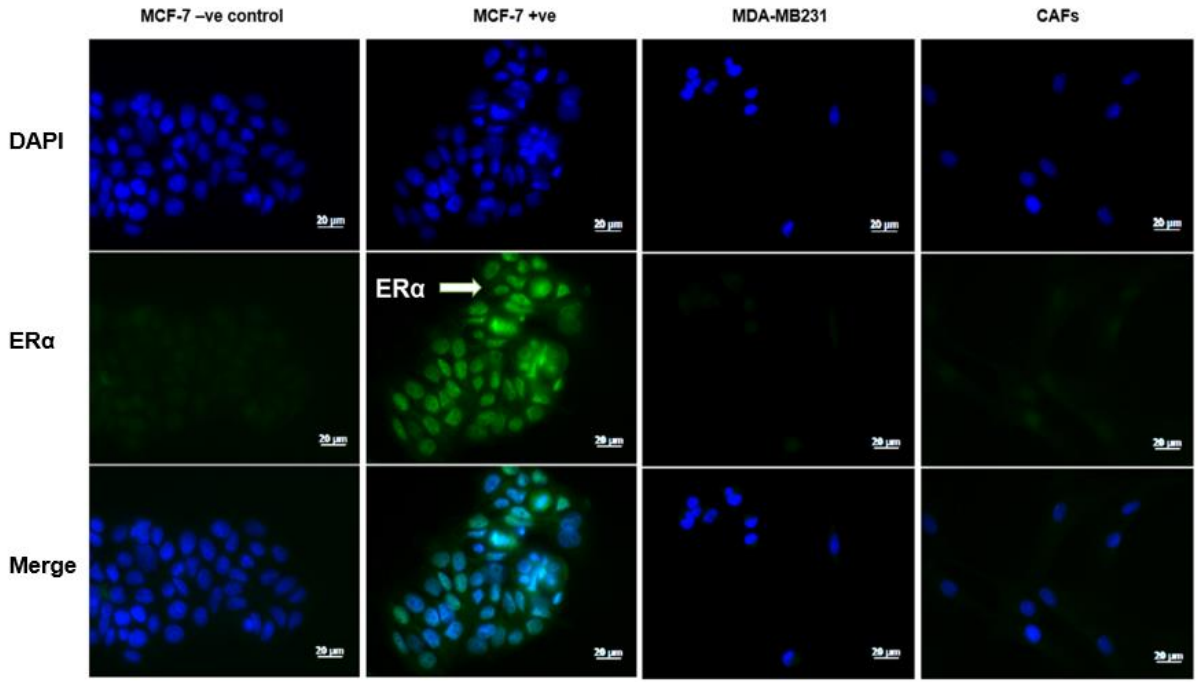

Figure 34 Immunofluorescent analysis of MCF-7 (+ve and –ve control), MDA-MB231 and CAFs using ERα antibody. ERα is expressed in the nuclei of MCF-7 cells but is absent from MDA-MB-231 cells and CAFs.

3.7 Raman Imaging

A pilot study examined one triple negative and one triple positive breast cancer sample. The mean raw spectra for each of the histological samples are shown in figure (35). Results revealed that Amide I and Amide III were clearly detected at (1620 –1680 cm^{-1}) and (1250 – 1270 cm^{-1}) respectively. Another vibration was also occurred at (2874 cm^{-1}) which attributes to a lipid region in both samples. [216]. Some vibrations occurred between 650 cm-1 and 1600 cm-1that attribute to amino acids, carbohydrates and nucleotides in the triple positive sample [217], whereas low intensity vibrations were seen in the triple negative sample. These preliminary findings revealed that it is possible to identify chemical components directly within samples. The exposure time should be increased to obtain a better signal-to-noise ratio and allow for larger areas to be mapped.

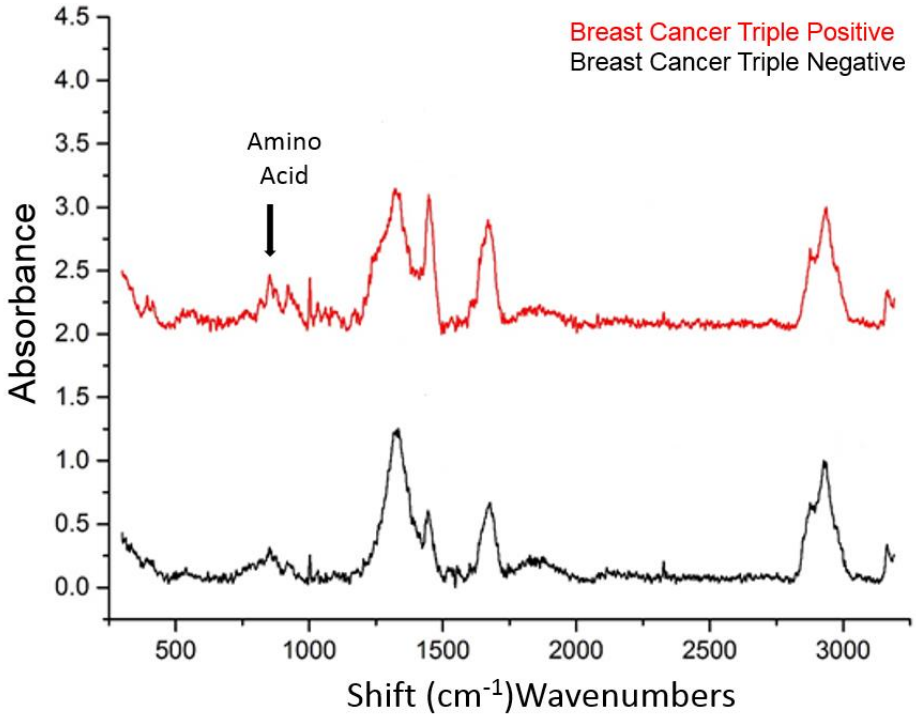

Figure 35 Raman map showing the intensity of the Raman shift at different points for triple positive and triple negative breast cancer tissue on stainless slides.

3.8 The effect of conditioned medium on breast cancer cell proliferation

This study was performed to test the effect of conditioned medium (CM) on cell proliferation, CM was generated from MCF-7, MDA-MB-231 and CAFs derived from ER+ and TNBC breast cancer patients as described in methods. Briefly, both epithelial cell lines and CAFs were cultured in a 96 well plate using regular culture medium and incubated for 24h at 37°C. Cells were then incubated with CM after washing and removal of the medium used for culture. Cell proliferation was tested using a live cell imaging system (Essen IncuCyte Zoom) which measures changes in true cell number (nuclear count) based on desired time-point using Incucyte Nuclight live cell labelling reagents. MCF-7 cell proliferation was affected by different CMs, both CMs of fibroblasts derived from ER+ and TNBC breast cancer inhibited MCF-7 cell proliferation in comparison with MDA-MB-231 CM that slightly effected MCF-7 cell proliferation (Figure 36).

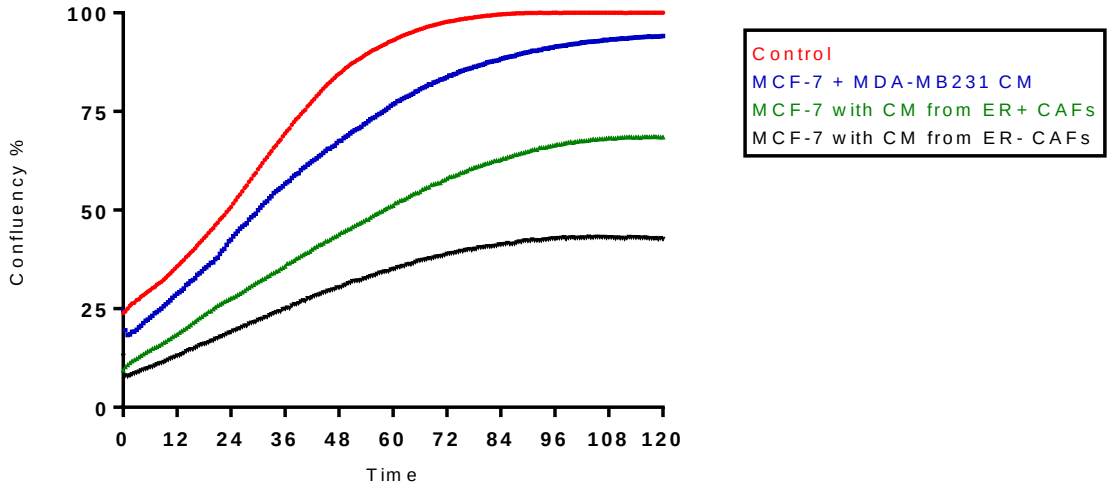

Figure 36 The effect of conditioned medium on MCF-7 cell growth. The experiemnt was conducted in 3 biological repeats and the mean value of 3 conducted experiemtns was calculated using GraphPad Prism V8.0.

Further investigation was performed on MDA-MB-231 cell in order to see the effect of CM on cell proliferation. However, fibroblasts derived from ER+ and TNBC breast cancer CM and MCF-7 CM slowed MDA-MB-231 cell growth with decreased cell number seen per well as is shown in figure (37).

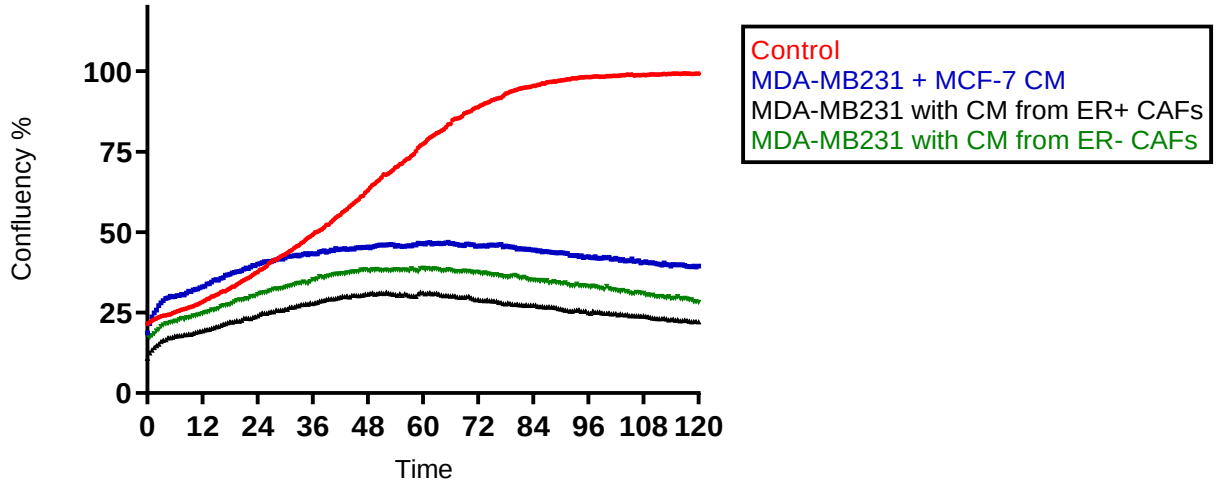

Figure 37 The effect of conditioned medium on MDA-MB231 Cell growth. The experiemnt was conducted in 3 biological repeats and the mean value of 3 conducted experiemtns was calculated using GraphPad Prism V8.0.

Moreover, fibroblasts derived from ER+ breast cancer patients showed the slowest cell growth in comparison with MCF-7 and MDA-MB-231 cells. CM from MCF-7, MDA-MB-231 and fibroblasts derived from TNBC breast cancer patients inhibited cell proliferation during incubation time as is shown in figure (38).

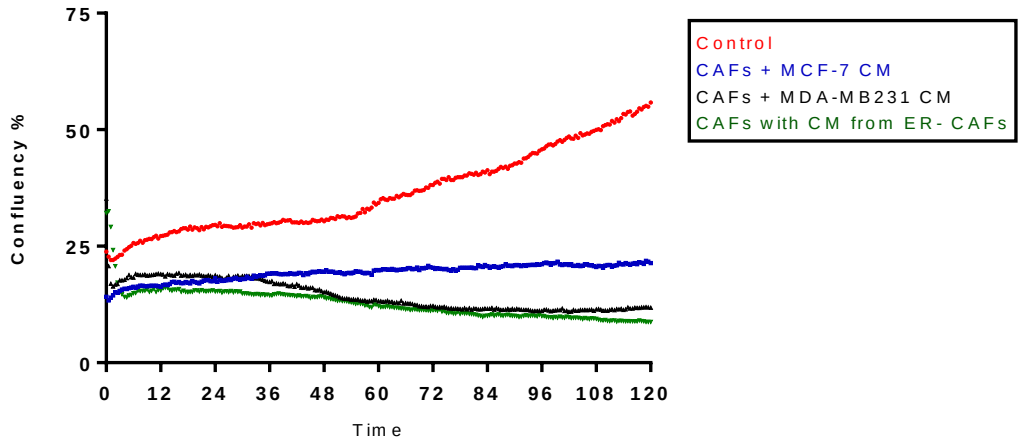

Figure 38 The effect of conditioned medium on cell growth of CAFs derived from ER+ breast cancer patient. The experiemnt was conducted in 3 biological repeats and the mean value of 3 conducted experiemtns was calculated using GraphPad Prism V8.0.

Interestingly, the growth of epithelial cell lines (MCF-7 and MDA-MB-231) and fibroblasts derived from ER+ breast cancer was differently effected by CM. Fibroblast CM slightly inhibited both epithelial cell lines.

3.9 The effect of Pirfenidone on cell proliferation

Pirfenidone (PFD) has been reported to have inhibitory effect on CAFs proliferation [218]. In this study the effect of PFD was evaluated in CAFs and breast epithelial cell lines, MCF-7 and MDA-MB-231. 5000 cells of each line and CAFs were seeded in 96 well plate as described in methods and treated with serial dilutions of PFD (100-1 µm). PFD significantly inhibited the proliferation of CAFs, MCF-7s and MDA-MB231 cells in a dose-dependent manner as shown in figures (39, 40 and 41). The proliferation of cells with 10µM of PFD was 15% in CAFs throughout the incubation time whereas it was higher in both MCF-7 and MDA-MB-231 when 50% confluency was seen after 60 hours. The effect of 1µM PFD showed no differences in MDA-MB-231 proliferation with that seen with 10µM PFD. Unlike MDA-MB-231s proliferation was slightly higher at 1µM PFD in CAFs compared with those that were treated with 10µM of PFD. MCF-

7 cell proliferation reached 100% after 60 hours with 1µM treatment, showing no overall effect on proliferation, however a growth delay was seen up until 60 hours. In agreement with the literature, we demonstrated that PFD inhibits cell proliferation in CAFs. A 100µM of PFD in each experiment was shown to be highly toxic to each cell line tested as shown in figure (42).

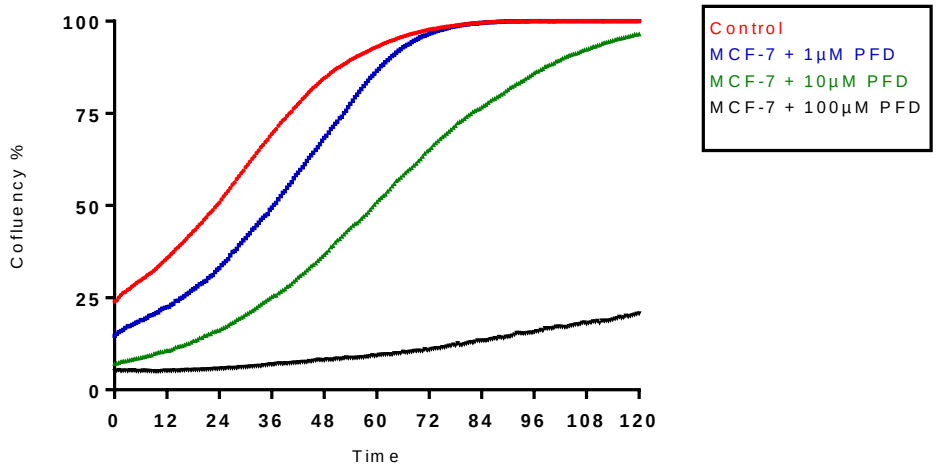

Figure 39 The effect of pirfenidone on MCF-7 cell growth. The experiemnt was conducted in 3 biological repeats and the mean value of 3 conducted experiemtns was calculated using GraphPad Prism V8.0.

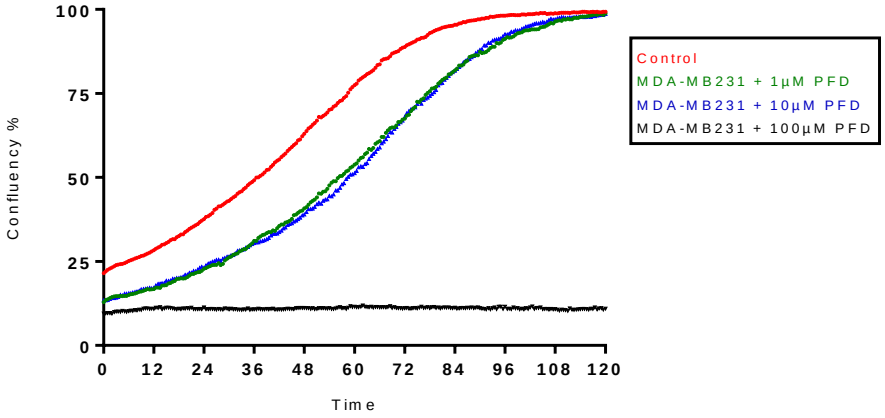

Figure 40 The effect of pirfenidone on MDA-MB231 cell growth. The experiemnt was conducted in 3 biological repeats and the mean value of 3 conducted experiemtns was calculated using GraphPad Prism V8.0.

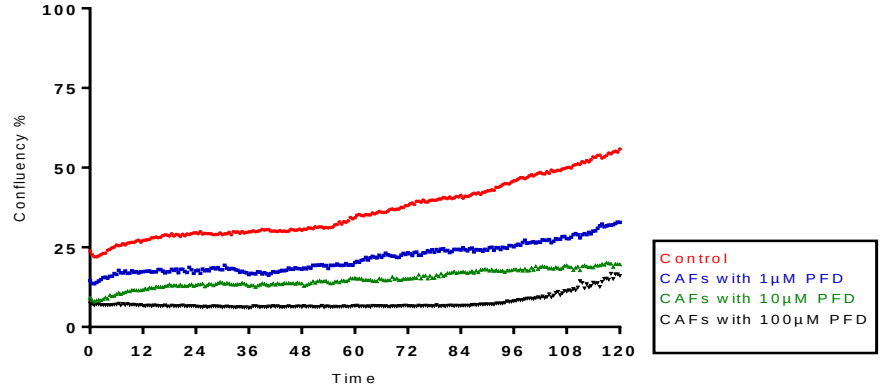

Figure 41 The effect of pirfenidone on CAFs cell growth. The experiemnt was conducted in 3 biological repeats and the mean value of 3 conducted experiemtns was calculated using GraphPad Prism V8.0.

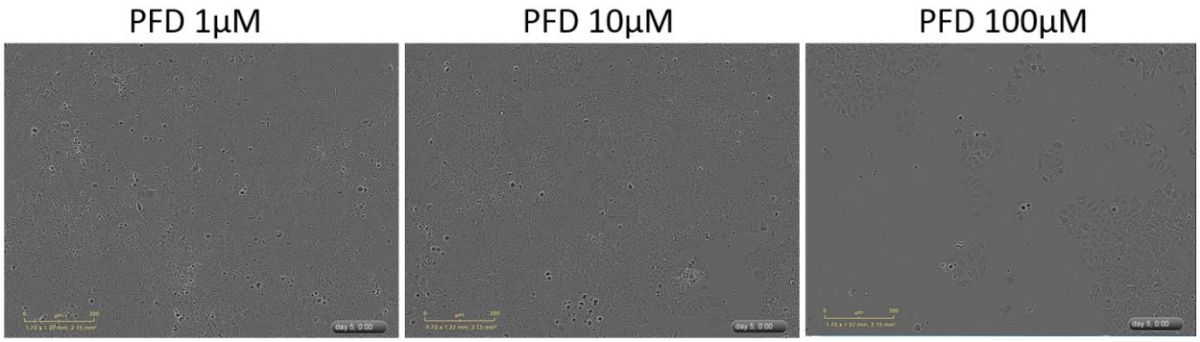

Figure 42 MCF-7 cell proliferation after 5 days incubation. Cells were treated with serial dilutions of PFD. 1 and 10 µM of PFD concentration slightly inhibited cell proliferation of MCF-7 while a sign of acute toxicity was seen with 100 µM of PFD.

Discussion

According to Gene expression profile studies, breast cancer is categorized into 3 subtypes based on the presence or absence of eostrogen receptor (ER), progesterone receptor (PR) and human epidermal growth factor-2 (HER-2). Lacking of all 3 receptors mentioned above, then the tumour is categorized as triple negative breast cancer (TNBC). The main focus of this project is to identify differences in the tumour microenvironment between ER+ and TNBC subtypes as ER+ represents the most common subtype among others, while TNBC is most likely to recur subtype as well as the most aggressive and metastatic disease due to lack of therapeutic targets [219].

Currently, breast cancer patients are treated with systemic therapy depending on which subtype was determined, patients with ER+ subtype are treated with endocrine therapy such as Tamoxifen to target oestrogen receptor, and patients with HER-2 positive are treated with HER-2 targeted antibody such as Herceptin to block HER-2 receptor. While patients with TNBC subtype are treated with specific chemotherapy such as doxorubicin, which binds to topoisomerase II enzyme that facilitates DNA replication [220]. In addition, immunotherapies have been also widely used in breast cancer treatment after promising outcomes were shown in early and late stages of breast cancer patients [221]. Immune checkpoint inhibitors such as Atezolizumab in combination with nab-paclitaxel are the most extensively immunotherapeutic agents used for blocking programmed cell deathligand-1 [222]. The PD-1/PD-L1 pathway represents an adaptive immune resistance mechanism of tumour cells. Blockage of this pathway via antibodies mentioned above releases the brakes of immune system to attach tumour cells [223-225].

Recent studies have evaluated that the cross-talk between tumour cells and immune cells play an essential role during variety of tumour progression such as tumour elimination, tumour growth, shaping immunogenicity, tumour migration, resistance to therapy and escaping immune surveillance [226]. Others studies have reported that high levels immune infiltration was associated with good prognosis [227]. In this study we performed IHC staining on 50 TNBC and 20 ER+ samples in order to evaluate the immune cells density and their association with clinicopathological characteristics of tumors. The prognostic value of tumour infiltrating T lymphocytes in breast cancer is still controversial [228]. However, the number of CD3+ and CD8+ cells was inversely correlated with high histologic grade in ER+ tumours, whereas, high numbers of CD3+ and CD8+ were positively associated with high histologic grade in TNBC tumours compared with low graded tumours. It was reported that increasing numbers of tumour infiltrated T lymphocytes in TNBC was associated with pCR, DFS and OS [229]. This indicates that TNBC tumours with high numbers of T lymphocytes are low proliferative and highly responsive to therapy. Contrarily, it was demonstrated that the number of T lymphocytes was negatively correlated clinicopathological outcome in ER+ patients, indicating that the distribution of T lymphocytes is associated with breast cancer molecular subtype [111]. The reason behind T cell distribution in breast cancer is still unknown, but according to best of our knowledge, high expression of CXCL9 and HLA class I histocompatibility antigen were found to play a big role in T lymphocytes recruitment and distribution among tumour cells [230-232]

Macrophages and fibroblasts are another contributors in tumour progression, which show a significant impact on clinical outcome of breast cancer patients [233, 234]. With regards to clinicopathological features of ER+ and TNBC tumours, macrophages and fibroblasts cell number was positively correlated with high histologic grade in both

molecular breast cancer subtypes. The mechanism of the positive correlation between histologic tumour grade and macrophages and fibroblasts is still controversial, however, it was reported that the increased levels of hypoxia-associated tumour necrosis was found to be positively associated with high histologic tumour grade. Based on this tumour cells therefor attract macrophages toward tumour nest in order to contribute to blood vessels formation known as angiogenesis [235]. Furthermore, breast cancer secreted factors such as CCL-2 promote macrophages recruitment toward tumour site [236]. Although in our study we were able to evaluate to distribution of immune infiltration in our breast cancer samples, our limited samples would have impacted our pooled estimates. Further studies are still needed in order to better understand the mechanism behind immune cells distribution and their relation with tumour cells.

Chapter 4

Assessment of macrophages differentiation and their role in breast cancer progression

4. Macrophages cell line selection and differentiation

Macrophages are versatile cells derived from monocyte precursors which have the ability to functionally ingest and destroy dead and living microbial and host cells, as well as they maintain tissue homeostasis and respond to micro-organisms [237, 238]. Monocytes migrate through peripheral blood and extravasate into damaged tissue where they differentiate to macrophages [239, 240]. Human peripheral macrophages are non-proliferative cells and their replenishment is believed to be confined to the bone marrow, as well as their lifespan is limited [241]. To overcome these issues, monocytic Thp-1 cells are spontaneously immortalised cell line derived from a child who was diagnosed with acute monocytic leukaemia. Thp-1 cells are an alternative option for human peripheral blood macrophages with the advantage that they continuously proliferate and are easy to maintain in the lab. Moreover, they have been widely used as a model to study the biological and functional role of human macrophages in many aspects including cancer research [242, 243].

Several studies were performed in order to evaluate whether Thp-1 cells can be used as a model for human peripheral blood macrophages, these studies revealed that Thp-1 cells demonstrate characteristics, adherent properties, enhanced IL-1β production and showed remarkable phenotypic changes of human peripheral blood macrophages [244, 245]. Thp-1 cells are small suspension round cells that gain a macrophage-like phenotype after exposure to phorbol 12-myristate 13-acetate (PMA) treatment [246-249]. The conditions of stimulating Thp-1 into macrophage-like cells are various, particularly the length of exposure to PMA stimuli and the concentration used to expose Thp-1 cells to PMA as high concentration could be toxic to cells or it might up-regulate undesired gene expressions. However, this study is aiming to determine the optimal PMA concentration and incubation period with PMA stimuli under different

conditions. Once determined, the length of time in which the differentiated macrophages can maintain their phenotype post PMA removal known as (resting period) in single culture (macrophage alone) and/or co-cultured with breast cancer cell will be established. Reportedly, the co-culture of macrophages with malignant cells was found to promote macrophage differentiation and polarisation [250, 251]. To enable breast cancer cells to be co-cultured for 30-days as the main focus of this chapter is to conduct long-term co-culture of breast cancer cells with macrophages, the macrophage source will need to be refreshed. As such, it was necessary to initially determine how long the Thp1 cells can maintain a differentiated macrophage phenotype under breast cancer cell provision as this itself would determine how frequent the co-culture model would need to be refreshed.

4.1 The optimal concentration of phorbol-12-myristate-13-acetate (PMA)

The human monocytic Thp-1 cell line is frequently used as an alternative to human peripheral-blood macrophages having similar morphological and metabolic properties [252-254]. The cell line has distinct technical advantages in that the purification, and subsequent differentiation, of primary peripheral blood monocytes can be problematic due to ease of finding healthy donors. This is a more relevant issue whereby any protocols that require the long-term culturing of primary macrophages (e.g. 30 days) will require weekly bleedings from the same individual.

The Thp-1 cells are monocytic in nature and can be differentiated into macrophages when exposed to PMA treatment [210, 255]. Functioning as a phorbol ester, PMA activates the protein kinase C (PKC) pathway [255] and various concentrations (10-100ng/ml) have been reported for differentiating Thp-1 cells [255-258]. It is noted that by activating the PKC pathway, the use of high PMA concentrations could be toxic to

cells due to increase levels of genes related cell death (e. g., TNF-α, IL-8, MIP-1β and IL-1β) [210, 257].

As the reported protocols of PMA-dependent differentiation of Thp-1 cells vary immensely, it was important to first determine the optimal concentration of PMA treatment in our lab. To achieve this, Thp-1 cells were exposed to different concentrations of PMA treatment 10, 25, 50 and 100ng/ml for 48hrs as described in methods.

In order to determine the optimal PMA concentration, both assessments of cell adherence and gene expression level were used to assess the successful differentiation of Thp-1 into macrophages. The finding from 3 independent experiments revealed that all PMA concentrations successfully induced differentiation of monocytic Thp-1 cells into macrophages-like phenotype, this was noticed by changing in cell morphology and increased cytoplasmic volume relative to untreated cells as shown in figure (43).

Cell attachment to plastic was assessed via washing adherent cells 3 times with PBS in order to remove PMA and unattached cells. Notably many cells treated with 10ng/ml PMA were easily detached from the surface of the flask relative to other concentrations 25-100ng/ml which showed a stronger attachment to plastic. As cellular adherence is a key characteristic of terminally differentiated macrophages, this observation suggested that differentiation of Thp-1 cells with 10ng/ml PMA was not optimal. As no overt deficiency in cell adherence was noted with the other PMA concentrations, the more accurate assessment of macrophage differentiation by gene expression analysis was examined.

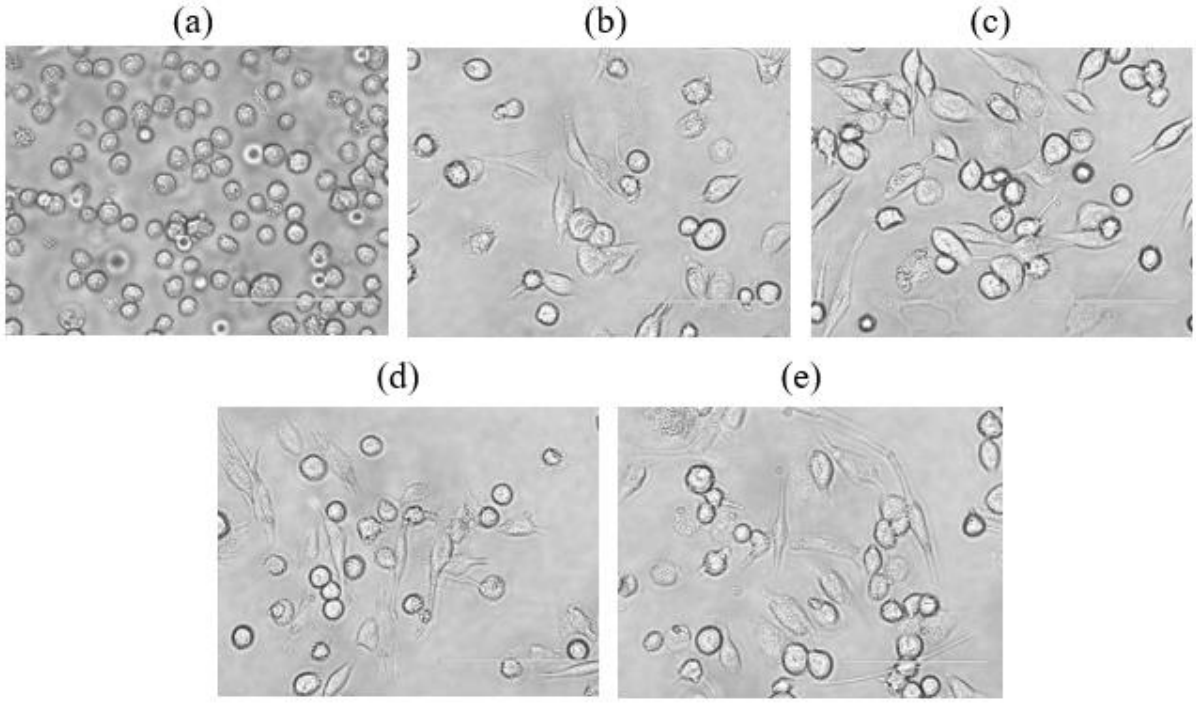

Figure 43 phase contrast microscopy of monocytic Thp-1 and macrophages-like cell morphology after exposure to different concentrations of PMA treatment for 48hrs as described in methods. **(A)** Untreated Thp-1 cells, **(B)** Thp-1 with 10ng/ml PMA, **(C)** Thp-1 with 25ng/ml PMA, **(D)** Thp-1 with 50ng/ml PMA, **(E)** Thp-1 with 100ng/ml PMA. Scale bar is 100 µm.

In the presence of different PMA concentrations, the relative transcript expression of macrophages-specific genes including CD11b, CD14, CD68 and TLR-4 was examined in order to determine the sufficient PMA treatment. Notably, expression of these chosen genes is widely used to discriminate between early-monocytes and terminally differentiated macrophages respectively [256, 258-260]. The treatment of Thp-1 cells with all PMA concentrations resulted in up-regulated expression of CD11b, CD14, CD68 and TLR-4 relative to undifferentiated Thp-1 which, notably, showed weak expression or no expression of indicated genes (Figure 44). This was an indication of successful Thp-1 differentiation regardless of PMA concentration. However, the induction of these macrophage-specific genes was weakest at 10ng/ml PMA which in support of the earlier findings, suggested a sub-optimal differentiation

of the cells. Treatment of the cells with higher PMA concentrations, (25, 50 and 100ng/ml), demonstrated a significant up-regulation of the CD11b, CD14, CD68 and TLR-4 genes. Of importance, there was no obvious significant changes in expression level of these four genes in cells treated with 25 and 50 or 100ng/ml as shown in figure (44). Collectively, these observations demonstrate that 25ng/ml PMA was found to be the lowest sufficient concentration to optimally stimulate monocytic Thp-1 to macrophage-like cells.

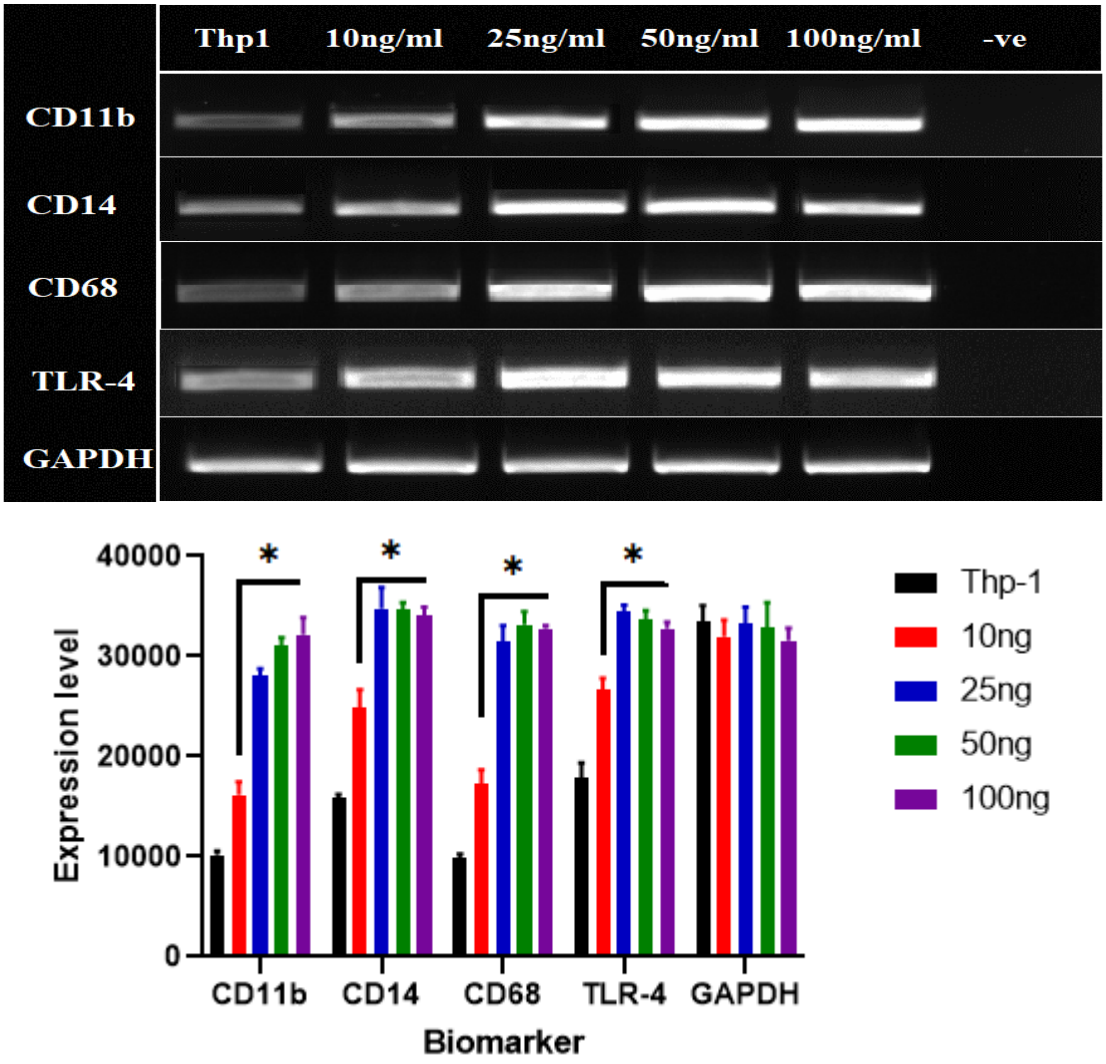

Figure 44 Gene expression of CD11b, CD14, CD68 and TLR-4 in macrophages-like differentiated from monocytic Thp-1 with 10, 25, 50 and 100ng/ml PMA for 48hrs. The expression level of the indicated genes was tested in different PMA concentrations using GraphPad Prism V 8.0. Data are displayed as mean values ± standard error of 3 independent experiments. A p-value of ≤ 0.05 was considered as statistical significance between the samples.

4.2 Determining resting phase period in stimulated Thp-1 post PMA removal

In our previous work it was possible to optimally differentiate Thp-1 cells into macrophages by incubation with 25ng/ml PMA for 2 days. However, a primary goal of this project is to co-culture the differentiated Thp1 macrophage with breast cancer cells and to then analyse the cross-talk activation between these two cells. In this regard, the presence of PMA cannot be maintained during the co-culture period as it would be very difficult to ascertain macrophage-specific activation of breast cancer cells to that of PMA itself. Notably, activation of the PKC pathway within breast cancer cells can induce growth arrest via several pathways such as mitogen-activated protein kinases (MAPKs), p21,p53 and c-Jun N-terminal Kinase (JNK) [261].

To determine that ability of Thp-1 cells to maintain the macrophage identity in the absence of PMA, cells were differentiated with 25ng/ml PMA for 2 days and the PMA washed out (2x PBS) with replenishment of fresh media. The macrophage phenotype of the cells was subsequently examined at both 2 and 4 days post-PMA respectively. In this study, the criteria in assessing the differentiated macrophages phenotype included (i) expression of macrophage-specific genes including CD11b, CD14, CD68 and TLR-4 as well as (ii) cell adherence. For clarity, samples included untreated Thp-1cells (Thp-1), cells treated with PMA for 2 days (no rest; NOR), 2 days rested cells (2DR) and 4 days rested cells (4DR) respectively. This experiment was performed in triplicate (3 independent biological repeats) and representative results from a single experiment is presented herein.

As previously demonstrated, the expression of all 4 macrophage genes were dramatically up-regulated upon PMA treatment for 2 days (NOR) compared to untreated cells (Thp-1) respectively (Figure 45). After removal of PMA and resting of the cells for a further 2 days (2DR), the relative expression of all genes was similar to

that of non-rested PMA-treated cells (NOR). A similar pattern was also identified when the cells had been rested for 4 days post PMA-removal (4DR) with the specific exception of TLR-4 transcripts which had a significant reduction in expression.

Albeit a limited analysis of genes, these observations nevertheless suggest a collapse of the macrophage network when Thp-1 cells are rested for 4 days post-PMA removal yet remain stable when rested for 2 days respectively.

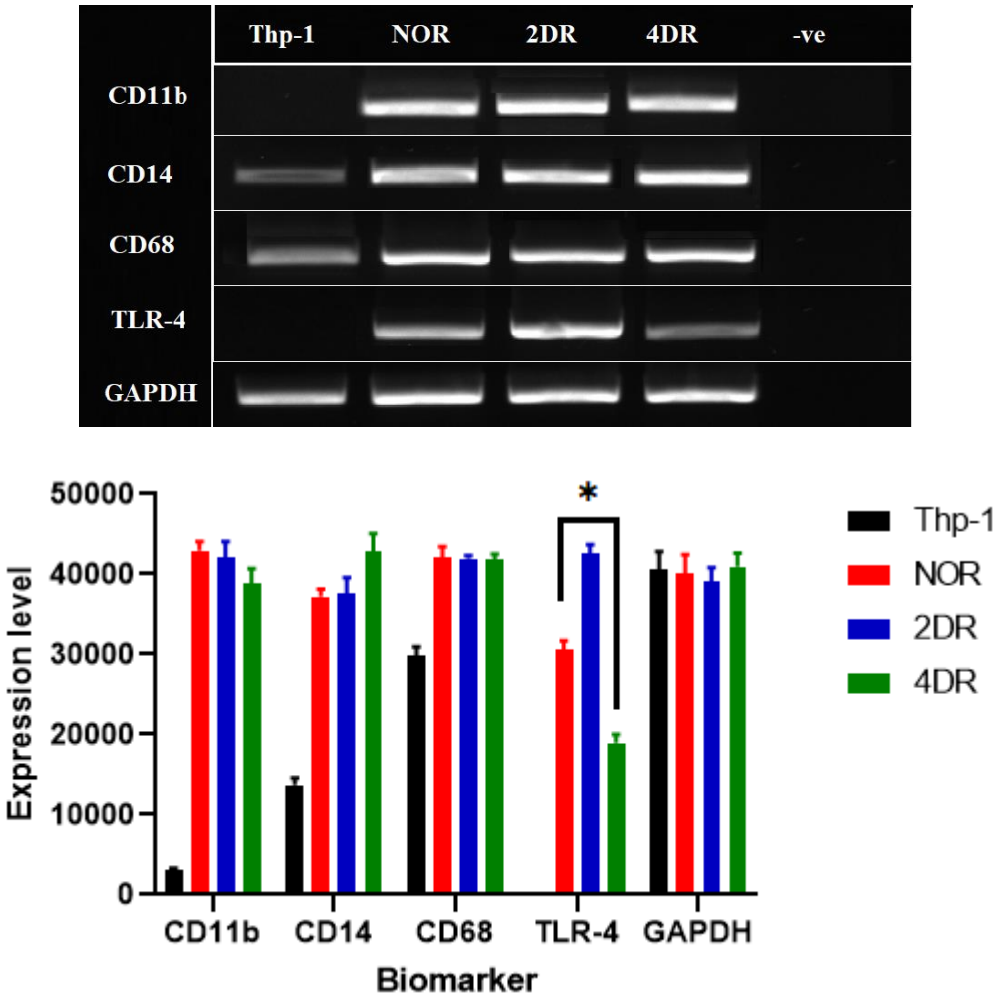

Figure 45 Representative image of gene expression including CD11b, CD14, CD68 and TLR-4 in Thp-1 cells (control), non-resting (NoR), 2 days rest (2DR) and 4 days rest (4DR). Data are displayed as mean values ± standard error of 3 independent experiments. The analysis were performed and plotted in Prism V8.0 (GraphPad software). A p-value of ≤ 0.05 was considered as statistical significance between the samples presented in the figure.

Cell adherence is a characteristic phenotype of macrophages [262] and this distinct property was used to further characterize the differentiation status of Thp-1 cells after the removal of PMA from the culture. As detailed above, the experimental conditions included PMA treated cells (2 days, NOR) and both 2 days (2DR) and 4 days (4DR) rest post-PMA removal respectively. In brief, 1-million Thp-1 cells were differentiated with 25ng/ml PMA and cellular adherence was assayed by removal of the culture media and the adherent cells washed 3x with PBS and subsequently trypsinised for counting of live cells by trypan blue exclusion.

The cell number in the figure below (Figure 46) represents the average of 3 independent experiments. In agreement with published reports [210], the PMA treatment of Thp-1 cells induced a rapid and efficient differentiation of the cells as approximately 94% of the population become adhered within 2 days (940,500 cells adhered, Figure 46). Once the PMA is washed from the media and cells allowed to rest for a further 2 days (2DR), the cells seem to maintain their macrophage phenotype with approximately 83% cells adhered. However, resting the cells for 4-days post-PMA removal resulted in a dramatic loss of adherence with only 51% of the cells adhered.

In conjunction with the gene expression profiling, it is clear that the macrophage cell state is unstable at 4 days resting post PMA removal as demonstrated by partial collapse of the gene network as well as the decrease of cellular adherence. Based on these findings, we evaluated that differentiated macrophages can keep their phenotype for no longer than 2 days post PMA removal as majority of cells still more adherent at 2 in comparison with cells at day 4 of rest.

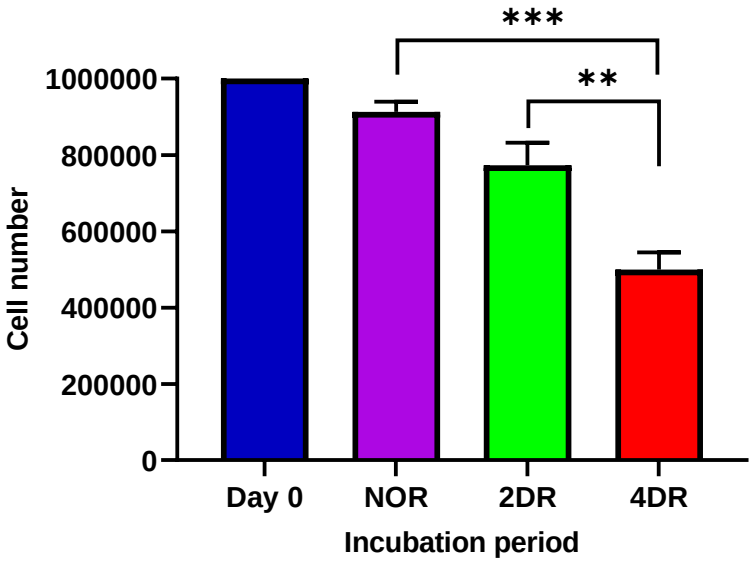

Figure 46 Cell survival rate in non-rested and resting cells macrophages post PMA removal relative to untreated Thp-1 (control). Data are displayed as mean values ± standard error of 3 independent experiments. The analysis were performed and plotted in Prism V8.0 (GraphPad software). A p-value of ≤ 0.05 was considered as statistical significance between the samples presented in the figure.

4.3 Evaluating gene expression of macrophages specific markers in detached cells

An interesting aspect of differentiated Thp-1 cells was the dramatic loss of cellular adherence when PMA was washed from the media; notably at 4 days of rest. The detached cells remained in the media suspension and were viable based on microscopic analysis (bright shiny cells with round circumference) and trypan blue exclusion (data not shown). This observation drew attention as to evaluate whether detached cells still express any macrophage phenotype or had reverted back the original Thp-1 lineage.

To further characterise these cells, Thp-1 cells were differentiated into macrophages with 25ng/ml PMA for 48hrs, cells were washed twice with PBS and incubated with

fresh media for 4 days. After 4th day of incubation detached cells were collected and RNA was isolated and analysed for expression of macrophage-specific genes by RT-PCR analysis. As a positive control, RNA from 2 days rested macrophages was included.

Data from a single experiment was performed showed that the gene expression profile revealed weak expression of CD14, CD68 and TLR-4 with an absence of any detectable transcripts for CD11b in comparison to the positive control (Figure 47). Although not the focus of this project, these results suggest that prolonged resting of differentiated Thp-1 cells (post-PMA removal) could promote a loss of the macrophage phenotype and reversion to the parental monocytic cell lineage.

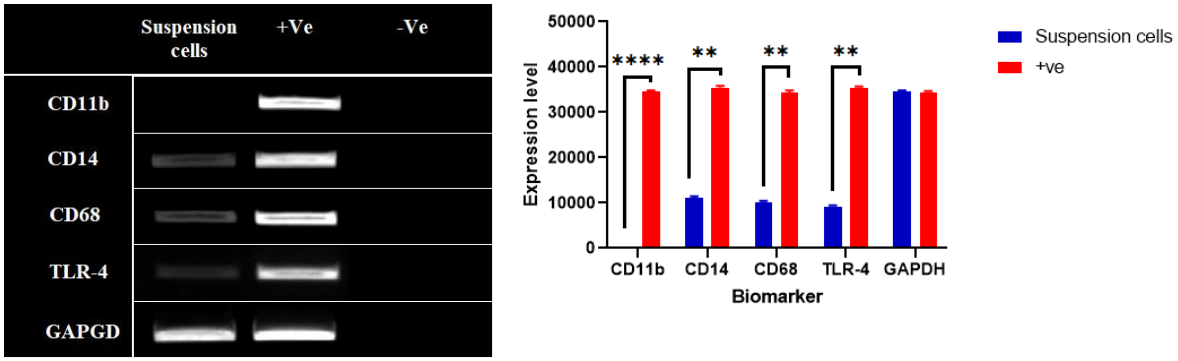

Figure 47 RT-PCR analysis of gene expression in suspension cells and differentiated macrophages post PMA removal. Bands intensity was calculated using ImageJ (V. 1.38), and plotted in Prism V8.0 (GraphPad software). A p-value of ≤ 0.05 was considered as statistical significance between the samples of each group presented in the figure.

4.4 Breast cancer cells promoted macrophage differentiation

The current characterization of the Thp-1 model has been performed in isolation with the cells analysed independent from interaction with other cells such as breast cancer lines. The findings herein demonstrate that differentiated Thp-1 macrophages can maintain their phenotype for no longer 2 days in single culture. Yet, it is well established that in the presence of tumour cells the survival and differentiation of macrophages is greatly enhanced primarily due to the provision of survival-signals from cancer cells which include IL10, TGF-β and M-CSF [263, 264]. From these observations, it is possible that the macrophage phenotype of Thp-1 cells (post-PMA removal) could be prolonged due to survival factors provided by cancer cells.

To explore this further, this experiment was designed to determine whether the presence of breast cancer cells could sustain the macrophage phenotype of Thp-1 cells compared to single Thp-1 culture. Briefly, $1x10^6$ Thp-1 cells were differentiated into macrophages with 25ng/ml PMA for 48hrs, cells were washed with PBS and incubated with fresh media for 48hrs to allow to cell recovery. After 48hrs resting (2DR), cells were incubated for further 2 days (4DR) or 4 days (6DR) in (i) single culture or (ii) co-cultured with 1-million breast cancer cells using the transwell system. Initial assessment of the macrophage phenotype was performed by quantifying cell adherence. Cell count was performed after every resting phase (48hrs of each incubation) as described in methods.

Data from 3 independent experiments demonstrate that in the absence of cancer cells, the average number of adhered macrophages markedly decreased to approximately 50% or 35% in 4DR and 6DR respectively. Yet, in the presence of MCF-7 or MDA-MB-231 breast cancer cells, the adherence of macrophages to plastic was sustained with 75% or 80% at day 4 or 65% or 75% at day 6 respectively as shown in figure (48).

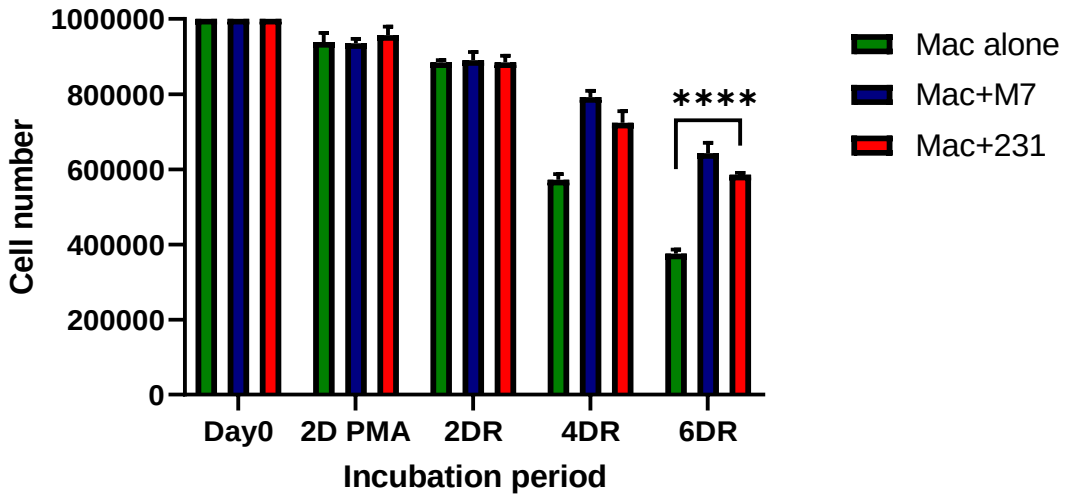

Figure 48 Macrophages cell survival in single culture and co-cultured with breast cancer cells post PMA removal. Data are displayed as mean values ± standard error of 3 independent experiments. The analysis were performed and plotted in Prism V8.0 (GraphPad software). A p-value of ≤ 0.05 was considered as statistical significance between the samples of each group presented in the figure.

Gene expression profiling was performed to further characterize the macrophage phenotype of the differentiated Thp1 cells in the presence, or absence, of breast cancer cells. Here, total RNA was isolated from macrophages as well as those co-cultured with either MDA-MB-231 or MCF-7 cells respectively. As control, expression of the CD11b, CD14, CD68 and TLR-4 transcripts was assessed in macrophages cultured in the absence of breast cancer cells at 2 days PMA treatment (NOR) as well as post-PMA removal for 2 days (2DR), 4 days (4DR) and 6 days (6DR) time points. Under identical conditions, the macrophage expression profile was also examined in the presence of either MDA-MB-231 or MCF-7 cells respectively.

As previously noted, in macrophages cultured alone, all 4 genes were markedly up-regulated in NOR and 2DR while the resting of the macrophages for 4 days (4DR) resulted in reduced expression for TLR-4. Moreover, at 6 days resting (6DR), there is

more collapse of the network with reduced expression in TLR-4, CD68 and CD14 (Figure 49a).

In macrophages co-cultured with MDA-MB-231 and/or MCF-7 breast cancer, the macrophage phenotype was sustained in the absence of PMA as all genes were expressed at similar levels. This suggests a preservation of the macrophage cells by cancer cells (Figures 49b, 49c). This indicates that breast cancer cells significantly enhanced, or maintained, macrophage differentiation phenotype via secreting factors during co-culture communication. In support of this, it has been reported that breast cancer cells secreted factors such as M-CSF, IL-10 which enhance macrophages differentiation and survival via up-regulating CD14 which functions as a recognition receptor on macrophage cell surface [250, 265].

In addition, this data suggests that during chronic co-culture (when the co-culture is extended to 30 days); the replenishment of the macrophages can be safely done at day3 or day4 of co-culture with breast cancer cells as macrophages are still good at this time point. Here we evaluate that macrophages survive longer when co-cultured with breast cancer cells in contrast with macrophages in single culture in which they lost their phenotype after 4^{th} day resting.

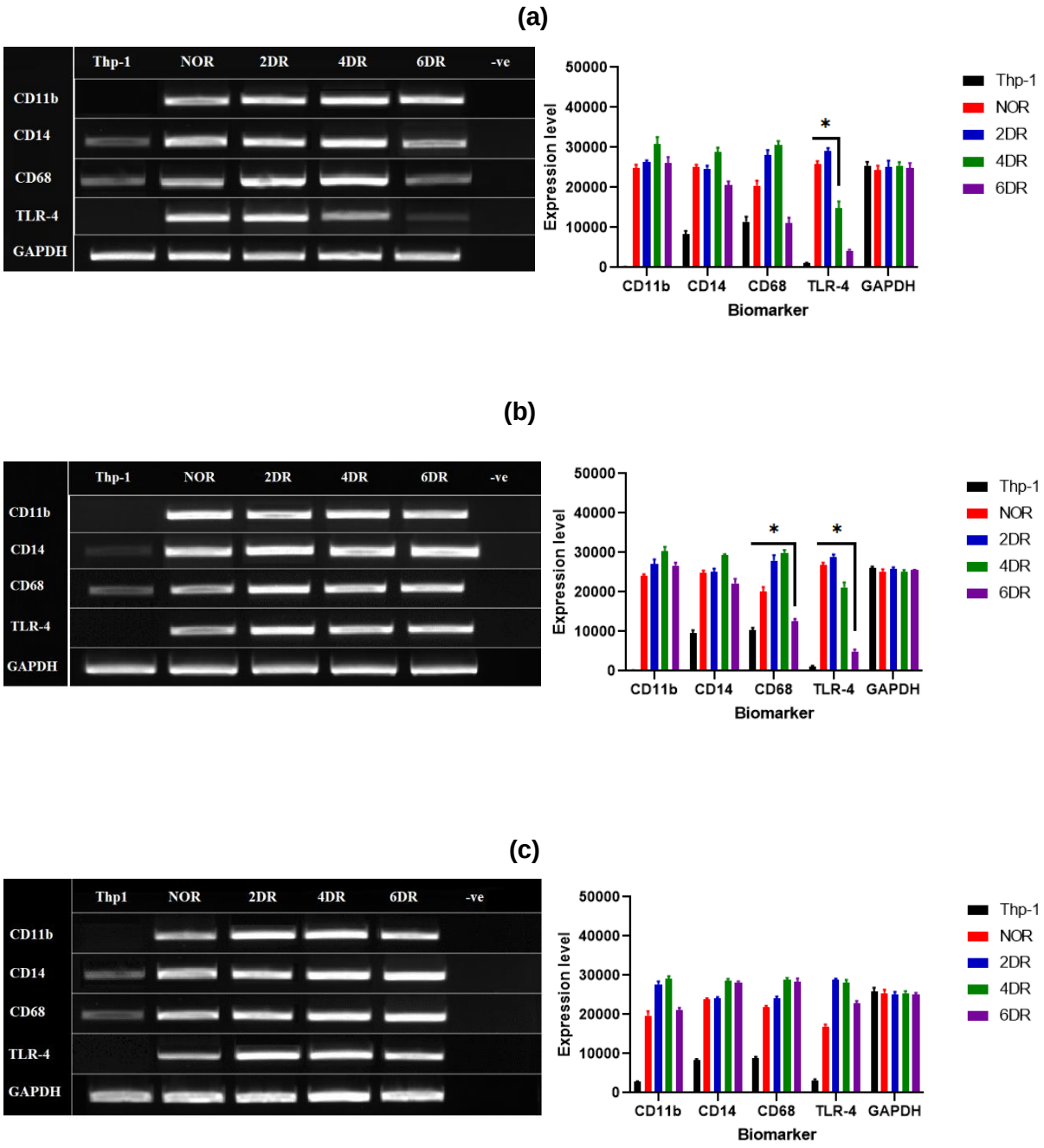

Figure 49 Gene expression analysis of macrophages-specific markers including CD11b, CD14, CD68 and TLR-4. Data were observed from different cultures **(A)** macrophages alone and/or macrophages under **(B)** MDA-MB-231. **(C)** MCF-7 culture condition over different time of incubation as described in methods. Bands intensity was calculated using ImageJ (V. 1.38), and plotted in Prism V8.0 (GraphPad software). A p-value of ≤ 0.05 was considered as statistical significance between the samples of each group presented in the figure.

4.5 Assessment of gene expression in breast cancer upon co-culture with differentiated Thp-1 cells.

Gene expression profile studies impressively reported that human monocytic Thp-1 cells represent a valuable tool to study the primary macrophages function in tumour progression [242, 248, 266]. A study performed by Hollmén M. et al. reported that co-culture of human primary macrophages with breast cancer cells up-regulated differential gene expression in breast cancer cells [267]. Based on these findings, for our pilot study, we investigated the most 10 and 5 most up-regulated genes in MDA-MB-231 and MCF-7 respectively in order to test whether breast cancer cells being activated upon co-culture with Thp-1.

Briefly, upon $1x10^6$ Thp-1 differentiation into macrophages, MDA-MB-231 or MCF-7 breast cancer cells were co-cultured with the macrophages (1:1 ratio) using transwell inserts of 6 well plates for 3 days. For RT-PCR analysis, the expression level of the indicated genes in MDA-MB-231 and MCF-7 breast cancer cells was investigated as described in methods. As for MDA-MB-231 cells upon co-culturing with Thp-1 macrophages, RT-PCR data from 2x experiment conduction revealed that of the 10 genes analysed, 5 were up-regulated (BIRC3, LAMC2, DKK1, PER1 and NR1D1) relative to control untreated MDA-MB-231 cells (Figure 50a). To ensure that these changes in gene expression were macrophage-dependent, a similar co-culture experiment was performed but using untreated monocytic Thp-1 cells. It is of great interest to note that no changes in gene expression was seen in MDA-MB-231 cells co-cultured with untreated Thp-1 cells (Figure 50a), demonstrating that activation of the breast cancer cells is mediated in a macrophage-specific manner.

Similar observations were noted when MCF-7 breast cancer cells were co-cultured with Thp-1 macrophages leading to the significant up-regulation of 3 genes including FAS, ICAM1 and SOCS3 relative to MCF-7 control. In agreement with earlier observations, the activation of the MCF-7 cells was macrophage dependent as the co-culture of these cells with untreated Thp-1 cells failed to induce the expression of tested genes (Figure 50b).

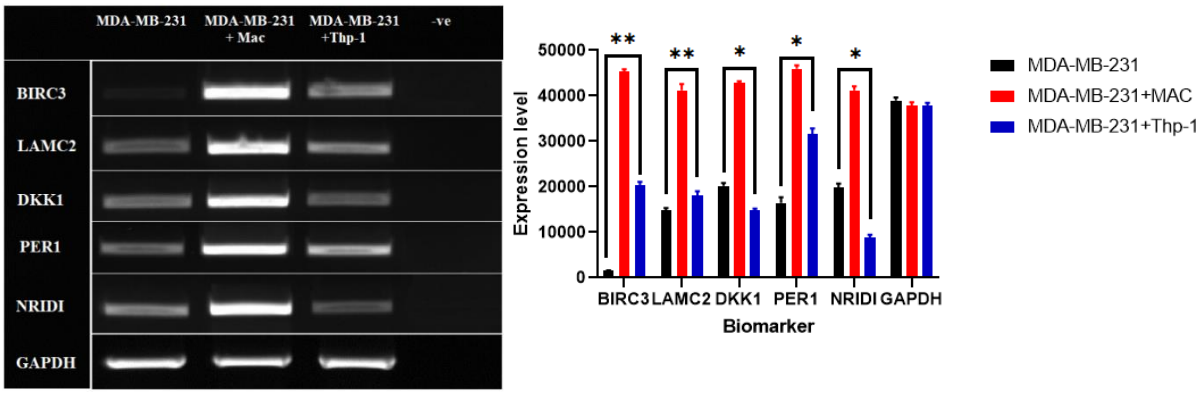

Figure 50A Up-regulated gene in MDA-MB-231 breast cancer cells co-cultured with macrophages represented by PCR analysis. Bands intensity was calculated using ImageJ (V. 1.38), and plotted in Prism V8.0 (GraphPad software). A p-value of ≤ 0.05 was considered as statistical significance between the samples of each group presented in the figure.

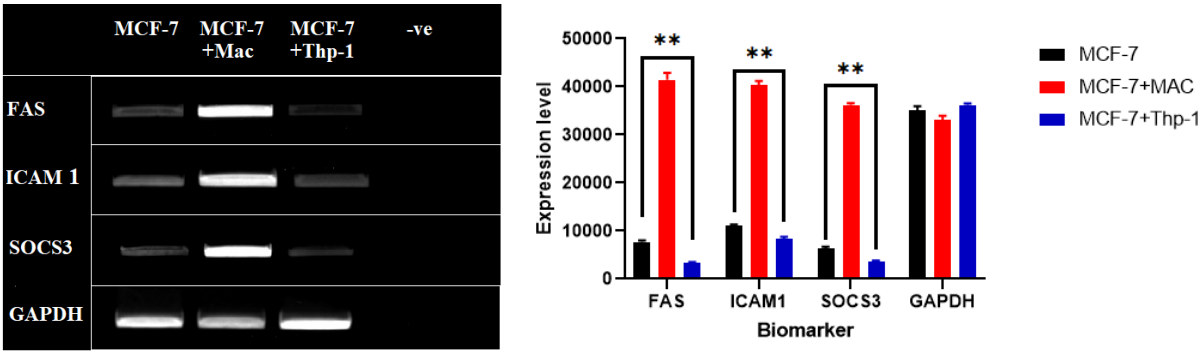

Figure 50B Up-regulated gene in MCF-7 breast cancer cells co-cultured with macrophages represented by PCR analysis. Bands intensity was calculated using ImageJ (V. 1.38), and plotted in Prism V8.0 (GraphPad software). A p-value of ≤ 0.05 was considered as statistical significance between the samples of each group presented in the figure.

4.6 Determining co-culture cell ratio

The tumour microenvironment of breast cancer collectively consists of not only malignant cells but also of residential stromal cells including immune cells, fibroblasts and others. The interaction between malignant cells and surrounding stromal cells at different ratios can profoundly promote or eliminate tumour progression [268]. In support of this notion, histopathological studies have reported that high densities of tumour infiltrated macrophages were found to be correlated with worse prognosis in breast cancer, such as stimulating breast cancer migration and metastasis, and promoting resistance to chemotherapy [269]. This indicates that high levels of macrophage-secreted factors were implicated directly or indirectly in tumour metastasis. Therefore determining cell-cell ratio of tumour cells and macrophages is important tool to perform in order to evaluate whether macrophages can positively or negatively impact tumour progression at the optimal cell ratio. Given these observations, this experiment was established to determine the optimal ratio of breast cancer cells co-cultured with macrophages at different ratios for 3 days of incubation and the ultimate cell ratio was chosen based on gene expression level in breast cancer cells.

Briefly, post Thp-1 differentiation and resting period, breast cancer cells including MDA-MB-231 and MCF-7 at density $1x10^6$ were co-cultured with macrophages at different ratios including 0.5, 1, 2 and $3x10^6$ for 3 days incubation. Optimal activation of the breast cancer cells by these varying co-culture ratios was determined by the relative induction in the expression of BIRC3, LAMC2, DKK1, PER1 and NR1D1 genes in MDA-MB-231, and FAS, ICAM1 and SOCS3 in MCF-7 breast cancer cells respectively.

Gene profiling analysis from 3 independent experiments revealed that weak induction of the indicated genes within either breast cancer subtypes when co-cultured with Thp-1 macrophages at a ratio of 1:0.5 (Figure 51a, 51b). As described previously, both MDA-MB-231 and MCF-7 cells were activated by macrophages when co-cultured at 1:1 ratio. Interestingly, the remaining ratios including 1:2 and 1:3 didn't show any further changes in the expression level in comparison to those co-cultured at 1:1 ratio (Fig 51a, 51b).

In summary, there was negligible activation of breast cancer cells at a 1:0.5 ratio with macrophages, yet optimally activated when co-cultured at equal ratio (1:1) of cell numbers which was sufficient to up-regulate gene expression in both breast cancer cells co-cultured with macrophages as depicted in figure (50a, 50b) below.

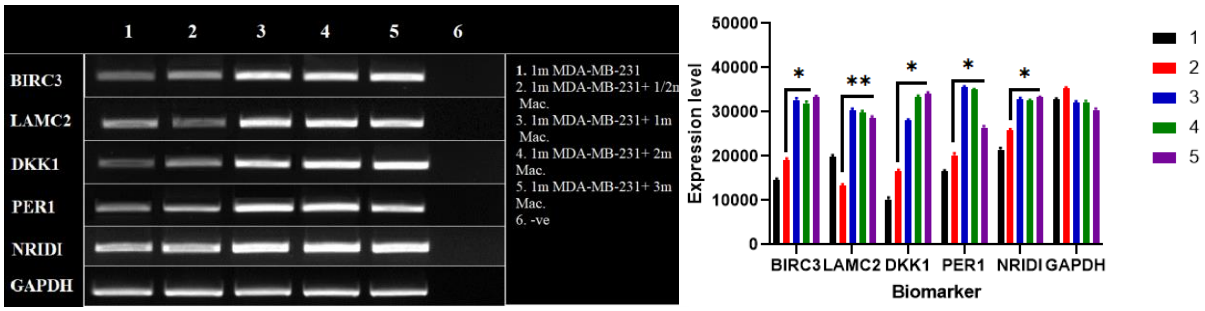

Figure 51A Gene expression level in MDA-MB-231 breast cancer cells co-cultured with macrophages at different ratios including (1) control (2) 0.5:1 (3) 1:1 (4) 2:1 (5) 3:1 and (6) – ve. Bands intensity was calculated using ImageJ (V. 1.38), and plotted in Prism V8.0 (GraphPad software). A p-value of ≤ 0.05 was considered as statistical significance between the samples of each group presented in the figure.

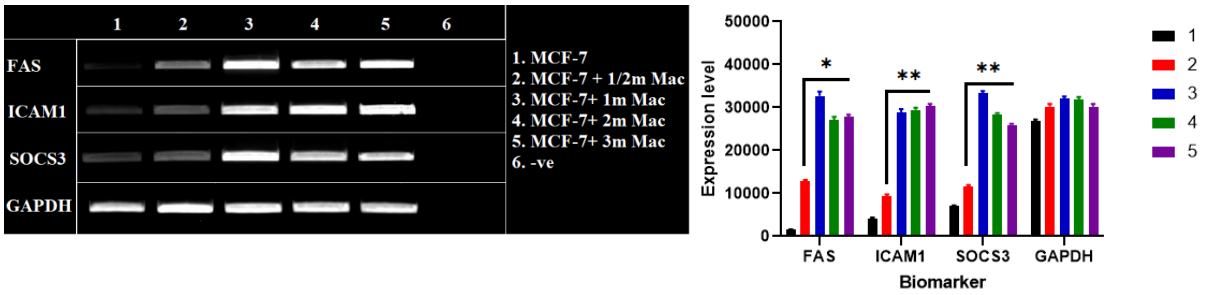

Figure 51B Gene expression level in MCF-7 breast cancer cells co-cultured with macrophages at different ratios including (1) control (2) 0.5:1 (3) 1:1 (4) 2:1 (5) 3:1 and (6) –ve. Bands intensity was calculated using ImageJ (V. 1.38), and plotted in Prism V8.0 (GraphPad software). A p-value of ≤ 0.05 was considered as statistical significance between the samples of each group presented in the figure.

4.7 Assessment of Macrophages cell morphology in the presence of breast cancer cells

Cell spreading and adherence are the hallmark of macrophages which are used to evaluate the successful differentiation of monocytic Thp-1 into macrophages. Previous work presented herein assessed the morphology of macrophages upon differentiation with PMA treatment. As demonstrated herein, as breast cancer cells promoted the survival of macrophages in single culture it was of interest as too whether this was associated with any morphological changes.

The assessment was achieved by differentiating Thp-1 into macrophages as mentioned previously. Macrophages were rested alone in fresh media and/or by incubating with breast cancer cells. Pictures were taken using florescence microscope (EVOS FL) at each indicated time points. The investigation of cell morphology from 3 independent experiments showed that the exposure of Thp-1 to a dose 25ng/ml PMA for 48hrs induced marked spreading morphology and cell adhesion which are the hallmark of macrophages (Figure 52). The morphology of Thp-1 was changed from

small round shape to fried-egg. Notably, on the 4th day resting phase the co-culture of macrophages with breast cancer cells markedly enhanced macrophages granularity and attachment relative to macrophages in single culture as shown in figure (51). This indicated that factors secreted by breast cancer cells enhanced macrophages differentiation and attachment to the surface relative to macrophages alone which significantly differed in appearance.

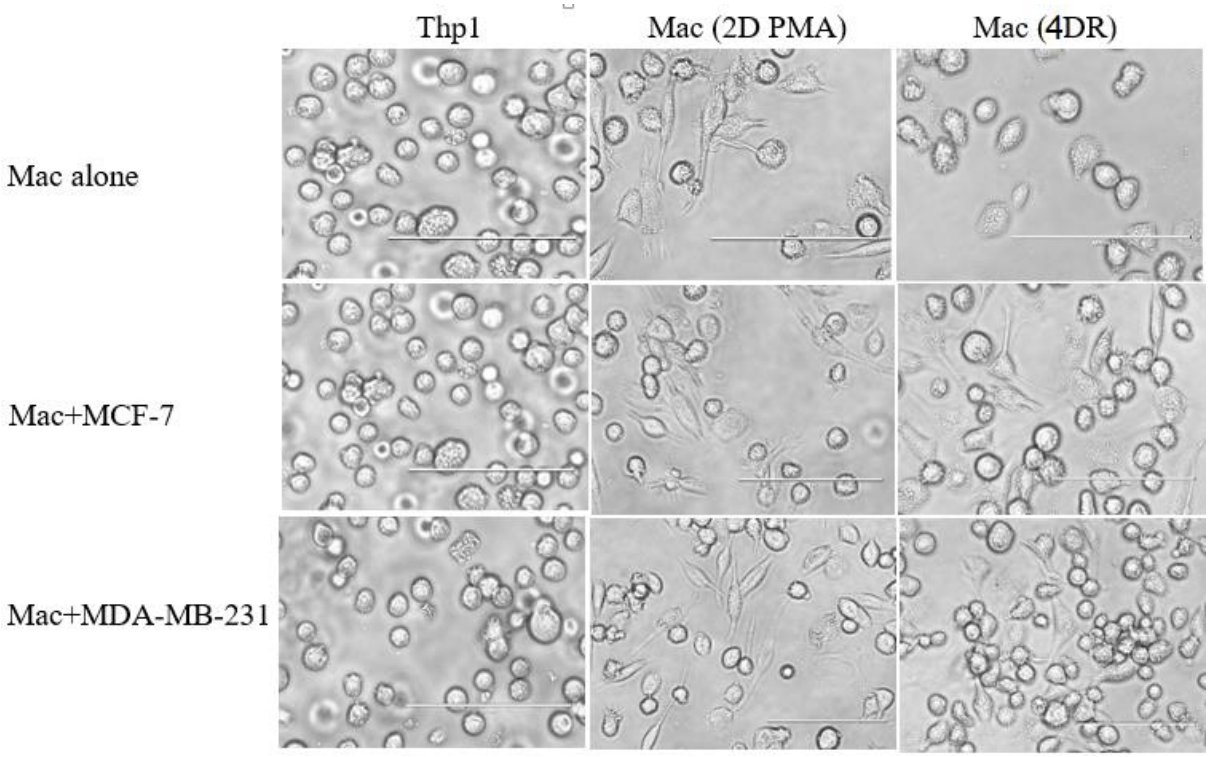

Figure 52 Representative images of macrophages cell morphology in single culture or co-cultured with breast cancer cells which promoted macrophages cells adhesion and differentiation. Scale bar is 100 µm.

4.8 Evaluation of macrophages conditioned media effect on breast cancer

The use of conditioned media has been widely utilised in many research areas as it contains several growth factors, amino acids, interleukins and extracellular proteins secreted by cultured cells. The current findings have identified several genes that are up-regulated within breast cancer cells (either MDA-MB-231 or MCF-7) upon co-culture with Thp-1 macrophages. The precise mechanism as too how the breast cancer cells become activated is unclear. Two scenarios could explain these observations (i) macrophages secreted factors as a result of co-culture with breast cancer cells which activates signaling pathways between two cell populations, or (ii) due to the ability of macrophages itself to up-regulate gene expression in cancer cells without being in communicate with breast cancer cells.

To distinguish between these two possibilities, conditioned media from several cultures was generated; (i) conditioned media from activated MDA-MB-231 or MCF-7 breast cancer cells were previously co-cultured with macrophages (3 days), (ii) conditioned media from co-culture of macrophages and breast cancer cells, (iii) conditioned media from macrophages, (iv) conditioned media from untreated Thp-1 cells.

MDA-MB-231 or MCF-7 cells were incubated with the generated conditioned media for 3 days. RNA from all cultures was collected and RT-PCR analysis was performed in order to test the expression level of the previously described genes that were identified to be up-regulated in the breast cancer cells upon co-culture with Thp-1 macrophages respectively.

Of the MDA-MB-231 cells cultured in the different condition media, data from 3 independent experiments demonstrate that conditioned media from co-culture of MDA-MB-231 with macrophages up-regulated genes including BIRC3, LAMC2, DKK1, PER1 and NR1D1. Of great interest, conditioned media from macrophages in single culture, untreated Thp-1cells and activated MDA-MB-231 did not show any changes in genes level in breast cancer cells as shown in figure (53).

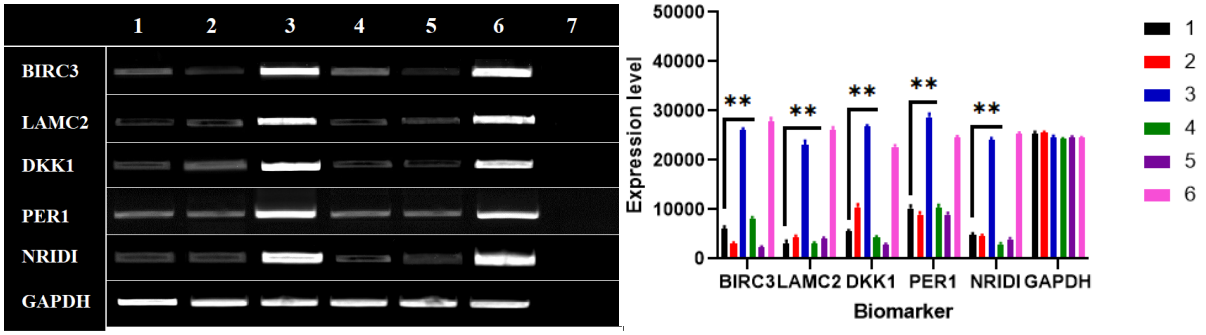

Figure 53 Representative image of RT-PCR analysis shows the expression levels of BIRC3, LAMC2, DKK1, PER1 and NR1D1 genes in MDA-MB-231 cells incubated with different conditioned media including (1) MDA-MB-231 in fresh media. (2) Conditioned media from activated breast cancer cells. (3) Conditioned media from co-culture of macrophages with breast cancer cells. (4) Conditioned media from macrophages in single culture. (5) Conditioned media from Thp-1 cells. (6) Positive control. (7) Negative control. Bands intensity was calculated using ImageJ (V. 1.38), and plotted in Prism V8.0 (GraphPad software). A p-value of ≤ 0.05 was considered as statistical significance between the samples of each group presented in the figure.

Similarly, for the MCF-7 cells cultured in the conditioned media the expression of 3 genes (FAS, ICAM1 and SOCS3) demonstrated that conditioned media from co-culture of macrophages was sufficient to activate the breast cancer cells. Notably, and distinct from the MDA-MB-231 cells, the MCF-7 cells were also activated when cultured in macrophages conditioned media; albeit that the level of induction of gene expression was not as strong. As described for the MDA-MB-231 cells, no changes in

gene expression within the MCF-7 cells was detected when cultured in conditioned media generated from Thp-1 and activated MCF-7 conditioned media; as shown in figure (54).

These observations demonstrate that conditioned media from macrophages up-regulated gene expression in MCF-7 but not in MDA-MB-231 cells. Conditioned media from co-culture of macrophages and breast cancer cells markedly up-regulated gene expression in both breast cancer subtypes. This indicated that macrophages secreted factors were sufficient to up-regulate gene expression in MCF-7 cells while, genes in breast cancer require a direct communication between 2 cells populations in order to activate signaling pathways in MDA-MB-231 which therefore lead to high expression of these 5 selected genes.

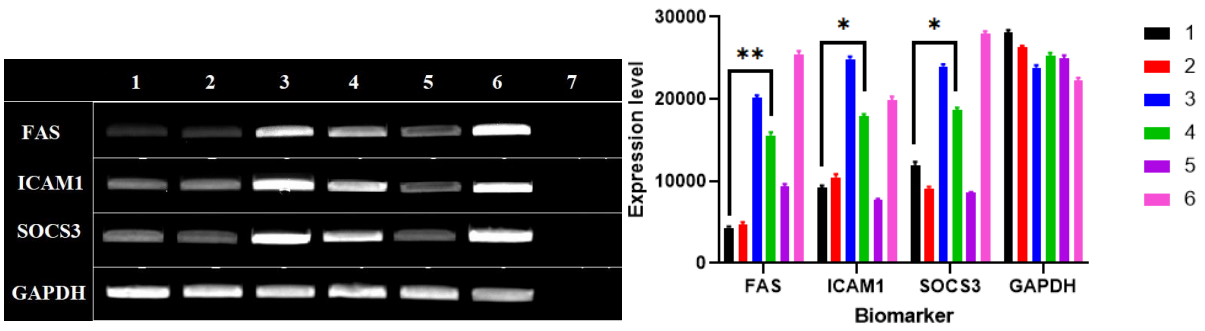

Figure 54 Representative image of RT-PCR analysis shows the expression levels of FAS, ICAM1, and SOCS3 genes in MCF-7 cells incubated with different conditioned media including (1) MCF-7 in fresh media (2) Conditioned media from activated MCF-7 cells. (3) Conditioned media from co-culture of macrophages with MCF-7 breast cancer cells. (4) Conditioned media from macrophages in single culture. (5) Conditioned media from Thp-1 cells. (6) Positive control. (7) Negative control. Bands intensity was calculated using ImageJ (V. 1.38), and plotted in Prism V8.0 (GraphPad software). A p-value of ≤ 0.05 was considered as statistical significance between the samples of each group presented in the figure.

4.9 Characterization of breast cancer using triple culture model

Breast cancer is the most leading disease to death among women across the globe due to it has the potential to spread to the other tissues of the body such us bone, lung, brain and others [270]. The reason behind it still not fully understood, although several studies have reported that the complex reciprocal between malignant cells and surrounds stromal cells involving fibroblasts, immune cells, adipocytes and extracellular matrix proteins was found to be implicated in tumour initiation and progression [14, 71].

Fibroblast and macrophages are prominent components of the tumour microenvironment and the complex relationship between fibroblasts and macrophages with malignant cells is not well determined. Activated fibroblasts are known as cancer associated fibroblasts (CAFs) have shown to play a critical role in tumour progression. Glycoprotein Chitinase-3-like-1 (Chi3L1) is secreted by CAFs and was found to be implicated in tumour promotion and macrophages activation [271, 272]. Knocking out of CAFs derived Chi3L1 decreased tumour growth and enhanced survival in mice. This indicated that tumours injected with shChi3L1-CAFs potentially influenced the signalling pathway in tumour cells hence reducing tumour growth. Furthermore, tumours with high expression of Chi3L1 were found to be abundantly infiltrated with CD206 (macrophages type 2 marker), suggesting that Chi3L1 functionally enhances anti-inflamatory factors secretion by recruiting macrophages into M2 phenotype and angiogenesis formation hence promoting tumour growth [273].

Macrophages that infiltrate within tumour cells are called tumour associated macrophages (TAMs) which have been reported to be associated with poor prognosis in many solid tumours including breast cancer. The mechanism of interaction between

CAFs and TAMs is largely unknown although accumulated studies demonstrated that the interaction between M2 and CAFs drive epithelial–mesenchymal transformation as well as tumours occurrence and progression [274]. Furthermore the histopathology studies have shown the abundance of CAFs and TAMs in the same area in many tumour tissues, this indicates that the cross-talk between CAFs and TAMs not only to recruiting monocytes into macrophages by secreting monocyte chemotactic protein-1 (MCP-1) and stromal cell-derived factor-1 (SDF-1), but also to promote tumour progression and escaping from immune surveillance via secreting IL-10 which polorises macrophages into M2 as well as it plays an important role in suppressing immune cells [274]. It was reported that CAFs promote macrophages adhesion via secreting collagen type I which acts as a substrate recognised by SR-A receptor on macrophages surface which mediate macrophages adhesion [275]. Based on these evidences, the individual, as well as combined, role of CAFs and TAMs in breast cancer proliferation, migration and invasion was explored respectively.

4.10 Determining fibroblasts and breast cancer cells ratio

In previous work we identified the importance of co-culture of tumour and macrophages cell ratio for optimal activation of breast cancer cells. I our current work we are aiming to perform triple culture model in order to evaluate the biological effect of fibroblasts and macrophages on breast cancer cells. The breast cells-fibroblasts co-culture cell ratio has not been determined yet. Therefore this experiment was established to determine the optimal cell ratio of normal fibroblasts co-cultured with breast cancer cells based on breast cancer cell proliferation rate. Breifly, $1x10^5$ of MDA-MB-231 or MCF-7 were incubated with various ratios of fibroblasts including 1: 0.5, 1:1, 1:2 and 1:3 for 5 days using transwell inserts of 6 well plates as described in methods. Breast cancer cell count was performed daily in order to evaluate the number of proliferated breast cancer cells under each ratio of fibroblasts.

The average of breast cancer cell number from 3 independent experiments revealed that the co-culture of MDA-MB-231 and MCF-7 with fibroblasts at ratio 0.5:1 increased breast cancer cell number to 12% compared to breast cancer cells in single culture. Other fibroblasts ratio including 1:1, 2:1 and 3:1 did show a remarkable increase in both breast cancer subtypes, and this was noticed by increasing breast cancer cell number to 15%, 15% and 16% at ratios 1:1, 2:1 and 3:1 respectively in MDA-MB-231 (Figure 55), while it was increased to 16% at all ratios including 1:1, 2:1 and 3:1 in MCF-7 cells (Figure 54). No changes were seen between 1:1 and 1:2 or 1:1 and 1:3 ratios. Based on our findings, 1:1 ratio was chosen to be the optimal cell ratio in our co-culture model.

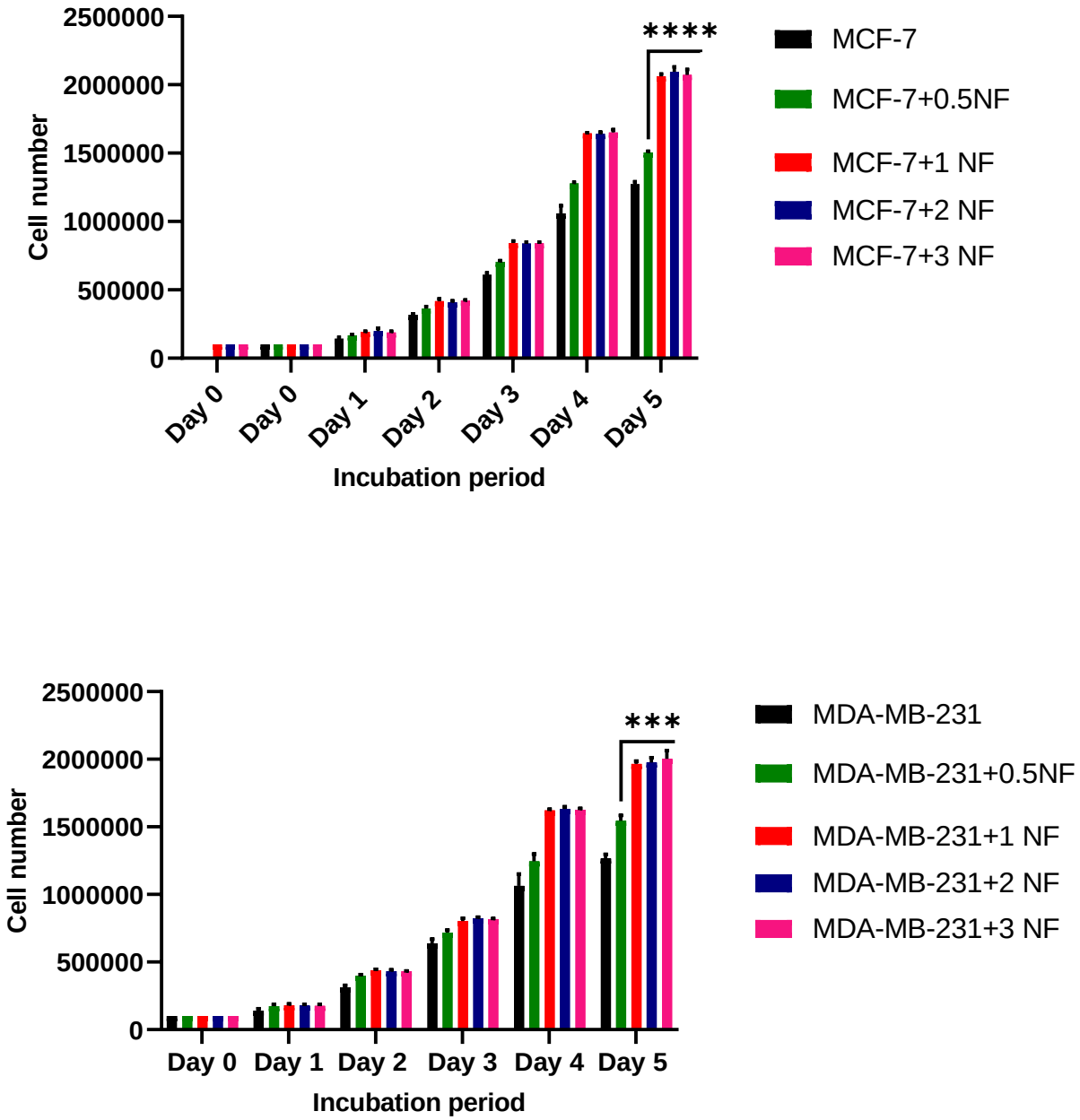

Figure 55 Determining fibroblasts cell ratio. MCF-7 and MDA-MB-231 were incubated with fibroblasts at different ratios including 1:0.5, 1:1, 1:2 and 1:3 respectively. Both cultures markedly show the significant increase in MCF-7 and MDA-MB-231 cell proliferation at 1:1 ratio. Data are displayed as mean values ± standard error of 3 independent experiments. The analysis were performed and plotted in Prism V8.0 (GraphPad software). A p-value of ≤ 0.05 was considered as statistical significance between the samples of each group presented in the figure.

4.11 Cell migration assay (wound healing)

Cancer cell migration is the ability of cell to move from their original site into another location of the tissue by adopting motility modes such as mesenchymal transition [276]. The tumour microenvironment plays an essential role in promoting cancer migration [277]. TAMs have been shown to facilitate malignant cells migration via secreting different cytokines and chemokines such us matrix metalloproteinases, serine proteases, and cathepsins [278]. Fibroblasts are the other major component of the tumour microenvironment which have been shown to actively promote breast cancer migration and metastasis. The mechanism behind this contribution is still poorly understood, however it was reported that up-regulation of FAK expression in activated fibroblasts (known CAFs) was found to promote breast cancer migration [279]. These studies were conducted using co-culture model in order to evaluate the functional interaction between 2 cell populations. In our study we performed a triple culture model to investigate the migratory capacity of MCF-7 and highly metastatic MDA-MB-231 breast cancer cell lines under co-culture of macrophages and fibroblasts. The procedure of wound healing assay was performed as described in methods. Briefly, we initially induced $1x10^6$ monocytic Thp-1 differentiation into macrophages, following macrophages differentiation and resting, fibroblasts at the same ratio were added to individual inserts and/or to inserts that contain macrophages. Breast cancer cells after reaching 95% confluence were starved using serum free media 24hrs prior running the experiments. Wounds in breast cancer cells were generated next day as indicated in methods. Wounded wells of breast cancer cells were incubated alone with fresh media contains 10% FBS and/or with macrophages or fibroblasts (double culture) or with both macrophages and fibroblasts using triple culture model.

Migrated cells were monitored at different time points. Results were expressed according to wound closure by adherent cells between two intact zones. The wound width was measured in µm and the scatter plot was used to present the wound closure over the time as shown in figures (56b, 57b).

The finding of measured wound width represents the mean value of 3 independent experiments. The co-culture of macrophages or fibroblasts with breast cancer cells increased both MCF-7 and MDA-MB-231 migration relative to breast cancer cells in single culture which showed slight changes or no difference in wound closure as shown in figures (56a, 57a). No difference was seen in wounds width of MDA-MB-231 under fibroblasts or macrophages culture condition. Contrarily, MCF-7 cells were faster in their migration when co-cultured with macrophages in comparison with those co-cultured with fibroblasts indicating that MCF-7 were more responsive to macrophages-secreted factors that drive cell migration than those co-cultured with fibroblasts.

Interestingly, the triple culture of macrophages and fibroblasts with breast cancer cell lines clearly promoted the migration of MDA-MB-231 cells compared with those cultured under double condition or control cells. No changes were seen in MCF-7 cell migration co-cultured under triple culture condition compared with those cultured with macrophages or fibroblasts using double culture model. The biological reason of promoting MDA-MB-231 under triple culture model is still unknown, but according to our best knowledge, fibroblasts potentially enhanced macrophages secreted factors such as IL-1β, CCL-18 which have been shown to be implicated in breast cancer migration and invasion [280, 281]. The cross-talk between fibroblasts and macrophages remains loosely defined, although some studies demonstrated that macrophage colony-stimulating factor (CSF1) secreted by CAFs plays an important

role in macrophages polarisation into M2 phenotype which have been shown to promote tumour progression [282]. Other studies have shown that activated fibroblasts by macrophages were shown to dynamically promote prostate cancer via secreting IL-10 and SDF-1 [283]. Based on initial work, we observed that the co-culture of macrophages and fibroblasts promoted breast cancer cell migration relative to double culture as shown in our data. Although several studies have shown the influential role of CAFs or TAMs in the tumour microenvironment, further investigation are needed to elucidate the interaction between both cell populations and their biological role in the tumour progression.

(A)

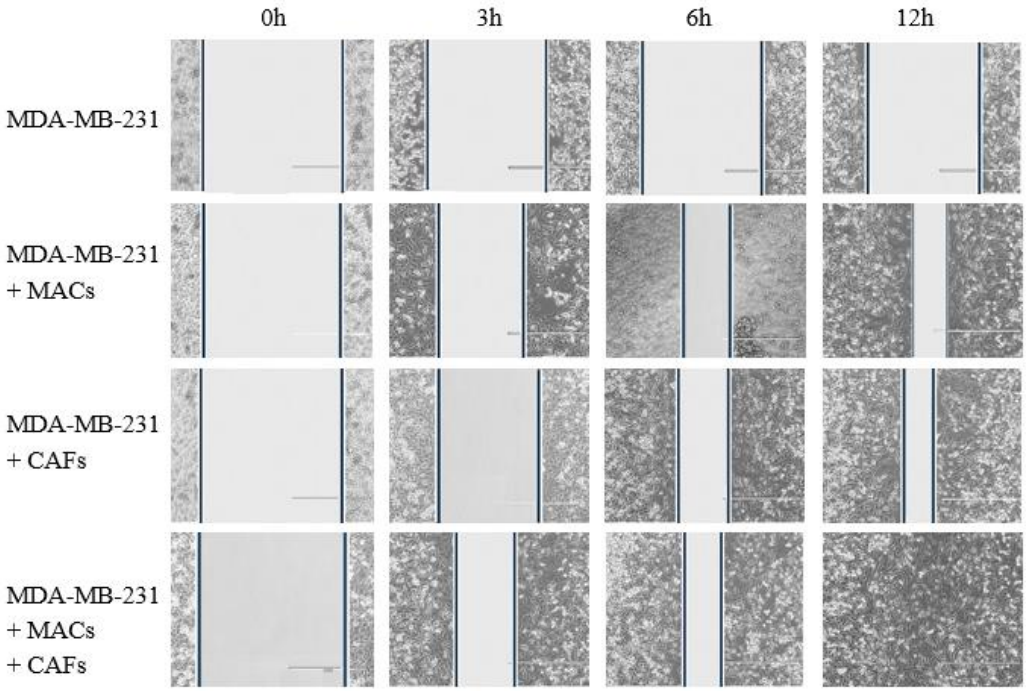

(B)

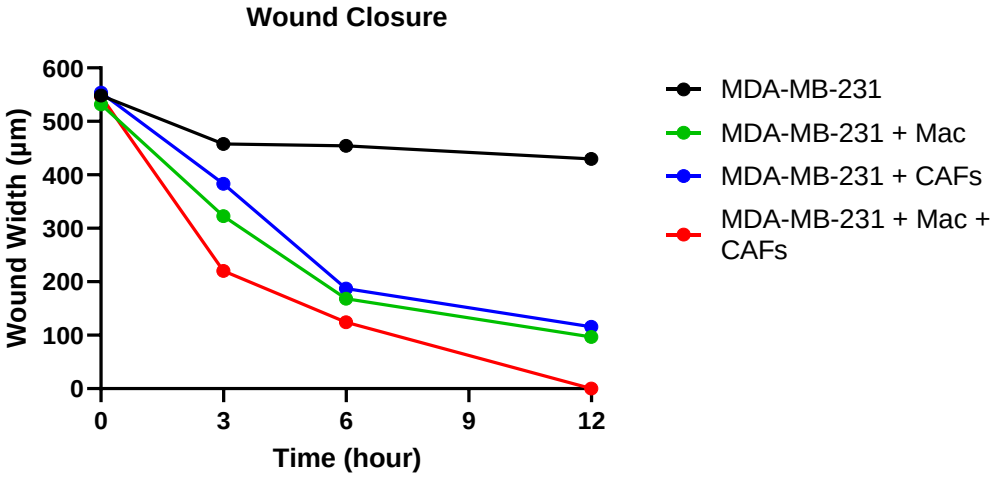

Figure 56 Representative images of MDA-MB-231 breast cancer wound healing during 12 hours and scale bars (400 µm) are added for wound width measurement. **(A)** Wound closure of MDA-MB-231 in single culture (control) or co-cultured with fibroblasts or macrophages and/or with both fibroblasts and macrophages in triple culture. **(B)** The rate of wound closure between 2 intact zones over the time.

(A)

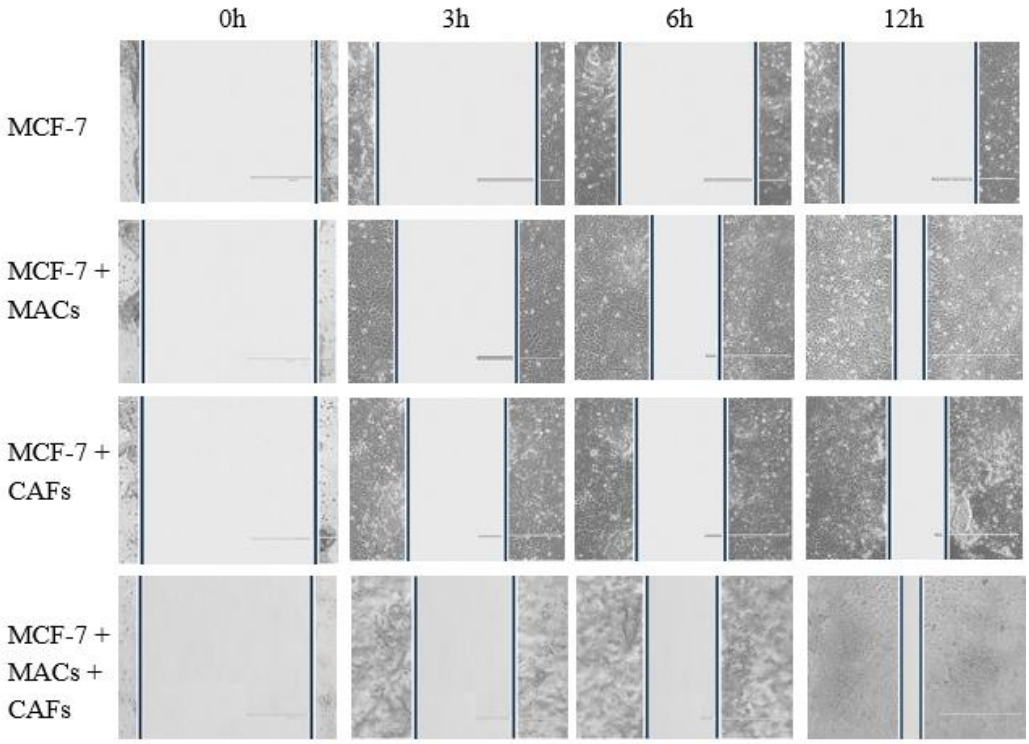

(B)

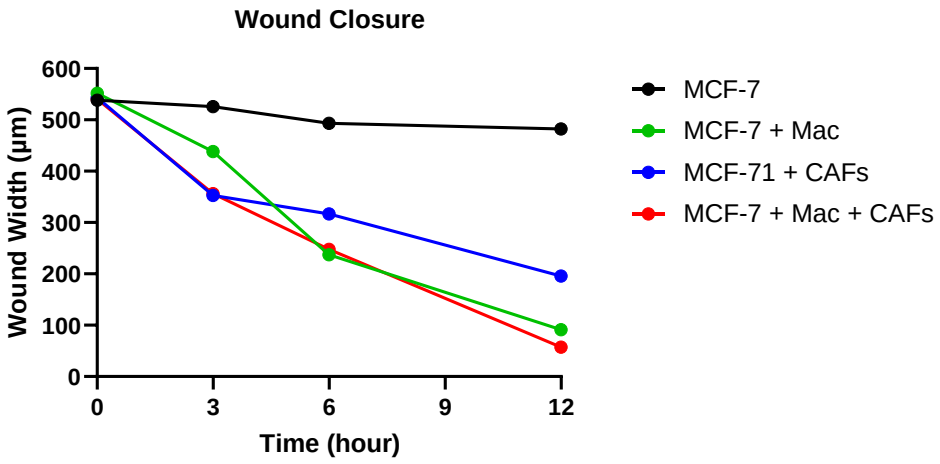

Figure 57 Representative images of MCF-7 breast cancer wound healing during 12 hours and scale bars (400 µm) are added for wound width measurement. **(A)** Wound closure of MCF-7 in single culture (control) or co-cultured with fibroblasts or macrophages and/or with both fibroblasts and macrophages in triple culture. **(B)** The rate of wound closure between 2 intact zones over the time. Data represent the mean value of 3 independent experiments.

4.12 The optimal concentration of matrix matrigel

Cell invasion is the ability of cancer cell to breach the local tissue in order to translocate to surrounding tissue or into another part of the body to establish another site of growth. The cross-talk between macrophages and fibroblasts with cancer cells in the tumour microenvironment has not been well established therefore, our model is aiming to examine the role of macrophages and fibroblasts co-cultured with breast cancer cells using our triple culture model. To achieve this, matrigel matrix which is a reconstituted basement membrane was used to examine the invasive ability of both breast cancer cells including MCF-7 and MDA-MB-231 in either single culture and/or co-cultured with macrophages or fibroblast or both.

Before starting our cell invasion assay we had to determine the optimal concentration of protein concentration that form a firm gel. As mentioned previously, inserts of 12 well plates were coated with a range of matrix matrigel concentrations including 0.3, 0.6 and 1.2 mg/ml as recommended by previous studies [284]. $3x10^5$ MDA-MB-231 or MCF-7 in serum free media were pipetted into coated inserts. 1ml of fresh media were added into lower chamber of 12 well plates. Control inserts were prepared by adding serum free media in the lower chambers. Cells were incubated for 72hrs and invasive cells were visualised using hematoxylin and Eosin staining as described in methods. The optimal protein concentration was determined based on the difference between invasive and noninvasive cells through matrix membrane and the average of invaded cells through matrix matrigel was evaluated from three independent experiments. Our finding revealed that cells invaded through matrix membrane of all protein concentrations toward attractants in the lower chambers relative to control inserts in which no invasive cells were seen as depicted in figure (58a). This indicates that inserts were successfully coated with matrix matrigel regardless protein concentration

of matrix matrigel. Notably cells were not uniformly scattered but they formed clusters and strings in different areas of the slide. The optimal concentration of matrix matrigel was determined according to number of cells invaded through the membrane. The mean number of cells was evaluated from 3 independent experiments as described previously. The number of MDA-MB-231 and MCF-7 invaded through matrix matrigel differed according to the protein concentration, 5.1%, 14.1% and 14.4% of MDA-MB-231 cells, 2.4%, 8% and 8.9% of MCF-7 cells were invaded through matrigel at concentrations 0.3, 0.6 and 1.2 mg/ml respectively. No cells were invaded through control inserts and the number of invaded cells was significantly increased when using 0.6 mg/ml in contrast with 0.3 mg/ml of protein concentration. This was the biggest difference we observed among 3 concentrations of matrix matrigel we used in this study as shown in figure (58b). However, our observation from these findings, 0.6 mg/ml was chosen as an optimal protein concentration to be used in our future experiment.

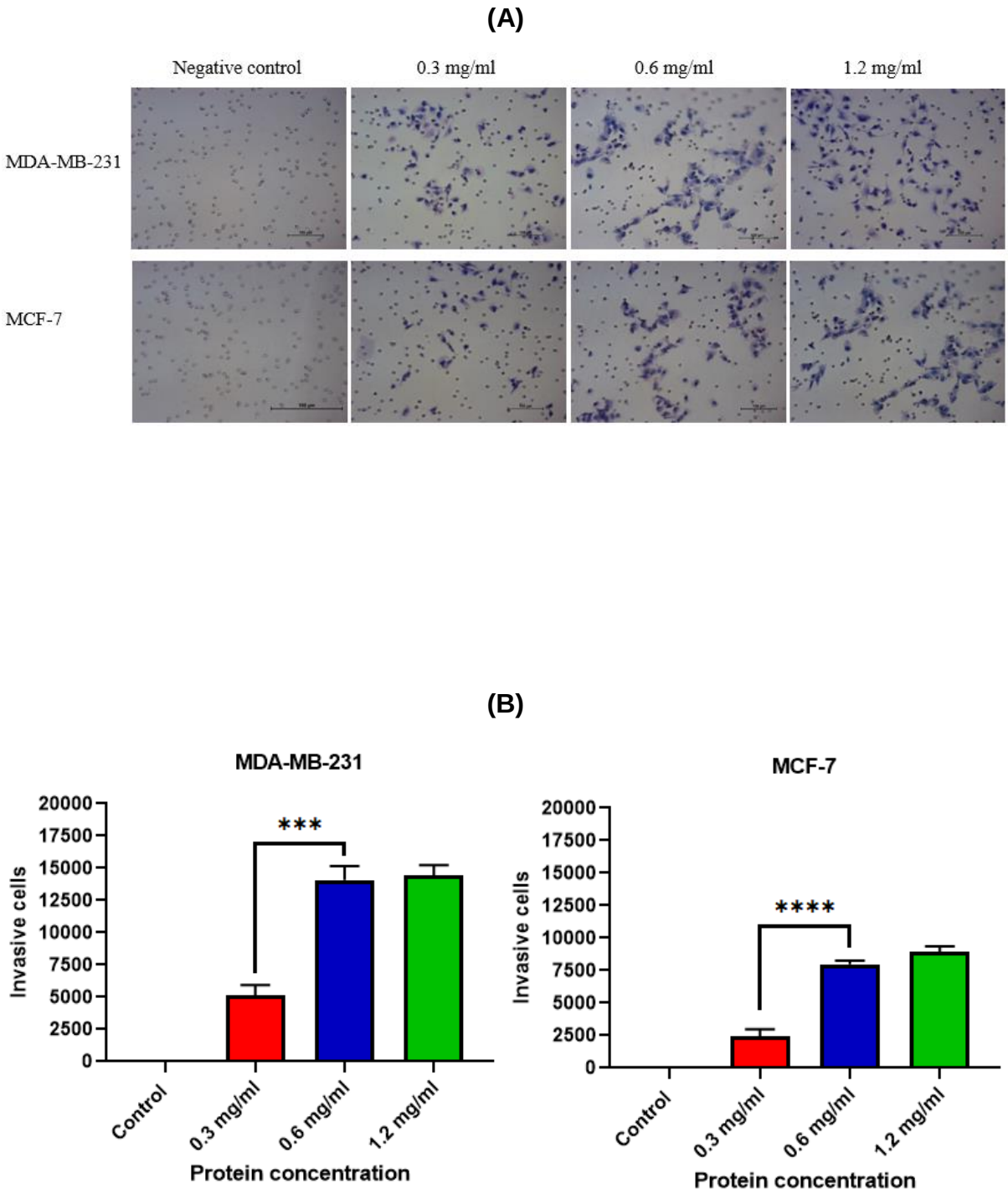

Figure 58 Optimization of matrix matrigel concentration. **(A)** Representative image of MDA-MB-231 and MCF-7 invasive cells through matrix matrigel. **(B)** Number of breast cancer cells (MDA-MB-231 and MCF-7) invaded through different concentrations of matrix matrigel. Data are displayed as mean values ± standard error of 3 independent experiments. The analysis were performed and plotted in Prism V8.0 (GraphPad software). A p-value of ≤ 0.05 was considered as statistical significance between the samples presented in the figure.

4.13 Macrophages and fibroblasts promoted breast cancer cells proliferation

Given the notion that the co-culture of breast cancer cells with fibroblasts or macrophages promote or suppress breast cancer proliferation. In our model, we hypothesized that the co-culture of breast cancer cells with fibroblasts and macrophages may influence tumour cells proliferation. To assess this, $1x10^5$ MDA-MB-231 and MCF-7 breast cancer cells were incubated with same amount of macrophages or fibroblasts in double culture or with macrophages and fibroblasts using our triple culture model as described in methods. Cells were incubated for 6 days and daily cell count was performed using hemocytometer technique. Our result showed that the fibroblasts significantly promoted MDA-MB-231 and MCF-7 breast cancer cell proliferation by 34% and 14%, whereas the incubation with macrophages decreased the proliferation rate of both breast cancer subtypes by 36% and 31% respectively. These effects fibroblasts and macrophages on breast cancer cell proliferation has been already reported in many studies [285, 286]. Interestingly, our triple culture model revealed that the co-culture of MDA-MB-231 and MCF-7 with fibroblasts and macrophages significantly promoted breast cancer cell proliferation by 51% and 42% respectively as depicted in figure (59). The cross-talk between breast cancer cells macrophages and fibroblasts is not fully understood yet. Notably macrophages played a dual roles in both cultures, in double culture experiment macrophages suppressed breast cancer cell proliferation and this function has already been shown previously [286]. While in triple culture macrophages became a tumour supporter which has shown to promote breast cancer proliferation. This indicated that the existence of macrophages among cancer cells and fibroblasts has changes their functional abilities in response to the microenvironment stimuli e.g. COX2 is expressed in cancer cells and fibroblasts which in turn plays an important role in macrophages

polarization into M2 subset, which has shown to activate PI3K/Akt pathways resulting in enhancing breast cancer cell proliferation [287, 288]. Based on these findings macrophages secreted factors can diversely play multiple roles in suppressing and promoting tumour progression based on their location of the tissue.

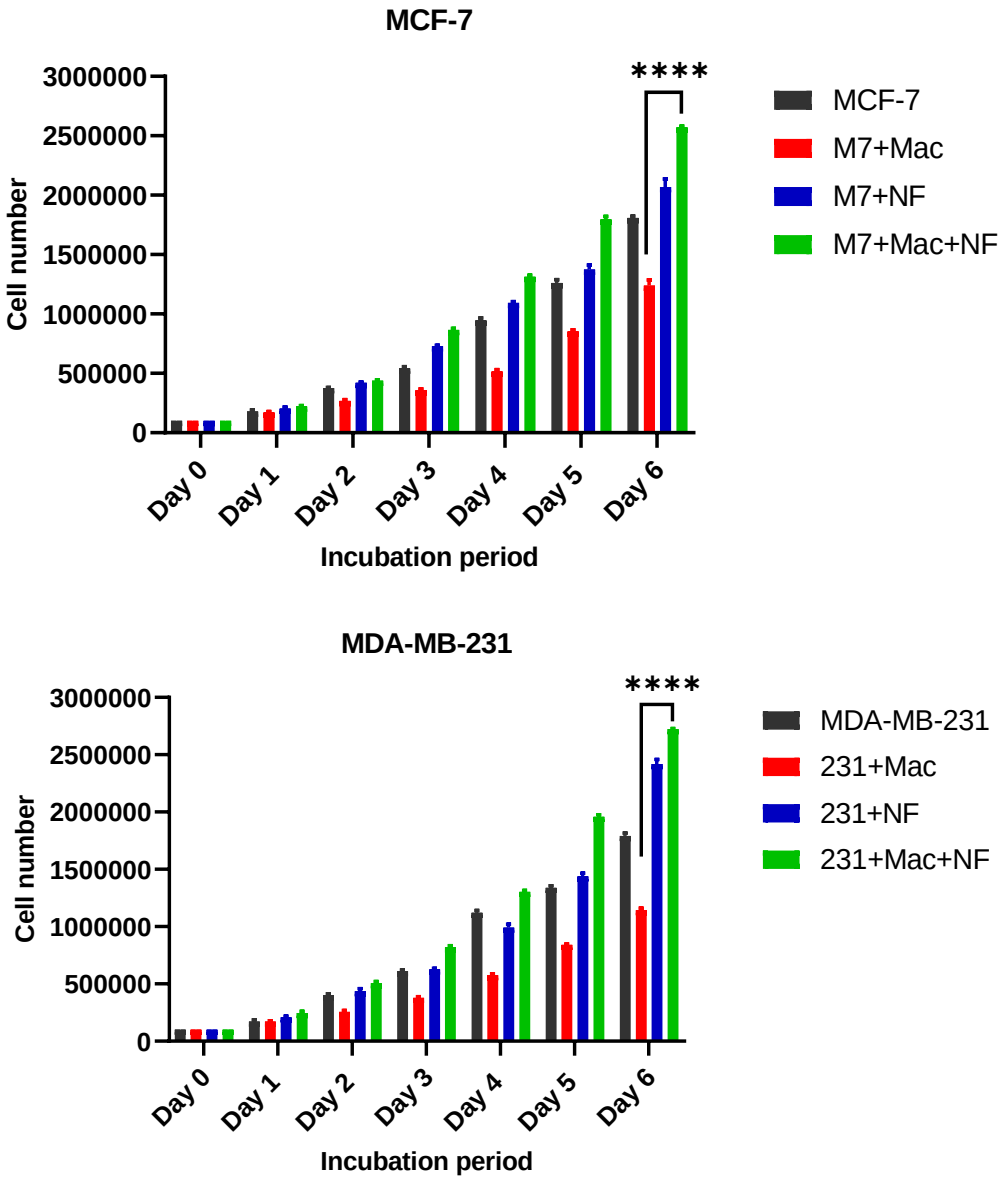

Figure 59 Proliferation assay of MDA-MB-231 and MCF-7 breast cancer cells in single culture as control or co-cultured with fibroblasts or macrophages or in triple culture with both fibroblasts and macrophages. Both figures show that the cell number of breast cancer cells was significantly increased in triple culture experiment. Data are displayed as mean values ± standard error of 3 independent experiments. The analysis were performed and plotted in Prism V8.0 (GraphPad software). A p-value of ≤ 0.05 was considered as statistical significance between the samples presented in the figure.

Discussion

Thp-1 cells are the most used cell line that mimic human primary macrophages in term of cell morphology, surface markers and cytokines production after exposure to PMA treatment [289]. For successful Thp-1 differentiation into macrophages and to evaluate whether Th-1 can be used as a model for primary macrophages, Thp-1 underwent three-step procedure.

The first step was to incubate Thp-1 cells with different PMA concentrations in order to determine the optimal PMA concentration. However, from various concentrations we used including 10, 25, 50 and 100ng/ml for 2 days incubation, 25ng/ml was the lowest optimal concentration that was sufficient to induce cell adhesion and up-regulate gene expression on cell surface in differentiated macrophages. It was reported that incubation of Thp-1 cells with 25ng/ml for 48hrs was sufficient to induce Thp-1 differentiation into macrophages [290].

The second step was to evaluate macrophages phenotype in single culture and/or co-cultured with breast cancer cells in free PMA media. However, macrophages phenotype was significantly promoted in the presence of breast cancer cells compared with those cultures under single culture condition. This indicates that tumour enhanced macrophages differentiation and adhesion due to the influence of various signal factors secreted by breast cancer cells during co-culture with macrophages. Previous studies have reported that the expression of colony stimulus factor 1 (CSF-1) and interleukin-6 (IL-6) in tumour cells was positively associated with macrophages differentiation and their infiltration within tumour cells [291]. Furthermore, the new discovered IL-34 cytokine is secreted by tumour cells, which functions same as CSF-1 which plays a key role in macrophages recruitment into tumour site [292].

The third step was to determine whether Thp-1 can be used as a model for primary macrophages as we cannot assume that the phenotype and molecular attributes of differentiated Thp-1 are similar to primary macrophages. However, upon co-culture with breast cancer cells, gene expression analysis revealed that differentiated Thp-1 were able to up-regulated gene expression in both breast cancer cells, and this was compared with undifferentiated Thp-1 which did not show any changes. This indicates that Thp-1 were successfully differentiated into macrophages and were able to display macrophages characteristic which lead to gene expression changes in breast cancer cells. Previous studies have also reported that macrophages-like differentiated from monocytic Thp-1 cells can serve as primary macrophages, thus they are widely used to study the biological interaction between macrophages and tumour cells [255, 293].

The breast tumour microenvironment is composed from malignant cells and stromal cells that are widely believed to drive tumour progression through a complex and dynamic communication with tumour cells [294, 295]. Our knowledge of cancer biology is not fully elucidated, but cell culture techniques including single culture or double culture of two populations of cells have been widely used in order to understand cell-cell interactions in cancer microenvironment through maximum simulation to *in vivo* microenvironment of human cancer. As the breast tumour microenvironment is composed from variety of cell types that are widely believed to play a key role during tumour progression [296], in our laboratory we used triple culture model in order to evaluate whether tumour cell characteristics under triple culture model differ from those cultured under double culture condition. In our triple culture model we used 3 cell populations including malignant cells co-cultured with macrophages and fibroblasts as they represent the predominant cells among immune cells and stroma respectively [297, 298]. However, upon double culture of breast cancer cells with

macrophages or fibroblasts and/or in triple culture with macrophages and fibroblasts, breast cancer cells showed different proliferative rates. In double culture with macrophages, breast cancer cells proliferation was inhibited compared with those cultured under triple culture condition. This indicates that the interaction between macrophages and fibroblasts favoured the tumour growth, and this have been reported that fibroblasts and macrophages interact to promote the progression of cancer [299, 300]. In addition, fibroblasts secreted collagen type I enhances macrophages adhesion and their recruitment into tumour site [301]. Moreover, activated fibroblasts secreted factors such as monocyte chemotactic protein-1 (MCP-1), stromal cell-derived factor-1 (SDF-1) and TGF-β play a big role in macrophages recruitment and polarisation into macrophages class II (M2), which have been reported to be associated with unfavourable prognosis and highly proliferative breast cancers [269, 302, 303]. Herein we evaluate that breast cancer proliferation differed when co-cultured under triple condition from those cultured under double. This well indicates that the biological interactions between stromal cells are considered pivotal for breast carcinogenesis and malignancy such as metastasis, proliferation, and angiogenesis in breast cancer. Based on the findings mentioned above and how breast cancer cells behaved under different culture conditions, more effort is required to study the biological interaction between the tumour microenvironment cells and how this interaction could positively/negatively influence tumour progression.

Chapter 5

Evaluation of cellular reprogramming of breast cancer after long-term co-culture with macrophages

5.1 Characterization of breast cancer after long-term co-culture with macrophages

Cell culture techniques have been widely used to evaluate the biological interaction between two or more cell populations. Several studies established their co-culture model by incubating two or more cell populations for 3-5 days (short-term) in order to evaluate the biological effect of these cells. These studies were able to identify gene expression level under short-term co-culture model but this could be inaccurate as tumours result from weeks-months communication with their surrounding cells such as macrophages. In addition, the promotion or suppression in the tumour progression could be either due to tumour heterogeneity which results in variety of tumour response to growth-stimulating factors, or due to cytokines and chemokines secreted factors via stromal cells such as macrophages. Here we addressed our question, whether the tumour progression under long-term (30 days) incubation of tumour cells with macrophages differs from those co-cultured under short-term condition.

To investigate this, in our study we are aiming to generate single cells clone from breast cancer cells and culture them with macrophages using our long-term co-culture condition. Upon long-term co-culture, macrophages inserts will be removed to allow breast cancer cells to grow in single culture for another 30days. Cell migration and proliferation analysis will be performed in order test any behavioral changes in cell migration and proliferation of breast cancer cells. In addition RNA-seq analysis will take a place in this study to identify gene expression changes underlying cell proliferation and migration of breast cancer.

5.1.1 Generating single cell clone

We established this experiment to generate single cells clone from both breast cancer cell lines in order to be co-cultured with macrophages using our long term model. Briefly, MDA-MB-231 and MCF-7 at density 15000 cells/ml were pipetted into 96 well plates then sequentially diluted to the last well of the second 96 well plates as described in methods. After 3 weeks a single expanded clones were transferred into 12 well plates and eventually cells were grown in T75 flask for cell expansion.

5.1.2 Assessment of gene expression in programmed breast cancer

In our previous work we tested genes expression including BIRC3, DKK, LAMC2, NRIDI and PER1 in MDA-MB-231 and FAS, ICAM1 and SOCS3 in MCF-7 cells which showed up-regulation in these genes after short–term (3-5 days) culture with macrophages relative to breast cancer cells in single culture. These changes in gene expression levels could relate to breast cancer heterogeneity which effectively respond to endocrine signals. In our current work, we hypothesised that long term incubation of breast cancer cells with macrophages will chronically up or down-regulate gene expression in breast cancer cells. To achieve this, $1x10^6$ of MDA-MB-231 or MCF-7 clones were incubated with same amount of macrophages for short-term incubation (3 days) or for short-term incubation (30 days) with bearing in mind that macrophages were replenished every 4 days. During macrophage replenishment, media of each culture (previous culture) was centrifuged and half amount of it was added to the new replenished macrophages in order to keep breast cancer cells exposed to growth factors secreted during previous culture. Post 30 days incubation

with macrophages, breast cancer cells were washed with PBS 3 times then incubated in single culture with a fresh media for another 30 days.

For clarity, clones from long-term culture and rested for 1 month post macrophages removal were termed as programmed (P), cells from short-term culture were termed as (S), and parental cells were termed as control (C). However, RNA from each culture sample was extracted and RT-PCR data a single pilot study demonstrate that genes including LAMC2, NRIDI and PER1 were significantly up-regulated in P MDA-MD-231 clones whereas BIRC3 and DKK1 showed weak or no expression in P relative to S MDA-MB-231 clones. Genes including ICAM1, FAS and SOCS3 were significantly up-regulated in P MCF-7 compared to C as shown in figure (60). This indicated the expression level of LAMC2, NRIDI and PER1 in P MDA-MB-231 clones and ICAM1, FAS and SOCS3 in P MCF-7 clones was chronically up-regulated in breast cancer cells.

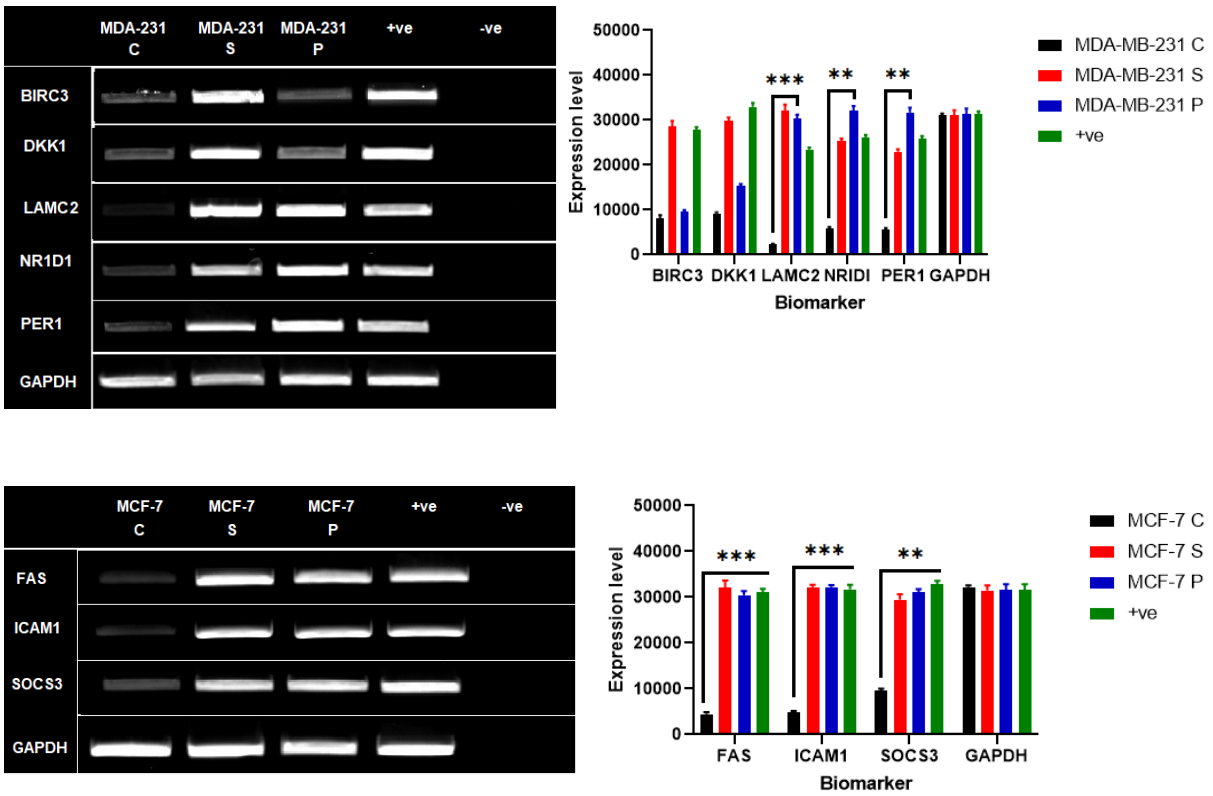

Figure 60 RT-PCR analysis of gene expression level in Programmed (P), short term incubation (S) and control MDA-MB-231 and MCF-7 clones. Bands intensity was calculated using ImageJ (V. 1.38), and plotted in Prism V8.0 (GraphPad software). A p-value of ≤ 0.05 was considered as statistical significance between the samples of each group presented in the figure.

5.1.3 Long term incubation with macrophages promoted MDA-MB-231 migration but not MCF-7

In our previous work we assessed breast cancer cell migration under co-culture with macrophages which clearly promoted breast cancer cell migration using short-term incubation model. This was due to either breast cancer heterogeneity which exhibits differential consequence of genetic changes and different levels of sensitivities to paracrine signals resulting in various morphological, metabolic and functional changes

among tumour cells, or macrophages-secreted factors itself promote cell migration of cancer cells. In this experiment we hypothesised that co-culture of breast cancer cells with macrophages for long-term incubation could chronically enhance breast cancer cell migration. Here we established this experiment to investigate programmed MDA-MB-231 and MCF-7 breast cancer clones migration under different conditions including “short-term “and “long-term” incubation with macrophages as described in methods.

Our data from 3 independent experiments demonstrate that co-culture of MDA-MB-231 and MCF-7 clones with macrophages for 3-5 days followed by 1 month incubation in single culture did not show any chronic changes in cell migration of both breast cancer subtypes as shown in figures (61, 62). Interestingly, the long-term incubation significantly promoted MDA-MB-231 migration but not MCF-7 clones. These date illustrate that macrophages have chronically enhanced MDA-MB-231 clones migration indicating that MDA-MB-231 were more responsive to macrophages signals relative to MCF-7 clone migration after long-term incubation with macrophages which did not differ from short-term incubation. To confirm our data, gene expression profile will reveal cell migration-related genes that could be used as a specific target for future studies.

(A)

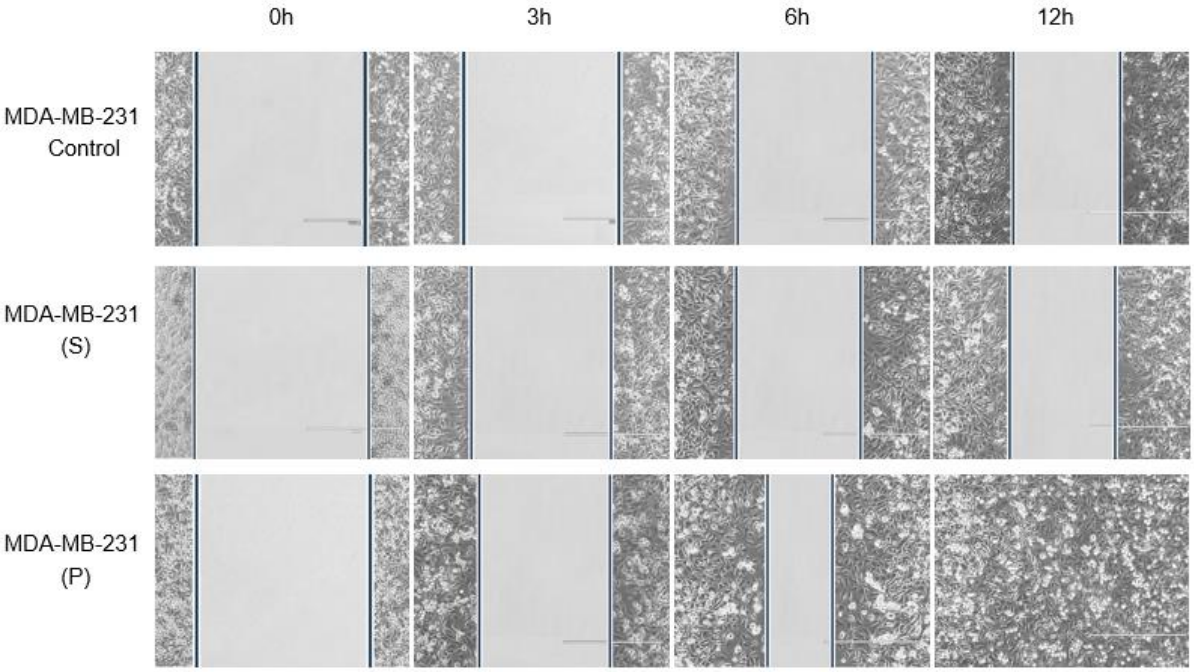

(B)

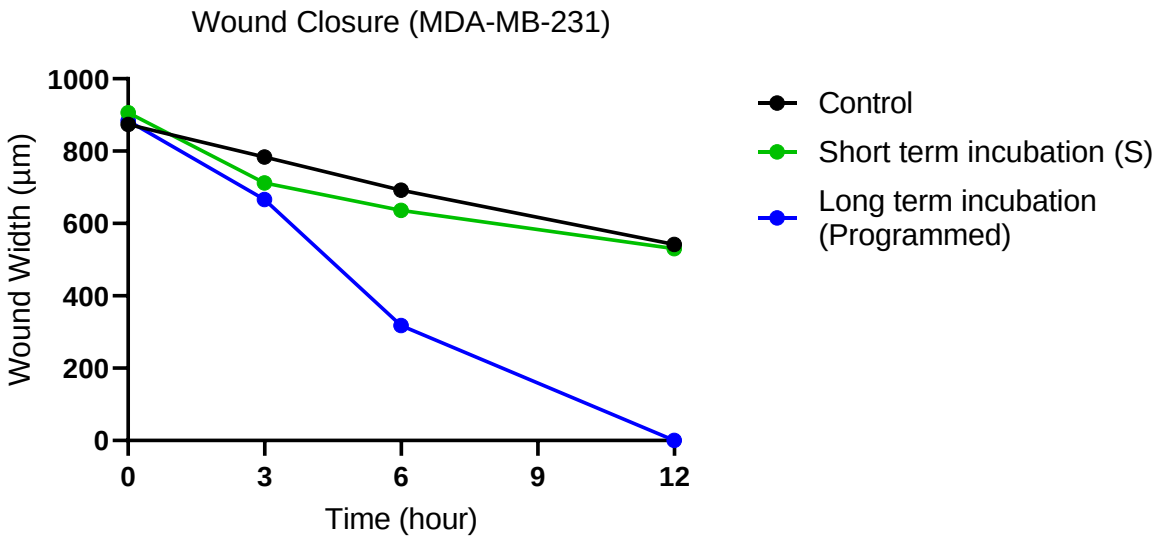

Figure 61 Representative images of MDA-MB-231 clones wound healing during 12 hours and scale bars (400 µm) are added for wound width measurement. **(A)** Wound closure of programmed (P), short-term incubation (S) MDA-MB-231 samples. **(B)** The rate of wound closure between 2 intact zones over the time. Data represent the mean value of 3 independent experiments.

(A)

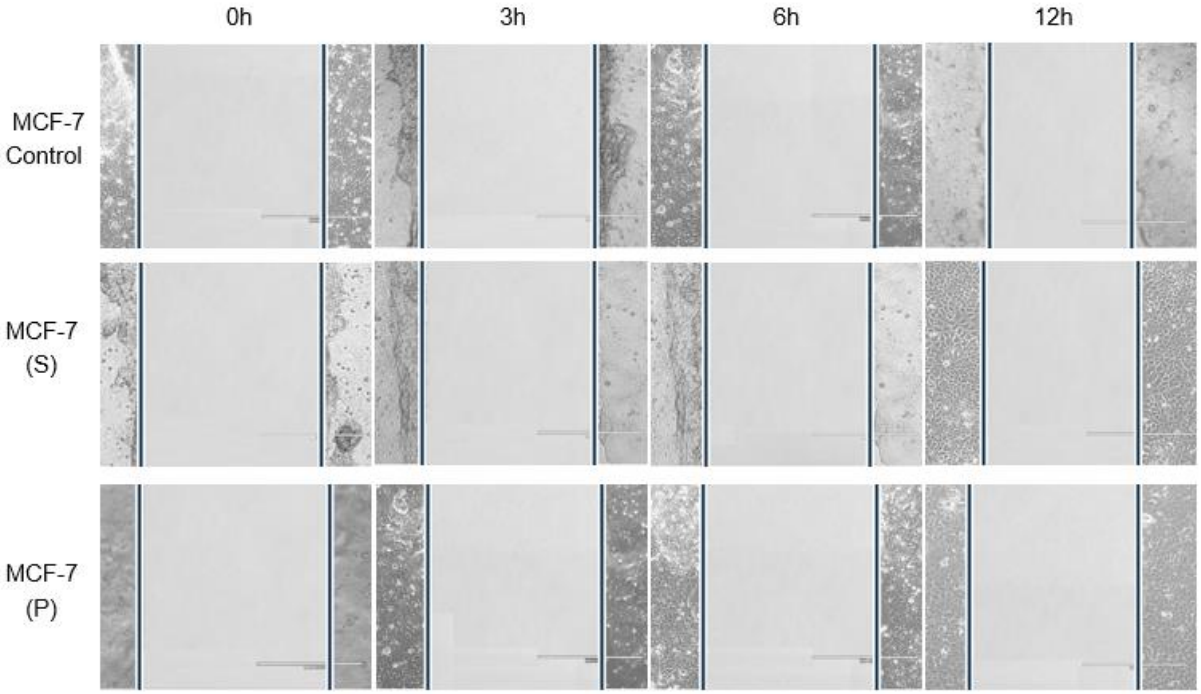

(B)

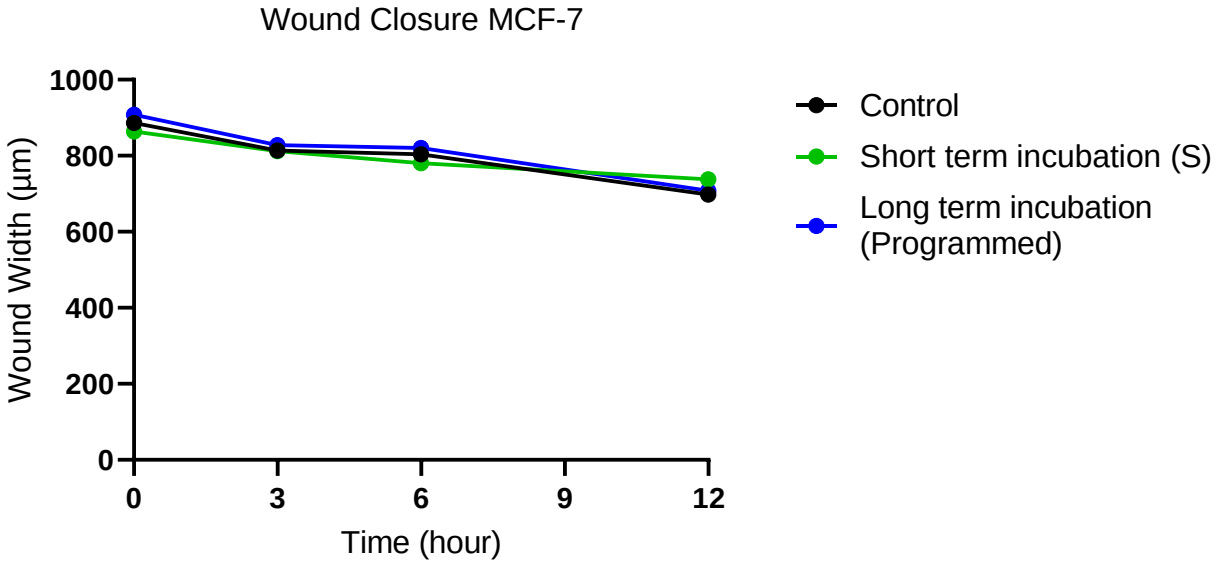

Figure 62 Representative images of MCF-7 clones wound healing during 12 hours and scale bars (400 µm) are added for wound width measurement. **(A)** Wound closure of programmed (P), short-term incubation (S) MCF-7 samples. **(B)** The rate of wound closure between 2 intact zones over the time. Data represent the mean value of 3 independent experiments.

5.1.4 Macrophages inhibited breast cancer cell proliferation

Cell growth and division is one of essential parts for cancer development and progression. Breast cancer is well known to have an aggressive progression via frequent proliferation and resistance to chemotherapy [304]. In our previous work we assessed cell proliferation of MDA-MB-231 and MCF-7 co-cultured with macrophages which resulted in low proliferation rate relative to breast cancer cells in single culture (Figure 58). Therefore we evaluated that macrophages suppressed breast cancer cell proliferation but this could be inaccurate either due to breast cancer cells heterogeneity which response differentially to external signaling molecules, or macrophages itself have the ability to suppress breast cancer cell proliferation. In addition, changes in proliferation rate of breast cancer was concluded under short-term co-culture (3-5 days) condition of both cell populations. Notably we noticed that breast cancer cell proliferation rate turn back to normal indicated that macrophages acutely educated breast cancer cells to occasionally divide. Here we addressed two questions. Firstly, will single cell clones of MDA-MB-231 and MCF-7 proliferate faster and respond differently to macrophage-secreted factors? Secondly, will the proliferation rate chronically change in breast cancer cells after conducting long-term co-culture (1 month) or cells will turn back to their normal phenotype once removing macrophages. To investigate this, MDA-MB-231 and MCF-7 breast cancer clones were incubated with macrophages for short-term (5 days) and long-term (30 days) incubation. After the indicated period of incubation we allowed breast cancer cells from both cultures to rest in fresh media for 30 days. Breast cancer cells at density $1x10^5$ were seeded into 6 well plates and incubated for 5 days. Daily cell count was performed as described in methods. However, the average of cell number from 3 independent experiments demonstrate that programmed MDA-MB-231 and MCF-7

clones significantly displayed lower proliferation rate compared with short-term incubation or control cells as determined by daily cell count as presented in figure (63). This indicates that macrophages inhibited breast cancer cell proliferation although their supporting role in breast cancer migration and resistance to therapy. To better elucidate this, macrophage educated breast cancer cells to reduce their proliferation rate via secreting high levels of TNF-α which has already been reported to be correlated with decreased cell proliferation in breast cancer [305]. On the other hand other studies demonstrated that the pro-inflammatory TNF-α plays an important role in inducing breast cancer cell proliferation [203, 306], so the mechanism behind this still unknown. However, our RNA-seq data will identify genes-related cell proliferating by which we better understand genes that could suppress breast cancer cell proliferation.

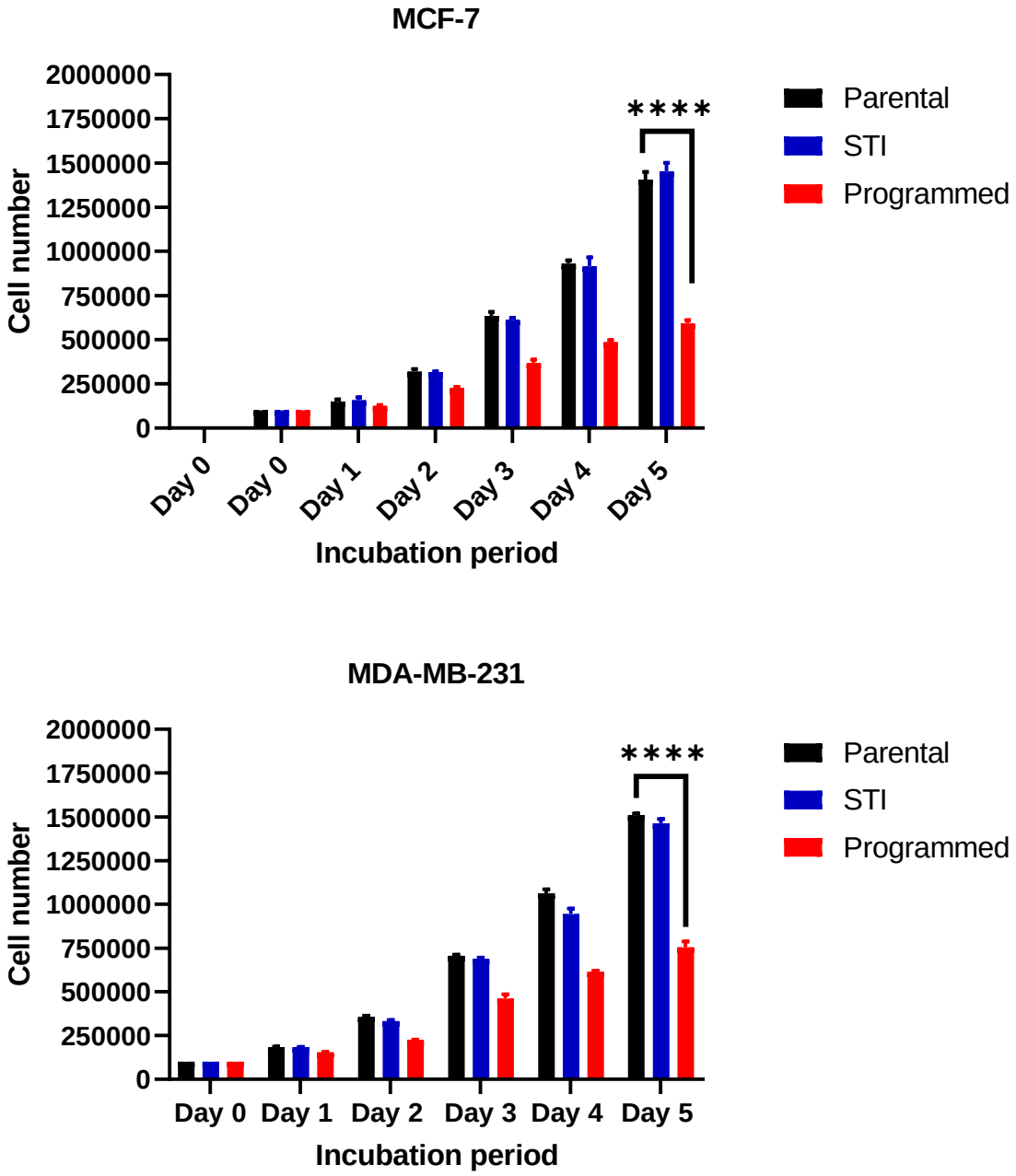

Figure 63 Cell proliferation assay of MCF-7 and MDA-MB-231 single cell clones. Breast cancer cells were incubated for short-term and long-term incubation with macrophages. This experiment was performed 1 month upon incubation with macrophages, cells from short-term and long-term cultures were termed S and P respectively. Data represent the mean value of 3 independent experiments. The analysis were performed and plotted in Prism V8.0 (GraphPad software). A p-value of ≤ 0.05 was considered as statistical significance between the samples presented in the figure.

5.2 Next Generation RNA Sequencing

5.2.1 Assessment of RNA isolation and integrity

RNA-sequencing is a technique that commonly used in many biological areas including drug discovery, cancer diagnosis and progression. The principle of utilising RNA-seq is to quantify and discover different populations of RNA including messenger RNA (mRNA), ribosomal RNA (rRNA) and transfer RNA (tRNA) using next generation sequencing (NGS). RNA-seq specifically reveals gene expression level known as “transcriptome” under different cellular conditions for instance, mutations, gene fusion and differences in gene expression level under different treatments and cultures.

The main focus of this study is to characterise breast cancer cells co-cultured with macrophages under different culture conditions, as we hypothesise that gene expression levels in short-term culture (3-5 days) will differ when using long-term culture (30 days). In addition, the reason behind performing 30 days co-culture is to evaluate how long genes will stay activated post macrophages removal. However, the total RNA from MDA-MB-231 clones was extracted and assessed as described in methods. RNA bands were assessed by observing the intensity at 28S:18S rRNA ratios as a standard measurement of RNA integrity. The 2 bands of all RNA samples were visualised at 28s and 18s which indicated that all RNA samples were isolated at good quality as shown in figure (64).

To further investigate RNA integrity, cDNA was synthesised from all RNA samples including control (C), short-term (S), long-term (L) and programmed (P) as described previously, RT-PCR was performed in order to test the expression level of the following genes BIRC3, LAMC2, DKK1, PER1 and NRIDI. RT-PCR data from 3 independent experiments revealed that LAMC2, PER1 and NR1D1 showed high expression in all

samples whereas BIRC3 and DKK1 showed weak or no expression in P relative to S and L samples. Same patterns were detected among L and S samples as presented in figure (64). Upon RNA isolation and assessment, 1ng/ml was taken from each RNA sample and mixed with RNase free water to get 20µl as a final volume for RNA-seq analysis. The expression profile of RNA was performed at Nonogene Europe (Cambridge Science Park, Cambridge, CB4 0FW, United Kingdom) using NGS (next generation sequencing).

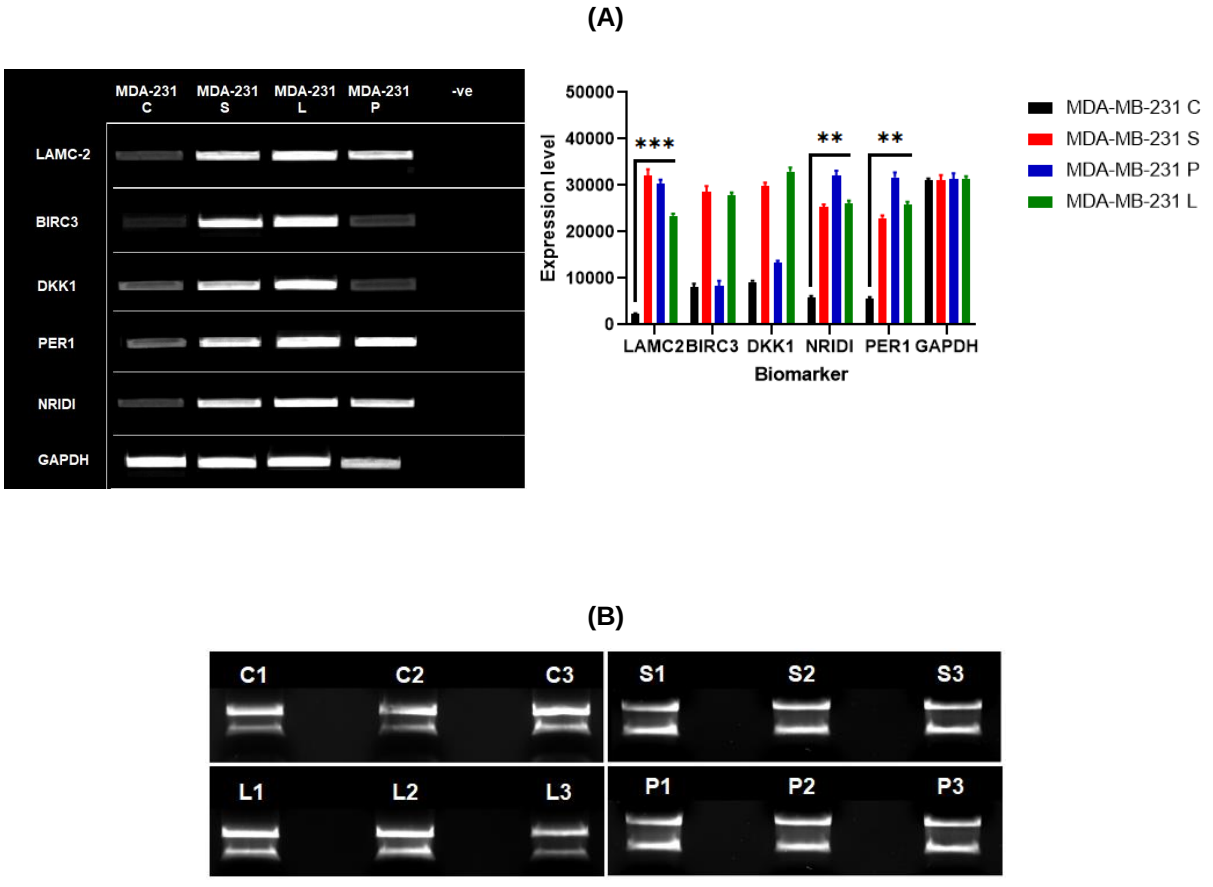

Figure 64 Analysis of gene expression and RNA quality. **(A)** Gene expression in MDA-MB-231 samples including control (C), short-term incubation (S), long-term incubation (L) and programmed (P). Bands intensity was calculated using ImageJ (V. 1.38), and plotted in Prism V8.0 (GraphPad software). A p-value of ≤ 0.05 was considered as statistical significance between the samples of each group presented in the figure. **(B)** RNA analysis by agarose gel of all indicated samples, which shows the 2 bands represented by 28s and 18s ratios of ribosomal RNA.

5.2.2 Analysis of KEGG pathways and Gene Ontology enrichment

Data of whole defined genes was further analysed in order to infer the biological role of up and down-regulated genes in MDA-MB-231 clones cultured under different cultures. We conducted enrichment analysis with Gene Ontology (GO) terms, Kyoto Encyclopedia of Genes and Genomes (KEGG) pathways in order to annotate the biological process in a directed acyclic graph structure and pathways level respectively. The GO analysis revealed top 20 significant functional enrichments involved in biological process, molecular function and cellular component in MDA-MB-231 clones under different cultures including short-term incubation, long-term incubation with macrophages and programmed MDA-MB-231 clones compared to control samples. Interestingly, the GO analysis showed that 19 pathways were mutually enriched among all samples (C, S, L and P), and these include cell cycle, intracellular, cytoplasm, mitotic cell cycle and others as shown in figure (65a, 65b and 65c). Notably, 3 cellular pathways including mitochondrion, protein containing complex and biosynthesis process were particularly enriched in L and P samples (Figure 65b, 65c). Interestingly, 5 cellular pathways including RNA binding, cellular protein modification process, enzyme binding and others were uniquely enriched in P samples (Figure 65c).

Additionally the KEGG annotations show top 20 significant pathways. 3 enriched pathways including metabolic pathways, PI3K-Akt signalling pathways and Epstin-barr virus infection were remarkably enriched in L and P populations (Figure 65d, 65e). Whereas, 5 pathways were uniquely enriched in P compared to L, C and S samples (Figure 65f). Similar pathways were enriched in all MDA-MB-231 samples, and these include metabolic pathways, HTLV-I infection and pathways in cancer (Figure 65d, 65e and 65f).

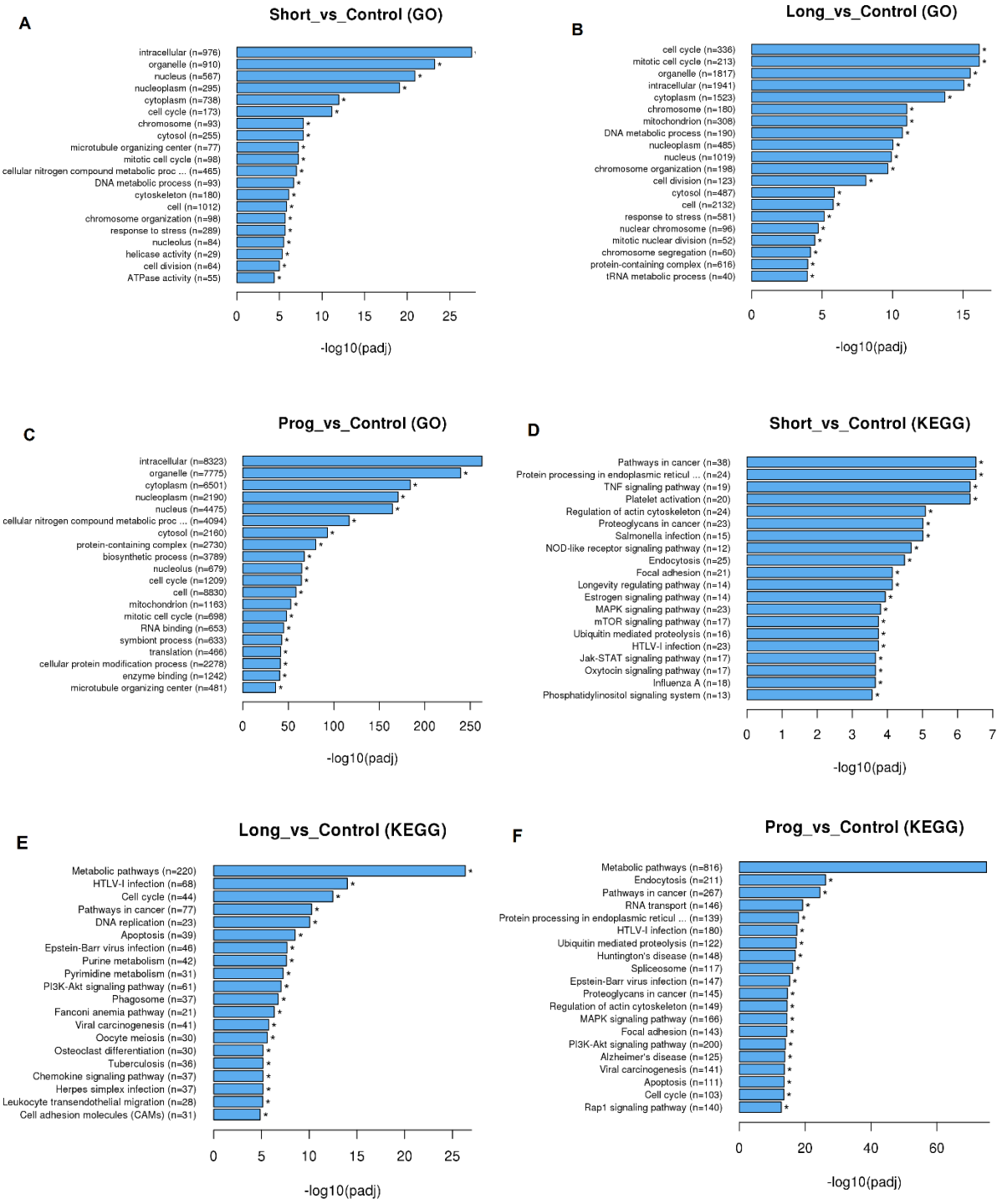

Figure 65 Top 20 functional enrichment analysis of Gene Ontology (GO) and Kyoto Encyclopedia of Genes and Genomes (KEGG) pathways. Both analysis were performed by comparing gene expression level in short-term (S), long-term (L) and programmed MDA-MB-231 to control (C) known as parental. **(A, B, C**) figures show the GO analysis of (S-*vs*-C), (L-*vs*-C) and (P-*vs*-C) respectively. (**D, E, F**) figures show the KEGG pathways of ((S-*vs*-C), (L-*vs*-C) and (P-*vs*-C) respectively.

5.2.3 Differential gene expression and overlapping genes between samples

The analysis of differential gene expression was performed in order to evaluate gene expression differences between our samples including control, short-term, long-term and programmed MDA-MB-231 clones. The significance in up and down-regulation in gene expression was calculated using Benjamini and Hochberg's method as described previously. Based on these adjustments we found that 1077 up-regulated and 145 down-regulated genes were significantly differentially expressed in short-term compared to control, while in long-term we found 653 up-regulated and 2482 down-regulated genes were differentially expressed relative to control. Furthermore, we found 5591 up-regulated and 6093 down-regulated genes were differentially expressed in programmed in contrast with control as presented in figure (66a, 66b and 66c). Furthermore, we found 149, 76 and 370 genes were overlapped between control *vs* short-term, control *vs* long-term and control *vs* programmed respectively as shown in figure (66d), indicating that programmed cells share high number of up and down-regulated genes.

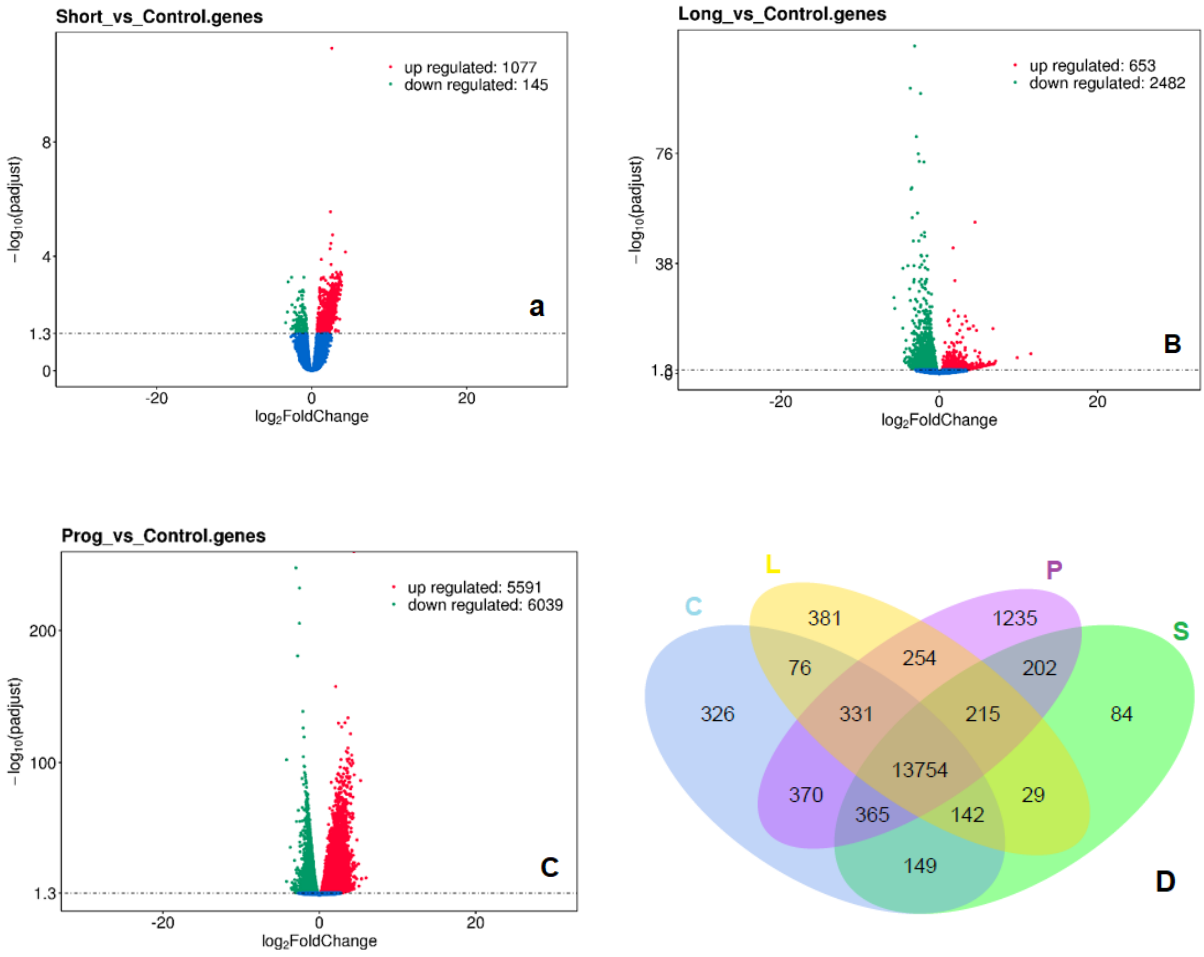

Figure 66 Differentially gene expression and Venn diagram in single cell clones of MDA-MB-23 samples under different cultures. **A, B** and **C**, volcano plots of identified differentially expressed genes between C *vs* S, C *vs* L and C *vs* P respectively. **D**, the Venn diagram shows the overlapping genes between C *vs* S, C *vs* L and C *vs* P.

5.2.4 Clustering and grouping of MDA-MB-231 samples

Hierarchical grouping of the index-coded samples of MDA-MB-231 samples including C, S, L and P were conducted on a cBot Cluster Generation System using PE Cluster Kit cBot-HS (Illumina). This analysis was performed on all MDA-MB-231 clones including C, S, L and P and each sample consisted of three biological replicates. Sequencing of gene expression library was performed on an Illumina platform and paired-end reads and each sample cluster was visualised using colour scheme. The

threshold of up-regulated and down regulated genes was adjusted with fold change >2 and $p < 0.05$. Data of gene expression are displayed in a grid and each column and row represent a sample and a gene respectively. The red and blue colours were used to annotate up-regulated and down-regulated genes respectively. Based on these adjustments, C and P clusters were grouped as expected which show the similarities between the three biological replicates of each sample as presented in figure (67). Unexpectedly, S1 and L3 samples showed different patterns from their pairs despite of using same cell population. This could relate to samples labelling or samples replacement during samples analysis.

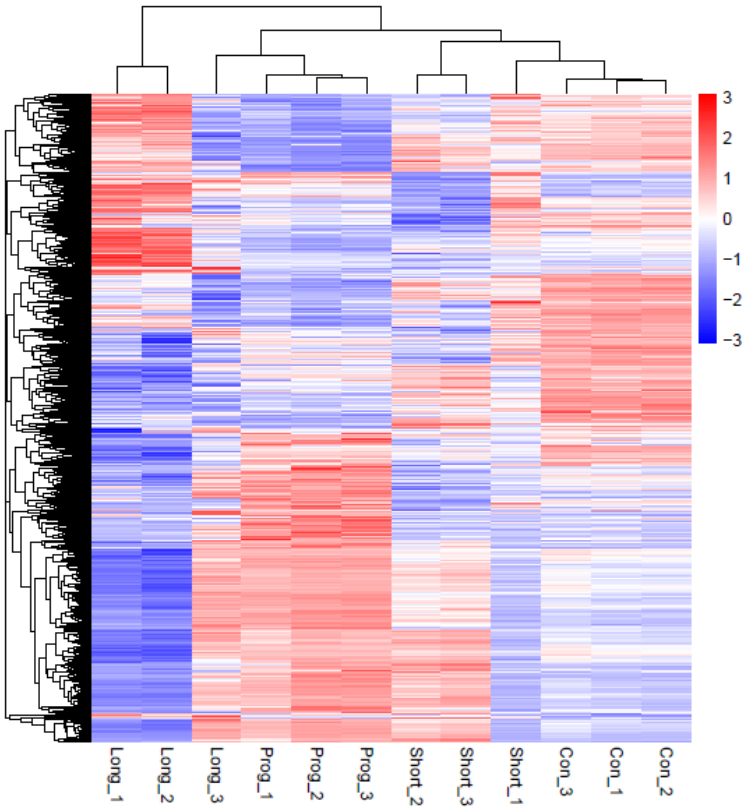

Figure 67 Gene expression pattern of the MDA-MB-231 clones represented by the heat map. The horizontal axis shows the sample clusters while the vertical axis shows the detected mRNA and lncRNA genes. The red and blue bars indicate an increase and decrease in the level of the corresponding genes, respectively. All samples were analysed in triplicate and the name of the samples was indicated as follows: control 1 (con 1), control 2 (con 2), control 3 (con 3) and the same is true for S, L and P.

5.3 Identification of genes-related cell migration

Cancer development and metastasis require advanced cancer progression including cell migration. We have previously characterized breast cancer under different conditions using various tissue culture models. Interestingly, we found that long-term incubation of breast cancer cells chronically promoted MDA-MB-231 cell clone migration relative to short-term incubation which did not show any changes post macrophages removal as described previously. To further explore molecular changes underlying migration gaining, we performed a whole RNA sequencing in order identify genes-related cell migration in MDA-MB-231. Analysis of RNA-seq revealed 69 genes implicated in MDA-MB-231 cell clone migration under different cultures. To categorize the up-regulation and down-regulation of gene expression level, the control MDA-MB-231 cells were used as a baseline for short-term, long-term and programmed MDA-MB-231 clone. The up-regulated genes were grouped with 2 fold-changes or more, while the down-regulated genes were grouped with 0.5 or less for a significant expression. Our date demonstrate that 26 genes were up-regulated in programmed MDA-MB-231 relative to control, whereas 12 genes were significantly down-regulated in programmed MDA-MB-231 in comparison with control which showed higher expression as presented in tables (12,13). All identified genes can be classified into three categories according to their functional involvement in cell migration.

Firstly those that accelerate tumour cell migration such as RAPGEF4, RAP1B, RAP1A, CLDN1 and MYL12A and the overexpression of these genes was found to be associated with poor prognosis in many cancers [307-315]. These genes were significantly up-regulated in programmed MDA-MB-231 clone indicating that co-culture of macrophages with MDA-MB-231 clone chronically up-regulated genes-specific migration. Secondly, genes that impair migration with cell proliferation were

down-regulated in programmed MDA-MB-231 clone such as RASSF5 and RAC2 and knocking down these genes promoted tumour cell migration, invasion and proliferation [316, 317]. Thirdly, those genes that didn't show significant changes in MDA-MB-231 under different condition cultures. Given these evidences, we evaluate that macrophages influenced breast cancer cell migration not only when using a direct co-culture but also they could chronically up-regulate migration-specific genes after long term co-cultured with MDA-MB-231 breast cancer clone.

Table 12. Top10 up-regulated genes-related MDA-MB-231 clone migration identified by next generation sequencing. The table shows the fold change (Log_2) gene expression in short-term (S), long-term (L) incubation and programmed MDA-MB-231 samples compared to control.

No	**Gene Name**	**Fold Change (Log_2)**		
		Fold (S)	**Fold (L)**	**Fold (P)**
1	RP11-359J14.2	1.38734371	1.53010056	19.5781071
2	RP11-677M14.6	0.99546147	3.33211047	16.2085577
3	PI3KCG	1.89107987	2.46403284	6.95873168
4	PIK3CA	8.03775054	3.13056271	10.7129843
5	ITGB1P1	2.83165934	2.17665098	6.12475318
6	PIK3R1	5.72222258	3.86003418	10.9838316
7	ROCK2	6.58467842	1.55969328	9.12253035
8	ARHGAPS	7.12468248	1.38690388	11.6696569
9	ROCK1	6.80985872	1.60796849	8.89500855
10	ITGB1	2.90570259	2.01692342	6.95413124

Table 13. Top 10 down-regulated genes-related MDA-MB-231 cell migration identified by next generation sequencing. The table shows the fold change (Log_2) gene expression in short-term (S), long-term (L) incubation and programmed MDA-MB-231 samples compared to control.

No	**Gene Name**	**Fold Change (Log_2)**		
		Fold (S)	**Fold (L)**	**Fold (P)**
1	MAPK11	0.82023026	0.81500367	0.46599577
2	CLDN23	0.50213146	0.29163093	0.28247925
3	CXCR4	0.83297391	1.12254364	0.32677378
4	PLCG2	0.70480338	0.49029103	0.2753846
5	RP11-281P11.1	0.43233947	0.19323765	0.44934146
6	CLDN4	0.87163201	0.66552494	0.35878987
7	SIPA1	0.86366391	0.7155029	0.48736649
8	MYL9	1.03122035	0.52950461	0.44651074
9	BCAR1	0.75004333	0.59945171	0.5091679
10	CDC42P6	0.69034638	0.34469634	0.39850181

5.4 Identification of genes-related cell proliferation

A continuous cell proliferation is one of cancer cells characteristic that have the ability to uncontrollably divide via sustaining their proliferative signalling as well as the ability to evade homeostatic signalling network that controls cell proliferation. In our previous work we investigated the proliferation of MDA-MB-231 and MCF-7 single cell clones after long term incubation with macrophages which significantly inhibited the proliferation of both breast cancer subtypes. In this experiment we investigated the expression profile of genes underlying proliferation signature of MDA-MB-231 samples including control (C), short-term (S), long-term (L) incubation and programmed (P) using RNA-sequencing. The analysis revealed 110 genes to be implicated in MDA-MB-231 cell proliferation. To stratify the up and down-regulated genes were used C

MDA-MB-231 clone as a baseline for P MDA-MB-231 clone as we mainly focused to analyse gene expression changes between C and P cell populations. The significance in gene expression changes of up-regulated and down-regulated genes was adjusted with 2 fold changes (log_2) and 0.05 or less respectively as a threshold for our analysis. Based on these adjustments we found 38 up-regulated and 14 down-regulated genes significantly expressed in P relative to C MDA-MB-231 clone as listed in tables (14, 15). We further investigate the biological role of some up-regulated genes and their involvement in tumour proliferation. Some of these genes were found to play an important role in cell cycle pathways such as STAG1 and ART. The overexpression of these genes was found to be associated with cell cycle arrest in many tumours including breast cancer [318-320]. The other example of up-regulated genes is SMAD4 which plays a pivotal role in regulating cell growth. However, Deckers *et al* have reported that high expression of SMAD4 was associated with reduced cell growth via mediating proapoptotic and antimitogenic effects of TGF-β [321]. Another example of down-regulated genes is MCM2, which plays a big role in breast cancer proliferation, and the expression of MCM2 was associated with poor prognosis and proliferation rate [322]. Some other genes have no effect on tumour proliferation such as SMAD2. The knockdown of over-expressed SMAD2 had no effect on MDA-MB-231 cell growth [323]. Furthermore we evaluated the role of some down-regulated genes in programmed MDA-MB-231 cells, PLK1 gene involved in cycle and the down-regulation or knockdown of PLK1 induced cell cycle arrest at G2/M phase in MDA-MB-231 breast cancer cells [324]. Based on these findings, we evaluate that long-term co-culture of macrophages with MDA-MB-231 breast cancer clones reduced cell growth via up-regulating and down-regulating genes related cell division which can be used as potential therapeutic target for breast cancer.

Table 14. Top 10 up-regulated genes related cell proliferation in MDA-MB-231 clones identified by next generation sequencing. The table shows the fold change (Log_2) gene expression in short-term (S), long-term (L) incubation and programmed MDA-MB-231 samples compared to control.

No	Gene Name	Fold Change (Log_2)		
		Fold (S)	Fold (L)	Fold (P)
1	STAG1	6.946601575	1.912467804	8.518424056
2	ATR	10.12199018	2.452642027	12.39866193
3	CDK6	6.482042746	2.785866867	16.23093174
4	SMC3	6.904141656	1.380779293	7.073400261
5	ATM	4.468899548	1.967680923	12.28616841
6	STAG2	10.09516827	1.123932998	7.5422664
7	RBL1	2.8689273	0.408785175	4.649919515
8	RB1	5.32304891	1.207863205	8.081195922
9	RBL2	1.238508953	1.412797016	4.802778928
10	CDC27	6.099015069	2.060839831	7.973956448

Table 15. Top 10 down-regulated genes related cell proliferation in MDA-MB-231 clones identified by next generation sequencing. The table shows the fold change (Log_2) gene expression in short-term (S), long-term (L) incubation and programmed MDA-MB-231 samples compared to control.

No	Gene Name	Fold Change (Log_2)		
		Fold (S)	Fold (L)	Fold (P)
1	MAD2L2	0.879480437	0.583264523	0.499932782
2	MCM2	0.65979936	0.249632075	0.487588003
3	MCM5	0.777005162	0.273552103	0.476274943
4	CDC20	0.871118592	0.263000968	0.260899073
5	GADD45G	0.458561798	1.230394294	0.218033326
6	CCNA1	0.955039642	0.424307011	0.322808589
7	E2F2	0.509734449	0.043490162	0.3894967
8	ORC1	0.592230758	0.089705291	0.353865157
9	CCNE1	0.615626737	0.163309022	0.369285458
10	CDC25A	0.614124686	0.10047909	0.313337309

5.5 Analysis of gene expression related cell migration and proliferation

In our previous work we characterised programmed (P) MDA-MB-231 and MCF-7 clones proliferation and migration after long-term co-culture with macrophages. Notably, both MDA-MB-231 and MCF-7 clones displayed low proliferation rates relative to control (C) breast cancer cells. In addition, MDA-MB-231 clone markedly migrated faster than C clone, MCF-7 clones did not show changes in their migration behaviour in comparison with C clone. This has increased our interest to further investigate the molecular changes underlying proliferation and migration gaining. We therefore conducted NGS (RNA-seq) which revealed numbers of up-regulated and down-regulated genes implicated in many cellular processes including migration and proliferation of MDA-MB-231 clone. To validate our RNA-seq data, we have selected some genes implicated in MDA-MB-231 cell clone migration and proliferation behaviour, and test them using RT-PCR analysis. Furthermore, these genes will be tested in MCF-7 cell clones in order to evaluate whether gene expression level in MCF-7 differs in MDA-MB-231 clones.

5.6 Validation of gene expression related cell migration

In our previous work we performed cell migration assay of programmed MDA-231 and MCF-7 clones which clearly showed that MDA-MB-231 significantly migrated faster than MCF-7 within 12hrs of incubation. This indicated that macrophages increased the aggressiveness of MDA-MB-231 clone after as result of 1 month of co-culture. We therefore performed RNA-seq analysis in order to identify gene expression underlying cell migration as described previously. In this experiment we tested the expression of some up-regulated using RT-PCR analysis in order to validate our RNA-seq data as

well as to examine their expression in MCF-7 clone to evaluate whether MCF-7 differ from MDA-MB-231 clones in term of gene expression. Data from RT-PCR revealed that all tested genes including ARHGAP5, ITGB1, PIK3CA, PIK3CG, ROCK1 and ROCK2 were significantly up-regulated in programmed MDA-MB-231clone relative to control as expected from our RNA-seq data. Same genes were tested in programmed MCF-7 clone which did not show any changes apart from ROCK1 gene which was weakly up-regulated compared to control MCF-7 clone as presented in figure (68). This indicated that long-term incubation of macrophages with breast cancer cells chronically up-regulated genes-related cell migration in MDA-MB-231 but not MCF-7 clones.

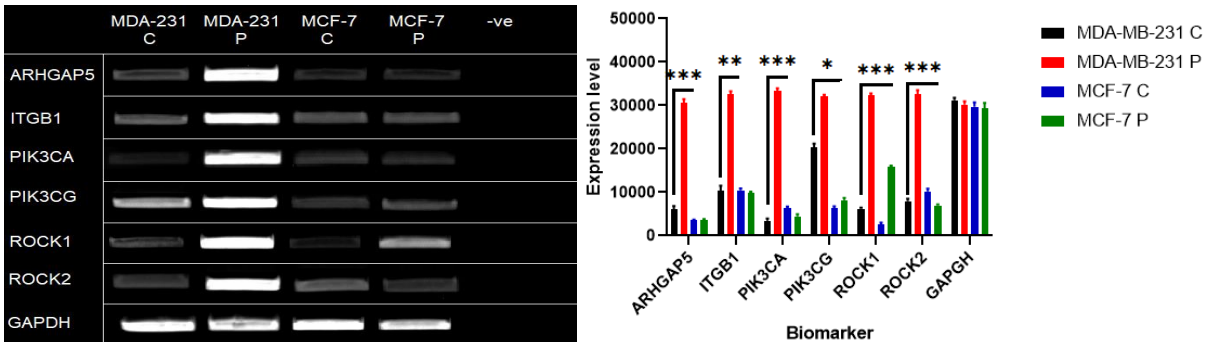

Figure 68 Validation of genes related cell migration using RT-PCR analysis in programmed (P) MDA-MB-231 and MCF-7 clones compared to control breast cancer cells. Gene expression level of all tested genes were normalised to GAPDH expression. Bands intensity was calculated using ImageJ (V. 1.38), and plotted in Prism V8.0 (GraphPad software). A p-value of ≤ 0.05 was considered as statistical significance between the samples of each group presented in the figure.

5.7 Validation of gene expression related cell proliferation

Accelerated cell proliferation is one of invasive breast cancer hallmark, we therefore examined MDA-MB-231 and MCF-7 cell clone proliferation under different cultures and conditions. One of our important experiments was to evaluate programmed breast cancer cell proliferation after long-term incubation with macrophages in order to evaluate whether macrophages can chronically promote or supress breast cancer cell division. Interestingly we noticed that macrophages supressed programmed breast cancer cell proliferation compared to control cells. This has increased our interest to identify genes expression changes underlying this process, we then performed RNA-seq analysis which revealed large number of up-regulated and down-regulated genes in programmed MDA-MB-231 that mediate cell proliferation as discussed previously. This experiment was established to validate our RNA-seq data via conducting RT-PCR analysis and to evaluate their expression in MCF-7 cells. Briefly, RNA from $1x10^6$ breast cancer cells including programmed and control MDA-MB-231 and MCF-7 clones was extracted and Reverse transcriptase was conducted. Some genes with 3 or more folds change were unbiasedly selected and RT-PCR analysis was performed as described previously.

The expression of all tested genes was normalise to GAPDH expression as an endogenous control. ATR expression was significantly up-regulated in both programmed MDA-MB-231 and MCF-7 clones, whereas the expression of MCM2 and MCM5 was markedly down-regulated in programmed breast cancer cells compared to control. CDC27 was highly expressed in programmed MDA-MB-231 relative to control cells, while it was weakly down-regulated in programmed MCF-7 clone compared to control. MAD2l2 was clearly down-regulated in programmed MDA-MB-231 clone in comparison with control cells, no changes were seen in all MCF-7 clone. RB1 gene

expression was clearly up-regulated in programmed MDA-MB-231 clone compared to control cells, MCF-7 clone did not show any significant changes when compared between programmed and control MCF-7 clones as shown in figure (69).

Here we observe similar expression patterns between MDA-MB-231 and MCF-7 clones when comparing ATR, MCM2 and MCM5, while both MDA-MB-231 and MCF-7 clones showed significant differences in their expression levels in CDC27, MAD2l2 and RBI genes as indicated above. In addition, the expression level of all tested genes in MDA-MB-231 cells validates our RNA-seq data as shown in table (14,15).

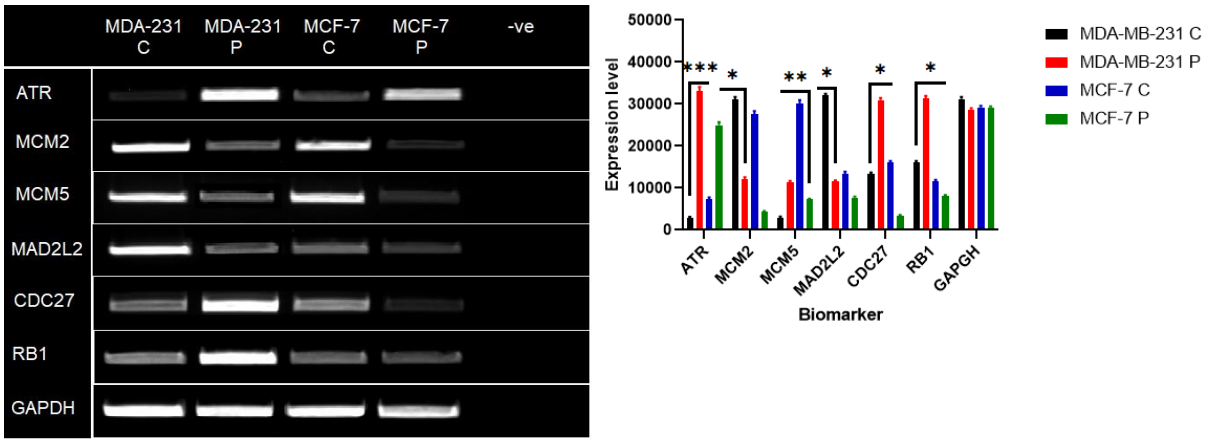

Figure 69 Validation of genes related cell proliferation using RT-PCR analysis in programmed (P) MDA-MB-231 and MCF-7 clones compared to control breast cancer cells. Gene expression level of all tested genes were normalised to GAPDH expression. Bands intensity was calculated using ImageJ (V. 1.38), and plotted in Prism V8.0 (GraphPad software). A p-value of ≤ 0.05 was considered as statistical significance between the samples of each group presented in the figure.

Discussion

Co-culture methodologies of two or more cell populations have been widely used in many laboratories including cancer research in order to study the biological interaction between malignant and stromal cells [325]. These cultures are mostly performed by placing cell types one on top of the other for 3-5 days incubation in order to evaluate tumour cell characterisation such as cell proliferation, invasion, migration and resistance to therapy. However these cultures could be associated with inaccurate outcomes as cancers are resulted from long-term “weeks-months” interaction with stromal cells to invade from their original site into another part of the body [326]. It has been reported that cancer cells acquire different molecular and morphological changes known as “cell reprogramming” as a result of the complex interaction between malignant and stromal cells [327]. If the tumour has not been well eliminated by immune system, tumour cells will continuously gain a cellular changes which therefore result in more aggressive and resistant to therapy tumours [328]. This indicates that the longer-term communication of tumour cells with their surrounding cells the more aggressive tumours become and are more able to manipulate immune system in order to survive and invade into another nearby tissues [329].

Based on these observations, our laboratory hypothesised that long-term incubation (30 days) of breast cancer cells with macrophages could lead to chronic gene expression in breast cancer compared with those cultured under short-term (3-5 days) incubation. However, in response to long-term communication of breast cancer cells with macrophages, MDA-231 cells from long-term co-culture condition migrated faster than those cultured under short-term condition. No changes were seen in MCF-7 cell migration cultured under the same conditions above. Herein we evaluate that during long-term co-culture with macrophages, MDA-MB-231 cells potentially gained a series

of mutations and epigenetic changes as a requirement for tumour survival and development [330]. In addition, in comparison with MCF-7, MDA-MB-231 by nature are the most heterogeneous among all subtypes and are always associated with aggressive behaviour such as high proliferative rate, migrate faster and invade from the local tissue into another parts of the body [331]. RNA-seq analysis revealed that several genes underlying cell migration were chronically up-regulated after long-term incubation with macrophages, whereas no changes in gene expression were seen MDA-231 cells after short-term culture. These data confirms our hypothesis that the long-term incubation with macrophages the more genes were chronically changed. Same genes that regulated MDA-MB-231 cell migration were tested in MCF-7. However, RT-PCR analysis did not show any changes in gene expression after long-term incubation with macrophages indicating that gene expression in MCF-7 revert back to normal expression after co-culture with macrophages. The mechanism under these changes in both breast cancer cells is unknown but further investigations still required which therefore facilitate molecular targets in future therapies.

Chapter 6

Discussion and summary of findings

6. Discussion

6.1 Analysis of immunohistochemistry study

The aim of this study was to identify differences in the tumour microenvironment between ER+ and ER- invasive ductal breast cancer. The tumour microenvironment is composed of fibroblasts, myofibroblasts, epithelial, myoepithelial, smooth muscle and various immune cells along with extracellular matrix (ECM). A range of stromal cells were stained using immunohistochemistry. In this project, 7 biomarkers were optimised using the standard immunohistochemistry protocol as mentioned in methods section 1. In order to achieve the appropriate concentration for each antibody, seven biomarkers were diluted using serial concentrations (1-50, 1-100, 1-200) including a negative control. 1-100 concentration was chosen for CD3, CD8, CD20, CD68, α-SMA, and Foxp3 antibodies while 1-50 was chosen for CD4 antibody. These concentrations enabled visualization of specific biomarker staining and minimized non-specific background signals. Taking these concentrations forward, 50 TNBC and 20 ER+ cases were retrieved, sectioned and immunohistochemically stained for each biomarker. The sections were then digitally scanned.

Analysis of CD3, CD4, CD8, CD20, CD68, Foxp3 and αSMA expressing cells in 50 TNBC and 20 ER+ samples revealed heterogeneity in biomarker positivity and their tissue distribution. The distribution of each targeted cell was evaluated whether intratumoural or stromal. Interestingly, CD3+ and CD8+ were largely distributed in stroma and the density of CD3+ and CD8+ cells associated with other immune cells that accumulated at the tumour edge and the distribution of these cells was modest in the tumour area in TNBC samples. Other studies have shown that CD8+ predominantly infiltrated in stroma and tumour edge [332]. Whereas with ER+ cases,

CD3+ and CD8+ cells were found within the tumour and some CD3+ and CD8+ cells were seen along at tumour edge. There was some evidence of CD3+ and CD8+ co-localisation in the stroma near the tumour, in both TNBC and ER+ cases. CD68+ cells predominantly infiltrated the stromal areas and but large numbers of CD68+ cells localised within the tumour in both TNBC and ER+ cases. It was demonstrated that the density of distant stromal macrophages was higher than intratumoural and adjacent stromal macrophages [333].

Results from PPC analysis revealed CD3+, CD4+ and CD8+ numbers were positively correlated with higher histological grade in TNBC cases. This is confirmed by literature showing that CD8+ cell in high abundance is associated with high tumour grade in breast cancer [334]. While in ER+ breast cancer cases, CD3+, CD4+ and CD8+ abundance was negatively correlated with high grade tumour. CD68+ cells were positively correlated with high grade in both TNBC and ER+ cases. This data is in agreement with reports that show the negative impact of CD68+ density in the tumour microenvironment, however, it has been reported that the number of CD68+ cells has been reported to be associated with aggressive clinicopathologic features such as high histological grade [155]. CD20 positive cells were only correlated with high tumour grade in TNBC and not in ER+ cases which were found to be negatively correlated with high tumour grade. Foxp3+ number showed no differences with low vs high grade in ER+ breast cancer cases, though it was seen to be negatively correlated with high grade tumour in TNBC cases. αSMA+ cells were largely infiltrated in the tumour and stroma, αSMA+ number was positively correlated with high tumour grade in TNBC and ER+ breast cancer cases.

The immunohistochemistry staining was conducted on 50 TNBC and 20 ER+ breast cancer cases. For our future work and additional 80 ER+ and 50 TNBC cases have

been requested from tissue bank. These cases will be sectioned, stained and scored using PPC analysis as described in this preliminary work. During the course of this work, a new faster way of assessing PPC became available called Qu-Path [335]. This could be used in future analysis. Using patient histopathological characteristics, we will use Kaplan-Meier survival analysis to determine if expression of inflammatory cells and/or CAFs in ER+ and ER- influence patient over all outcome or disease free survival.

Tissues from TNBC and ER+ breast cancer subtypes were successfully submitted to Raman analysis and our data revealed that although the sort time of samples exposure to light, various vibrations occurred through the analysis, this indicates that experiment was successfully performed. Here we evaluate that the confocal Raman spectroscopy combined with statistical methods allows these tissues to be analysed by determining their chemical composition and thus provides feedback for the spinning process. A whole map of both tissues took between 25 and 35 minutes, meaning that the exposure time could be increased to obtain a better signal-to-noise ratio and allow greater areas to be mapped overnight. This promising data could contribute to therapeutic targets as by revealing the abundance of chemicals distribution in tumour tissue compared with normal tissues.

Various CM was generated from MCF-7, MDA-MB-231 and CAFs derived from ER+ breast cancer patient samples. Our preliminary data shows the role of CM generated from breast epithelial cell lines and CAFs derived from ER+ breast cancer, which have a measurable effects on cell proliferation. In future work, we aim to conduct additional experiments using these cell lines at the same ratio of conditioned medium (100%) as well as with decreasing concentrations of conditioned medium (75%, 50%, 25% and 12.5%). In addition we will culture each cell line using the same conditioned medium

derived from that line to determine whether cell proliferation is inhibited due to nutrition depletion in the conditioned medium or by soluble factors of other cell line.

Pirfenidone is an anti-fibrotic drug which has been shown to decrease collagen synthesis in several studies [336]. In this study we investigated the effect of serial dilutions of PFD (100-1µM) on cell proliferation of MCF-7, MDA-MB231 and CAFs derived from ER+ breast cancer. A 100µM PFD had noticeable inhibitory effect on breast epithelial cell lines and CAFs. A sign of acute toxicity to PFD was seen at the highest concentration used (100µm). Therefore, no growth was seen during incubation time (120h). While the cell proliferation of MCF-7, MDA-MB-231 and CAFs derived from ER+ breast cancer gradually increased with both 10µm and 1µm. Interestingly, we noticed that PFD inhibited the cell growth of epithelial cells, although PFD was reported to be an anti-fibrotic drug [337]. The rational for this observation could have due to PFDs ability to abrogate the TGF-β pathway via inhibition SMADs resulting in inhibitory of cell proliferation [338].

Several techniques including immunohistochemistry, qRT-PCR, flow cytometry and immunofluorescence are used to detect ER expression in breast cancer cells. However, in this work we used qRT-PCR to detect the ER expression in both CAFs derived from ER+ and ER- breast cancer. Briefly, MCF-7 (positive control), MDA-MB231 (negative control), CAFs derived from ER+ breast cancer patient (LS12-041) and CAFs derived from ER- breast cancer patient (TCBI) were investigated for ER-α expression. Our data shows that MCF-7 was positive for ER-α expression, while MDA-MB-231 showed negative expression of ERα, as expected. These cell lines are extensively used in biomedical research as ER+ and negative controls. MCF-7 cell line has been reported to be positive for ER-α [339]. Both CAFs showed negative expression of ER-α. Although fibroblasts were derived from ER+ breast cancer

patients, the expression of ERα was negative. The interpretation of negative expression of ERα in CAFs is due to the ER is mainly expressed in epithelial cells where breast cancer initiates.

To confirm our qRT-PCR data the same cells were tested using immunofluorescence technique. Cells were fixed, permeabilised and incubated with ER-α antibody as described in methods section 6. However, our data from this experiment showed that MCF-7 displayed diffuse staining for ER-α that was localized to the cell nuclei as this cell line expressed ER-α gene when using qRT-PCR. While MDA-MB-231 and CAFs derived from ER+ breast cancer did not express ER-α receptor as expected according to the qRT-PCR results.

6.2 PMA and Thp1 Differentiation

Although the use of human monocytic Thp-1 cell line as an alternative model for peripheral blood macrophages, the optimal concentration of PMA treatment has not given much attention yet. In this study we used the predominant PMA concentrations ranged between 10-100ng/ml over 48hrs incubation in order to determine the optimal PMA concentration based on the expression level of surface markers and cell adherence. However, the finding of several treatments revealed that 25ng/ml was sufficient to induce successful differentiation of Thp-1 into macrophages-like as we consider that 10ng/ml was too low as it showed weak expression of CD11b. CD14, CD68 and TLR-4 genes. In addition there was no difference between 25, 50 and 100ng/ml in the expression level of the indicated genes therefore 25ng/ml was chosen as the minimal effective concentration among other as high concentrations of PMA potentially leads to up-regulating undesired genes as this has been reported by Park,

E K *et al.* studies which demonstrate that high PMA concentrations could overwhelm gene expression in differentiated Thp-1 [257]. Therefore our study suggest that optimizing PMA concentration is required and essential for differentiating monocytic Thp-1 into macrophages-like.

Following Thp-1 cells differentiation into macrophages-like, differentiated Thp-1 were allowed to grow in the absence of PMA to allow a cellular recovery in single culture and/or co-cultured with breast cancer cells. Determining the resting period in the absence of PMA treatment was assessed via cellular adhesion and the expression level of surface markers including CD11b, CD14, CD68 and TLR-4 (The hallmark of macrophages). However, using both assessments as an accepted criteria of the successful differentiation of monocytic Thp-1 into macrophages like, we observed that differentiated macrophages lost their phenotype at day 4 represented by cell adherence and the expression level of surface markers compared with those rested for 2 days post PMA removal. In support of our findings, it has been reported that extended period of rest post PMA removal was associated with regained proliferative ability and decreased levels of surface markers indicating reversion of differentiated macrophages to monocytic phenotype [340, 341]. Other studies suggested that macrophages derived Thp-1 cells possibly keep their differentiation properties even longer than 3 days post PMA [257, 260]. Contrarily, the presence of breast cancer cells MDA-MB-231 and MCF-7 in co-culture with differentiated macrophages markedly promoted macrophages differentiation and adhesion for longer than 3 days therefore, the variations of phenotypic features of differentiated macrophages such as resting period in the absence of PMA is impacted via several factors such as, PMA concentration, cell passage, the duration of cells that are exposed to PMA treatment as well as the supervision of tumour cells which has been reported to play an essential

role in promoting macrophages survival and differentiation [342-344]. Based on the finding above, we demonstrate that macrophages phenotype is gained not only via PMA concentration and the incubation period but also external factors provided via tumour cells which proved to play a big role in macrophages survival.

The co-culture system has been widely used to evaluate the biological effect of 2 or 3 cell populations. For our study it was critical to determine the optimal cell ratio of macrophages or fibroblasts with breast cancer cells. However, the co-culture of macrophages at different ratios with breast cancer cells revealed weak expression level of tested genes at 0.5:1 ratio compared to those co-cultured at 1:1, 2:1 and 3:1 ratios. Same ratio was determined based on breast cancer cell number co-cultured with fibroblasts. To support our data, many studies have widely used 1:1 cell ratio to evaluate the physiological effect of different stromal cells involving fibroblasts and macrophages co-cultured with breast cancer cell at 1:1 cell ratio [286, 345, 346].

Conditioned media from macrophages up-regulated gene expression in MCF-7 but not in MDA-MB-231 breast cancer cells. This indicates that macrophages-secreted factors were able to up-regulate gene expression in MCF-7 cells unlike MDA-MB-231 which require a direct cross-talk with macrophages in order to trigger signalling pathways, hence up-regulated the indicated gene expression.

Several studies have used co-culture of two cell populations (i.e. cancer cells with macrophages or fibroblasts) in order to evaluate the effective role of macrophages or fibroblasts on tumour progression [347]. Accumulating research data have reported that macrophages or fibroblasts in double culture system where found to promote breast cancer cell migration [348, 349]. Macrophages and fibroblast are the major component of the breast tumour microenvironment [350] and this was also determined

by our IHC data , therefore we thought that the crosstalk between fibroblasts and macrophages with breast cancer favours the tumour progression. However, the triple culture model of macrophages and fibroblasts with MDA-MB-231 or MCF-7 accelerated breast cancer cell migration more than those co-cultured with macrophages or fibroblasts using double culture model.

Breast cancer cell proliferation was also tested using our triple and double culture models, macrophages inhibited breast cancer cell proliferation whereas the co-culture of fibroblast with breast cancer cells promoted MCF-7 and MDA-MB-231 cell proliferation, these effects of fibroblasts and macrophages on breast cancer cell proliferation has been already reported in many studies [285, 286]. Interestingly, the presence of macrophages and fibroblasts co-cultured with breast cancer cells significantly promoted MDA-MB-231 and MCF-7 breast cancer cell proliferation. The mechanism in which macrophages inhibit and promote breast cancer cell proliferation in different cultures is unknown, but this potentially could accept two mechanisms underlying breast cancer proliferation (i) the presence of macrophages in the triple culture potentially promoted fibroblasts activation which therefore enhanced fibroblasts-secreted factors that promote breast cancer cell proliferation [350] or (ii) macrophages change their functional effect based on their existence and factors secreted by tumour microenvironment component, such as COX2 secreted fibroblasts and breast cancer cells play an important role in polarizing macrophages into M2 phenotype which have been shown to promote breast cancer progression via activating PI3K/Akt pathways [287, 288].

6.3 Long-term co-culture

In the last decades, extensive co-culture studies were conducted to evaluate the biological effect of macrophages on breast cancer progression such as cell migration using short-term incubation (3-5 days) [305, 351]. However, taken together, these studies demonstrate that macrophages co-cultured with breast cancer cells enabled malignant cells to migrate faster than those cultured alone under short-term 'acute' conditions. [352-354]. In this work, we focused on studying whether long-term incubation (30 days) of MDA-MB-231 or MCF-7 breast cancer clones with macrophages could chronically change the metabolic pathways underlie cell migration and proliferation. For clarification, breast cancer cells that co-cultured with macrophages for 3 days or 30 days followed by 1 month recovery in fresh media without macrophages were termed short-term or programmed cells respectively, parental cells were termed control that grew in single culture. However, programmed MDA-MB-231 clone migrated faster than those co-cultured under short-term or control samples, this indicates that programmed MDA-MB-231 clone underwent cellular reprogramming under long-term co-culture condition by macrophages which has chronically changed the signalling pathway underlying cell migration. Programmed MCF-7 clone did not show any changes in their migratory behaviour post long-term co-culture activation indicating that MCF-7 clone respond only under cell-cell cross-talk with macrophages. MDA-MB-231 is highly aggressive disease and more resistance to therapy due to its heterogeneity, therefore the long-term exposure to macrophages-secreted factors such as matrix metalloproteinases MMPs, transforming growth factor beta TGF-β1, cathepsin B and platelet-derived factor (PDGF) potentially resulted in epigenetic changes that drive tumour progression and metastasis during tumour evolution [355, 356]. In contrast, MCF-7 is less aggressive

tumour and more responsive to anti-hormone therapy which therefore has been clinically reported to be associated with favourable prognosis. In addition, breast cancer cells heterogeneity plays an effective role in macrophages activation depending on tumour-secreted factors. It was reported that high levels of CCL2, M-CSF secreted via MDA-231cell educate macrophages polarisation toward M2 phenotype which was found to be positively correlated with highly metastatic breast cancer. Contrarily, high levels of macrophages in ER+ cases was associated with antigen presenting pathways, IL-17 signalling and acute phase inflammatory response. These findings show how different tumour cells govern macrophages phenotype in order to support tumour migration [345]. The long-term communication with host microenvironment cells, the more aggressive tumours as a result of a potential epigenetic changes that drive tumour progression, we therefore observe from our long-term co-culture model that breast cancer cells mainly MDA-MB-231 have chronically changed their gene expression underlying cell migration. Based on these findings, we observe that MDA-MB-231 are highly metastatic than MCF-7 breast cancer cells and this has been reported by several studies that MDA-MB-231 migrate faster than MCF-7 cells [357].

The proliferation rate of both breast cancer cell populations under the same condition mentioned above was also tested. Both programmed MCF-7 and MDA-MB-231 clones displayed low proliferative rate compared to short-term and control samples, this indicates that the long-term exposure of breast cancer cells to macrophages-secreted factors has negatively impacted cell proliferation of both breast cancer subtypes. To support our finding, Wenzhe Song and his group have reported that the proliferation rate of both MCF-7 and MDA-MB-231 clones was decreased via macrophages through down-regulating proliferating cell nuclear antigen (PCNA) gene in breast

cancer cells [358]. Comprehensive studies of several tumours including breast and pancreatic cancers have demonstrated the positive correlation between *PCNA* expression and high proliferative rate [359-361]. Both analysis of cell mobility and proliferation have shown different actions of macrophages in breast cancer progression which indicates macrophages have chronically regulated gene expression in breast cancer cells after long-term incubation with macrophages. Clinically, this could be used as a useful indicator of tumour progression relative to macrophages abundance in tumour tissues.

Programmed MDA-MB-231 clones show distinctive gene expression patterns that differentiate them from other samples including long-term, short-term and control. We observed the increased numbers of up-regulated (5591) and down-regulated (6039) genes in programmed samples was as a result from long-term co-culture condition with macrophages. This indicates that the long-term incubation of MDA-Mb-231 clone with macrophages chronically changed the cellular mechanisms that drive tumour progression.

The up-regulated and down-regulated of selected genes in programmed MDA-MB-231 clone that drive cell migration and proliferation were distinctive in their expression level compared to short-term and control, this confirms our data from the migration and proliferation assays. In comparison with programmed MDMB-231 clone which showed high migration rate, programmed MCF-7 clone did not show any changes in their migratory behaviour and this due to low expression of ARHGAP5, ITGB1, PIK3CA, PIK3CG, ROCK2 was detected. The expression level of 6 selected genes implicated in P MDA-MB-231 cell proliferation tested via RT-PCR analysis confirms our data of the whole RNA-seq. Same genes including ATR, MCM2, MCM5, MAD2L2, CDC27 and RB1 were also tested in P MCF-7. The expression level of CDC27 and

RB1 differs in both breast cancer subtypes, they were highly expressed in P MDA-MB-231 but not in MCF-7 clones. Interestingly, ATR was up-regulated in both P MDA-MB-231 and MCF-7 clones which has been showed to be prognostically associated with cell cycle arrest which therefore results in low proliferative rate in both breast cancer subtypes [362].

Summary of findings

Current breast cancer treatments focus on targeting breast tumour cells only but there is now good evidence to suggest that targeting cells in the stroma such as CAFs and/or inflammatory cells could lead to outcome. More recently attention has focused on the potential prognostic value that tumour-stromal percentage (TSP) may have in an increasing number of different cancer types. For example, previous studies of TSP in triple-negative breast cancer showed that a high percentage of stroma, defined as >50%, predicted poor survival in triple-negative breast cancers [363]. Contrarily, recent work in a cohort of 118 female ER+ breast cancers showed that a high proportion of stroma was associated with better survival [364]. Therefore, the work in this PhD project was established to test the hypothesis that cells within the tumour microenvironment influence breast cancer outcome and this differs in ER+ versus TNBC disease. To test this (i) determine if CAFs and/or inflammatory cells in breast stroma of ER+ and TNBC populations contribute to outcome, (ii) Interactive effects and functional role of CAFs and/or inflammatory cells with MCF-7 and MDA-MB-231 breast cancer cells.

The mean number of CAFs and inflammatory cells determined using immunohistochemistry analysis. However, CAFs were predominantly expressed in both ER+ and TNBC populations, notably, macrophages were the second predominant stromal cells infiltrated within tumour cells in TNBC but not in ER+ which showed modest expression within tumour cells.

We further investigated the expression of ER-α in both breast cancer subtypes, however, it was significantly expressed in ER+ samples whereas no expression was detected in MDA-MB-231 breast cancer cells. To validate this, immunofluorescence

analysis confirm the expression of ER-α in MCF-7 but it was absent in MDA-MB-231 samples.

The pilot study of Raman imaging technique revealed that some chemicals such as Amide I and Amide III were clearly detected at (1620 –1680 cm-1) and (1250 – 1270 cm-1) respectively in both TNBC and triple positive tissue samples. Interestingly, some vibrations occurred between 650 cm-1 and 1600 cm-1that attribute to amino acids, carbohydrates and nucleotides in the triple positive sample. Whereas low intensity vibrations were seen in the triple negative sample.

It was possible to use monocytic Thp-1 cells as an alternative cell line for blood peripheral monocytes after incubation with 25ng/ml PMA, which was chosen as an optimal concentration among other concentrations including 10, 50 and 100ng/ml. Gene expression and cell adherence analysis showed that the co-culture of MDA-MB-231 or MCF-7 breast cancer cells with macrophages promoted macrophages survival compared to those cultured under single culture condition.

The assessment of macrophages cell morphology revealed that MDA-MB-231 or MCF-7 breast cancer cells promoted macrophages cell adherence and cytoplasm spreading relative to those cultured alone.

Conditioned media from macrophages up-regulated gene expression in MCF-7 cells but not in MDA-MB-231 compared to conditioned media from macrophages-breast cancer cells co-culture which induced gene up-regulation in both breast cancer subtypes.

The double co-culture of MDA-MB-231 or MCF-7 with macrophages or fibroblasts promoted breast cancer cell migration compared to breast cancer cells in single culture. Interestingly, the migration rate of MDA-MB-231 in the presence of

macrophages and fibroblasts was faster than those co-cultured with macrophages or fibroblasts. Notably, the cell migration of MCF-7 cell in the triple culture with macrophages and fibroblasts did not show changes compared with those cultured with macrophages using double culture model.

The proliferation rate of MDA-MB-231 or MCF-7 was promoted when co-cultured with fibroblasts but not macrophages which showed an inhibitory effect on both breast cancer subtypes. Interestingly, the cell proliferation rate of MDA-MB-231 or MCF-7 was significantly promoted in the presence of macrophages and fibroblasts using triple culture model.

The RT-PCR gene expression analysis revealed that 3 genes including LAMC2, NR1D1 and PER1 were up-regulated in programmed MDA-MB-231 cell whereas the expression of BIRC3 and DKK1genes did not show any changes relative to control. All tested genes including FAS, ICAM1 and SOSC3 were up-regulated in programmed MCF-7 in comparison with control.

Cell migration assay of both MDA-MB-231 and MCF-7 breast cancer cells showed that programmed MDA-MB-231 migrated faster than those were cultured under short-term condition and control cells. Programmed MCF-7 cells did not exhibit any changes in their migratory behaviour in comparison with those cultured under short-term and control cultures. Cell proliferation of programmed MCF-7 and MDA-MB-231 was significantly suppressed relative to those cultured under short-term and control.

Gene expression profiling analysis revealed that several genes were implicated in cell migratory and proliferative behaviour of programmed MDA-MB-231 and MCF-7 cells. However, genes that accelerate cell migration including ARHGAP5, ITGB1, PIK3CA, PIK3CG, ROCK1 and ROCK2 were highly expressed in programmed MDA-MB-231

but not in programmed MCF-7 apart from ROCK1. In addition, we further investigated the expression of genes underlying cell proliferation in both breast cancer subtypes. However, MCM2, MCM5 and MAD2L2 were mutually dow-regulated in programmed MDA-MB-231 and MCF-7 samples. Whereas, ATR that drives cell cycle arrest was up-regulated in both programmed MDA-MB-231 and MCF-7 cells.

Analysis of KEGG pathways and gene ontology enrichments revealed that some pathways such as cell cycle, metabolic pathways and mitotic cell cycle were mutually enriched in all MDA-MB-231 samples. Interestingly, some pathways were uniquely enriched in programmed MDA-MB-231 samples such as RNA binding, RAP1 signalling pathway compared with short-term and long-term samples.

Future direction

1. Conduct Raman imaging to determine if the metastatic signatures are different in ER+ and TNBC breast cancer. Raman Imaging, it is a laser-based microscopic device allows to generate chemical images and reveals anatomical layers without labelling. This microscopic system has been used to identify chemical components in tissue and cell samples. To date, a study was conducted on FFBE colon tissue mounted on stainless steel, the results showed various signals represented different chemicals that allowed the study to identify the chemical structure in the tissue samples [365]. In my preliminary study conducted on one triple positive and triple negative breast cancer samples revealed that it is possible to identify chemical components directly within samples. For future study, I recommend expanding the analysis on breast cancer cells as it is now possible to identify the chemical components of tumour cells [366], as well as it allows exploring differences between not only tumours of one subtype but also between different tumours of two or more subtypes.

2. Our finding for the first time revealed that Pirfenidone drug has shown a proliferation inhibitor activity in all investigated cell lines including MDA-MB-231 and MCF-7 at dose 10µM/mL. The mechanism behind this activity has not explored yet, but our observation indicates that PFD potentially inhibited SMAD pathways via abrogating TGF-β pathway which eventually resulted in decreased a proliferation rate in tumour cells. Therefore, I highly recommend to conduct gene expression analysis in order to evaluate PFD activity in tumour progression.

3. Data from triple co-culture experiments showed that fibroblasts with macrophages significantly promoted MCF-7 and MDA-MB-231 cell proliferation and migration. The mechanism underlying tumour progression under co-culture with both fibroblasts and macrophages still open mechanistic questions. Here, I highly recommend to evaluate gene expression changes under triple culture condition as it might be a good therapeutic target in future studies.

4. Analysis of RNA-seq conducted on MDA-MB-231 breast cancer cells revealed that thousands of genes were chronically up-regulated or down-regulated under long-term co-culture condition with macrophages. Based on this promising results, I recommend performing same analysis on MCF-7 cultured under the same condition as it could be a potential targeted pathways for future therapies.

5. Performing gene silencing experiments on different genes that underlie tumour progression in order to assess their biological effect on tumour cell proliferation, migration and resistance to therapy.

6. We initially determined the optimal protein concentration of matrix matrigel used to perform cell invasion assay as described previously. Evaluating of MDA-MB-231 and MCF-7 breast cancer cell invasion under different culture conditions is still needed.

7. Conducting functional experiment of MDA-MB-231 and MCF-7 cells cultured under conditions used in this project in the presence of Doxorubicin alone and/or in combination with other effective drugs such cyclophosphamide. This will allow us to determine the tumour cells resistance to therapy.

APPENDIXES

Appendix 1. Chemicals were used for this project

Novolink Polymer Detection Kit

- Manufactured by: Leica Biosystem
- Product Code: RE7280-K
- 1250 test

TBS (Tris-buffer Saline 20x)

- Manufactured by: A.Menarini diagnostic
- Product Code: MP-945-X500
- Dissolve in 950 ml distilled water
- PH: 7.6

Access Revelation (Antigen Access Solution 10x)

- Manufactured by: A.Menarini diagnostic
- Product Code: MP-607-X500
- Dissolve in 900 ml distilled water
- PH: 6.4

Antibody Diluent Reagent Solution (500 ml)

- Manufactered by: Life Technologies
- 500 ml
- Contains 0.1% Sodium Azide
- PH: 7

Appendix 2. Up-regulated genes-related MDA-MB-231 clone migration identified by next generation sequencing. The table shows differential gene expression in control (C), short-term (S), long-term (L) incubation and programmed MDA-MB-23. Highlighted genes represent the significant expression in P compared to C.

No	Gene ID	Gene Name	Expression level				Fold Change (Log_2)		
			C	S	L	P	Fold (S)	Fold (L)	Fold (P)
1	ENSG00000256973	RP11-359J14.2	0.04458479	0.06185443	0.06821921	0.87288576	1.38734371	1.53010056	19.5781071
2	ENSG00000171217	CLDN20	0.0462694	0.00672539	0.06246374	0.41955688	0.14535298	1.35000124	9.06769731
3	ENSG00000254509	RP11-677M14.6	0.0785124	0.07815607	0.261612	1.27257283	0.99546147	3.33211047	16.2085577
4	ENSG00000091428	RAPGEF4	0.11971597	0.0957518	0.1174828	0.69761886	0.79982477	0.98134608	5.82728306
5	ENSG00000254893	RAP1B	0.15429296	0.76553319	0.40359458	0.52161639	4.96155607	2.61576788	3.38068814
6	ENSG00000263006	ROCK1P1	0.15835681	0.1081161	0.3371377	0.95355852	0.68273729	2.12897501	6.02158188
7	ENSG00000179295	PTPN11	16.3091914	40.9024418	31.5166948	96.175889	2.50793805	1.93244986	5.897036
8	ENSG00000105851	PI3KCG	0.20774091	0.39285466	0.51188043	1.44561328	1.89107987	2.46403284	6.95873168
9	ENSG00000213937	CLDN9	0.4183674	0.36147435	1.26651584	1.4763404	0.86401176	3.02728138	3.52881319
10	ENSG00000121879	PIK3CA	0.51560279	4.14428663	1.61412688	5.52364464	8.03775054	3.13056271	10.7129843
11	ENSG00000127314	RAP1B member of RAS	16.961606	74.0476117	33.9544659	47.2191253	4.36560146	2.00184263	2.78388293
12	ENSG00000269378	ITGB1P1	0.70119273	1.98553896	1.52625185	4.29463242	2.83165934	2.17665098	6.12475318
13	ENSG00000145675	PIK3R1	0.78460738	4.48969804	3.02861128	8.61799529	5.72222258	3.86003418	10.9838316

14	ENSG00000074966	TXK	0.79699726	1.61638156	1.49341326	3.53488285	2.02808924	1.87379975	4.43525095
15	ENSG00000134318	ROCK2	0.91827141	6.04652193	1.43222175	8.3769588	6.58467842	1.55969328	9.12253035
16	ENSG00000100852	ARHGAPS	0.94500215	6.73284027	1.31062715	11.0278508	7.12468248	1.38690388	11.6696569
17	ENSG00000065135	GNAI3	0.97284216	3.20066052	1.66701478	4.31277873	3.29001007	1.71355112	4.43317415
18	ENSG00000197822	OCLN	1.6167004	2.27820663	1.97111308	3.52090654	1.40917058	1.21921976	2.1778349
19	ENSG00000067900	ROCK1	1.22034367	8.31036801	1.96227417	10.8549674	6.80985872	1.60796849	8.89500855
20	ENSG00000116473	RAP1A	7.19892075	16.0719091	8.76344462	21.7034724	2.23254425	1.21732756	3.01482308
21	ENSG00000051382	PIK3CB	7.91284351	12.2108244	8.27021133	23.9503855	1.54316516	1.04516301	3.02677356
22	ENSG00000127955	GNAI1	7.01169872	11.9410162	6.38843717	21.1514818	1.70301331	0.91111119	3.01659878
23	ENSG00000163347	CLDN1	8.87119295	7.39627518	8.2850409	13.902192	0.83374076	0.93392636	1.5671164
24	ENSG00000130396	MLLT4	28.871607	25.9827605	17.1820223	47.1337965	0.89994161	0.59511832	1.63253111
25	ENSG00000101608	MYL12A	145.971407	266.655715	263.179389	520.171012	1.82676677	1.80295165	3.56351305
26	ENSG00000150093	ITGB1	156.554935	454.90208	315.759315	1088.70356	2.90570259	2.01692342	6.95413124
27	ENSG00000118680	MYL12B	212.80558	462.269207	301.569551	719.06702	2.17226074	1.41711299	3.37898574
28	ENSG00000169398	PTK2	75.1818594	79.5290777	54.49692	160.490513	1.0578227	0.72486795	2.13469731

Appendix 3. Down-regulated genes-related cell migration identified by next generation sequencing. The table shows differential gene expression in control (C), short-term (S), long-term (L) incubation and programmed MDA-MB-231 clone. Highlighted genes represent the significant expression in P compared to C.

No	**Gene ID**	**Gene Name**	**Expression level**				**Fold Change (Log_2)**		
			C	**S**	**L**	**P**	**Fold (S)**	**Fold (L)**	**Fold (P)**

1	ENSG00000185386	MAPK11	1.52095633	1.24753441	1.23958499	0.70875922	0.82023026	0.81500367	0.46599577
2	ENSG00000183250	LINC01547	7.89878622	5.37683787	3.33365285	4.96554091	0.68071698	0.42204622	0.62864607
3	ENSG00000249936	RAC1P2	2.78516549	2.64921867	2.16130229	1.73269379	0.95118896	0.77600498	0.6221152
4	ENSG00000253958	CLDN23	3.42823212	1.72142319	0.99977851	0.96840445	0.50213146	0.29163093	0.28247925
5	ENSG00000121966	CXCR4	9.64609359	8.03494428	10.828161	3.15209047	0.83297391	1.12254364	0.32677378
6	ENSG00000116701	NCF2	10.9441666	9.03582821	16.0004297	8.76597344	0.82562963	1.46200531	0.80097222
7	ENSG00000197943	PLCG2	12.1115099	8.53623305	5.93816472	3.3353233	0.70480338	0.49029103	0.2753846
8	ENSG00000217801	RP11-465B22.3	16.2187299	10.1667531	18.0209876	8.42679265	0.62685261	1.111122	0.51957168
9	ENSG00000266094	RASSF5	3.61032342	2.18285957	3.23554858	2.08409565	0.60461607	0.89619355	0.5772601
10	ENSG00000243635	RP11-281P11.1	1.50364003	0.65008293	0.29055986	0.6756478	0.43233947	0.19323765	0.44934146
11	ENSG00000160293	VAV2	26.2460197	17.9908171	17.7700881	17.7009947	0.6854684	0.6770584	0.67442587
12	ENSG00000156711	MAPK13	33.1085478	27.9594742	41.9348245	24.4665369	0.84447902	1.26658604	0.73897946
13	ENSG00000171608	PIK3CD	37.3696871	34.5734268	36.5212422	23.5663703	0.92517303	0.9772959	0.63062798
14	ENSG00000189143	CLDN4	41.6902052	36.3385174	27.7458714	14.9580235	0.87163201	0.66552494	0.35878987
15	ENSG00000213445	SIPA1	60.2708381	52.0537478	43.1239592	29.3739867	0.86366391	0.7155029	0.48736649
16	ENSG00000160255	ITGB2	72.9864334	61.4858811	88.8082042	66.938432	0.8424289	1.21677687	0.91713527
17	ENSG00000101335	MYL9	88.069914	90.8194876	46.6334259	39.3241625	1.03122035	0.52950461	0.44651074
18	NSG00000154229	PRKCA	94.3203897	66.4016007	32.80733	60.3677936	0.70400049	0.34782861	0.64002909
19	ENSG00000035403	VCL	102.656629	81.8564636	49.2214477	84.2232276	0.79738118	0.47947656	0.82043633
20	ENSG00000124181	PLCG1	129.950268	107.523885	98.33314	80.4239951	0.82742334	0.75669825	0.61888287
21	ENSG00000112062	MAPK11	134.801601	108.812976	95.5383868	111.783002	0.80720834	0.70873332	0.82924091

22	ENSG00000149564	ESAM	141.461994	122.017852	133.391812	106.044685	0.86254865	0.94295158	0.74963374
23	ENSG00000089159	PXN	216.32402	186.629872	141.828164	124.241007	0.86273301	0.65562837	0.5743283
24	ENSG00000168036	CTNNB1	247.986625	175.139787	119.688606	223.275636	0.70624691	0.48264138	0.90035354
25	ENSG00000092820	EZR	249.73904	210.450228	178.661027	171.589109	0.84268054	0.71539086	0.68707363
26	ENSG00000002586	CD99	262.229017	268.607921	312.120138	180.120928	1.0243257	1.19025782	0.68688404
27	ENSG00000050820	BCAR1	263.455422	197.602982	157.928804	134.143043	0.75004333	0.59945171	0.5091679
28	ENSG00000070831	CDC42	288.484469	239.648422	116.008762	263.472366	0.83071516	0.40213174	0.91329827
29	ENSG00000114353	GNAI2	337.25339	302.505392	318.751156	211.399713	0.89696768	0.94513848	0.62682754
30	ENSG00000128340	RAC2	372.152245	357.773023	435.938452	256.718254	0.96136199	1.17139815	0.68982052
31	ENSG00000051523	CYBA	391.55289	503.634445	581.131117	341.180765	1.28624883	1.48417016	0.87135295
32	ENSG00000125753	VASP	416.660098	362.625931	435.108463	246.177719	0.87031596	1.04427678	0.59083584
33	ENSG00000072110	ACTN1	856.885106	788.369809	823.90503	581.34736	0.92004144	0.96151167	0.6784426
34	ENSG00000067560	RHOA	942.269361	1023.0329	964.738502	696.949204	1.08571173	1.02384577	0.73964965
35	ENSG00000044115	CTNNA1	1506.58013	1189.26843	1008.67851	1104.91106	0.78938279	0.66951534	0.73339017
36	ENSG00000130402	ACTN4	1745.33109	1369.55204	1216.67163	1329.92832	0.78469469	0.69710076	0.761992
37	ENSG00000184009	ACTG1	2740.04468	2791.08298	1893.25108	1483.66512	1.01862681	0.69095628	0.54147479
38	ENSG00000075624	ACTB	8059.7161	8192.64259	4855.11296	4152.30621	1.0164927	0.60239255	0.51519261
39	ENSG00000184113	CLDN5	0.16933111	0.04476595	0.03130956	0.0243601	0.26436933	0.18490142	0.14386074
40	ENSG00000165215	CLDN3	0.63045708	0.39537737	0.1483315	0.06752768	0.62712813	0.23527613	0.10710908
41	ENSG00000237350	CDC42P6	1.12024798	0.77335914	0.38614538	0.44642085	0.69034638	0.34469634	0.39850181

Appendix 4. Up-regulated genes related cell proliferation in MDA-MB-231 clones identified by next generation sequencing. The table shows gene expression level of all genes involved in cell proliferation in control (C), short-term (S), long-term (L) incubation and programmed MDA-MB-231 clone. Highlighted genes represent the significant expression in P compared to C.

No	Gene ID	Gene Name	Expression level				Fold Change (Log_2)		
			C	S	L	P	Fold (S)	Fold (L)	Fold (P)
1	ENSG00000118007	STAG1	0.583802592	4.055444006	1.116503661	4.973078045	6.946601575	1.912467804	8.518424056
2	ENSG00000175054	ATR	0.679060109	6.873439755	1.665491362	8.419436726	10.12199018	2.452642027	12.39866193
3	ENSG00000105810	CDK6	0.953281376	6.179210627	2.655714999	15.47264494	6.482042746	2.785866867	16.23093174
4	ENSG00000175305	CCNE2	1.052202243	2.503379974	0.219449509	2.293416414	2.379181371	0.2085621	2.179634599
5	ENSG00000006634	DBF4	1.354559666	7.205762293	1.317276762	3.460518804	5.319634471	0.972475997	2.554718622
6	ENSG00000079335	CDC14A	1.468528268	2.020595647	1.100430712	3.511138115	1.375932415	0.749342546	2.390923069
7	ENSG00000108055	SMC3	1.654752019	11.42464234	2.284847323	11.70472336	6.904141656	1.380779293	7.073400261
8	ENSG00000149311	ATM	1.718803419	7.681159823	3.382056698	21.11750827	4.468899548	1.967680923	12.28616841
9	ENSG00000115947	ORC4	1.749296353	6.918390289	2.290005829	6.150917204	3.954956105	1.309101128	3.516223649
10	ENSG00000231259	AC125232.1	1.786702607	2.202744431	4.911653844	3.004089554	1.232854546	2.749004689	1.681359585
11	ENSG00000225507	AC069282.6	1.806452914	0.743646528	0.804491367	4.273155693	0.411661174	0.445343115	2.365495198
12	ENSG00000101972	STAG2	2.187613165	22.08432301	2.458730623	16.49956127	10.09516827	1.123932998	7.5422664
13	ENSG00000175387	SMAD2	2.483713211	4.031955881	2.96154814	6.081016477	1.623358068	1.19238732	2.44835694
14	ENSG00000080839	RBL1	2.67130785	7.663788015	1.091991046	12.4213665	2.8689273	0.408785175	4.649919515
15	ENSG00000097046	CDC7	2.869537676	6.808006775	1.434562122	9.198483112	2.37250998	0.499927962	3.20556276
16	ENSG00000135336	ORC3	3.283649598	8.621664116	2.520720648	7.937561536	2.625634636	0.767658233	2.417298588

17	ENSG00000112742	TTK	3.305570758	10.75778633	0.401142845	6.125871742	3.254441402	0.12135358	1.853196374
18	ENSG00000133740	E2F5	3.537891112	3.020900326	4.241411382	6.584770693	0.853870351	1.198853003	1.861213498
19	ENSG00000139687	RB1	4.160009965	22.14393651	5.024722971	33.61785557	5.32304891	1.207863205	8.081195922
20	ENSG00000176386	CDC26	4.559304525	10.30530884	5.960109594	9.594725893	2.260280879	1.307240953	2.104427515
21	ENSG00000053900	ANAPC4	4.603010942	11.7383273	9.315286873	16.74357993	2.550141081	2.023737721	3.637527727
22	ENSG00000141646	SMAD4	5.031270421	7.983684579	4.835136169	17.34355593	1.586812855	0.961016953	3.447152403
23	ENSG00000103479	RBL2	5.808645195	7.194059079	8.206436597	27.89763874	1.238508953	1.412797016	4.802778928
24	ENSG00000115942	ORC2	7.021196853	10.03941584	5.94626062	16.38986279	1.429872435	0.846901283	2.334340303
25	ENSG00000129055	ANAPC13	7.520514408	16.25249453	10.98341179	20.99512594	2.161088145	1.460460175	2.791714077
26	ENSG00000164815	ORC5	7.929702941	8.920643048	5.254636936	13.86963265	1.124965603	0.662652432	1.749073422
27	ENSG00000164162	ANAPC10	8.164030988	9.91979875	5.250408528	15.38513754	1.215061379	0.643114723	1.88450259
28	ENSG00000134480	CCNH	8.362814775	22.87034659	15.38002554	26.3333496	2.734766607	1.839096758	3.148861993
29	ENSG00000135679	MDM2	8.63799633	15.42570275	6.270822277	22.43097848	1.7857964	0.72595797	2.596780274
30	ENSG00000055130	CUL1	8.663370975	11.45161774	6.741405025	17.78386301	1.321843168	0.778150335	2.052764802
31	ENSG00000092969	TGFB2	9.626045097	20.55505868	11.53107272	38.62657699	2.135358652	1.197903459	4.012715149
32	ENSG00000004897	CDC27	10.2151433	62.3023129	21.05177418	81.45510776	6.099015069	2.060839831	7.973956448
33	ENSG00000164109	MAD2L1	14.51849264	35.13415669	4.954927649	37.88103971	2.419958984	0.34128389	2.609157896
34	ENSG00000082701	GSK3B	14.98188439	21.01017715	27.41719372	45.16419355	1.402372131	1.830023046	3.014586975
35	ENSG00000156970	BUB1B	16.06999203	29.86212624	4.54881498	37.88940922	1.858253954	0.283062678	2.357773989
36	ENSG00000081377	CDC14B	16.47746533	14.55220306	8.815225818	23.07258848	0.883157862	0.534986762	1.400251071
37	ENSG00000196591	HDAC2	20.61510124	50.78327255	29.14611597	73.51199082	2.46340156	1.413823567	3.565929169

38	ENSG00000145386	CCNA2	21.16026423	38.42500722	4.641469597	35.50990559	1.815903941	0.219348376	1.678140934
39	ENSG00000134058	CDK7	24.87500077	45.35439173	48.6963953	71.54688108	1.823292073	1.957643971	2.876256436
40	ENSG00000111276	CDKN1B	41.51909321	33.44402712	32.05194044	69.6207699	0.805509575	0.771980743	1.676837438
41	ENSG00000116809	ZBTB17	37.9708442	27.39408662	31.81624983	22.2877113	0.721450555	0.837912627	0.586969075
42	ENSG00000170312	CDK1	29.4271323	43.80713874	5.405359392	72.02453412	1.488664893	0.183686244	2.447555317
43	ENSG00000253729	PRKDC	32.47696886	73.26876871	24.03621469	106.1801556	2.256022384	0.740100309	3.269398573
44	ENSG00000169679	BUB1	27.14710099	68.34002223	12.47396924	72.62970519	2.517396692	0.459495445	2.675412936
45	ENSG00000164754	RAD21	40.04940323	136.4776214	51.73844293	196.9463974	3.40773171	1.291865515	4.917586318
46	ENSG00000132646	PCNA	88.26579414	90.85314798	20.26438058	124.2373678	1.029313211	0.22958362	1.407536963
47	ENSG00000130177	CDC16	93.18681662	104.921893	59.52330019	137.7103664	1.12593065	0.638752372	1.477788075
48	ENSG00000166913	YWHAB	303.1793984	340.6204106	217.9066627	402.8581948	1.123494579	0.718738357	1.328778264
49	ENSG00000164924	YWHAZ	486.3794514	941.6372975	500.7187378	1076.862317	1.936013734	1.029481686	2.214037443
50	ENSG00000113558	SKP1	25.38250404	74.57510078	46.96155689	65.99574848	2.93805137	1.850154611	2.600048773
51	ENSG00000127564	PKMYT1	57.01297985	38.338288	5.705632783	15.83610298	0.672448416	0.100076032	0.277763117
52	ENSG00000101412	E2F1	56.22537386	41.04601812	10.34693335	32.17072109	0.730026593	0.184026048	0.572174427

Appendix 5. Down-regulated genes related cell proliferation in MDA-MB-231 clones identified by next generation sequencing. The table shows gene expression level of all genes involved in cell proliferation in control (C), short-term (S), long-term (L) incubation and programmed MDA-MB-231 clone. Highlighted genes represent the significant expression in P compared to C.

No	Gene ID	Gene Name	Expression level				Fold Change (Log_2)		
			C	S	L	P	Fold (S)	Fold (L)	Fold (P)
1	ENSG00000158402	CDC25C	25.5815919	19.20919319	8.784045052	13.96315479	0.750899055	0.343373668	0.545828221
2	ENSG00000091651	ORC6	27.01605414	15.06133885	4.673184099	18.17653611	0.557495879	0.17297804	0.672804993
3	ENSG00000135476	ESPL1	27.90080012	18.48469898	7.904444278	14.44977102	0.662515014	0.28330529	0.517898087
4	ENSG00000196510	ANAPC7	33.40289761	27.5819289	12.27913558	22.12772559	0.825734618	0.367606898	0.662449284
5	ENSG00000005339	CREBBP	41.45155188	26.57205583	20.0764921	28.57337215	0.641038866	0.48433632	0.68931972
6	ENSG00000100387	RBX1	44.07117112	42.81894472	24.09003956	34.35414567	0.971586269	0.546616733	0.779515152
7	ENSG00000129355	CDKN2D	46.26417544	33.7108546	27.7150073	28.00732596	0.728660011	0.599059792	0.605378259
8	ENSG00000097007	ABL1	51.8321738	42.43354014	52.39876612	35.56667821	0.818671822	1.010931286	0.686189207
9	ENSG00000072501	SMC1A	55.78597489	44.80494945	13.23540571	47.91607758	0.803157954	0.237253283	0.858926956
10	ENSG00000105325	FZR1	61.11408088	53.36661973	48.54410276	34.91937013	0.873229524	0.794319444	0.571380108
11	ENSG00000157456	CCNB2	63.70591302	54.92702161	20.13724923	40.3888248	0.8621966	0.31609702	0.633988635
12	ENSG00000123374	CDK2	66.20920449	41.28886358	33.2519427	41.89854585	0.623612138	0.502225377	0.63282056
13	ENSG00000176248	ANAPC2	69.22203522	55.72850888	55.73009207	46.66100467	0.805068916	0.805091788	0.67407733
14	ENSG00000116670	MAD2L2	75.01258967	65.97210516	43.75218236	37.50125268	0.879480437	0.583264523	0.499932782
15	ENSG00000123080	CDKN2C	78.49329984	48.96932732	26.55872581	38.17233969	0.623866335	0.338356597	0.486313351
16	ENSG00000170027	YWHAG	88.0649823	69.19228503	51.03212991	69.00424271	0.785695781	0.579482657	0.783560513

17	ENSG00000116717	GADD45A	94.83835241	81.23774117	51.19344243	68.91747895	0.856591654	0.539796835	0.726683638
18	ENSG00000135446	CDK4	103.5012927	88.45831269	82.69409327	63.63165916	0.854659013	0.798966768	0.614790961
19	ENSG00000166851	PLK1	110.3356682	96.46655574	31.68373333	35.64131254	0.874300735	0.287157669	0.323026208
20	ENSG00000073111	MCM2	111.2136604	73.37870192	27.76249683	54.22644652	0.65979936	0.249632075	0.487588003
21	ENSG00000101224	CDC25B	116.3147945	102.2456009	62.33775459	65.45531611	0.879042097	0.535940031	0.562742825
22	ENSG00000002822	MAD1L1	120.4745281	117.8187514	148.3813602	65.56426816	0.977955699	1.231640933	0.54421685
23	ENSG00000094804	CDC6	124.7812525	89.98682149	11.59187711	68.57776689	0.721156581	0.092897586	0.549583896
24	ENSG00000100297	MCM5	127.1414258	98.78954417	34.77980438	60.55427538	0.777005162	0.273552103	0.476274943
25	ENSG00000141552	ANAPC11	128.4134382	112.0642063	131.2861771	92.34062515	0.872682858	1.022371014	0.719088488
26	ENSG00000141510	TP53	133.9934669	117.8966918	86.17320727	80.50543025	0.879868956	0.643114991	0.600816085
27	ENSG00000089053	ANAPC5	141.8467507	127.476348	112.4596605	112.0272488	0.898690646	0.792825073	0.789776631
28	ENSG00000105329	TGFB1	151.3866645	192.4184465	377.1001826	145.7928706	1.271039606	2.490973586	0.963049626
29	ENSG00000128245	YWHAH	160.345628	121.6425765	63.5921199	91.68052247	0.758627335	0.396594037	0.571768146
30	ENSG00000205250	E2F4	180.6421339	149.5473218	140.7786301	114.7359534	0.827865119	0.779323334	0.635156101
31	ENSG00000175793	SFN	190.9009753	197.2791624	119.8895397	61.41988141	1.033410972	0.628019525	0.321736865
32	ENSG00000166949	SMAD3	197.4350344	154.7014291	142.1225745	183.1999483	0.783556118	0.719844758	0.927899898
33	ENSG00000164611	PTTG1	199.9735846	192.7494989	86.73920636	143.1002018	0.9638748	0.433753321	0.715595523
34	ENSG00000124762	CDKN1A	215.0335346	221.3853729	424.5976423	145.9909866	1.029538827	1.974564773	0.67892195
35	ENSG00000112118	MCM3	220.9391955	147.9436976	46.80277511	125.284307	0.669612729	0.211835546	0.567053332
36	ENSG00000104738	MCM4	237.3593007	123.6869851	45.4473177	130.8380071	0.521096012	0.191470558	0.551223427
37	ENSG00000166508	MCM7	253.2657306	191.0545181	102.7234023	148.344282	0.754363876	0.405595349	0.585725837

38	ENSG00000134057	CCNB1	272.1891584	265.2569964	62.63140784	151.2344736	0.974531822	0.230102507	0.555622694
39	ENSG00000198176	TFDP1	307.0731238	208.5467744	84.1517652	193.3768775	0.67914369	0.27404471	0.629742112
40	ENSG00000112576	CCND3	326.3434235	246.1687993	106.2689863	123.4747663	0.754324376	0.325635446	0.378358372
41	ENSG00000117399	CDC20	347.5786721	302.7822433	91.41352713	90.68295346	0.871118592	0.263000968	0.260899073
42	ENSG00000116478	HDAC1	350.2423434	297.013998	221.2466585	240.3149469	0.848024243	0.631695918	0.686139045
43	ENSG00000110092	CCND1	830.7301239	559.2542912	340.8822941	761.3855713	0.673208152	0.410340596	0.916525776
44	ENSG00000108953	YWHAE	1202.528003	885.0347337	813.8343882	1004.078708	0.735978482	0.676769594	0.834973244
45	ENSG00000130222	GADD45G	0.557617148	0.255701922	0.686088956	0.121579121	0.458561798	1.230394294	0.218033326
46	ENSG00000133101	CCNA1	2.156045342	2.059108771	0.914825154	0.695989954	0.955039642	0.424307011	0.322808589
47	ENSG00000007968	E2F2	6.734025781	3.432564924	0.292863873	2.622880819	0.509734449	0.043490162	0.3894967
48	ENSG00000093009	PIGW	8.816482959	6.323742163	2.263986556	6.870024002	0.717263584	0.256790215	0.779225008
49	NSG00000085840	ORC1	9.88322343	5.853148906	0.886577437	3.497328412	0.592230758	0.089705291	0.353865157
50	ENSG00000105173	CCNE1	10.33382042	6.361776146	1.687606109	3.816129602	0.615626737	0.163309022	0.369285458
51	ENSG00000164045	CDC25A	18.19675812	11.17507837	1.82839369	5.701723215	0.614124686	0.10047909	0.313337309

References

1. Ghoncheh, M., Z. Pournamdar, and H. Salehiniya, *Incidence and Mortality and Epidemiology of Breast Cancer in the World.* Asian Pac J Cancer Prev, 2016. **17**(S3): p. 43-6.
2. Harbeck, N., et al., *Breast cancer.* Nature Reviews Disease Primers, 2019. **5**(1): p. 66.
3. Blows, F.M., et al., *Subtyping of breast cancer by immunohistochemistry to investigate a relationship between subtype and short and long term survival: a collaborative analysis of data for 10,159 cases from 12 studies.* PLoS Med, 2010. **7**(5): p. e1000279.
4. Richie, R.C. and J.O. Swanson, *Breast cancer: a review of the literature.* J Insur Med, 2003. **35**(2): p. 85-101.
5. Hu, Z., et al., *The molecular portraits of breast tumors are conserved across microarray platforms.* BMC Genomics, 2006. **7**: p. 96.
6. Tsutsui, S., et al., *Prognostic significance of the coexpression of p53 protein and c-erbB2 in breast cancer.* Am J Surg, 2003. **185**(2): p. 165-7.
7. Johnson, K.S., E.F. Conant, and M.S. Soo, *Molecular Subtypes of Breast Cancer: A Review for Breast Radiologists.* Journal of Breast Imaging, 2020. **3**(1): p. 12-24.
8. Heitz, F., et al., *Triple-negative and HER2-overexpressing breast cancers exhibit an elevated risk and an earlier occurrence of cerebral metastases.* Eur J Cancer, 2009. **45**(16): p. 2792-8.
9. Wu, X., et al., *The tamoxifen metabolite, endoxifen, is a potent antiestrogen that targets estrogen receptor alpha for degradation in breast cancer cells.* Cancer Res, 2009. **69**(5): p. 1722-7.
10. Nahta, R., *New developments in the treatment of HER2-positive breast cancer.* Breast Cancer : Targets and Therapy, 2012. **4**: p. 53-64.
11. McKenna, M.T., et al., *A Predictive Mathematical Modeling Approach for the Study of Doxorubicin Treatment in Triple Negative Breast Cancer.* Scientific Reports, 2017. **7**(1): p. 5725.
12. Nguyen, Q.H., et al., *Profiling human breast epithelial cells using single cell RNA sequencing identifies cell diversity.* Nature Communications, 2018. **9**(1): p. 2028.
13. Polyak, K., *Breast cancer: origins and evolution.* The Journal of clinical investigation, 2007. **117**(11): p. 3155-3163.
14. Soysal, S.D., A. Tzankov, and S.E. Muenst, *Role of the Tumor Microenvironment in Breast Cancer.* Pathobiology, 2015. **82**(3-4): p. 142-52.
15. Gangadhara, S., et al., *Pro-metastatic tumor-stroma interactions in breast cancer.* Future Oncol, 2012. **8**(11): p. 1427-42.
16. Veronesi, U., et al., *Breast cancer.* The Lancet, 2005. **365**(9472): p. 1727-1741.
17. Colditz, G.A., et al., *Family history and risk of breast cancer: nurses' health study.* Breast Cancer Research and Treatment, 2012. **133**(3): p. 1097-1104.
18. Allison, K.H., *Molecular Pathology of Breast Cancer: What a Pathologist Needs to Know.* American Journal of Clinical Pathology, 2012. **138**(6): p. 770-780.
19. Shruti, S., et al., *Cluster of Differentiation 10 Positive Stromal Sarcoma of Breast: A Diagnostic Challenge.* Cureus, 2019. **11**(7): p. e5143.
20. Pencavel, T.D. and A. Hayes, *Breast sarcoma – a review of diagnosis and management.* International Journal of Surgery, 2009. **7**(1): p. 20-23.
21. van Seijen, M., et al., *Ductal carcinoma in situ: to treat or not to treat, that is the question.* British Journal of Cancer, 2019. **121**(4): p. 285-292.
22. Salvatorelli, L., et al., *Ductal Carcinoma In Situ of the Breast: An Update with Emphasis on Radiological and Morphological Features as Predictive Prognostic Factors.* Cancers, 2020. **12**(3): p. 609.
23. Sontag, L. and D.E.J.J.o.t.b. Axelrod, *Evaluation of pathways for progression of heterogeneous breast tumors.* 2005. **232**(2): p. 179-189.

24. Casasent, A.K., et al., *Multiclonal invasion in breast tumors identified by topographic single cell sequencing.* 2018. **172**(1-2): p. 205-217. e12.
25. Casasent, A.K., M. Edgerton, and N.E.J.T.J.o.p. Navin, *Genome evolution in ductal carcinoma in situ: invasion of the clones.* 2017. **241**(2): p. 208-218.
26. Narod, S.A. and V. Sopik, *Is invasion a necessary step for metastases in breast cancer?* Breast cancer research and treatment, 2018. **169**(1): p. 9-23.
27. Ashworth, A., C.J. Lord, and J.S.J.C. Reis-Filho, *Genetic interactions in cancer progression and treatment.* 2011. **145**(1): p. 30-38.
28. Cowell, C.F., et al., *Progression from ductal carcinoma in situ to invasive breast cancer: revisited.* 2013. **7**(5): p. 859-869.
29. Hernandez, L., et al., *Genomic and mutational profiling of ductal carcinomas in situ and matched adjacent invasive breast cancers reveals intra-tumour genetic heterogeneity and clonal selection.* The Journal of pathology, 2012. **227**(1): p. 42-52.
30. Kim, S.Y., et al., *Genomic differences between pure ductal carcinoma in situ and synchronous ductal carcinoma in situ with invasive breast cancer.* 2015. **6**(10): p. 7597.
31. Harrell, J.C., et al., *Estrogen receptor positive breast cancer metastasis: altered hormonal sensitivity and tumor aggressiveness in lymphatic vessels and lymph nodes.* Cancer Res, 2006. **66**(18): p. 9308-15.
32. Gruvberger, S., et al., *Estrogen receptor status in breast cancer is associated with remarkably distinct gene expression patterns.* Cancer Res, 2001. **61**(16): p. 5979-84.
33. Perou, C.M., et al., *Molecular portraits of human breast tumours.* 2000. **406**(6797): p. 747-752.
34. Nishimura, R., et al., *Ki-67 as a prognostic marker according to breast cancer subtype and a predictor of recurrence time in primary breast cancer.* Experimental and Therapeutic Medicine, 2010. **1**(5): p. 747-754.
35. Yersal, O. and S. Barutca, *Biological subtypes of breast cancer: Prognostic and therapeutic implications.* World J Clin Oncol, 2014. **5**(3): p. 412-24.
36. Zhang, M.H., et al., *Estrogen receptor-positive breast cancer molecular signatures and therapeutic potentials (Review).* Biomed Rep, 2014. **2**(1): p. 41-52.
37. Sotiriou, C., et al., *Breast cancer classification and prognosis based on gene expression profiles from a population-based study.* Proceedings of the National Academy of Sciences, 2003. **100**(18): p. 10393.
38. Sorlie, T., et al., *Repeated observation of breast tumor subtypes in independent gene expression data sets.* Proc Natl Acad Sci U S A, 2003. **100**(14): p. 8418-23.
39. Naderi, A., et al., *A gene-expression signature to predict survival in breast cancer across independent data sets.* Oncogene, 2007. **26**(10): p. 1507-16.
40. Ahr, A., et al., *Molecular classification of breast cancer patients by gene expression profiling.* J Pathol, 2001. **195**(3): p. 312-20.
41. Criscitiello, C., et al., *Tamoxifen in early-stage estrogen receptor-positive breast cancer: overview of clinical use and molecular biomarkers for patient selection.* OncoTargets and therapy, 2010. **4**: p. 1-11.
42. Krauss, K. and E. Stickeler, *Endocrine Therapy in Early Breast Cancer.* Breast Care, 2020. **15**(4): p. 337-346.
43. Lee, S.-y. and J.H. Seo, *Current Strategies of Endocrine Therapy in Elderly Patients with Breast Cancer.* BioMed Research International, 2018. **2018**: p. 6074808.
44. Abubakar, M., et al., *Breast cancer risk factors, survival and recurrence, and tumor molecular subtype: analysis of 3012 women from an indigenous Asian population.* Breast Cancer Research, 2018. **20**(1): p. 114.
45. Marotti, J.D., et al., *Triple-Negative Breast Cancer: Next-Generation Sequencing for Target Identification.* Am J Pathol, 2017. **187**(10): p. 2133-2138.

46. Gupta, A., et al., *Triple Negative Breast Cancer-An Overview and Review of Literature.* 2013, 2013. **3**(2): p. 5.
47. Fadare, O. and F.A. Tavassoli, *The phenotypic spectrum of basal-like breast cancers: a critical appraisal.* Adv Anat Pathol, 2007. **14**(5): p. 358-73.
48. Fulford, L.G., et al., *Specific morphological features predictive for the basal phenotype in grade 3 invasive ductal carcinoma of breast.* Histopathology, 2006. **49**(1): p. 22-34.
49. Nielsen, T.O., et al., *Immunohistochemical and clinical characterization of the basal-like subtype of invasive breast carcinoma.* Clin Cancer Res, 2004. **10**(16): p. 5367-74.
50. Livasy, C.A., et al., *Phenotypic evaluation of the basal-like subtype of invasive breast carcinoma.* Mod Pathol, 2006. **19**(2): p. 264-71.
51. Pintens, S., et al., *Triple negative breast cancer: a study from the point of view of basal CK5/6 and HER-1.* J Clin Pathol, 2009. **62**(7): p. 624-8.
52. Matos, I., et al., *p63, cytokeratin 5, and P-cadherin: three molecular markers to distinguish basal phenotype in breast carcinomas.* Virchows Arch, 2005. **447**(4): p. 688-94.
53. Abd El-Rehim, D.M., et al., *Expression of luminal and basal cytokeratins in human breast carcinoma.* J Pathol, 2004. **203**(2): p. 661-71.
54. Cakir, A., I.I. Gonul, and O. Uluoglu, *A comprehensive morphological study for basal-like breast carcinomas with comparison to nonbasal-like carcinomas.* Diagnostic pathology, 2012. **7**: p. 145-145.
55. Venkitaraman, A.R., *Cancer susceptibility and the functions of BRCA1 and BRCA2.* Cell, 2002. **108**(2): p. 171-82.
56. Wooster, R. and B.L. Weber, *Breast and ovarian cancer.* N Engl J Med, 2003. **348**(23): p. 2339-47.
57. Sørlie, T., et al., *Gene expression patterns of breast carcinomas distinguish tumor subclasses with clinical implications.* Proc Natl Acad Sci U S A, 2001. **98**(19): p. 10869-74.
58. Carey, L.A., et al., *Race, breast cancer subtypes, and survival in the Carolina Breast Cancer Study.* Jama, 2006. **295**(21): p. 2492-502.
59. Vousden, K.H. and D.P. Lane, *p53 in health and disease.* Nat Rev Mol Cell Biol, 2007. **8**(4): p. 275-83.
60. Hynes, N.E. and H.A. Lane, *ERBB receptors and cancer: the complexity of targeted inhibitors.* Nat Rev Cancer, 2005. **5**(5): p. 341-54.
61. Thiery, J.P., *Epithelial-mesenchymal transitions in tumour progression.* Nat Rev Cancer, 2002. **2**(6): p. 442-54.
62. Sarrió, D., et al., *Epithelial-mesenchymal transition in breast cancer relates to the basal-like phenotype.* Cancer Res, 2008. **68**(4): p. 989-97.
63. Blick, T., et al., *Epithelial mesenchymal transition traits in human breast cancer cell lines.* Clin Exp Metastasis, 2008. **25**(6): p. 629-42.
64. Octavia, Y., et al., *Doxorubicin-induced cardiomyopathy: from molecular mechanisms to therapeutic strategies.* J Mol Cell Cardiol, 2012. **52**(6): p. 1213-25.
65. Pareja, F., et al., *Triple-negative breast cancer: the importance of molecular and histologic subtyping, and recognition of low-grade variants.* NPJ Breast Cancer, 2016. **2**: p. 16036.
66. Ismail-Khan, R. and M.M. Bui, *A review of triple-negative breast cancer.* Cancer Control, 2010. **17**(3): p. 173-6.
67. Yuan, Y., et al., *Role of the tumor microenvironment in tumor progression and the clinical applications (Review).* Oncol Rep, 2016. **35**(5): p. 2499-515.
68. Deshmukh, S.K., et al., *Emerging evidence for the role of differential tumor microenvironment in breast cancer racial disparity: a closer look at the surroundings.* Carcinogenesis, 2017. **38**(8): p. 757-765.
69. Eftekhari, R., et al., *Study of the tumor microenvironment during breast cancer progression.* Cancer Cell International, 2017. **17**: p. 123.

70. D Soysal, S., A. Tzankov, and S. E Muenst, *Role of the Tumor Microenvironment in Breast Cancer*. Vol. 82. 2015. 142-52.
71. Hill, B.S., et al., *Recruitment of stromal cells into tumour microenvironment promote the metastatic spread of breast cancer.* Seminars in Cancer Biology, 2020. **60**: p. 202-213.
72. Bonnans, C., J. Chou, and Z. Werb, *Remodelling the extracellular matrix in development and disease.* Nat Rev Mol Cell Biol, 2014. **15**(12): p. 786-801.
73. Wang, J.P. and A. Hielscher, *Fibronectin: How Its Aberrant Expression in Tumors May Improve Therapeutic Targeting.* Journal of Cancer, 2017. **8**(4): p. 674-682.
74. Place, A.E., S. Jin Huh, and K. Polyak, *The microenvironment in breast cancer progression: biology and implications for treatment.* Breast Cancer Res, 2011. **13**(6): p. 227.
75. Dore-Savard, L., et al., *The Angiogenic Secretome in VEGF overexpressing Breast Cancer Xenografts.* Scientific Reports, 2016. **6**(1): p. 39460.
76. Ali, E.M., M. Sheta, and M.A. El Mohsen, *Elevated serum and tissue VEGF associated with poor outcome in breast cancer patients.* Alexandria Journal of Medicine, 2011. **47**(3): p. 217-224.
77. Rody, A., et al., *T-cell metagene predicts a favorable prognosis in estrogen receptor-negative and HER2-positive breast cancers.* Breast Cancer Research, 2009. **11**(2): p. R15.
78. Plitas, G., et al., *Regulatory T Cells Exhibit Distinct Features in Human Breast Cancer.* Immunity, 2016. **45**(5): p. 1122-1134.
79. Morris, B.A., et al., *Collagen Matrix Density Drives the Metabolic Shift in Breast Cancer Cells.* EBioMedicine, 2016. **13**: p. 146-156.
80. Khamis, Z., Z. Sahab, and Q.-X. Amy Sang, *Active Roles of Tumor Stroma in Breast Cancer Metastasis*. Vol. 2012. 2012. 574025.
81. Dandekar, R.C., A.V. Kingaonkar, and G.S. Dhabekar, *Role of macrophages in malignancy.* Annals of maxillofacial surgery, 2011. **1**(2): p. 150-154.
82. Pandya, P.H., et al., *The Immune System in Cancer Pathogenesis: Potential Therapeutic Approaches.* Journal of Immunology Research, 2016. **2016**: p. 4273943.
83. Hussein, M.R. and H.I. Hassan, *Analysis of the mononuclear inflammatory cell infiltrate in the normal breast, benign proliferative breast disease, in situ and infiltrating ductal breast carcinomas: preliminary observations.* Journal of Clinical Pathology, 2006. **59**(9): p. 972.
84. Ruffell, B., et al., *Leukocyte composition of human breast cancer.* Proceedings of the National Academy of Sciences, 2012. **109**(8): p. 2796.
85. Bhatia, A. and Y. Kumar, *Cancer-Immune Equilibrium: Questions Unanswered.* Cancer Microenvironment, 2011. **4**(2): p. 209-217.
86. Fu, C. and A. Jiang, *Dendritic Cells and CD8 T Cell Immunity in Tumor Microenvironment.* 2018. **9**(3059).
87. García-Aranda, M. and M. Redondo, *Targeting Protein Kinases to Enhance the Response to anti-PD-1/PD-L1 Immunotherapy.* Int J Mol Sci, 2019. **20**(9).
88. Campoli, M., et al., *Mechanisms of tumor evasion.* 2005: p. 61-88.
89. García-Aranda, M., E. Pérez-Ruiz, and M. Redondo, *Bcl-2 Inhibition to Overcome Resistance to Chemo- and Immunotherapy.* Int J Mol Sci, 2018. **19**(12).
90. Kroemer, G. and L. Zitvogel, *Cancer immunotherapy in 2017: The breakthrough of the microbiota.* Nat Rev Immunol, 2018. **18**(2): p. 87-88.
91. Emens, L.A., et al., *Cancer immunotherapy: opportunities and challenges in the rapidly evolving clinical landscape.* 2017. **81**: p. 116-129.
92. Butte, M.J., et al., *Programmed death-1 ligand 1 interacts specifically with the B7-1 costimulatory molecule to inhibit T cell responses.* Immunity, 2007. **27**(1): p. 111-22.
93. Latchman, Y., et al., *PD-L2 is a second ligand for PD-1 and inhibits T cell activation.* Nat Immunol, 2001. **2**(3): p. 261-8.
94. Zielinski, C., et al., *Rationale for targeting the immune system through checkpoint molecule blockade in the treatment of non-small-cell lung cancer.* Ann Oncol, 2013. **24**(5): p. 1170-9.

95. Wang, C., et al., *In vitro characterization of the anti-PD-1 antibody nivolumab, BMS-936558, and in vivo toxicology in non-human primates.* Cancer Immunol Res, 2014. **2**(9): p. 846-56.
96. Loi, S., et al., *Prognostic and predictive value of tumor-infiltrating lymphocytes in a phase III randomized adjuvant breast cancer trial in node-positive breast cancer comparing the addition of docetaxel to doxorubicin with doxorubicin-based chemotherapy: BIG 02-98.* J Clin Oncol, 2013. **31**(7): p. 860-7.
97. Wimberly, H., et al., *PD-L1 Expression Correlates with Tumor-Infiltrating Lymphocytes and Response to Neoadjuvant Chemotherapy in Breast Cancer.* Cancer Immunol Res, 2015. **3**(4): p. 326-32.
98. Schmid, P., et al., *KEYNOTE-522: Phase III study of pembrolizumab (pembro)+ chemotherapy (chemo) vs placebo+ chemo as neoadjuvant therapy followed by pembro vs placebo as adjuvant therapy for triple-negative breast cancer (TNBC)*. 2018, American Society of Clinical Oncology.
99. Zhang, J.-y., et al., *PD-1/PD-L1 Based Combinational Cancer Therapy: Icing on the Cake.* Frontiers in Pharmacology, 2020. **11**: p. 722.
100. Speiser, D.E., P.-C. Ho, and G. Verdeil, *Regulatory circuits of T cell function in cancer.* Nature Reviews Immunology, 2016. **16**(10): p. 599-611.
101. Halama, N., et al., *Localization and density of immune cells in the invasive margin of human colorectal cancer liver metastases are prognostic for response to chemotherapy.* Cancer Res, 2011. **71**(17): p. 5670-7.
102. Li, X., et al., *Infiltration of CD8(+) T cells into tumor cell clusters in triple-negative breast cancer.* Proceedings of the National Academy of Sciences of the United States of America, 2019. **116**(9): p. 3678-3687.
103. Andersen, M.H., et al., *Cytotoxic T Cells.* Journal of Investigative Dermatology, 2006. **126**(1): p. 32-41.
104. Burugu, S., K. Asleh-Aburaya, and T.O. Nielsen, *Immune infiltrates in the breast cancer microenvironment: detection, characterization and clinical implication.* Breast Cancer, 2017. **24**(1): p. 3-15.
105. Zeng, D.-Q., et al., *Prognostic and predictive value of tumor-infiltrating lymphocytes for clinical therapeutic research in patients with non-small cell lung cancer.* Oncotarget, 2016. **7**(12): p. 13765-13781.
106. Wang, Z., et al., *Infiltrating CD4/CD8 high T cells shows good prognostic impact in pancreatic cancer*. Vol. 10. 2017. 8820-8828.
107. Ziai, J., et al., *CD8+ T cell infiltration in breast and colon cancer: A histologic and statistical analysis.* PLoS ONE, 2018. **13**(1): p. e0190158.
108. Wang, K., et al., *The CD4/CD8 ratio of tumor-infiltrating lymphocytes at the tumor-host interface has prognostic value in triple-negative breast cancer.* Human Pathology, 2017. **69**: p. 110-117.
109. Yu, X., et al., *Prognostic and predictive value of tumor-infiltrating lymphocytes in breast cancer: a systematic review and meta-analysis.* Clinical and Translational Oncology, 2016. **18**(5): p. 497-506.
110. Mahmoud, S.M.A., et al., *Tumor-Infiltrating CD8+ Lymphocytes Predict Clinical Outcome in Breast Cancer.* Journal of Clinical Oncology, 2011. **29**(15): p. 1949-1955.
111. Seo, A.N., et al., *Tumour-infiltrating CD8+ lymphocytes as an independent predictive factor for pathological complete response to primary systemic therapy in breast cancer.* Br J Cancer, 2013. **109**(10): p. 2705-13.
112. Baker, K., et al., *Prognostic significance of CD8+ T lymphocytes in breast cancer depends upon both oestrogen receptor status and histological grade.* Histopathology, 2011. **58**(7): p. 1107-16.
113. Ahn, S., et al., *Changes and prognostic values of tumor-infiltrating lymphocyte subsets after primary systemic therapy in breast cancer.* PLOS ONE, 2020. **15**(5): p. e0233037.

114. Varn, F.S., et al., *Adaptive immunity programmes in breast cancer.* Immunology, 2017. **150**(1): p. 25-34.
115. Romagnani, S., *Th1/Th2 cells.* Inflamm Bowel Dis, 1999. **5**(4): p. 285-94.
116. den Haan, J.M.M., G. Kraal, and M.J. Bevan, *Cutting Edge: Lipopolysaccharide Induces IL-10-Producing Regulatory CD4⁺ T Cells That Suppress the CD8⁺ T Cell Response.* The Journal of Immunology, 2007. **178**(9): p. 5429.
117. Stanton, S.E. and M.L. Disis, *Clinical significance of tumor-infiltrating lymphocytes in breast cancer.* J Immunother Cancer, 2016. **4**: p. 59.
118. Matsumoto, H., et al., *Increased CD4 and CD8-positive T cell infiltrate signifies good prognosis in a subset of triple-negative breast cancer.* Breast Cancer Res Treat, 2016. **156**(2): p. 237-47.
119. Huang, Y., et al., *CD4+ and CD8+ T cells have opposing roles in breast cancer progression and outcome.* Oncotarget, 2015. **6**(19): p. 17462-78.
120. Matkowski, R., et al., *The Prognostic Role of Tumor-infiltrating CD4 and CD8 T Lymphocytes in Breast Cancer.* Anticancer Research, 2009. **29**(7): p. 2445-2451.
121. Jamiyan, T., et al., *Prognostic impact of a tumor-infiltrating lymphocyte subtype in triple negative cancer of the breast.* Breast Cancer, 2020. **27**(5): p. 880-892.
122. Jamiyan, T., et al., *Prognostic impact of a tumor-infiltrating lymphocyte subtype in triple negative cancer of the breast.* Breast cancer (Tokyo, Japan), 2020. **27**(5): p. 880-892.
123. Watanabe, M.A., et al., *Regulatory T cells and breast cancer: implications for immunopathogenesis.* Cancer Metastasis Rev, 2010. **29**(4): p. 569-79.
124. Rowshanravan, B., N. Halliday, and D.M. Sansom, *CTLA-4: a moving target in immunotherapy.* Blood, 2018. **131**(1): p. 58-67.
125. Takeuchi, Y. and H. Nishikawa, *Roles of regulatory T cells in cancer immunity.* Int Immunol, 2016. **28**(8): p. 401-9.
126. Arce-Sillas, A., et al., *Regulatory T Cells: Molecular Actions on Effector Cells in Immune Regulation.* Journal of Immunology Research, 2016. **2016**: p. 12.
127. Jiang, D., et al., *Clinicopathological and prognostic significance of FOXP3+ tumor infiltrating lymphocytes in patients with breast cancer: a meta-analysis.* BMC Cancer, 2015. **15**: p. 727.
128. Yeong, J., et al., *Higher densities of Foxp3(+) regulatory T cells are associated with better prognosis in triple-negative breast cancer.* Breast Cancer Res Treat, 2017. **163**(1): p. 21-35.
129. Lee, S., et al., *Prognostic impact of FOXP3 expression in triple-negative breast cancer.* Acta Oncol, 2013. **52**(1): p. 73-81.
130. Qian, F., et al., *High tumor-infiltrating FoxP3(+) T cells predict poor survival in estrogen receptor-positive breast cancer: A meta-analysis.* Eur J Surg Oncol, 2017. **43**(7): p. 1258-1264.
131. Liu, F., et al., *CD8(+) cytotoxic T cell and FOXP3(+) regulatory T cell infiltration in relation to breast cancer survival and molecular subtypes.* Breast Cancer Res Treat, 2011. **130**(2): p. 645-55.
132. Li, Z., et al., *PD-L1 Expression Is Associated with Tumor FOXP3⁺ Regulatory T-Cell Infiltration of Breast Cancer and Poor Prognosis of Patient.* Journal of Cancer, 2016. **7**(7): p. 784-793.
133. Li, Z., et al., *PD-L1 Expression Is Associated with Tumor FOXP3(+) Regulatory T-Cell Infiltration of Breast Cancer and Poor Prognosis of Patient.* Journal of Cancer, 2016. **7**(7): p. 784-793.
134. Shimokawara, I., et al., *Identification of lymphocyte subpopulations in human breast cancer tissue and its significance: an immunoperoxidase study with anti-human T- and B-cell sera.* Cancer, 1982. **49**(7): p. 1456-64.
135. Coronella, J.A., et al., *Evidence for an antigen-driven humoral immune response in medullary ductal breast cancer.* Cancer Res, 2001. **61**(21): p. 7889-99.
136. Yuen, G.J., E. Demissie, and S. Pillai, *B lymphocytes and cancer: a love-hate relationship.* Trends Cancer, 2016. **2**(12): p. 747-757.

137. Kalampokis, I., A. Yoshizaki, and T.F. Tedder, *IL-10-producing regulatory B cells (B10 cells) in autoimmune disease.* Arthritis Res Ther, 2013. **15 Suppl 1**: p. S1.
138. Shen, M., J. Wang, and X. Ren, *New Insights into Tumor-Infiltrating B Lymphocytes in Breast Cancer: Clinical Impacts and Regulatory Mechanisms.* Front Immunol, 2018. **9**: p. 470.
139. Shen, M., J. Wang, and X. Ren, *New Insights into Tumor-Infiltrating B Lymphocytes in Breast Cancer: Clinical Impacts and Regulatory Mechanisms.* Frontiers in immunology, 2018. **9**: p. 470-470.
140. Singh, S., et al., *Initiative action of tumor-associated macrophage during tumor metastasis.* Biochimie Open, 2017. **4**: p. 8-18.
141. Duan, Z. and Y. Luo, *Targeting macrophages in cancer immunotherapy.* Signal Transduction and Targeted Therapy, 2021. **6**(1): p. 127.
142. Tsuyada, A., et al., *CCL2 mediates cross-talk between cancer cells and stromal fibroblasts that regulates breast cancer stem cells.* Cancer research, 2012. **72**(11): p. 2768-2779.
143. O'Hayre, M., et al., *Chemokines and cancer: migration, intracellular signalling and intercellular communication in the microenvironment.* 2008. **409**(3): p. 635-649.
144. Yao, Y., X.-H. Xu, and L. Jin, *Macrophage Polarization in Physiological and Pathological Pregnancy.* 2019. **10**(792).
145. Qian, B.Z., et al., *CCL2 recruits inflammatory monocytes to facilitate breast-tumour metastasis.* Nature, 2011. **475**(7355): p. 222-5.
146. Yu, T. and G. Di, *Role of tumor microenvironment in triple-negative breast cancer and its prognostic significance.* Chinese Journal of Cancer Research, 2017. **29**(3): p. 237-252.
147. Obeid, E., et al., *The role of tumor-associated macrophages in breast cancer progression (review).* Int J Oncol, 2013. **43**(1): p. 5-12.
148. Brady, N.J., P. Chuntova, and K.L. Schwertfeger, *Macrophages: Regulators of the Inflammatory Microenvironment during Mammary Gland Development and Breast Cancer.* Mediators of Inflammation, 2016. **2016**: p. 13.
149. Murray, P.J. and T.A.J.J.o.l.b. Wynn, *Obstacles and opportunities for understanding macrophage polarization.* 2011. **89**(4): p. 557-563.
150. Solinas, G., et al., *Tumor-associated macrophages (TAM) as major players of the cancer-related inflammation.* J Leukoc Biol, 2009. **86**(5): p. 1065-73.
151. Gordon, S., *Alternative activation of macrophages.* Nature Reviews Immunology, 2003. **3**(1): p. 23-35.
152. Jubb, A.M., et al., *Expression of Vascular Notch Ligand Delta-Like 4 and Inflammatory Markers in Breast Cancer.* The American Journal of Pathology, 2010. **176**(4): p. 2019-2028.
153. Tsutsui, S., et al., *Macrophage infiltration and its prognostic implications in breast cancer: the relationship with VEGF expression and microvessel density.* Oncol Rep, 2005. **14**(2): p. 425-31.
154. Jamiyan, T., et al., *CD68- and CD163-positive tumor-associated macrophages in triple negative cancer of the breast.* Virchows Archiv, 2020.
155. Gwak, J.M., et al., *Prognostic Value of Tumor-Associated Macrophages According to Histologic Locations and Hormone Receptor Status in Breast Cancer.* PLoS ONE, 2015. **10**(4): p. e0125728.
156. Zhao, X., et al., *Prognostic significance of tumor-associated macrophages in breast cancer: a meta-analysis of the literature.* Oncotarget, 2017. **8**(18): p. 30576-30586.
157. Pelekanou, V., et al., *CD68, CD163, and matrix metalloproteinase 9 (MMP-9) co-localization in breast tumor microenvironment predicts survival differently in ER-positive and -negative cancers.* Breast Cancer Research, 2018. **20**(1): p. 154.
158. Quail, D.F. and J.A. Joyce, *Microenvironmental regulation of tumor progression and metastasis.* Nature Medicine, 2013. **19**(11): p. 1423-1437.
159. Maman, S. and I.P. Witz, *A history of exploring cancer in context.* Nature Reviews Cancer, 2018. **18**(6): p. 359-376.

160. Turley, S.J., V. Cremasco, and J.L. Astarita, *Immunological hallmarks of stromal cells in the tumour microenvironment.* Nat Rev Immunol, 2015. **15**(11): p. 669-82.
161. Kalluri, R., *The biology and function of fibroblasts in cancer.* Nature Reviews Cancer, 2016. **16**(9): p. 582-598.
162. Chen, X. and E. Song, *Turning foes to friends: targeting cancer-associated fibroblasts.* Nat Rev Drug Discov, 2019. **18**(2): p. 99-115.
163. Löhr, M., et al., *Transforming growth factor-beta1 induces desmoplasia in an experimental model of human pancreatic carcinoma.* Cancer Res, 2001. **61**(2): p. 550-5.
164. Aoyagi, Y., et al., *Overexpression of TGF-beta by infiltrated granulocytes correlates with the expression of collagen mRNA in pancreatic cancer.* Br J Cancer, 2004. **91**(7): p. 1316-26.
165. LeBleu, V.S. and R. Kalluri, *A peek into cancer-associated fibroblasts: origins, functions and translational impact.* Disease Models & Mechanisms, 2018. **11**(4): p. dmm029447.
166. Suda, T., et al., *ER-activating ability of breast cancer stromal fibroblasts is regulated independently of alteration of TP53 and PTEN tumor suppressor genes.* Biochemical and Biophysical Research Communications, 2012. **428**(2): p. 259-263.
167. Eiro, N., et al., *Cancer-associated fibroblasts affect breast cancer cell gene expression, invasion and angiogenesis.* Cellular Oncology, 2018. **41**(4): p. 369-378.
168. Ziani, L., S. Chouaib, and J. Thiery, *Alteration of the Antitumor Immune Response by Cancer-Associated Fibroblasts.* Front Immunol, 2018. **9**: p. 414.
169. Zhao, C.L., et al., *Stromal ColXα1 expression correlates with tumor-infiltrating lymphocytes and predicts adjuvant therapy outcome in ER-positive/HER2-positive breast cancer.* BMC cancer, 2019. **19**(1): p. 1036-1036.
170. Catalano, S., et al., *Tamoxifen through GPER upregulates aromatase expression: a novel mechanism sustaining tamoxifen-resistant breast cancer cell growth.* Breast Cancer Res Treat, 2014. **146**(2): p. 273-85.
171. Brechbuhl, H.M., et al., *Fibroblast Subtypes Regulate Responsiveness of Luminal Breast Cancer to Estrogen.* Clin Cancer Res, 2017. **23**(7): p. 1710-1721.
172. Louault, K., et al., *Interactions between cancer-associated fibroblasts and tumor cells promote MCL-1 dependency in estrogen receptor-positive breast cancers.* Oncogene, 2019. **38**(17): p. 3261-3273.
173. Zhou, J., et al., *Cancer-Associated Fibroblasts Correlate with Tumor-Associated Macrophages Infiltration and Lymphatic Metastasis in Triple Negative Breast Cancer Patients.* Journal of Cancer, 2018. **9**(24): p. 4635-4641.
174. Zhou, J., et al., *Cancer-Associated Fibroblasts Correlate with Tumor-Associated Macrophages Infiltration and Lymphatic Metastasis in Triple Negative Breast Cancer Patients.* J Cancer, 2018. **9**(24): p. 4635-4641.
175. Barcellos-Hoff, M.H. and S.A. Ravani, *Irradiated mammary gland stroma promotes the expression of tumorigenic potential by unirradiated epithelial cells.* Cancer Res, 2000. **60**(5): p. 1254-60.
176. Skobe, M. and N.E. Fusenig, *Tumorigenic conversion of immortal human keratinocytes through stromal cell activation.* Proc Natl Acad Sci U S A, 1998. **95**(3): p. 1050-5.
177. Bissell, M.J. and D. Radisky, *Putting tumours in context.* Nat Rev Cancer, 2001. **1**(1): p. 46-54.
178. Rønnov-Jessen, L., O.W. Petersen, and M.J. Bissell, *Cellular changes involved in conversion of normal to malignant breast: importance of the stromal reaction.* Physiol Rev, 1996. **76**(1): p. 69-125.
179. de Kruijf, E.M., et al., *Tumor-stroma ratio in the primary tumor is a prognostic factor in early breast cancer patients, especially in triple-negative carcinoma patients.* Breast Cancer Res Treat, 2011. **125**(3): p. 687-96.
180. Mesker, W.E., et al., *The carcinoma-stromal ratio of colon carcinoma is an independent factor for survival compared to lymph node status and tumor stage.* Cell Oncol, 2007. **29**(5): p. 387-98.

181. Courrech Staal, E.F., et al., *Reproducibility and validation of tumour stroma ratio scoring on oesophageal adenocarcinoma biopsies.* Eur J Cancer, 2011. **47**(3): p. 375-82.
182. Gujam, F.J., et al., *The relationship between the tumour stroma percentage, clinicopathological characteristics and outcome in patients with operable ductal breast cancer.* Br J Cancer, 2014. **111**(1): p. 157-65.
183. de Kruijf, E.M., et al., *Tumor–stroma ratio in the primary tumor is a prognostic factor in early breast cancer patients, especially in triple-negative carcinoma patients.* Breast cancer research and treatment, 2011. **125**(3): p. 687-696.
184. Moorman, A., et al., *The prognostic value of tumour-stroma ratio in triple-negative breast cancer.* European Journal of Surgical Oncology (EJSO), 2012. **38**(4): p. 307-313.
185. Downey, C., et al., *The prognostic significance of tumour–stroma ratio in oestrogen receptor-positive breast cancer.* British journal of cancer, 2014. **110**(7): p. 1744-1747.
186. Vangangelt, K.M.H., et al., *The prognostic value of the tumor-stroma ratio is most discriminative in patients with grade III or triple-negative breast cancer.* Int J Cancer, 2020. **146**(8): p. 2296-2304.
187. Vangangelt, K.M.H., et al., *The prognostic value of the tumor–stroma ratio is most discriminative in patients with grade III or triple-negative breast cancer.* 2020. **146**(8): p. 2296-2304.
188. Grivennikov, S.I., F.R. Greten, and M. Karin, *Immunity, inflammation, and cancer.* Cell, 2010. **140**(6): p. 883-99.
189. Hanahan, D. and R.A. Weinberg, *Hallmarks of cancer: the next generation.* Cell, 2011. **144**(5): p. 646-74.
190. Mantovani, A., et al., *Cancer-related inflammation.* Nature, 2008. **454**(7203): p. 436-44.
191. Fukuda, J., et al., *Micropatterned cell co-cultures using layer-by-layer deposition of extracellular matrix components.* Biomaterials, 2006. **27**(8): p. 1479-86.
192. Dominguez-Andres, J. and M.G. Netea, *Long-term reprogramming of the innate immune system.* J Leukoc Biol, 2019. **105**(2): p. 329-338.
193. Shalapour, S. and M. Karin, *Immunity, inflammation, and cancer: an eternal fight between good and evil.* J Clin Invest, 2015. **125**(9): p. 3347-55.
194. Zamarron, B.F. and W. Chen, *Dual roles of immune cells and their factors in cancer development and progression.* Int J Biol Sci, 2011. **7**(5): p. 651-8.
195. Gonzalo-Gil, E. and M. Galindo-Izquierdo, *Role of transforming growth factor-beta (TGF) beta in the physiopathology of rheumatoid arthritis.* Reumatol Clin, 2014. **10**(3): p. 174-9.
196. Duvernelle, C., V. Freund, and N. Frossard, *Transforming growth factor-beta and its role in asthma.* Pulm Pharmacol Ther, 2003. **16**(4): p. 181-96.
197. Liu, S., S. Chen, and J. Zeng, *TGF-β signaling: A complex role in tumorigenesis (Review).* Mol Med Rep, 2018. **17**(1): p. 699-704.
198. Kretzschmar, M., *Transforming growth factor-beta and breast cancer: Transforming growth factor-beta/SMAD signaling defects and cancer.* Breast cancer research : BCR, 2000. **2**(2): p. 107-115.
199. Teicher, B.A., et al., *Reversal of in vivo drug resistance by the transforming growth factor-beta inhibitor decorin.* Int J Cancer, 1997. **71**(1): p. 49-58.
200. Akhurst, R.J. and A. Hata, *Targeting the TGFβ signalling pathway in disease.* Nat Rev Drug Discov, 2012. **11**(10): p. 790-811.
201. Derynck, R. and R.J. Akhurst, *Differentiation plasticity regulated by TGF-beta family proteins in development and disease.* Nat Cell Biol, 2007. **9**(9): p. 1000-4.
202. Keystone, E.C. and C.F. Ware, *Tumor Necrosis Factor and Anti-Tumor Necrosis Factor Therapies.* The Journal of Rheumatology, 2010. **85**: p. 27.
203. Cai, X., et al., *Inflammatory factor TNF-α promotes the growth of breast cancer via the positive feedback loop of TNFR1/NF-κB (and/or p38)/p-STAT3/HBXIP/TNFR1.* Oncotarget, 2017. **8**(35): p. 58338-58352.

204. Wang, X. and Y. Lin, *Tumor necrosis factor and cancer, buddies or foes?* Acta Pharmacologica Sinica, 2008. **29**(11): p. 1275-1288.
205. Whiteside, T.L., *The tumor microenvironment and its role in promoting tumor growth.* Oncogene, 2008. **27**(45): p. 5904-5912.
206. Yuan, Y., et al., *Role of the tumor microenvironment in tumor progression and the clinical applications (Review).* Oncol Rep, 2016. **35**(5): p. 2499-2515.
207. Wright, A.I., H.I. Grabsch, and D.E. Treanor, *RandomSpot: A web-based tool for systematic random sampling of virtual slides.* Journal of pathology informatics, 2015. **6**: p. 8-8.
208. Takai, K., et al., *Targeting the cancer-associated fibroblasts as a treatment in triple-negative breast cancer.* Oncotarget, 2016. **7**(50): p. 82889-82901.
209. Movasaghi, Z., S. Rehman, and D.I. ur Rehman, *Fourier transform infrared (FTIR) spectroscopy of biological tissues.* Applied Spectroscopy Reviews, 2008. **43**(2): p. 134-179.
210. Starr, T., et al., *The phorbol 12-myristate-13-acetate differentiation protocol is critical to the interaction of THP-1 macrophages with Salmonella Typhimurium.* PLOS ONE, 2018. **13**(3): p. e0193601.
211. Lund, M.E., et al., *The choice of phorbol 12-myristate 13-acetate differentiation protocol influences the response of THP-1 macrophages to a pro-inflammatory stimulus.* J Immunol Methods, 2016. **430**: p. 64-70.
212. Traore, K., et al., *Signal transduction of phorbol 12-myristate 13-acetate (PMA)-induced growth inhibition of human monocytic leukemia THP-1 cells is reactive oxygen dependent.* Leuk Res, 2005. **29**(8): p. 863-79.
213. Park, E.K., et al., *Optimized THP-1 differentiation is required for the detection of responses to weak stimuli.* Inflammation Research, 2007. **56**(1): p. 45-50.
214. Hall, D.M.S. and S.A. Brooks, *In Vitro Invasion Assay Using Matrigel™: A Reconstituted Basement Membrane Preparation*, in *Metastasis Research Protocols*, M. Dwek, U. Schumacher, and S.A. Brooks, Editors. 2014, Springer New York: New York, NY. p. 1-11.
215. Chistiakov, D.A., et al., *CD68/macrosialin: not just a histochemical marker.* Laboratory Investigation, 2017. **97**(1): p. 4-13.
216. Chiriboga, L., et al., *Infrared spectroscopy of human tissue. I. Differentiation and maturation of epithelial cells in the human cervix.* Biospectroscopy, 1998. **4**(1): p. 47-53.
217. Chiang, H.P., et al., *Fourier transform Raman spectroscopy of carcinogenic polycyclic aromatic hydrocarbons in biological systems: Binding to heme proteins.* Journal of Raman spectroscopy, 1999. **30**(7): p. 551-555.
218. Macías-Barragán, J., et al., *The multifaceted role of pirfenidone and its novel targets.* Fibrogenesis & tissue repair, 2010. **3**(1): p. 16.
219. Lee, K.-L., et al., *Triple-Negative Breast Cancer: Current Understanding and Future Therapeutic Breakthrough Targeting Cancer Stemness.* 2019. **11**(9): p. 1334.
220. Waks, A.G. and E.P. Winer, *Breast Cancer Treatment: A Review.* Jama, 2019. **321**(3): p. 288-300.
221. Beckers, R.K., et al., *Programmed death ligand 1 expression in triple-negative breast cancer is associated with tumour-infiltrating lymphocytes and improved outcome.* Histopathology, 2016. **69**(1): p. 25-34.
222. Force, J., J.H.S. Leal, and H.L. McArthur, *Checkpoint Blockade Strategies in the Treatment of Breast Cancer: Where We Are and Where We Are Heading.* Curr Treat Options Oncol, 2019. **20**(4): p. 35.
223. Bayraktar, S., et al., *Immunotherapy in breast cancer.* Journal of carcinogenesis, 2019. **18**: p. 2-2.
224. McArthur, H.L. and D.B. Page, *Immunotherapy for the treatment of breast cancer: checkpoint blockade, cancer vaccines, and future directions in combination immunotherapy.* Clin Adv Hematol Oncol, 2016. **14**(11): p. 922-933.

225. Adams, S., et al., *Current Landscape of Immunotherapy in Breast Cancer: A Review.* JAMA Oncology, 2019. **5**(8): p. 1205-1214.
226. Dunn, G.P., L.J. Old, and R.D.J.A.R.I. Schreiber, *The three Es of cancer immunoediting.* 2004. **22**: p. 329-360.
227. Manuel, M., et al., *Lymphopenia combined with low TCR diversity (divpenia) predicts poor overall survival in metastatic breast cancer patients.* Oncoimmunology, 2012. **1**(4): p. 432-440.
228. Oda, N., et al., *Intratumoral regulatory T cells as an independent predictive factor for pathological complete response to neoadjuvant paclitaxel followed by 5-FU/epirubicin/cyclophosphamide in breast cancer patients.* Breast Cancer Res Treat, 2012. **136**(1): p. 107-16.
229. Gao, G., et al., *Prognostic value of tumor-infiltrating lymphocytes in patients with triple-negative breast cancer: a systematic review and meta-analysis.* BMC Cancer, 2020. **20**(1): p. 179.
230. Walser, T.C., et al., *Immune-mediated modulation of breast cancer growth and metastasis by the chemokine Mig (CXCL9) in a murine model.* J Immunother, 2007. **30**(5): p. 490-8.
231. Ohtani, H., et al., *Abundant expression of CXCL9 (MIG) by stromal cells that include dendritic cells and accumulation of CXCR3+ T cells in lymphocyte-rich gastric carcinoma.* J Pathol, 2009. **217**(1): p. 21-31.
232. Dong, D.D., et al., *Importance of HLA-G expression and tumor infiltrating lymphocytes in molecular subtypes of breast cancer.* Hum Immunol, 2012. **73**(10): p. 998-1004.
233. Ireland, L.V. and A. Mielgo, *Macrophages and Fibroblasts, Key Players in Cancer Chemoresistance.* Frontiers in cell and developmental biology, 2018. **6**: p. 131-131.
234. Chiarugi, P., *Cancer-associated fibroblasts and macrophages: Friendly conspirators for malignancy.* Oncoimmunology, 2013. **2**(9): p. e25563-e25563.
235. Leek, R.D., et al., *Necrosis correlates with high vascular density and focal macrophage infiltration in invasive carcinoma of the breast.* Br J Cancer, 1999. **79**(5-6): p. 991-5.
236. Kitamura, T., et al., *CCL2-induced chemokine cascade promotes breast cancer metastasis by enhancing retention of metastasis-associated macrophages.* The Journal of experimental medicine, 2015. **212**(7): p. 1043-1059.
237. Epelman, S., K.J. Lavine, and G.J. Randolph, *Origin and functions of tissue macrophages.* Immunity, 2014. **41**(1): p. 21-35.
238. Gordon, S. and P.R. Taylor, *Monocyte and macrophage heterogeneity.* Nat Rev Immunol, 2005. **5**(12): p. 953-64.
239. van oud Alblas, A.B. and R. van Furth, *Origin, Kinetics, and characteristics of pulmonary macrophages in the normal steady state.* J Exp Med, 1979. **149**(6): p. 1504-18.
240. Landsman, L. and S. Jung, *Lung macrophages serve as obligatory intermediate between blood monocytes and alveolar macrophages.* J Immunol, 2007. **179**(6): p. 3488-94.
241. Hettinger, J., et al., *Origin of monocytes and macrophages in a committed progenitor.* Nat Immunol, 2013. **14**(8): p. 821-30.
242. Genin, M., et al., *M1 and M2 macrophages derived from THP-1 cells differentially modulate the response of cancer cells to etoposide.* BMC Cancer, 2015. **15**(1): p. 577.
243. Smith, M., et al., *Differentiation of THP1 Cells into Macrophages for Transwell Co-culture Assay with Melanoma Cells.* Bio-protocol, 2015. **5**.
244. Stokes, R.W. and D. Doxsee, *The receptor-mediated uptake, survival, replication, and drug sensitivity of Mycobacterium tuberculosis within the macrophage-like cell line THP-1: a comparison with human monocyte-derived macrophages.* Cell Immunol, 1999. **197**(1): p. 1-9.
245. Tominaga, T., et al., *Establishment of an activated macrophage cell line, A-THP-1, and its properties.* Tohoku J Exp Med, 1998. **186**(2): p. 99-119.
246. Risko, P., et al., *THP-I cells as a model of human monocytes in iron-loading conditions.* Atherosclerosis, 2015. **241**(1): p. e80.

247. Takemura, H., et al., *Evaluation of a human monocytic cell line THP-1 model for assay of the intracellular activities of antimicrobial agents against Legionella pneumophila.* Journal of Antimicrobial Chemotherapy, 2000. **46**(4): p. 589-594.
248. Auwerx, J., *The human leukemia cell line, THP-1: A multifacetted model for the study of monocyte-macrophage differentiation.* Experientia, 1991. **47**(1): p. 22-31.
249. Bosshart, H. and M. Heinzelmann, *THP-1 cells as a model for human monocytes.* Ann Transl Med, 2016. **4**(21): p. 438.
250. Sousa, S., et al., *Human breast cancer cells educate macrophages toward the M2 activation status.* Breast Cancer Research, 2015. **17**(1): p. 101.
251. Ushach, I. and A. Zlotnik, *Biological role of granulocyte macrophage colony-stimulating factor (GM-CSF) and macrophage colony-stimulating factor (M-CSF) on cells of the myeloid lineage.* J Leukoc Biol, 2016. **100**(3): p. 481-9.
252. Baxter, E.W., et al., *Standardized protocols for differentiation of THP-1 cells to macrophages with distinct M(IFNγ+LPS), M(IL-4) and M(IL-10) phenotypes.* Journal of Immunological Methods, 2020. **478**: p. 112721.
253. Smith, M.P., et al., *Differentiation of THP1 Cells into Macrophages for Transwell Co-culture Assay with Melanoma Cells.* Bio-protocol, 2015. **5**(21): p. e1638.
254. Tedesco, S., et al., *Convenience versus Biological Significance: Are PMA-Differentiated THP-1 Cells a Reliable Substitute for Blood-Derived Macrophages When Studying in Vitro Polarization?* 2018. **9**(71).
255. Richter, E., et al., *Induction of Macrophage Function in Human THP-1 Cells Is Associated with Rewiring of MAPK Signaling and Activation of MAP3K7 (TAK1) Protein Kinase.* 2016. **4**(21).
256. Daigneault, M., et al., *The Identification of Markers of Macrophage Differentiation in PMA-Stimulated THP-1 Cells and Monocyte-Derived Macrophages.* PLOS ONE, 2010. **5**(1): p. e8668.
257. Park, E.K., et al., *Optimized THP-1 differentiation is required for the detection of responses to weak stimuli.* Inflamm Res, 2007. **56**(1): p. 45-50.
258. Maeß, M.B., et al., *Reduced PMA enhances the responsiveness of transfected THP-1 macrophages to polarizing stimuli.* J Immunol Methods, 2014. **402**(1-2): p. 76-81.
259. Mittar, D., R. Paramban, and C.J.B.B. McIntyre, *Flow cytometry and high-content imaging to identify markers of monocyte-macrophage differentiation.* 2011. **20**.
260. Daigneault, M., et al., *The identification of markers of macrophage differentiation in PMA-stimulated THP-1 cells and monocyte-derived macrophages.* PloS one, 2010. **5**(1): p. e8668-e8668.
261. Tahara, E., et al., *Activation of Protein Kinase C by Phorbol 12-Myristate 13-Acetate suppresses the growth of lung cancer cells through KLF6 induction.* Cancer Biology & Therapy, 2009. **8**(9): p. 801-807.
262. McWhorter, F.Y., C.T. Davis, and W.F. Liu, *Physical and mechanical regulation of macrophage phenotype and function.* Cellular and molecular life sciences : CMLS, 2015. **72**(7): p. 1303-1316.
263. Grugan, K.D., et al., *Tumor-associated macrophages promote invasion while retaining Fc-dependent anti-tumor function.* J Immunol, 2012. **189**(11): p. 5457-66.
264. Poh, A.R. and M. Ernst, *Targeting Macrophages in Cancer: From Bench to Bedside.* Frontiers in oncology, 2018. **8**: p. 49-49.
265. Ushach, I. and A. Zlotnik, *Biological role of granulocyte macrophage colony-stimulating factor (GM-CSF) and macrophage colony-stimulating factor (M-CSF) on cells of the myeloid lineage.* Journal of leukocyte biology, 2016. **100**(3): p. 481-489.
266. Bosshart, H. and M. Heinzelmann, *THP-1 cells as a model for human monocytes.* Annals of translational medicine, 2016. **4**(21): p. 438-438.
267. Hollmen, M., et al., *Characterization of macrophage--cancer cell crosstalk in estrogen receptor positive and triple-negative breast cancer.* Sci Rep, 2015. **5**: p. 9188.

268. Balkwill, F.R., M. Capasso, and T. Hagemann, *The tumor microenvironment at a glance.* Journal of Cell Science, 2012. **125**(23): p. 5591.
269. Qiu, S.-Q., et al., *Tumor-associated macrophages in breast cancer: Innocent bystander or important player?* Cancer Treatment Reviews, 2018. **70**: p. 178-189.
270. Bahcecioglu, G., et al., *Breast cancer models: Engineering the tumor microenvironment.* 2020. **106**: p. 1-21.
271. Lee, C.G., et al., *Role of chitin and chitinase/chitinase-like proteins in inflammation, tissue remodeling, and injury.* Annu Rev Physiol, 2011. **73**: p. 479-501.
272. Eurich, K., et al., *Potential role of chitinase 3-like-1 in inflammation-associated carcinogenic changes of epithelial cells.* World J Gastroenterol, 2009. **15**(42): p. 5249-59.
273. Cohen, N., et al., *Fibroblasts drive an immunosuppressive and growth-promoting microenvironment in breast cancer via secretion of Chitinase 3-like 1.* Oncogene, 2017. **36**(31): p. 4457-4468.
274. An, Y., et al., *Crosstalk between cancer-associated fibroblasts and immune cells in cancer.* Journal of cellular and molecular medicine, 2020. **24**(1): p. 13-24.
275. Mazur, A., et al., *Cleavage of Type I Collagen by Fibroblast Activation Protein-alpha Enhances Class A Scavenger Receptor Mediated Macrophage Adhesion.* PLoS One, 2016. **11**(3): p. e0150287.
276. Yamaguchi, H., J. Wyckoff, and J. Condeelis, *Cell migration in tumors.* Curr Opin Cell Biol, 2005. **17**(5): p. 559-64.
277. Yang, W., et al., *Regulation of breast cancer cell behaviours by the physical microenvironment constructed via projection microstereolithography.* Biomater Sci, 2016. **4**(5): p. 863-70.
278. Chen, Y., et al., *Tumor-associated macrophages: an accomplice in solid tumor progression.* Journal of Biomedical Science, 2019. **26**(1): p. 78.
279. Wu, H.J., et al., *FAK signaling in cancer-associated fibroblasts promotes breast cancer cell migration and metastasis by exosomal miRNAs-mediated intercellular communication.* Oncogene, 2020. **39**(12): p. 2539-2549.
280. Little, A.C., et al., *IL-4/IL-13 Stimulated Macrophages Enhance Breast Cancer Invasion Via Rho-GTPase Regulation of Synergistic VEGF/CCL-18 Signaling.* 2019. **9**(456).
281. Storr, S.J., et al., *Macrophage-derived interleukin-1beta promotes human breast cancer cell migration and lymphatic adhesion in vitro.* Cancer immunology, immunotherapy : CII, 2017. **66**(10): p. 1287-1294.
282. Zhang, A., et al., *Cancer-associated fibroblasts promote M2 polarization of macrophages in pancreatic ductal adenocarcinoma.* Cancer Med, 2017. **6**(2): p. 463-470.
283. Comito, G., et al., *Cancer-associated fibroblasts and M2-polarized macrophages synergize during prostate carcinoma progression.* Oncogene, 2014. **33**(19): p. 2423-31.
284. Hall, D.M. and S.A. Brooks, *In vitro invasion assay using matrigel™: a reconstituted basement membrane preparation.* Methods Mol Biol, 2014. **1070**: p. 1-11.
285. Bu, L., et al., *Biological heterogeneity and versatility of cancer-associated fibroblasts in the tumor microenvironment.* Oncogene, 2019. **38**(25): p. 4887-4901.
286. Ward, R., et al., *Monocytes and macrophages, implications for breast cancer migration and stem cell-like activity and treatment.* Oncotarget, 2015. **6**(16): p. 14687-14699.
287. Li, H., et al., *Cyclooxygenase-2 in tumor-associated macrophages promotes breast cancer cell survival by triggering a positive-feedback loop between macrophages and cancer cells.* Oncotarget, 2015. **6**.
288. Gilroy, D.W., M.A. Saunders, and K.K. Wu, *COX-2 expression and cell cycle progression in human fibroblasts.* Am J Physiol Cell Physiol, 2001. **281**(1): p. C188-94.
289. Meijer, K., et al., *Quantitative proteomics analyses of activation states of human THP-1 macrophages.* J Proteomics, 2015. **128**: p. 164-72.

290. Ai, W., et al., *Optimal method to stimulate cytokine production and its use in immunotoxicity assessment.* International journal of environmental research and public health, 2013. **10**(9): p. 3834-3842.
291. Pei, B.X., et al., *Interstitial tumor-associated macrophages combined with tumor-derived colony-stimulating factor-1 and interleukin-6, a novel prognostic biomarker in non-small cell lung cancer.* J Thorac Cardiovasc Surg, 2014. **148**(4): p. 1208-1216.e2.
292. Ségaliny, A.I., et al., *Interleukin-34 promotes tumor progression and metastatic process in osteosarcoma through induction of angiogenesis and macrophage recruitment.* Int J Cancer, 2015. **137**(1): p. 73-85.
293. Qin, Z., *The use of THP-1 cells as a model for mimicking the function and regulation of monocytes and macrophages in the vasculature.* Atherosclerosis, 2012. **221**(1): p. 2-11.
294. Miki, Y., et al., *Controversies of aromatase localization in human breast cancer—stromal versus parenchymal cells.* 2007. **106**(1-5): p. 97-101.
295. Paget, S.J.T.L., *The distribution of secondary growths in cancer of the breast.* 1889. **133**(3421): p. 571-573.
296. Damaghi, M., et al., *The harsh microenvironment in early breast cancer selects for a Warburg phenotype.* 2021. **118**(3): p. e2011342118.
297. Mwafy, S.E. and D.M. El-Guindy, *Pathologic assessment of tumor-associated macrophages and their histologic localization in invasive breast carcinoma.* Journal of the Egyptian National Cancer Institute, 2020. **32**(1): p. 6.
298. Ping, Q., et al., *Cancer-associated fibroblasts: overview, progress, challenges, and directions.* Cancer Gene Therapy, 2021.
299. Tiainen, S., et al., *High numbers of macrophages, especially M2-like (CD163-positive), correlate with hyaluronan accumulation and poor outcome in breast cancer.* Histopathology, 2015. **66**(6): p. 873-83.
300. Grossman, J.G., et al., *Recruitment of CCR2(+) tumor associated macrophage to sites of liver metastasis confers a poor prognosis in human colorectal cancer.* Oncoimmunology, 2018. **7**(9): p. e1470729.
301. Mazur, A., et al., *Cleavage of Type I Collagen by Fibroblast Activation Protein-α Enhances Class A Scavenger Receptor Mediated Macrophage Adhesion.* PLoS One, 2016. **11**(3): p. e0150287.
302. Gok Yavuz, B., et al., *Cancer associated fibroblasts sculpt tumour microenvironment by recruiting monocytes and inducing immunosuppressive PD-1(+) TAMs.* Sci Rep, 2019. **9**(1): p. 3172.
303. Chen, Y., et al., *Tumor-recruited M2 macrophages promote gastric and breast cancer metastasis via M2 macrophage-secreted CHI3L1 protein.* Journal of Hematology & Oncology, 2017. **10**(1): p. 36.
304. Saeki, T., et al., *Drug resistance in chemotherapy for breast cancer.* Cancer Chemother Pharmacol, 2005. **56 Suppl 1**: p. 84-9.
305. Castellaro, A.M., et al., *Tumor-Associated Macrophages Induce Endocrine Therapy Resistance in ER+ Breast Cancer Cells.* Cancers, 2019. **11**(2): p. 189.
306. Rubio, M.F., et al., *TNF-α enhances estrogen-induced cell proliferation of estrogen-dependent breast tumor cells through a complex containing nuclear factor-kappa B.* Oncogene, 2006. **25**(9): p. 1367-1377.
307. Zhang, Y.-L., et al., *Roles of Rap1 signaling in tumor cell migration and invasion.* Cancer biology & medicine, 2017. **14**(1): p. 90-99.
308. Yang, Y., et al., *Expression of RAP1B is associated with poor prognosis and promotes an aggressive phenotype in gastric cancer.* Oncol Rep, 2015. **34**(5): p. 2385-2394.
309. Zhang, Y.-L., et al., *Roles of Rap1 signaling in tumor cell migration and invasion.* 2017. **14**(1): p. 90.

310. Lin, K.-T., et al., *Glucocorticoids mediate induction of microRNA-708 to suppress ovarian cancer metastasis through targeting Rap1B.* Nature Communications, 2015. **6**(1): p. 5917.
311. Mitra, R.S., et al., *Rap1A and rap1B ras-family proteins are prominently expressed in the nucleus of squamous carcinomas: nuclear translocation of GTP-bound active form.* Oncogene, 2003. **22**(40): p. 6243-6256.
312. Wu, X., et al., *Claudin1 promotes the proliferation, invasion and migration of nasopharyngeal carcinoma cells by upregulating the expression and nuclear entry of β-catenin.* Experimental and therapeutic medicine, 2018. **16**(4): p. 3445-3451.
313. Nakagawa, S., et al., *Expression of CLDN1 in colorectal cancer: a novel marker for prognosis.* Int J Oncol, 2011. **39**(4): p. 791-6.
314. Park, I., et al., *Myosin regulatory light chains are required to maintain the stability of myosin II and cellular integrity.* The Biochemical journal, 2011. **434**: p. 171-80.
315. Maryan, N., et al., *Regulation of the expression of claudin 23 by the enhancer of zeste 2 polycomb group protein in colorectal cancer.* Mol Med Rep, 2015. **12**(1): p. 728-736.
316. Liu, Y., et al., *RAC2 acts as a prognostic biomarker and promotes the progression of clear cell renal cell carcinoma.* Int J Oncol, 2019. **55**(3): p. 645-656.
317. Park, J., et al., *Tumor suppressor ras association domain family 5 (RASSF5/NORE1) mediates death receptor ligand-induced apoptosis.* The Journal of biological chemistry, 2010. **285**(45): p. 35029-35038.
318. Benedetti, L., et al., *Synthetic lethal interaction between the tumour suppressor STAG2 and its paralog STAG1.* 2017. **8**(23): p. 37619.
319. Karnitz, L.M. and L. Zou, *Molecular Pathways: Targeting ATR in Cancer Therapy.* Clinical cancer research : an official journal of the American Association for Cancer Research, 2015. **21**(21): p. 4780-4785.
320. Kim, H.J., et al., *Anti-tumor activity of the ATR inhibitor AZD6738 in HER2 positive breast cancer cells.* 2017. **140**(1): p. 109-119.
321. Deckers, M., et al., *The tumor suppressor Smad4 is required for transforming growth factor beta-induced epithelial to mesenchymal transition and bone metastasis of breast cancer cells.* Cancer Res, 2006. **66**(4): p. 2202-9.
322. Yousef, E.M., et al., *MCM2: An alternative to Ki-67 for measuring breast cancer cell proliferation.* Mod Pathol, 2017. **30**(5): p. 682-697.
323. Singha, P.K., et al., *Increased Smad3 and reduced Smad2 levels mediate the functional switch of TGF-β from growth suppressor to growth and metastasis promoter through TMEPAI/PMEPA1 in triple negative breast cancer.* Genes & cancer, 2019. **10**(5-6): p. 134-149.
324. Ueda, A., et al., *Therapeutic potential of PLK1 inhibition in triple-negative breast cancer.* Laboratory Investigation, 2019. **99**(9): p. 1275-1286.
325. Miki, Y., et al., *Aromatase localization in human breast cancer tissues: possible interactions between intratumoral stromal and parenchymal cells.* 2007. **67**(8): p. 3945-3954.
326. Feng, Y., et al., *Breast cancer development and progression: Risk factors, cancer stem cells, signaling pathways, genomics, and molecular pathogenesis.* Genes & diseases, 2018. **5**(2): p. 77-106.
327. Gong, L., et al., *Cancer cell reprogramming: a promising therapy converting malignancy to benignity.* Cancer Communications, 2019. **39**(1): p. 48.
328. Dominiak, A., et al., *Communication in the Cancer Microenvironment as a Target for Therapeutic Interventions.* Cancers, 2020. **12**(5): p. 1232.
329. Aunan, J.R., W.C. Cho, and K. Søreide, *The Biology of Aging and Cancer: A Brief Overview of Shared and Divergent Molecular Hallmarks.* Aging Dis, 2017. **8**(5): p. 628-642.
330. Fane, M. and A.T. Weeraratna, *How the ageing microenvironment influences tumour progression.* Nature Reviews Cancer, 2020. **20**(2): p. 89-106.
331. de Ruijter, T.C., et al., *Characteristics of triple-negative breast cancer.* Journal of cancer research and clinical oncology, 2011. **137**(2): p. 183-192.

332. Mahmoud, S.M., et al., *Tumor-infiltrating CD8+ lymphocytes predict clinical outcome in breast cancer.* Journal of Clinical Oncology, 2011. **29**(15): p. 1949-1955.
333. Mahmoud, S., et al., *Tumour-infiltrating macrophages and clinical outcome in breast cancer.* Journal of clinical pathology, 2012. **65**(2): p. 159-163.
334. Ali, H., et al., *Association between CD8+ T-cell infiltration and breast cancer survival in 12 439 patients.* Annals of oncology, 2014: p. mdu191.
335. Bankhead, P., et al., *QuPath: Open source software for digital pathology image analysis.* bioRxiv, 2017: p. 099796.
336. Di Sario, A., et al., *The anti-fibrotic effect of pirfenidone in rat liver fibrosis is mediated by downregulation of procollagen α1 (I), TIMP-1 and MMP-2.* Digestive and liver disease, 2004. **36**(11): p. 744-751.
337. Takai, K., et al., *Targeting the cancer-associated fibroblasts as a treatment in triple-negative breast cancer.* Oncotarget, 2016.
338. Wang, J., et al., *Pirfenidone inhibits migration, differentiation, and proliferation of human retinal pigment epithelial cells in vitro.* Molecular vision, 2013. **19**: p. 2626.
339. Ford, C.H., et al., *Reassessment of estrogen receptor expression in human breast cancer cell lines.* Anticancer research, 2011. **31**(2): p. 521-527.
340. Spano, A., et al., *Expression of cell kinetics and death during monocyte-macrophage differentiation: effects of Actinomycin D and Vinblastine treatments.* Histochem Cell Biol, 2007. **127**(1): p. 79-94.
341. Spano, A., S. Barni, and L. Sciola, *PMA withdrawal in PMA-treated monocytic THP-1 cells and subsequent retinoic acid stimulation, modulate induction of apoptosis and appearance of dendritic cells.* Cell Prolif, 2013. **46**(3): p. 328-47.
342. Feng, Y.H., et al., *Differential regulation of resveratrol on lipopolysacchride-stimulated human macrophages with or without IFN-gamma pre-priming.* Int Immunopharmacol, 2004. **4**(6): p. 713-20.
343. Tulk, S.E., et al., *Vitamin D_3 metabolites enhance the NLRP3-dependent secretion of IL-1β from human THP-1 monocytic cells.* J Cell Biochem, 2015. **116**(5): p. 711-20.
344. Daigneault, M., et al., *The identification of markers of macrophage differentiation in PMA-stimulated THP-1 cells and monocyte-derived macrophages.* PLoS One, 2010. **5**(1): p. e8668.
345. Hollmén, M., et al., *Characterization of macrophage - cancer cell crosstalk in estrogen receptor positive and triple-negative breast cancer.* Scientific Reports, 2015. **5**(1): p. 9188.
346. Heneweer, M., et al., *Co-culture of Primary Human Mammary Fibroblasts and MCF-7 Cells as an In Vitro Breast Cancer Model.* Toxicological Sciences, 2004. **83**(2): p. 257-263.
347. Müller-Quernheim, U.C., et al., *Tumor-cell co-culture induced alternative activation of macrophages is modulated by interferons in vitro.* Journal of interferon & cytokine research : the official journal of the International Society for Interferon and Cytokine Research, 2012. **32**(4): p. 169-177.
348. Li, K., et al., *Leptin promotes breast cancer cell migration and invasion via IL-18 expression and secretion.* Int J Oncol, 2016. **48**(6): p. 2479-87.
349. Lugo-Cintrón, K.M., et al., *Breast Fibroblasts and ECM Components Modulate Breast Cancer Cell Migration Through the Secretion of MMPs in a 3D Microfluidic Co-Culture Model.* Cancers, 2020. **12**(5): p. 1173.
350. Ireland, L.V. and A. Mielgo, *Macrophages and Fibroblasts, Key Players in Cancer Chemoresistance.* 2018. **6**(131).
351. Wei, C., et al., *Crosstalk between cancer cells and tumor associated macrophages is required for mesenchymal circulating tumor cell-mediated colorectal cancer metastasis.* Molecular Cancer, 2019. **18**(1): p. 64.
352. Wang, N., et al., *CXCL1 derived from tumor-associated macrophages promotes breast cancer metastasis via activating NF-κB/SOX4 signaling.* Cell Death & Disease, 2018. **9**(9): p. 880.

353. Gan, L., et al., *Cyclooxygenase-2 in tumor-associated macrophages promotes metastatic potential of breast cancer cells through Akt pathway.* International Journal of Biological Sciences, 2016. **12**(12): p. 1533-1543.
354. Zhang, L.-N., Y.-H. Huang, and L. Zhao, *Fusion of macrophages promotes breast cancer cell proliferation, migration and invasion through activating epithelial-mesenchymal transition and Wnt/β-catenin signaling pathway.* Archives of biochemistry and biophysics, 2019. **676**: p. 108137-108137.
355. Bögels, M., et al., *Carcinoma origin dictates differential skewing of monocyte function.* Oncoimmunology, 2012. **1**(6): p. 798-809.
356. Mantovani, A., et al., *Role of tumor-associated macrophages in tumor progression and invasion.* Cancer Metastasis Rev, 2006. **25**(3): p. 315-22.
357. Sun, N., et al., *Potential Indexing of the Invasiveness of Breast Cancer Cells by Mitochondrial Redox Ratios.* Advances in experimental medicine and biology, 2016. **923**: p. 121-127.
358. Song, W., et al., *Conditioned medium from stimulated macrophages inhibits growth but induces an inflammatory phenotype in breast cancer cells.* Biomedicine & Pharmacotherapy, 2018. **106**: p. 247-254.
359. Smith, S.J., et al., *Molecular Targeting of Cancer-Associated PCNA Interactions in Pancreatic Ductal Adenocarcinoma Using a Cell-Penetrating Peptide.* Molecular Therapy - Oncolytics, 2020. **17**: p. 250-256.
360. Qiu, X., et al., *Correlation analysis between expression of PCNA, Ki-67 and COX-2 and X-ray features in mammography in breast cancer.* Oncol Lett, 2017. **14**(3): p. 2912-2918.
361. Malkas, L.H., et al., *A cancer-associated PCNA expressed in breast cancer has implications as a potential biomarker.* Proc Natl Acad Sci U S A, 2006. **103**(51): p. 19472-7.
362. Pedram, A., et al., *Estrogen inhibits ATR signaling to cell cycle checkpoints and DNA repair.* Molecular biology of the cell, 2009. **20**(14): p. 3374-3389.
363. Moorman, A.M., et al., *The prognostic value of tumour-stroma ratio in triple-negative breast cancer.* Eur J Surg Oncol, 2012. **38**(4): p. 307-13.
364. Downey, C.L., et al., *The prognostic significance of tumour–stroma ratio in oestrogen receptor-positive breast cancer.* British Journal of Cancer, 2014. **110**(7): p. 1744-1747.
365. Lewis, A.T., et al., *Mirrored stainless steel substrate provides improved signal for Raman spectroscopy of tissue and cells.* J Raman Spectrosc, 2017. **48**(1): p. 119-125.
366. Gao, P., et al., *The Clinical Application of Raman Spectroscopy for Breast Cancer Detection.* Journal of Spectroscopy, 2017. **2017**: p. 5383948.